UNIVERSITY OF CALIFORNIA
RIVERSIDE

Rapid Changes in Neuronal Excitability During Osmotic Edema in Juvenile and Adult Hippocampus Through NMDA Receptor Activation

A Dissertation submitted in partial satisfaction
of the requirements for the degree of

Doctor of Philosophy

in

Neuroscience

by

Kelli Amber Lauderdale

August 2015

Dissertation Committee:
Dr. Todd A. Fiacco, Chairperson
Dr. Peter W. Hickmott
Dr. Devin K. Binder

The Dissertation of Kelli Amber Lauderdale is approved:

_____

_____

_____

Committee Chairperson

University of California, Riverside

Acknowledgements

I would like to acknowledge my committee for their guidance and support over the past several years. I consider Dr. Hickmott, Dr. Binder, and Dr. Fiacco as mentors and friends. Dr. Hickmott was always there to discuss electrophysiology and experiments, and I thank him for that. Dr. Binder was a constant source of inspiration and welcomed source of information from the clinical side neuroscience. Additionally I would like to acknowledge my advisor, Dr. Fiacco, someone who has been influential in making me a neuroscientist, educator, and the person I am today. I will never forget their kindness, patience, and support throughout the years.

I would also like to thank my family for their support over the years. My mother, Gail Lauderdale: thank you for pushing me to attend college, your support, and love over the years. Also I would like to thank my sister, Nicole Lauderdale, for her constant support over the years and her willingness to editing my writing, including this dissertation.

I would also like to thank all of my lab members over the years Allison Xiaoqiao Xie, Prakash Devaraju, and especially Tom Murphy for their support and our many discussions over the years on neuroscience, electrophysiology, experiments, teaching and life. I would also like to thank the undergraduates who have assisted my research Taylor Harris, Ilona Kravtsova, Festus Ohan, Sahaj

Nijjar, and Logan Maples. A special thanks to Tina Tung an amazing undergraduate researcher for her enthusiasm, interest, and research contributions over the years.

ABSTRACT OF THE DISSERTATION

Rapid Changes in Neuronal Excitability
During Osmotic Edema in Juvenile and Adult Hippocampus
Through NMDA Receptor Activation

by

Kelli Amber Lauderdale

Doctor of Philosophy, Graduate Program in Neuroscience
University of California, Riverside, August 2015
Dr. Todd A. Fiacco, Chairperson

Cerebral edema affects millions of people worldwide and is associated with a plethora of diseases, disorders, and conditions such as traumatic brain injury, stroke, cardiac arrest, autism and epilepsy. Cellular edema has been known to increase epileptiform activity and seizure susceptibility *in vitro* and *in vivo*. However, the identity of the cell types undergoing volume increases and the types of excitability changes that occur in neurons remain unclear. Electrophysiological whole-cell patch clamp techniques were used to record currents and potentials from CA1 pyramidal neurons during the application of hypoosmolar ACSF (hACSF) in acutely isolated hippocampal slices from mice. Hypoosmolar ACSF evoked slow inward currents (SICs) in neurons, which initiated after ~1 minute of hACSF application. Neuronal excitability increased as osmolarity decreased in a dose-dependent manner. Even 5% reductions in osmolarity were sufficient to significantly increase neuronal excitability. In

addition, hACSF induced neuronal firing of action potentials (APs), independent of AMPA receptor activation. Neuronal excitability was also increased during application of hACSF while blocking both APs and AMPA receptors. Increased sub-threshold EPSPs, neuronal APs, and bursting activity were also evoked in the presence of Mg^{2+}, suggesting that hypoosmolar insults increase neuronal excitability under more physiological conditions. Hypoosmolar insults increased neuronal excitability in both juvenile (P15-P21) and adult 2- to 5-month-old) mice. Bursting activity in adult mice during osmotic insult was elevated compared to juvenile mice. During hypoosmolar insults the frequency of SICs recorded at physiological temperature were significantly elevated from SICs recorded at room temperature. SICs were potentiated by D-serine, and blocked by both DL-AP5 and the NR2B specific compound Ro25-6981. Together, these results indicate that osmotic insults produce cellular edema in both neurons and astrocytes, and increase neuronal excitability within minutes through a combination of synaptic and non-synaptic activation of glutamate receptors.

TABLE OF CONTENTS

(1 - 45) Chapter 1: Introduction

References

(46 - 76) Chapter 2: Methods

Figures

References

(77 - 115) Chapter 3: Osmotic edema evokes rapid excitatory slow inward currents in neurons.

Abstract

Introduction

Results

Discussion

Figures

References

(116 - 150) Chapter 4: Osmotic stress evokes action potentials and excitatory potentials in CA1 pyramidal neurons of the hippocampus.

Abstract

Introduction

Results

Discussion

Figures

References

(151 - 191) Chapter 5: Osmotic insults in adult mice compared to juveniles and during the development of epilepsy.

Abstract

Introduction

Results

Discussion

Figures

References

(192 - 207) Chapter 6: A closer examination of NMDAR activation and specificity during osmotic stress, and mechanisms of astrocytic glutamate release.

Abstract

Introduction

Results

Discussion

Figures

References

(208 - 223) Chapter 7: Conclusion and Perspective

Reference

List of Figures

(p 54) Figure 2.1: Diagram of hippocampus with patched neuron along with representative recordings of current profiles from an astrocyte and a neuron.

(p 55) Figure 2.2: Single and bursts of action potentials classification.

(p 97) Figure 3.1 AMPA receptors contribute to neuronal excitability during hypoosmolar stress.

(p 100) Figure 3.2: Large neuronal SICs are evoked in hypoosmolar conditions.

(p 103) Figure 3.3: Hypoosmolar ACSF increases neuronal SICs in a dose-dependent manner.

(p 104) Figure 3.4: Neuronal excitability at physiological and room temperature during osmotic stress.

(p 106) Figure 3.5 Synaptic and non-synaptic components of SICs during osmotic edema.

(p 108) Figure 3.6: Large neuronal SICs are evoked by hypoosmolar ACSF and occur during astrocyte volume increases.

(p 130) Figure 4.1: AMPA receptor activation is not required for APs or EPSPs induced by mild osmotic stress in acute hippocampal slices.

(p 133) Figure 4.2: AMPA receptor activation is not required for APs, bAPs, or EPSPs induced by moderate osmotic stress.

(p 137) Figure 4.3: 17% hACSF evokes neuronal action potentials and increased bursting activity that is independent of AMPA receptor activation.

(p 140) Figure 4.4: 40% hACSF evokes neuronal action potentials and increased bursting activity that is partly dependent on AMPA receptor activation.

(p 144) Figure 4.5: Neuronal action potentials and EPSPs evoked by hACSF in increasingly physiological conditions.

(p 147) Figure 4.6: Action potentials evoked by osmotic edema are non-synaptic and NMDA receptor-dependent.

(p 170) Figure 5.1: Adult slice health experiments comparing adult slicing buffer solutions and protocols.

(p 173) Figure 5.2: Adult slice health experiments examining effects of AP5, pyruvate and kynurenic acid.

(p 176) Figure 5.3 Neuronal excitability is elevated to a greater extent in adults compared to juvenile mice within the hippocampus.

(p 179) Figure 5.4: Changes in neuronal excitability following osmotic edema in the adult and juvenile CA1 region of the hippocampus.

(p 182) Figure 5.5: Neuronal excitability in adults and juveniles during moderate osmotic stress.

(p 186) Figure 5.6: Epileptiform-like activity during mild osmotic stress in the CA1 region of adult control and IH KA acute hippocampal slices.

(p 200) Figure 6.1: SICs are enhanced by D-Serine a coactivator of the NMDA receptor.

(p 202) Figure 6.2: SICs are blocked by the NR2B subunit NMDA receptor antagonist Ro 25-6981.

(p 204) Figure 6.3: Neuronal SICs appear to be enhanced during moderate osmotic stress when astrocytes are loaded with glutamate.

(p 219) Figure 7.1: Hypothesized model for neuronal excitability increases in hACSF.

List of Tables

(p 99) Table 3.1: Frequency and kinetics of SICs, contributions of mild osmotic stress, AMPA receptors, and neuronal firing of action potentials.

(p 102) Table 3.2: Mean and SE for frequency, amplitude, rise time and decay tau of SICs during a continuous application nACSF, mild, and moderate osmotic stress.

(p 105) Table 3.3: Neuronal SICs during mild osmotic stress at room and physiological temperature.

(p 107) Table 3.4: Mean and SE for frequency of SICs during mild osmotic stress while blocking vesicular release of neurotransmitters, and NMDA receptors.

(p 110) Table 3.5: Neuronal excitability before, during, and after mild or moderate osmotic stress.

(p 132) Table 4.1: Contributions of AMPA receptors to neuronal excitability during mild osmotic stress.

(p 135) Table 4.2: Contributions of AMPA receptors to neuronal excitability during moderate osmotic stress.

(p 139) Table 4.3: AMPA receptor contributions to neuronal excitability before, during and after mild osmotic insult.

(p 142) Table 4.4: AMPA receptor contributions to neuronal excitability before, during and after moderate osmotic insult.

(p 146) Table 4.5: APs, bAPs, and EPSPs before, during, and after moderate osmotic stress, contributions of Mg^{2+} and NBQX.

(p 149) Table 4.6: Frequency of APs, bAPs, and EPSPs, contributions of vesicular release, and NMDA receptors during mild osmotic stress.

(p 172) Table 5.1: Adult slice heath experiments evaluating the adult slicing buffers and protocols.

(p 175) Table 5.2: The effects of AP5, pyruvate, and kynurenic acid on adult slice health.

(p 178) Table 5.3: Frequency and amplitude of SICs in juvenile and adult mice during mild and moderate osmotic insult.

(p 181) Table 5.4: Frequency, rise time and decay tau of SICs in juvenile and adult mice before, during and following mild and moderate osmotic insult.

(p 184) Table 5.5: Action potentials and EPSPs for adult and juvenile mice during moderate osmotic stress.

(p 118) Table 5.6: SIC frequency and kinetics in 7-day post-injection saline control and IH KA mouse contralateral hippocampal slices before, during and after a 17% hACSF application.

(p 201) Table 6.1: Frequency of SICs/minute increases during osmotic insult in the presence of D-serine.

(p 203) Table 6.2: Frequency of SICs/minute during mild and moderate osmotic insult in the presence of the NR2B subunit containing NMDA antagonist Ro 25-6981.

List of Abbreviations

4-AP: 4-Aminopyridine

AED: antiepileptic drugs

AP(s): action potential(s)

AQP4: aquaporin 4

baf: bafilomycin A1

bAP(s): bursts of action potential(s)

BBB: blood brain barrier

CBF: cerebral blood flow

CBV: cerebral blood volume

CNS: central nervous system

CSD: cortical spreading depression

Cx(s): connexin(s)

ECS: extracellular space

EPSC(s): excitatory postsynaptic current(s)

EPSP(s): excitatory postsynaptic potential(s)

GS: glutamine synthetase

hACSF: hypoosmolar artificial cerebrospinal fluid

IACUC: Institutional Animal Care and Use Committee

ICP: intracranial pressure

ISI: interspike interval

nACSF: normosmolar artificial cerebrospinal fluid

NMDA: N-methyl-D-aspartate

PDS(s): paroxysmal depolarizing shift(s)

PSP(s): postsynaptic potential(s)

RVD: regulatory volume degrease

sAP(s): single action potential(s)

SIC(s): slow inward current(s)

s.r: stratum radiatum

STC(s): slow decayed transient inward current(s)

TTX: tetrodotoxin

VRAC(s): volume regulated anion channel(s)

Chapter 1: Introduction

Cerebral edema: definition and types

Cerebral edema is characterized by swelling of the brain tissue paralleled by an increase in brain water content (Fishman, 1975). It is a common life threatening clinical complication within many pathologies such as hypoxia (Hackett and Roach, 2001) ischemia (Badaut et al., 2002) traumatic brain injury (Unterberg et al., 2004), water intoxication (Radojevic et al., 2012; Kozler and Pokorný, 2014) and tumors (Papadopoulos and Verkman, 2007a). In clinical situations, cerebral edema translates into disruption of brain homeostasis, swelling of the brain tissue, increased intracranial pressure, reduced cerebral blood flow, hyperexcitability, seizures and can even result in cerebral herniation and death (Fishman, 1975; Tasleem and Chowdhary, 2003; Unterberg et al., 2004; Ho et al., 2012). Two main categories of cerebral edema were categorized by Klatzo as vasogenic and cytotoxic edema (Klatzo, 1967).

Vasogenic edema is characterized by leakage of the blood brain barrier, entry of fluid and swelling within the interstitial space, often as a result of adjacent traumatic injury (Unterberg et al., 2004). Cellular edema (previously known as cytotoxic edema) is divided into two main categories, cytotoxic edema and osmotic edema. Both swell cells in the CNS by entry of fluid into the intracellular compartment, but by means of different mechanisms; either through

metabolic disturbance (cytotoxic edema) or osmotic swelling (osmotic edema), resulting in a reduction of the extracellular space (ECS) (Kimelberg, 2004a). Cellular edema is a major complication of various pathologies including diabetic ketoacidosis, cardiac arrest, ischemic stroke, traumatic brain injury, and hyponatremia (Thrane et al., 2014)

Osmotic edema

Osmotic edema, such as syndrome of inappropriate antidiuretic hormone secretion and water intoxication, is another subset of cerebral edema which results from the dilution of the ions within the body, and subsequently changes the delicate homeostasis of the body and the brain. The term water intoxication implies that water is the culprit in this type of edema. However, water intoxication can occur from an excess of any fluid which dilutes the osmolarity within the body and thus is sometimes referred to as fluid intoxication as well. Water intoxication is also capable of inducing hyponatremia, another type of cerebral edema which is due to low levels of sodium in the blood (Yamashiro et al., 2013). Thus any insult to the ionic homeostasis of the body which results in low blood osmolarity and subsequently drives net water influx into the brain could cause osmotic edema. Interestingly, cerebral edema via osmotic edema possesses elements of both vasogenic edema, via entry of water into the brain, and cytotoxic edema, via

intracellular swelling of cells (Risher et al., 2009a; Ho et al., 2012; Kozler et al., 2013).

Mechanisms of brain swelling/cell swelling

Cerebral edema is an increase in brain water content and pathological swelling of the brain. Mechanistically, cerebral edema occurs in one of three ways: either by the excessive accumulation of fluid in the extracellular compartment (vasogenic), or by the swelling of the CNS cells (Cellular edema), or a combination of both (osmotic edema) (Klatzo, 1967). In all of these situations the rigid skull restricts the expansion of the brain during cerebral edema and increases intracranial pressure (Mortazavi et al., 2012). One major consequence of elevated intracranial pressure is that it opposes cerebral perfusion pressure thereby reducing cerebral blood flow and potentially compromising the metabolic homeostasis (Bouzat et al., 2013). Another aspect of cerebral edema is the loss of autoregulation within the vasculature of the brain (Hemphill et al., 2001) which may lead to blood pressure fluctuations, increased brain blood volume and swelling of the brain and spinal cord.

Mechanisms of astrocytic swelling

On the cellular level, the development of cellular edema is also associated with astrocytic swelling (Andrew et al., 2007a; Risher et al., 2009b). Astrocytes constitute a neuropil-spanning network, that maintain the homeostatic equilibrium

within the brain under normal physiological conditions by the uptake of potassium, water, glutamate, and other ions (Anderson and Swanson, 2000; Kofuji and Newman, 2004). During cerebral edema, these cells have the ability to swell, which contributes to reduction of the ECS (Andrew and MacVicar, 1994; Risher et al., 2009b; Thrane et al., 2014). Astrocytes have been found to swell under a variety of different conditions, including: elevated KCl, in the presence of metabolic inhibitors such as 6 aminonicotinamide, elevated extracellular neurotransmitter concentrations including glutamate and adenosine, polyunsaturated fatty acids and oxygen-derive free radicals, changes in osmolarity and oxygen glucose deprivation (Andrew et al., 2007b; Risher et al., 2009b; Fedorff, 2012).

Astrocytes are involved in the clearance of glutamate and potassium from the ECS, which is one of the reasons they are thought to be more prone to swelling than neurons. In situations with elevated potassium and glutamate, astrocytes become overloaded with osmolytes, which promotes the influx of water in order to balance their osmolarity. Research has shown that elevated levels of potassium and cell swelling up regulates NKCC in astrocytes but not in neurons (Mongin et al., 1996; Su et al., 2002a, 2002b). The co-transporter NKCC1 has been found in culture to swell cells during the coupling between water and salt transport based on the osmotic gradient, and could be one mechanism by which cells swell (MacAulay et al., 2004; Hamann et al., 2010).

Aquaporin-4 channels which, as their name suggests, primarily transport water across cell membranes and are present in astrocytes. These channels are discussed in further detail below and represent another mechanism by which astrocytes can swell. Evidence for this comes from studies in AQP4-deficient mice, which show reduced brain edema during osmotic edema, ischemic stroke, and transient focal cerebral edema (Manley et al., 2000; Yao et al., 2015).

Other mechanisms that have been suggested for astrocytic swelling are electrically neutral anion and cation co- and exchange transport in astrocytes. In this mechanism, astrocytic swelling involves coupled Na^+/H^+ and Cl^-/ HCO_3^- exchange which is stimulated by increases in intracellular astrocytic hydration of CO^2 to form HCO_3^- and H^+, which are then exchanged for extracellular Cl^- and Na^+ ions (Kimelberg et al., 1979a, 1979b; Kimelberg and Bourke, 1982).

Background on seizures, epilepsy and mechanisms of hyperexcitability

Approximately 2% of the world's population has epilepsy, which is characterized by unprovoked periodic and unpredictable seizures (Hesdorffer et al. 2011). The main treatment method for seizures and epilepsy is administration of antiepileptic drugs (AED). Two serious problems with AEDs prevail. First, AEDs are nonspecific and primarily rely on chronic depression of excitatory neuronal activity. Second, AEDs are incapable of treating one third of the population with epilepsy. A major concern within the scientific and clinical community is that the development of new AEDs over the past several decades

has failed to substantially improve the treatment of epilepsy (Loscher and Schmidt, 2011). The lack of improved AEDs could stem from the fact that the mechanisms underlying the generation and initiation of epileptic activity are not clearly understood.

The majority of the research on epilepsy is based on neuronal mechanisms for seizure induction. Recently, the role of astrocytic Ca^{2+} has begun to be explored. Several neuronal mechanisms have been proposed, including global decrease in inhibitory input via defective GABAergic inhibition (Lloyd et al., 1986) or global increases in excitatory inputs such as increased synchrony and/or activation due to recurrent excitatory collaterals (Wong et al., 1986). High extracellular levels of excitatory neurotransmitters and ions such as glutamate and potassium, as well as low extracellular levels of magnesium and calcium have also been implicated in increasing neuronal excitability (Traynelis and Dingledine, 1988, 1989; Bikson et al., 2003; Angulo et al., 2004; Fellin et al., 2004; Le Meur et al., 2007). The neuronal mechanisms of epilepsy may explain, in part, why current antiepileptic drugs focus on global chronic depression of excitatory networks.

Many of the studies conducted so far to examine astrocytic contributions to seizures have focused on studying the role of astrocytic Ca^{2+}, despite the fact that swelling-evoked glutamate release by astrocytes can be a Ca^{2+}-independent process (Somjen et al., 1993; Kimelberg, 2004b, 2005; Liu et al., 2006; Haskew-Layton et al., 2008; Hirrlinger et al., 2008). Presently, researchers have started to

examine the potential role of astrocytes as a primary source of non-synaptic swelling-induced glutamate release contributing to seizures. However, progress is limited and slow due to lack of astrocyte specific pharmacological reagents and techniques. For instance, studies examining the role of VRACs in epilepsy have used nonspecific VRAC antagonists such as flufenamic acid and NPPB, which directly inhibit neuronal postsynaptic excitability and block neuronal VRACs, respectively (Fernández et al., 2010; Zhang et al., 2011). Therefore, the effects of blocking VRACs could not be conclusively attributed to blocking astrocytic VRACs. While astrocytes appear to be playing a role in epileptiform activity, the mechanisms and pathways require further elucidation and research.

Role of slow inward currents (SICs) in interictal and ictal activity

The relationship of SICs to epileptic activity and the generation of seizures has been heavily debated and is not completely understood (Fellin et al., 2004; Tian et al., 2005). Early research in this area suggested that SICs were responsible for a current called the paroxysmal depolarizing shift (PDS), which underlies epileptic discharges called interictal and ictal bursts (Kang et al., 2005a; Tian et al., 2005). However, others consider SICs and PDSs to be entirely separate events (Angulo et al., 2004; Fellin et al., 2004, 2006a; Wetherington et al., 2008). A brief summary of the research examining and defining the events behind this debate follows.

Some of the first research to suggest a connection between astrocytes in the generation of epileptiform activity was conducted by Kang and others in 2005. They provided the first evidence that Ca^{2+}-dependent release of glutamate from astrocytes may produce epileptiform-like activity (Kang et al., 2005b). It should be noted that other researchers had previously observed this phenomenon in astrocytes but not in the context of disease (Pasti et al., 1997; Araque et al., 1998). They infused IP3 via patch pipette into astrocytes to increase calcium, which was followed by a current that they called, slow decayed transient inward currents (STCs) in CA1 hippocampal neurons. The STC's were large enough to depolarize the pyramidal neurons and induce neuronal firing of action potentials. The STC depolarization itself was similar to that of the PDS thought to underlie epileptic discharges.

Further studies by the same group demonstrated that STCs/PDSs remained even when interictal epileptiform activity was evoked in hippocampal slices by applying 4-AP, along with Ca^{2+} channel blockers to suppress presynaptic release of neurotransmitters and TTX to block neuronal firing (Tian et al., 2005). These results suggested that the PDSs were driven by a non-neuronal source of glutamate. Next, they decided to examine the role of calcium signaling in astrocytes and its role in evoking PDSs. They examined the role of calcium signaling in astrocytes by photolysis of caged Ca^{2+}, which still produced PDSs in the presence of TTX, indicating that glutamate was released due to the calcium elevations in astrocytes.

Other researchers at the time, Fellin and Haydon, conducting similar experiments claimed that glutamate released from astrocytes was not necessary for the generation of epileptiform activity (Fellin et al., 2004, 2006a). In their experiments, they removed magnesium and added in picrotoxin, a noncompetitive channel blocker of $GABA_A$ receptors, to induce ictal and interictal epileptiform activity. During epileptiform activity, they recorded SICs from neurons in hippocampal slices. SICs share similar characteristics to the PDSs. However, when they applied D-AP5 to block NMDA receptors, they still observed ictal and interictal activity, but AP5 did reversibly reduce the duration of both interictal and ictal epileptiform events. Thus they suggested that glutamate release from astrocytes may have a modulatory role in determining the strength of the epileptic activity. However, these experiments failed to address activation of AMPA receptors by glutamate released from astrocytes, claiming gliotransmission is exclusively mediated by NMDA receptors.

Years later, another researcher examining astrocytic release of glutamate in the generation of in focal ictal discharges found that calcium elevations were only associated with the ictal discharges (Gómez-Gonzalo et al., 2010). In addition, they observed that the duration of ictal discharges, frequency, and astrocytic calcium elevations were reduced by antagonists of mGluR5 and P2Y receptors. Furthermore, they concluded that in the presence of 0 Mg^{2+} and picrotoxin, stimulating astrocytes to release glutamate through activation of the PAR-1 thrombin receptor with the peptide TFLLR-NH2 induced SICs which were

sufficient to generate ictal discharges. These findings are difficult to reconcile given that PDSs are often larger than SICs and recur very regularly without directly producing ictal discharges.

In-between the early research examining STCs, PDSs, and SICs and Gomez-Gonzalo's later experiments, the characteristics of PDSs and SICs were further debated and finally concluded that they were two distinct current types. While they both have a similar time course, there are a couple of criteria that distinguish each current: 1) PDSs are sensitive to tetrodotoxin, (TTX) a voltage-gated Na^+ channel blocker, while SICs are not; and 2) PDSs are synchronized over larger areas of the brain (several millimeters) whereas SICs are considered to be locally synchronized among neurons (< 100 μm). (Korn et al., 1987; Wetherington et al., 2008). Furthermore, SICs are irregular in terms of inter-event interval and amplitude, whereas PDSs recur with very evenly spaced intervals and very similar large amplitudes. Even when examining one type of epileptiform-type current, there is discrepancy as to the components contributing to the activity between varying conditions. For example, when PDSs are evoked in low Ca^{2+}, they are insensitive to the NMDAR antagonist D-APV (Heinemann et al., 1985). However, when PDSs are evoked following $GABA_A$ receptor inhibition, D-APV truncates the PDS activity but does not fully suppress it (Dingledine et al., 1986). Of the two main types of epileptiform activity *in vitro*, the ictal state is defined as the fully generalized seizure discharge, while the interictal state is a

form of synchronized epileptiform activity that gradually builds up to the full seizure state (Traynelis and Dingledine, 1988). The interictal state, now thought to be mediated by PDSs, is further characterized as being shorter than the ictal discharge, approximately 50-200 ms consisting of a brief burst of neuronal discharges synchronous over several millimeters of the tissue (Wetherington et al., 2008). SICs, on the other hand, have been shown to synchronize local networks of neurons and may contribute to ictal discharges under certain situations (Angulo et al., 2004; Fellin et al., 2004, 2006a; Gómez-Gonzalo et al., 2010).

Still much is uncertain regarding SICs. They appear to be induced by different types of stimuli while retaining the hallmarks and characteristics of SICs, unlike PDSs. The majority of the research published thus far regarding SICs reports them to be due to Ca^{2+}-dependent glutamate release by astrocytes, through astrocytic vesicular exocytosis. However, other researchers have found that SICs can be induced in conditions completely independent of calcium elevations (Fiacco et al., 2007a). In fact, there is some evidence to support at least six different mechanisms by which astrocytes could release glutamate (discussed later). Whether any or all of these mechanisms are capable of producing SICs and ictal discharges is unclear. The experiments outlined in this dissertation will further define the contribution of SICs during osmotic edema and possible implications to neuronal excitability and seizures.

Pathological changes during cerebral edema and seizures/epilepsy

Epilepsy is characterized by an over-excitation of neurons. One of the main functions of astrocytes is to prevent excitotoxicity by the uptake of glutamate and potassium along with water (Anderson and Swanson, 2000; Kofuji and Newman, 2004). However, several studies indicate that the ability of astrocytes to maintain the osmotic balance may be impaired in epilepsy due to loss and redistribution of different channels and receptors including the water channel Aquaporin-4 and the Kir4.1 inwardly rectifying K^+ channel (Binder and Steinhuaser, 2006). Potassium and water uptake can lead to astrocyte swelling (Andrew et al., 2007). Astrocytic swelling may be of particular importance to epilepsy because several studies have demonstrated that tissue swells prior to the initiation of a seizure (Hsu et al., 2007; Traynelis and Dingledine, 1988). In fact there are many changes that occur during the pathogenesis of epilepsy which vary depending on the type of epilepsy and/or the model of epilepsy. Briefly, I will describe a few of the changes observed during the pathogenesis of epilepsy.

During epilepsy there is significant neuronal cell loss, reactive gliosis, synaptic reorganization, and microvascular proliferation (Hinterkeuser et al., 2000; Jabs et al., 2008; Kahle et al., 2010; Volman et al., 2013). Glutamine synthetase (GS), the astrocytic enzyme that breaks down glutamate into glutamine, may change during the pathogenesis of epilepsy. Research conducted by Eid and coworkers (2004) indicates loss of GS in sclerotic vs. non-sclerotic tissue from patients with

temporal lobe epilepsy (Lee et al., 2004). In addition, several experimental and clinical studies have shown that glutamate clearance from the extracellular space may be delayed (During and D, 1993; Petroff et al., 2002; Campbell and Hablitz, 2004). An increase in AMPA receptor density, and change in expression of AMPA receptor subunits has been observed in patients with medial temporal lobe epilepsy (Lanerolle et al., 1998; Eid et al., 2002). NMDA receptors are also affected. Initially there is significant loss of NMDARs, probably due to neuronal loss, and then similar to AMPA receptors, there is a change in subunit composition with an increase in the NR2B subunit subtype (Frasca et al., 2011).

Heterogeneity of Astrocytes in the CNS

It is generally acknowledged that within the brain, the non-neuronal cell types - glia - are classified into three major groups: microglia, oligodendrocytes, and astrocytes. Michael Von Lenhossek first coined the name 'astrocyte' in 1893. Later, astrocytes were divided into fibrous and protoplasmic subtypes by Kolliker (1893) and Andriezen (1896) (Fedoroff and Vernadakis, 1986). Protoplasmic astrocytes are located in the gray matter and have short yet highly ramified processes, while fibrous astrocytes have rather long processes running between myelinated fibers and are generally located in the white matter (Miller and Raff, 1984; Boulton et al., 1992; Oberheim et al., 2006). While there are many other types of specialized glia including Tanycytes, Bergmann glia, Pituicytes, Muller Cells, Radial glia, and Ependymal cells, of particular interest is the identification

of subtypes within the protoplasmic astrocytes. Found mainly in the juvenile animals, NG2 cells are similar to astrocytes in morphology. However, they have higher input resistances (~200 mΩ), as well as voltage-gated inward and outward potassium currents (Lin and Bergles, 2002). In younger mice we come across these cells in hippocampal slices, but exclude them based on their electrophysiological properties (Lin and Bergles, 2002; Trotter et al., 2010). This study focuses on the hippocampus and specifically protoplasmic astrocytes within the stratum radiatum in the CA1 region. We chose to use slightly older juvenile mice (P15 to P 21) to avoid the younger age group (P7 to P13) where NG2 cells are encountered quite often, and also only included astrocytes with a passive electrophysiological profile. However, it should be noted that while our interests compelled us to examine the role of passive astrocytes in cellular edema more closely, NG2 glia could potentially be swelling during osmotic edema as well.

Physiological roles of astrocytes

In the late 1800s and early 1900s, Ramon Y Cajal and his colleagues were quite insightful when they hypothesized that glia not only insulate neurons, but could secrete trophic factors supporting neuronal growth (Kimelberg, 2004c). Nearly a century later, these concepts have been convincingly demonstrated. The long-standing notion that glia are simply glue or space fillers is long gone due to the dedication and contributions of glial scientists and novel techniques

specifically examining astrocytes. Researchers have discovered numerous other functions for glia, and astrocytes in particular. Astrocytes have been shown to play a role in recycling neurotransmitters, synapse formation, maintenance of the blood brain barrier, nutrient provision for neurons, and ion buffering (Sofroniew and Vinters, 2010). As this study is mainly concerned with the relationship between neurons and astrocytes during osmotic edema, I will briefly review some of the physiological roles of astrocytes followed by neuronal excitatory receptors in the CA1 region of hippocampus.

Potassium buffering

Early experiments measuring extracellular potassium levels with K^+-selective microelectrodes revealed spontaneous as well as stimulated elevations of potassium (Kriz et al., 1974; Sykova et al., 1974; Svoboda and Sykova, 1991). However, studies found that in the adult spinal cord and mammalian cortex, potassium concentration does not exceed a certain steady state of ~ 8 to 10 mM, even during intense stimulation (Kriz et al., 1974; Heinemann and Lux, 1977; Czeh et al., 1981; Svoboda and Sykova, 1991). Extracellular potassium is quickly redistributed back to normal levels by several localized mechanisms including astrocytic spatial potassium buffering. Astrocytes clear potassium ions from the ECS through: 1) opening of Ca^{2+} activated K^+ channels (MacVicar, 1984) 2) Na^+/K^+-ATPase transport; 3) K^+ spatial buffering through uptake by astrocytic Kir4.1 and redistribution through the glial syncytium into the vasculature at

astrocytic endfeet (Orkand et al., 1966) and 4) KCl uptake through Cl^- channels activated through depolarization of the membrane (Walz and Hertz, 1983; Walz and Hinks, 1986). The idea of potassium buffering comes from the glial cell membrane's high permeability for K^+, as well as astrocytic coupling by gap junctions which allows movement of ions such as K^+, Ca^{2+}, and others into the astrocytic syncytium (Coles and Orkand, 1983; Kettenmann et al., 1983).

Astrocytic regulation and homeostasis of the ECS

Hydrated ions cross the cell membrane and this transmembrane movement of ions and water can lead to cellular swelling, especially astrocytic swelling. Swelling activates transport mechanisms in an effort to reduce the concentration of osmolytes in the cell, resulting in a decrease in cell volume. The reduction in cell volume is thought to occur in a couple of different ways. Studies have suggested that cells might undergo a process called a regulatory volume decrease (RVD), which is thought to occur when cells swell and thereby open stretch-activated channels (Pasantes-Morales et al., 2000; Mongin and Orlov, 2001; Abdullaev et al., 2006). Intracellular pH and intracellular concentrations of Ca^{2+} might modulate these mechanisms regulating cell volume (Kempski et al., 1990; Mccarty and O'Neil, 1992). Several studies have also shown the importance of aquaporins in volume regulation (Solenov et al., 2004; Eid et al., 2005).

Aquaporins

Aquaporins (AQP) are a family of transmembrane proteins identified by six membrane-spanning domains containing intracellular amino (N) and carboxyl (C) termini. The aquaporin channels are commonly called "water channels", and can be classified into three subgroups: 1) Aquaglyceroporins, which are involved in water diffusion, as well as urea, glycerol, and some monocarboxylate transport (Gonen and Walz, 2006); 2) Super-aquaporins localized to the cytoplasm, which possibly contribute to intra-vesicular homeostasis, organelle volume, and regulation of intracellular water transport (Gonen and Walz, 2006); and, 3) Aquaporins, which are primarily only permeable to water (Badaut et al., 2002; Yang et al., 2009).

There are many different subtypes of the aquaporin channels, of which AQP1, AQP4 and AQP9 have been found to be expressed in the brain. Of these three, AQP4 has been studied extensively in the context of injury, edema, epilepsy and disease (Lee et al., 2004; Binder et al., 2006b; Hsu et al., 2007; Fukuda et al., 2012; Hubbard et al., 2013). Expression of AQP4 is predominantly found in Muller cells and astrocytes, where it is mainly localized to the pial surface, the vitreous body, and in the endfeet near the blood vessels under normal physiological conditions (Nagelhus et al., 2002; Oshio et al., 2004). Aquaporin-4 has been shown to colocalize with the potassium channel Kir4.1 and TRPV4 (Benfenati et al., 2011). During activity-dependent K^+ redistribution, water flux through these channels follows the osmotic gradient. These channels are

involved in maintaining homeostasis within the brain through regulation of the extracellular ionic gradients as well as intracellular and extracellular volume. In fact, knock-out of AQP4 reduces water permeability in astrocytes (Solenov et al., 2002; Nicchia et al., 2003).

Astrocytic mechanisms of glutamate release

One hallmark of many different types of cerebral edema, including osmotic edema, is an increase in brain activity following the initial swelling of the brain tissue (Traynelis and Dingledine, 1989; Binder et al., 2004). This increase in neuronal excitability can then lead to synchronization of neuronal networks and seizures (Saly and Andrew, 1993; Mccormick and Contreras, 2001; Fellin et al., 2004). Neurons within a local network have been shown to be synchronized by slow inward currents (SICs) (also sometimes referred to as slow transient inward currents, or STCs (Kang et al., 2005b)) within the hippocampus, and are produced by glutamate binding to NMDA receptors (Angulo et al., 2004; Fellin et al., 2004) . At least part of this glutamate is considered to be non-synaptic in origin, implicating either ambient glutamate and/or astrocytic-dependent release of glutamate. Astrocyte-dependent glutamate release could occur through six different mechanisms: 1) glutamate exchange via the cystine-glutamate antiporter; 2) Ca^{2+}-dependent vesicular exocytosis; 3) connexin or pannexin hemichannels; 4) volume regulated anion channels (VRACs); 5) reversal of glutamate transport; and, 6) ionotropic purinergic receptors such as P2X7

(Szatkowski et al., 1990; Parpura and Haydon, 2000; Rossi et al., 2000; Mongin and Orlov, 2001; Baker et al., 2002; Duan et al., 2003; Ye et al., 2003; Fellin et al., 2006b; Liu et al., 2006; Pedersen et al., 2015). The VRAC and hemichannel-mediated release pathways will be discussed further as they may play an especially prominent role during cell volume changes.

VRACs

When cells are exposed to hypotonic solutions, outwardly rectifying Cl^- currents are activated due to opening of volume-regulated anion channels (VRACs). These channels are known by several different names: volume sensitive outwardly rectifying (VSOR) anion channels, volume-sensitive organic osmolyte and anion channels (VSOAC), volume sensitive anion channels (VSACs), and stretch activated anion channels. These channels are expressed by nearly all cells and are permeable to organic osmolytes and anions such as aspartate and glutamate. For a long time, the identity of these channels remained elusive. However, recently two groups independently identified one of the family members from the (LRRC8A-E), which are distantly related to pannexins, as a possible candidate for VRACs. The protein leucine-rich repeat containing 8A (LRRC8A) was identified as the likely pore-forming subunit of VRAC (Qiu et al., 2014; Voss et al., 2014).

The VRACs have traditionally been thought to be activated by cell swelling. However, VRACs can be activated in a number of different ways,

thereby releasing a variety of different organic osmolytes, including glutamate (Pedersen et al., 2015). Research by Nilius and colleagues determined the full permeability sequence as follows: SCN^- > I^- > $NO3^-$ > Br^- > HCO_3^- > glycine > F^- > taurine > lactate > gluconate > glutamate > aspartate (Nilius et al., 1994, 1997; Nilius and Droogmans, 2001, 2003). The ways in which VRACs may be activated are as follows: 1) when intracellular ionic strength is reduced; 2) during astrocytic swelling; 3) apoptotic stimuli; 4) purinergic signaling; and 5) bradykinin receptor signaling (Wang et al., 1996; Nilius et al., 1998; Voets et al., 1999; Maeno et al., 2000; Sabirov et al., 2000; Akita et al., 2011). Neuronal SICs are thought to be induced by astrocytic release of glutamate potentially through VRACs, but the significance of this observation in regard to seizure induction and the ictal discharge is not fully understood (Zhang et al., 2011).

Gap junctions/Hemichannels

Gap junctions form pores between cells to mediate cytoplasm-to-cytoplasm communication. A family of proteins called connexins (Cxs) form gap junctions channels in vertebrates. Astrocytes express Cx30, Cx43, and possibly Cx26, with Cx43 being the most prevalent (Lynn et al., 2011; Wasseff and Scherer, 2011). Evidence indicates that the unpaired connexons may act as functional hemichannels that can open into the extracellular space (Stout et al., 2002). In this respect, they are considered to be a potential mechanism by which glutamate might be released from astrocytes. Ye and colleagues reported that

hippocampal astrocytes release glutamate in response to conditions with low extracellular divalent cations (Ye et al., 2003). Hemichannels are a potential mechanism by which astrocytes release glutamate to generate neuronal SICs.

Excitatory receptors in the CA1 region of the hippocampus

Glutamate is the main excitatory neurotransmitter in the central nervous system (Fonnum, 1984; Meldrum, 2000). Release of glutamate from presynaptic terminals acts on both metabotropic and ionotropic glutamate receptors (Nakanishi, 1994; Gao et al., 2000). N-methyl-D-aspartate (NMDA) and α-amino-3-hydroxy-5-methyl-4-isoxazolepropionic acid (AMPA) receptors are both ionotropic glutamate receptors located throughout the brain and within the hippocampus (Dingledine et al., 1999; Gao et al., 2000).

Briefly, AMPA receptors are generally considered to mediate fast synaptic transmission within the central nervous system. Each AMPA receptor has four binding sites for glutamate, and when activated is permeable to sodium and potassium ions. Some receptor channels also exhibit high calcium permeability depending on the subunit composition (Mahanty and Sah, 1998; Liu and Cull-candy, 2000). Influx of sodium through AMPA receptors depolarizes the cell membrane producing EPSPs and possibly action potentials depending on the amount and duration of the depolarization.

The NMDA receptors are important for synaptic transmission and plasticity, and have been extensively studied in the context of long-term

potentiation and learning and memory (Shen and Linden, 2005). NMDA receptors are both ligand- and voltage-gated channels. The voltage dependency of NMDA receptors is due to blockade of the receptor channel by magnesium ions at negative membrane potentials (Flatman et al., 1983; Mayer et al., 1984). After the neuron depolarizes sufficiently to remove magnesium block, then the receptor can be activated when glutamate binds along with its co-agonist, glycine or d-serine. Unlike AMPA receptors, the NMDA receptor ion channels are highly permeable to calcium, in addition to sodium and potassium. NMDA receptors can be located extrasynaptically and within the synapse, forming a heterotetramer composed of multiple subunits. Glutamate release from astrocytes during swelling, ambient glutamate concentration increasing during reduction of the ECS, or a combination of both may activate the NMDA receptors to produce SICs.

Purpose of this research/dissertation

Among local networks of neurons, SICs have been found to synchronize and depolarize neurons above firing threshold, which has brought about the idea that they may have a role in epilepsy (Kang et al., 2005b; Tian et al., 2005; Fellin et al., 2006a; Wetherington et al., 2008). Furthermore, SICs might play an important role in the ictal part of a seizure (Angulo et al., 2004; Fellin et al., 2004; Gómez-Gonzalo et al., 2010). However, the specific cellular contributions to the neuronal excitability, and the identity of the cells involved in swelling are

minimally understood due to the lack of tools and techniques to isolate astrocytic contributions from neuronal ones. The purpose of the experiments in this dissertation was to further investigate and understand the cellular mechanisms of neuronal excitability during osmotic edema.

All of the experiments done in these chapters were originally completed with the idea in mind that hypoosmolar solutions were only capable of swelling astrocytes but not neurons. Volume imaging experiments of neurons and astrocytes during elevated potassium, oxygen glucose deprivation, and hypoosmolar insults by other researchers noted neuronal and astrocytic swelling during elevated potassium and oxygen glucose deprivation. However, during hypoosmolar insults only astrocytes were reported to swell (Andrew et al., 2007b; Risher et al., 2009a).Thus, the central hypothesis of this research was that astrocytic swelling contributes to the generation of epileptiform activity by releasing glutamate through volume regulated anion channels (VRAC). We further proposed that astrocytic glutamate contributes to seizures by activating neuronal extrasynaptic NMDA receptors, producing slow inward currents (SICs). In order to test our central hypothesis, we used a hypoosmolar solution to swell astrocytes and measure neuronal activity under varying conditions. However, our laboratory discovered within the first couple of months of this year (2015) that the hypoosmolar solution also swelled neurons, confounding interpretation of the effects of our model of osmotic edema. Despite this caveat, the experiments still

reveal important insights into the effects of osmotic edema on neuronal excitability while challenging the prevailing dogma in the field.

References

Abdullaev IF, Rudkouskaya A, Schools GP, Kimelberg HK, Mongin A a (2006) Pharmacological comparison of swelling-activated excitatory amino acid release and Cl- currents in cultured rat astrocytes. J Physiol 572:677–689.

Aghajanian GK, Rasmussen K (1989) Intracellular Studies in the Facial Nucleus Illustrating a Simple New Method for Obtaining Viable Motoneurons in Adult Rat Brain Slices. Synapse 338:331–338.

Akita T, Fedorovich S V, Okada Y (2011) Cellular Physiology and Biochemistr y Biochemistry Ca 2 + Nanodomain-Mediated Component of Swelling-Induced Volume-Sensitive Outwardly Rectifying Anion Current Triggered by Autocrine Action of ATP in Mouse Astrocytes. Cell Physiol Biochem.

Alarcon G, Valentin A (2010) Mesial temporal lobe epilepsy with hippocampal sclerosis. In: Atlas of Epilepsies. 1ed. (Panayiotopoulos CP, ed). SpringerLink.

Anderson CM, Swanson RA (2000) Astrocyte Glutamate Transport : Review of Properties , Regulation , and Physiological Functions. Glia 32:1–14.

Andrew RD, Fagan M, Ballyk B a, Rosen a S (1989a) Seizure susceptibility and the osmotic state. Brain Res 498:175–180.

Andrew RD, Fagan M, Ballyk B a, Rosen a S (1989b) Seizure susceptibility and the osmotic state. Brain Res 498:175–180.

Andrew RD, Labron MW, Boehnke SE, Carnduff L, Kirov S a (2007a) Physiological evidence that pyramidal neurons lack functional water channels. Cereb Cortex 17:787–802.

Andrew RD, Labron MW, Boehnke SE, Carnduff L, Kirov SA (2007b) Physiological Evidence That Pyramidal Neurons Lack Functional Water Channels. Cereb Cortex 17:787–802.

Andrew RD, Lobinowich ME, Osehobo EP (1997) Evidence against volume regulation by cortical brain cells during acute osmotic stress. Exp Neurol 143:300–312.

Andrew RD, MacVicar B a (1994) Imaging cell volume changes and neuronal excitation in the hippocampal slice. Neuroscience 62:371–383.

Angulo MC, Kozlov AS, Charpak S, Audinat E (2004) Glutamate released from glial cells synchronizes neuronal activity in the hippocampus. J Neurosci 24:6920–6927.

Arabadzisz D, Antal K, Parpan F, Emri Z, Fritschy J-M (2005) Epileptogenesis and chronic seizures in a mouse model of temporal lobe epilepsy are associated with distinct EEG patterns and selective neurochemical alterations in the contralateral hippocampus. Exp Neurol 194:76–90.

Araque A, Carmignoto G, Haydon PG, Oliet SHR, Robitaille R, Volterra A (2014) Gliotransmitters travel in time and space. Neuron 81:728–739.

Araque A, Sanzgiri RP, Parpura V, Haydon PG (1998) Calcium elevation in astrocytes causes an NMDA receptor-dependent increase in the frequency of miniature synaptic currents in cultured hippocampal neurons. J Neurosci 18:6822–6829.

Aronica E, Vliet EA Van, Mayboroda OA, Troost D, Lopes FH, Gorter JA (2000) Upregulation of metabotropic glutamate receptor subtype mGluR3 and mGluR5 in reactive astrocytes in a rat model of mesial temporal lobe epilepsy. 12:2333–2344.

Auzmendi J, González N, Girardi E (2008) The NMDAR Subunit NR2B Expression is Modified in Hippocampus after Repetitive Seizures. Neurochem Res 34:819–826.

Azouz R, Alroy G, Yaari Y (1997) Modulation of endogenous firing patterns by osmolarity in rat hippocampal neurones. :175–187.

Badaut J, Lasbennes F, Magistretti PJ, Regli L (2002) Aquaporins in brain: distribution, physiology, and pathophysiology. J Cereb Blood Flow Metab 22:367–378.

Baker DA, Xi Z, Shen H, Swanson CJ, Kalivas PW (2002) The Origin and Neuronal Function of In Vivo Nonsynaptic Glutamate. J Neurosci 22:9134–9141.

Ballyk BA, Quackenbush SJ, Andrew RD (1991) Osmotic Effects on the CA1 Neuronal Population in Hippocampal Slices with Special Reference to Glucose. J Neurophysiol 65.

Bardutzky J, Schwab S (2007) Antiedema therapy in ischemic stroke. Stroke 38:3084–3094.

Benfenati V, Caprini M, Dovizio M, Mylonakou MN, Ferroni S, Ottersen OP, Amiry-Moghaddam M (2011) An aquaporin-4/transient receptor potential vanilloid 4 (AQP4/TRPV4) complex is essential for cell-volume control in astrocytes. Proc Natl Acad Sci 108:2563–2568.

Bikson M, Hahn PJ, Fox JE, Jefferys JGR (2003) Depolarization block of neurons during maintenance of electrographic seizures. J Neurophysiol 90:2402–2408.

Binder DK, Auser CS, Words KEY (2006a) Functional Changes in Astroglial Cells in Epilepsy. 368:358–368.

Binder DK, Papadopoulos MC, Haggie PM, Verkman a S (2004) In vivo measurement of brain extracellular space diffusion by cortical surface photobleaching. J Neurosci 24:8049–8056.

Binder DK, Yao X, Zador Z, Sick TJ, Verkman AS (2006b) Increased Seizure Duration and Slowed Potassium Kinetics in Mice Lacking Aquaporin-4 Water Channels. 636:631–636.

Boulton AA, Baker GB, Walz W eds. (1992) Neuromethods Practical Cell Culture Techniques. Totowa, New Jersey: Humana Press Inc.

Bouzat P, Sala N, Payen J-F, Oddo M (2013) Beyond intracranial pressure: optimization of cerebral blood flow, oxygen, and substrate delivery after traumatic brain injury. Ann Intensive Care 3:23.

Bowens NH, Dohare P, Kuo Y, Mongin AA (2013) DCPIB , the Proposed Selective Blocker of Volume-Regulated Anion Channels , Inhibits Several Glutamate Transport Pathways in Glial Cells s. :22–32.

Campbell SL, Hablitz JJ (2004) Glutamate transporters regulate excitability in local networks in rat neocortex. Neuroscience 127:625–635.

Carey H V, Andrews MT, Martin SL (2003) Mammalian Hibernation : Cellular and Molecular Responses to Depressed Metabolism and Low Temperature. :1153–1181.

Chebabo SR, Hester M a, Aitken PG, Somjen GG (1995a) Hypotonic exposure enhances synaptic transmission and triggers spreading depression in rat hippocampal tissue slices. Brain Res 695:203–216.

Chebabo SR, Hester MA, Jing J, Aitken PG, Somjen GG (1995b) Interstitial space , electrical resistance and ion concentrations during hypotonia of rat hippocampal slices. J Physiol:685–697.

Cocatre-Zilgien JH, Delcomyn F (1992) Identification of bursts in spike trains. J Neurosci Methods 41:19–30.

Coles JA, Orkand RK (1983) Modification of potassium movement through the retina of the drone (Apis Mellifera) by glial uptake. J Physiol 340:157–174.

Collingridge GL (1995) The brain slice preparation : a tribute to the pioneer Henry Mcllfwain. 59:5–9.

Czeh G, Kriz N, Sykovat E (1981) Extracellular potassium accumulation in the frog spinal cord induced by stimulation of the skin and ventrolateral columns. J Physiol:57–72.

Danysz W, Parsons CG (1998) Glycine and N-Methyl-D-Aspartate Receptors: Physiological Significance and Possible Therapeutic Applications. Pharmacol Rev 50.

Delaney AJ, Power JM, Sah P (2012) Ifenprodil reduces excitatory synaptic transmission by blocking presynaptic P/Q type calcium channels. J Neurophysiol 107:1571–1575.

Desagher S, Glowinski J, Premont J (1997) Pyruvate Protects Neurons against Hydrogen Peroxide-Induced Toxicity. J Neurosci 17:9060–9067.

Diamond JS (2005) Deriving the Glutamate Clearance Time Course from Transporter Currents in CA1 Hippocampal Astrocytes : Transmitter Uptake Gets Faster during Development. 25:2906–2916.

Ding S, Fellin T, Zhu Y, Lee S-Y, Auberson YP, Meaney DF, Coulter D a, Carmignoto G, Haydon PG (2007) Enhanced astrocytic Ca2+ signals contribute to neuronal excitotoxicity after status epilepticus. J Neurosci 27:10674–10684.

Dingledine R, Borges K, Bowie D, Traynelis SF (1999) The glutamate receptor ion channels. Pharmacol Rev 51:7–61.

Dingledine R, Hynes MA, King GL (1986) Involvement of N-methyl-D-aspartate receptors in epileptiform bursting in the rat hippocampal slice. J Physiol 380:175–189.

Djukic B, Casper KB, Philpot BD, Chin L-S, McCarthy KD (2007) Conditional knock-out of Kir4.1 leads to glial membrane depolarization, inhibition of potassium and glutamate uptake, and enhanced short-term synaptic potentiation. J Neurosci 27:11354–11365.

Duan S, Anderson CM, Keung EC, Chen Y, Chen Y, Swanson RA (2003) P2X 7 Receptor-Mediated Release of Excitatory Amino Acids from Astrocytes. J Neurosci 23:1320–1328.

Dudek FE, Obenaus a, Tasker JG (1990) Osmolality-induced changes in extracellular volume alter epileptiform bursts independent of chemical synapses in the rat: importance of non-synaptic mechanisms in hippocampal epileptogenesis. Neurosci Lett 120:267–270.

Dudek FE, Patrylo PR, J.P. W (1999) Mechanisms of neuronal synchronization during epileptiform activity. Adv Neurol 79:699–708.

Duffy S, Labrie V, Roder JC (2008) D-serine augments NMDA-NR2B receptor-dependent hippocampal long-term depression and spatial reversal learning. Neuropsychopharmacology 33:1004–1018.

During MJ, D SD (1993) Extracellular hippocampal glutamate and spontaneous seizure in the conscious human brain. Lancet 341:1607–1610.

Eid T, Kovacs I, Spencer DD, Lanerolle NC De (2002) Novel expression of AMPA-receptor subunit GluR1 on mossy cells and CA3 pyramidal neurons in the human epileptogenic hippocampus. Eur J Neurosci 15.

Eid T, Lee T-SW, Thomas MJ, Amiry-Moghaddam M, Bjørnsen LP, Spencer DD, Agre P, Ottersen OP, de Lanerolle NC (2005) Loss of perivascular aquaporin 4 may underlie deficient water and K+ homeostasis in the human epileptogenic hippocampus. Proc Natl Acad Sci U S A 102:1193–1198.

Ellender TJ, Harwood J, Kosillo P, Capogna M, Bolam JP (2013) Heterogeneous properties of central lateral and parafascicular thalamic synapses in the striatum. J Physiol 591:257–272.

Elmslie KS, Yoshikami D (1985) Effects of Kynurenate on Root Potentials Evoked by Synaptic Activity and Amino Acids in the Frog Spinal Cord. Brain Res 330:265–272.

Fedorff S ed. (2012) Astrocytes Pt 3: Biochemistry, Phyisiology, and Pharmacology of Astrocytes, 3rd ed. Elsevier.

Fedoroff S, Vernadakis A eds. (1986) Astrocytes Development, Morphology, and Regional Specialization of Astrocytes. London: Academic Press Inc.

Fellin T, Gomez-Gonzalo M, Gobbo S, Carmignoto G, Haydon PG (2006a) Astrocytic glutamate is not necessary for the generation of epileptiform neuronal activity in hippocampal slices. J Neurosci 26:9312–9322.

Fellin T, Pascual O, Gobbo S, Pozzan T, Haydon PG, Carmignoto G (2004) Neuronal synchrony mediated by astrocytic glutamate through activation of extrasynaptic NMDA receptors. Neuron 43:729–743.

Fellin T, Pozzan T, Carmignoto G (2006b) Purinergic receptors mediate two distinct glutamate release pathways in hippocampal astrocytes. J Biol Chem 281:4274–4284.

Fernández M, Lao-Peregrín C, Martín ED (2010) Flufenamic acid suppresses epileptiform activity in hippocampus by reducing excitatory synaptic transmission and neuronal excitability. Epilepsia 51:384–390.

Fiacco T a, McCarthy KD (2004) Intracellular astrocyte calcium waves in situ increase the frequency of spontaneous AMPA receptor currents in CA1 pyramidal neurons. J Neurosci 24:722–732.

Fiacco TA, Agulhon C, Taves SR, Petravicz J, Casper KB, Dong X, Chen J, McCarthy KD (2007a) Selective stimulation of astrocyte calcium in situ does not affect neuronal excitatory synaptic activity. Neuron 54:611–626.

Fiacco TA, Agulhon C, Taves SR, Petravicz J, Casper KB, Dong X, Chen J, McCarthy KD (2007b) Selective Stimulation of Astrocyte Calcium In Situ Does Not Affect Neuronal Excitatory Synaptic Activity. Neuron 54:611–626.

Fishman RA (1975) Brain edema. N Engl J Med 293:706–711.

Flatman JA, Schwindt PC, Crill WE, Stafstrom CE (1983) Multiple actions of N-methyl-D-aspartate on cat neocortical neurons in vitro. Brain Res 266:169–173.

Fonnum F (1984) Glutamate: A Neurotransmitter in Mammalian Brain. J Neurochem.

Frasca A, Aalbers M, Frigerio F, Fiordaliso F, Salio M, Gobbi M, Cagnotto A, Gardoni F, Battaglia GS, Hoogland G, Di Luca M, Vezzani A (2011) Misplaced NMDA receptors in epileptogenesis contribute to excitotoxicity. Neurobiol Dis 43:507–515.

Fukuda a M, Pop V, Spagnoli D, Ashwal S, Obenaus a, Badaut J (2012) Delayed increase of astrocytic aquaporin 4 after juvenile traumatic brain injury: possible role in edema resolution? Neuroscience 222:366–378.

Gao X, Sakai K, Roberts RC, Ph D, Conley RR, Dean B, Tamminga CA (2000) Ionotropic Glutamate Receptors and Expression of N-Methyl-D-Aspartate Receptor Subunits in Subregions of Human Hippocampus: Effects of Schizophrenia. Am J Psychiatry 157:1141–1149.

Gill MB, Frausto S, Ikoma M, Sasaki M, Oikawa M, Sakai R, Swanson GT (2010) A series of structurally novel heterotricyclic alpha-amino-3-hydroxyl-5-methyl-4-isoxazole-propionate receptor-selective antagonists. Br J Pharmacol 160:1417–1429.

Gómez-Gonzalo M, Losi G, Chiavegato A, Zonta M, Cammarota M, Brondi M, Vetri F, Uva L, Pozzan T, de Curtis M, Ratto GM, Carmignoto G (2010) An

excitatory loop with astrocytes contributes to drive neurons to seizure threshold. PLoS Biol 8:e1000352.

Gonen T, Walz T (2006) The structure of aquaporins. Q Rev Biophys 39:361–396.

Gray WP, Sundstrom LR (1998) Kainic acid increases the proliferation of granule cell progenitors in the dentate gyrus of the adult rat. Brain Res:52–59.

Green JD (1969) The hippocampus. Physiol Rex 44:561–608.

Gunnarson E, Song Y, Kowalewski JM, Brismar H, Brines M, Cerami A, Andersson U, Zelenina M, Aperia A (2009) Erythropoietin modulation of astrocyte water permeability as a component of neuroprotection. Proc Natl Acad Sci U S A 106:1602–1607.

Gunnarson E, Zelenina M, Axehult G, Song Y, Bondar A, Krieger P, Brismar H, Zelenin S, Aperia A (2008) Identification of a molecular target for glutamate regulation of astrocyte water permeability. Glia 56:587–596.

Hackett PH, Roach RC (2001) High-altitude illness. N Engl J Med 345:107–114.

Haglund MM, Hochman DW (2005) Furosemide and mannitol suppression of epileptic activity in the human brain. J Neurophysiol 94:907–918.

Hamann S, Herrera-Perez JJ, Zeuthen T, Alvarez-Leefmans FJ (2010) Cotransport of water by the Na+-K+-2Cl(-) cotransporter NKCC1 in mammalian epithelial cells. J Physiol 588:4089–4101.

Han D, Sun M, He P-P, Wen L-L, Zhang H, Feng J (2015) Ischemic Postconditioning Alleviates Brain Edema After Focal Cerebral Ischemia Reperfusion in Rats Through Down-Regulation of Aquaporin-4. J Mol Neurosci.

Harris AZ, Pettit DL (2007) Extrasynaptic and synaptic NMDA receptors form stable and uniform pools in rat hippocampal slices. J Physiol 584:509–519.

Harris KD, Hirase H, Leinekugel X, Henze DA (2001) Temporal Interaction between Single Spikes and Complex Spike Bursts in Hippocampal Pyramidal Cells. 32:141–149.

Haskew-Layton RE, Rudkouskaya A, Jin Y, Feustel PJ, Kimelberg HK, Mongin A a (2008) Two distinct modes of hypoosmotic medium-induced release of excitatory amino acids and taurine in the rat brain in vivo. PLoS One 3:e3543.

Heinemann U, Franceschetti B, Hamon S, Konnerth A, Yaari Y (1985) Effects of anticonvulsants on spontaneous epileptiform activity which develops in the absence of chemical synaptic transmission in hippocampal slices. Brain Res 325:349–352.

Heinemann UWE, Lux HD (1977) Ceiling of stimulus induced rises in extracellular potassium concentraion in the cerebral cortex of cat. Brain Res 120:231–249.

Heldmaier G, Ruf T (1992) Body temperature and metabolic rate during natural hypothermia in endotherms. :696–706.

Helmchen F, Svoboda K, Denk W, Tank DW, Spring C, Harbor CS, York N (1999) In vivo dendritic calcium dynamics in deep-layer cortical pyramidal neurons.

Hemphill JC, Knudson MM, Derugin N, Morabito D, Manley GT (2001) Carbon dioxide reactivity and pressure autoregulation of brain tissue oxygen. Neurosurgery 48:377–384.

Henshall DC, Meldrum BS (2012) Cell death and survival mechanisms after single and repeated brief seizures. In: Jasper's basic mechanisms of the epilepsies. 4th edn. Bethesda, MD: Oxford University Press.

Hinterkeuser S, Schröder W, Hager G, Seifert G, Blümcke I, Elger CE, Schramm J, Steinhäuser C (2000) Astrocytes in the hippocampus of patients with temporal lobe epilepsy display changes in potassium conductances. Eur J Neurosci 12:2087–2096.

Hirrlinger PG, Wurm A, Hirrlinger J, Bringmann A, Reichenbach A (2008) Osmotic swelling characteristics of glial cells in the murine hippocampus, cerebellum, and retina in situ. J Neurochem 105:1405–1417.

Hirtz D, Thurman DJ, Mohamed M (2007) How common are the " common " neurologic disorders ?

Ho M-L, Rojas R, Eisenberg RL (2012) Cerebral edema. AJR Am J Roentgenol 199:W258–73.

Hsu MS, Lee DJ, Binder DK (2007) Potential role of the glial water channel aquaporin-4 in epilepsy. Neuron Glia Biol:287–297.

Huang R, Bossut DF, Somjen GG (1997) Enhancement of Whole Cell Synaptic Currents by Low Osmolarity and by Low [NaCl] in Rat Hippocampal Slices. :2349–2359.

Hubbard J a, Hsu MS, Fiacco T a, Binder DK (2013) Glial cell changes in epilepsy: overview of the clinical problem and therapeutic opportunities. Neurochem Int 63:638–651.

Hyzinski-García MC, Vincent MY, Haskew-Layton RE, Dohare P, Keller RW, Mongin A a (2011) Hypo-osmotic swelling modifies glutamate-glutamine cycle in the cerebral cortex and in astrocyte cultures. J Neurochem 118:140–152.

Igelmund P (1995) Modulation of synaptic transmission at low temperatures by hibernation related changes in ionic microenvironment in hippocampal slices of golden hamsters.pdf. Cryobiology 32:334–343.

Igelmund P, Heinemann U (1995) Synaptic transmission and paired-pulse behaviour of CA1 pyramidal cells in hippocampal slices from a hibernator at low temperature : importance of ionic environment. 689:9–20.

Jabs R, Seifert G, Steinhäuser C (2008) Astrocytic function and its alteration in the epileptic brain. Epilepsia 49 Suppl 2:3–12.

Jensen FE, Wang C, Stafstrom CE, Liu Z, Geary C, Stevens MC, Rakhade SN, Fitzgerald EF, Klein PM, Zhou C, Sun H, Richard L, Jensen FE, Jun HY, Yeom Y Il, Park SH, Kim KH, Shin H, Kim D (2015) Acute and Chronic Increases in Excitability in Rat Hippocampal Slices After Perinatal Hypoxia In Vivo Acute and Chronic Increases in Excitability in Rat Hippocampal Slices After Perinatal Hypoxia In Vivo. :73–81.

Jensen MS, Yaari Y (1988) The Relationshp Between Interictal and Ictal Paroxysms in an In Vitro Model o f rocal Hippocampal kpuepsy. :591–598.

Jensen MS, Yaari Y (1997) Role of Intrinsic Burst Firing , Potassium Accumulation , and Electrical Coupling in the Elevated Potassium Model of Hippocampal Epilepsy.

Jones RS, Heinemann U (1988) Synaptic and intrinsic responses of medial entorhinal cortical cells in normal and magnesium-free medium in vitro. J Neurophysiol 59:1476–1496.

Kahle KT, Gerzanich V, Simard JM (2010) Molecular mechanisms of microvascular failure in CNS injury - synergistic roles of NKCC1 and SUR1/TRPM4. J Neurosurg 113:622–629.

Kang N, Xu J, Xu Q, Nedergaard M, Kang J (2005a) Astrocytic Glutamate Release-Induced Transient Depolarization and Epileptiform Discharges in Hippocampal CA1 Pyramidal Neurons. J Neurophysiol 94:4121–4130.

Kang N, Xu J, Xu Q, Nedergaard M, Kang J (2005b) Astrocytic glutamate release-induced transient depolarization and epileptiform discharges in hippocampal CA1 pyramidal neurons. J Neurophysiol 94:4121–4130.

Kempski O, Staub F, Jansen M, Baethmann A (1990) Molecular mechanisms of glial cell swelling in acidosis. Adv Neurol 52:39–45.

Kettenmann H, Orkand RK, Schachner M (1983) Coupling among identified cells in mammalian nervous system cultures. J Neurosci 3:506–516.

Kilb W, Dierkes PW, Syková E, Vargová L, Luhmann HJ (2006) Hypoosmolar conditions reduce extracellular volume fraction and enhance epileptiform activity in the CA3 region of the immature rat hippocampus. J Neurosci Res 84:119–129.

Kim HG, Connors BW (1993) Apical Dendrites of the Neocortex : Correlation between Sodium- Spiking and Pyramidal Cell Morphology. 13.

Kimelberg HK (2004a) Water homeostasis in the brain: basic concepts. Neuroscience 129:851–860.

Kimelberg HK (2004b) Increased release of excitatory amino acids by the actions of ATP and peroxynitrite on volume-regulated anion channels (VRACs) in astrocytes. 45:511–519.

Kimelberg HK (2004c) The problem of astrocyte identity. Neurochem Int 45:191–202.

Kimelberg HK (2005) Astrocytic swelling in cerebral ischemia as a possible cause of injury and target for therapy. Glia 50:389–397.

Kimelberg HK, Biddlecome S, S BR (1979a) SITS-inhibitable Cl- transport and Na+-dependent H+ production in primary astroglial cultures. Brain Res 173:11–124.

Kimelberg HK, Bourke RS (1982) Chemical and Cellular Architecture (Lajtha A, ed). Springer.

Kimelberg HK, Bowman C, Biddlecome S, Bourke RS (1979b) Cation transport and membrane potential properties of primary astroclial cultures form neonatl rat brains. Brain Res 177:533–550.

Kimelberg HK, Macvicar BA, Sontheimer H (2006) Anion Channels in Astrocytes : Biophysics , Pharmacology , and Function. 757:747–757.

Klatzo I (1967) Neuropathological aspects of brain edema. J Neuropathol Exp Neurol 26:1–14.

Kofuji P, Newman E a (2004) Potassium buffering in the central nervous system. Neuroscience 129:1045–1056.

Korn SJ, Giacchino JL, Chamberlin NL, Dingledine R (1987) Epileptiform Burst Activity Induced by Potassium in the Hippocampus and its Regulation by GABA-Mediated Inhibition. J Neurophysiol 57.

Kozler P, Pokorný J (2014) CT density decrease in water intoxication rat model of brain oedema. 35:608–612.

Kozler P, Riljak V, Pokorný J (2013) Both Water Intoxication and Osmotic BBB Disruption Increase Brain Water Content in Rats. 62.

Kozlov a S, Angulo MC, Audinat E, Charpak S (2006a) Target cell-specific modulation of neuronal activity by astrocytes. PNAS 103:10058–10063.

Kozlov AS, Angulo MC, Audinat E, Charpak S (2006b) Target cell-specific modulation of neuronal activity by astrocytes. PNAS 103.

Kriz N, Sykova E, Ujec E, Vyklicky L (1974) Changes of extracellular potassium concentration induced by neuronal activity in the spinal cord of the cat. J Paediatr Child Heal:1–15.

Lanerolle NC De, Eid T, Campe G Von, Kovacs I, Spencer DD, Brines M (1998) Glutamate receptor subunits GluR1 and GluR2/3 distribution shows reorganization in the human epileptogenic hippocampus. Eur J Neurosci 10:1687–1703.

Larkum ME, Zhu JJ (2002) Signaling of Layer 1 and Whisker-Evoked Ca 2 ⁒ and Na ⁒ Action Potentials in Distal and Terminal Dendrites of Rat Neocortical Pyramidal Neurons In Vitro and In Vivo. 22:6991–7005.

Lassmann H, Petsche U, Kitz K, Baran H, Sperk G, Seitelberger F, Hornykiewicz O (1984) The role of brain edema in epileptic brain damage induced by systemic kainic acid injection. Neuroscience 13:691–704.

Le Meur K, Galante M, Angulo MC, Audinat E (2007) Tonic activation of NMDA receptors by ambient glutamate of non-synaptic origin in the rat hippocampus. J Physiol 580:373–383.

Lee TS, Eid T, Mane S, Kim JH, Spencer DD, Ottersen OP, De Lanerolle NC (2004) Aquaporin-4 is increased in the sclerotic hippocampus in human temporal lobe epilepsy. Acta Neuropathol 108:493–502.

Lehmenkühler A, Syková E, Svoboda J, Zilles K, Nicholson C (1993) Extracellular space parameters in the rat neocortex and subcortical white

matter during postnatal development determined by diffusion analysis. Neuroscience 55:339–351.

Lin S-C, Bergles DE (2002) Physiological characteristics of NG2-expressing glial cells. J Neurocytol 31:537–549.

Liu H, Tashmukhamedov BA, Inoue H, Okada Y (2006) Roles of Two Types of Anion Channels in Glutamate Release from Mouse Astrocytes Under Ischemic or Osmotic Stress. 357:343–357.

Liu SJ, Cull-candy SG (2000) Synaptic activity at calcium- permeable AMPA receptors induces a switch in receptor subtype. Nature 405:1–5.

Lloyd KG, Bossi L, Morselli C, Rougier M, Loiseau H (1986) Alterations in human epilepsy. Adv Neurol 44:1033–1044.

Lynn BD, Tress O, May D, Willecke K, Nagy JI (2011) Ablation of connexin30 in transgenic mice alters expression patterns of connexin26 and connexin32 in glial cells and leptomeninges. Eur J Neurosci 34:1783–1793.

MacAulay N, Hamann S, Zeuthen T (2004) Water transport in the brain: role of cotransporters. Neuroscience 129:1031–1044.

MacVicar BA (1984) Voltage-dependent calcium channels in glial cells. Science (80-):1345–1347.

Maeno E, Ishizaki Y, Kanaseki T, Hazama A, Okada Y (2000) Normotonic cell shrinkage because of disordered volume regulation is an early prerequisite to apoptosis. PNAS.

Mahanty NK, Sah P (1998) Calcium-permeable AMPA receptors mediate long-term potentiation in interneurons in the amygdala. Nature 394:683–687.

Manley GT, Fujimura M, Ma T, Noshita N, Filiz F, Bollen a W, Chan P, Verkman a S (2000) Aquaporin-4 deletion in mice reduces brain edema after acute water intoxication and ischemic stroke. Nat Med 6:159–163.

Mares P, Mikulecká A (2009) Different effects of two N-methyl-D-aspartate receptor antagonists on seizures, spontaneous behavior, and motor performance in immature rats. Epilepsy Behav 14:32–39.

Mayer ML, Westbrook GL, Guthrie PB (1984) Voltage-dependent block by Mg2+ of NMDA responses in spinal cord neurones. Nature 309:261–263.

Mccarty NA, O'Neil RG (1992) Calcium Signaling in Cell Volume Regulation. Physiol Rev 72.

McCool BA, Lovinger DM (1995) Ifenprodil Inhibition of the 5-Hydroxytryptamine3 Receptor. Neuropharmacology 34:621–629.

Mccormick DA, Contreras D (2001) On the cellular and network bases of epileptic seizures. Annu Rev Physiol 63:815–846.

Meldrum BS (2000) Glutamate and Glutamine in the Brain Glutamate as a Neurotransmitter in the Brain : Review of Physiology and Pathology 1. 8:1007–1015.

Meldrum BS, Akbar MT, Chapman AG (1999) Glutamate receptors and transporters in genetic and acquired models of epilepsy. 36:189–204.

Miller RH, Raff MC (1984) Fibrous and protoplasmic astrocytes are biochmically and developmentally distinct. J Neurosci 4:585–592.

Mongin AA, Aksentsev SL, Orlov SN, Kyacheva ZB, Mezen NI, Fedulov AS, Konev SV (1996) Swelling-induced activation of Na+, K+, 2Cl cotransport in C6 glioma cells: kinetic properties and intracellular signaling mechanisms. Biochim Biophys Acta:229–236.

Mongin AA, Kimelberg HK (2005) ATP regulates anion channel-mediated organic osmolyte release from cultured rat astrocytes via multiple Ca2+-sensitive mechanisms. Am J Physiol Cell Physiol:204–213.

Mongin AA, Orlov SN (2001) Mechanisms of cell volume regulation and possible nature of the cell volume sensor. Pathophysiology 8:77–88.

Montero TD, Orellana J a (2015) Hemichannels: new pathways for gliotransmitter release. Neuroscience 286:45–59.

Mortazavi MM, Romeo AK, Deep A, Griessenauer CJ, Shoja MM, Tubbs RS, Fisher W (2012) Hypertonic saline for treating raised intracranial pressure: literature review with meta-analysis. J Neurosurg 116:210–221.

Mosley C a, Myers SJ, Murray EE, Santangelo R, Tahirovic Y a, Kurtkaya N, Mullasseril P, Yuan H, Lyuboslavsky P, Le P, Wilson LJ, Yepes M, Dingledine R, Traynelis SF, Liotta DC (2009) Synthesis, structural activity-relationships, and biological evaluation of novel amide-based allosteric binding site antagonists in NR1A/NR2B N-methyl-D-aspartate receptors. Bioorg Med Chem 17:6463–6480.

Murtha L a, McLeod DD, Pepperall D, McCann SK, Beard DJ, Tomkins AJ, Holmes WM, McCabe C, Macrae IM, Spratt NJ (2015) Intracranial pressure elevation after ischemic stroke in rats: cerebral edema is not the only cause, and short-duration mild hypothermia is a highly effective preventive therapy. J Cereb Blood Flow Metab 35:592–600.

Nagelhus EA, Mathiisen TM, Ottersen OP (2002) Aquaporin-4 in the central nervous system: Cellular and subcellular distribution and coexpression with KIR4.1. Neuroscience 112:921–934.

Nakanishi S (1994) Metabotropic Glutamate Receptors: Synaptic Transmission, Modulation, and Plasticity. Neuron 13:1031–1037.

Neusch C, Papadopoulos N, Müller M, Maletzki I, Winter SM, Hirrlinger J, Handschuh M, Bähr M, Richter DW, Kirchhoff F, Hülsmann S (2006) Lack of the Kir4.1 channel subunit abolishes K+ buffering properties of astrocytes in the ventral respiratory group: impact on extracellular K+ regulation. J Neurophysiol 95:1843–1852.

Nicchia GP, Frigeri A, Liuzzi GM, Svelto M (2003) Inhibition of aquaporin-4 expression in astrocytes by RNAi determines alteration in cell morphology, growth, and water transport and induces changes in ischemia-related genes. FASEB 17:1508–1510.

Nilius B, Droogmans G (2003) Amazing chloride channels: an overview. Acta Physio 177:119–147.

Nilius B, Droogmans GUY (2001) Ion Channels and Their Functional Role in Vascular Endothelium. Physiol Rev 81.

Nilius B, Eggermont J, Voets T, Buyse G, Manolopoulos V, Droogmans GUY (1997) Properties of volume-regulated anion channels in mammalian cells. Prog Biophys Mol Biol 68:69–119.

Nilius B, Oike M, Zahradnik I, Droogmans G (1994) Activation of a C1- Current by Hypotonic Volume Increase in Human Endothelial Cells. J Gen Physiol:787–805.

Nilius B, Prenen J, Droogmans G (1998) Modulation of volume-regulated anion channels by extra- and intracellular pH. J Physiol 9:742–748.

Noebels J, Avoli M, Rogawski M, Olsen R, Delgado-Escueta A eds. (2012) Jasper's Basic Mechanisms of the Epilepsies. Oxford University Press.

Oberheim NA, Wang X, Goldman S, Nedergaard M (2006) Astrocytic complexity distinguishes the human brain. Trends Neurosci 29:547–553.

Orkand RK, Nicholls JG, Kuffler SW (1966) Effect of nerve impulses on the membrane potential of glia cells in the central nervous system of amphibia. J Neurophysiol 29:788–806.

Oshio K, Binder DK, Yang B, Schecter S, Verkman a S, Manley GT (2004) Expression of aquaporin water channels in mouse spinal cord. Neuroscience 127:685–693.

Ozturk SS, Hu W eds. (2005) Cell culture technology for pharmaceutical and cell-based therapies. CRC Press.

Paoletti P, Ascher P (1994) Mechanosensitivity of NMDA Receptors in Cultured Mouse Central Neurons. Neuron 13:645–655.

Papadopoulos MC, Verkman AS (2007a) Aquaporin-4 and brain edema. Pediatr Nephrol 22:778–784.

Papadopoulos MC, Verkman AS (2007b) Aquaporin-4 and brain edema. Pediatr Nephrol 22:778–784.

Parpura V, Haydon PG (2000) Physiological astrocytic calcium levels stimulate glutamate release to modulate adjacent neurons. PNAS 97:8629–8634.

Pasantes-Morales H, Franco R, Torres-Marquez E, Hernández-Fonseca K, Ortega A (2000) Amino Acid Osmolytes in Regulatory Volume Decrease and Isovolumetric Regulation in Brain Cells: Contribution and Mechanisms. Cell Physiol Biochem:361–370.

Pasti L, Volterra A, Pozzan T, Carmignoto G (1997) Intracellular Calcium Oscillations in Astrocytes : A Highly Plastic , Astrocytes In Situ. 17:7817–7830.

Pawlak R, Melchor JP, Matys T, Skrzypiec AE, Strickland S (2005) Ethanol-withdrawal seizures are controlled by tissue plasminogen activator via modulation of NR2B-containing NMDA receptors. 102:443–448.

Pedersen SF, Klausen TK, Nilius B (2015) The identification of a volume-regulated anion channel: an amazing Odyssey. Acta Physiol (Oxf):1–14.

Petravicz J, Fiacco T a, McCarthy KD (2008) Loss of IP3 receptor-dependent Ca2+ increases in hippocampal astrocytes does not affect baseline CA1 pyramidal neuron synaptic activity. J Neurosci 28:4967–4973.

Petroff OAC, Errante LD, Rothman DL, Kim JH, Spencer DD (2002) Glutamate – glutamine Cycling in the Epileptic Human Hippocampus. Epilepsia 43:703–710.

Porter JT, McCarthy KD (1996) Hippocampal astrocytes in situ respond to glutamate released from synaptic terminals. J Neurosci 16:5073–5081.

Qiu Z, Dubin AE, Mathur J, Tu B, Reddy K, Miraglia LJ, Reinhardt J, Orth AP, Patapoutian A (2014) SWELL1, a Plasma Membrane Protein, Is an Essential Component of Volume-Regulated Anion Channel. Cell 157:447–458.

Radojevic N, Bjelogrlic B, Aleksic V, Rancic N, Samardzic M, Petkovic S, Savic S (2012) Forensic aspects of water intoxication: four case reports and review of relevant literature. Forensic Sci Int 220:1–5.

Ramos-mandujano G, Vazquez-Juarez E, Hernandez-Benitez R, Pasantes-Moreales H (2007) Thrombin Potently Enhances Swelling-Sensitive Glutamate Efflux from Cultured Astrocytes. Glia:917–925.

Rauner C, Köhr G (2011) Triheteromeric NR1/NR2A/NR2B receptors constitute the major N-methyl-D-aspartate receptor population in adult hippocampal synapses. J Biol Chem 286:7558–7566.

Risher WC, Andrew RD, Kirov S a (2009a) Real-time passive volume responses of astrocytes to acute osmotic and ischemic stress in cortical slices and in vivo revealed by two-photon microscopy. Glia 57:207–221.

Risher WC, Andrew RD, Kirov SA (2009b) Real-Time Passive Volume Responses of Astrocytes to Acute Osmotic and Ischemic Stress in Cortical Slices and In Vivo Revealed by Two-Photon Microscopy. 221:207–221.

Roper SN, Obenaus a, Dudek FE (1992) Osmolality and nonsynaptic epileptiform bursts in rat CA1 and dentate gyrus. Ann Neurol 31:81–85.

Rosen AS, Andrew RD (1990) Osmotic effects upon excitability in rat neocortical slices. Neuroscience 38:579–590.

Rossi DJ, Oshima T, Attwell D (2000) Glutamate release in severe brain ischaemia is mainly by reversed uptake. Nature 403:1–6.

Rossi S, Zanier ER, Mauri I, Columbo A, Stocchetti N (2001) Brain temperature , body core temperature , and intracranial pressure in acute cerebral damage. Neurol Neurosurg Psychiatry 71:448–454.

Rungta RL, Choi HB, Tyson JR, Malik A, Dissing-Olesen L, Lin PJC, Cain SM, Cullis PR, Snutch TP, MacVicar BA (2015) The Cellular Mechanisms of Neuronal Swelling Underlying Cytotoxic Edema. Cell 161:610–621.

Sabirov RZ, Prenen J, Tomita T, Droogmans G, Nilius B (2000) Reduction of ionic strength activates single volume-regulated anion channels (VRAC) in endothelial cells. Pflugers Arch:315–320.

Saly V, Andrew RD (1993) CA3 neuron excitation and epileptiform discharge are sensitive to osmolality. J Neurophysiol 69:2200–2208.

Schwartzkroin P a, Baraban SC, Hochman DW (1998a) Osmolarity, ionic flux, and changes in brain excitability. Epilepsy Res 32:275–285.

Schwartzkroin P a., Baraban SC, Hochman DW (1998b) Osmolarity, ionic flux, and changes in brain excitability. Epilepsy Res 32:275–285.

Shelton MK, McCarthy KD (1999) Mature hippocampal astrocytes exhibit functional metabotropic and ionotropic glutamate receptors in situ. Glia 26:1–11.

Shen Y, Linden DJ (2005) Long-term potentiation of neuronal glutamate transporters. Neuron 46:715–722.

Shigetomi E, Bowser DN, Sofroniew M V, Khakh BS (2008) Two Forms of Astrocyte Calcium Excitability Have Distinct Effects on NMDA Receptor-Mediated Slow Inward Currents in Pyramidal Neurons. 28:6659–6663.

Shu Y, Duque A, Yu Y, Haider B, Mccormick DA (2007) Properties of Action-Potential Initiation in Neocortical Pyramidal Cells : Evidence From Whole Cell Axon Recordings. :746–760.

Siegel AJ (2015) Fatal Water Intoxication and Cardiac Arrest in Runners during Marathons: Prevention and Treatment Based on Validated Clinical Paradigms. Am J Med.

Sofroniew M V, Vinters H V (2010) Astrocytes: biology and pathology. Acta Neuropathol 119:7–35.

Solenov E, Watanabe H, Manley GT, Verkman a S (2004) Sevenfold-reduced osmotic water permeability in primary astrocyte cultures from AQP-4-deficient mice, measured by a fluorescence quenching method. Am J Physiol Cell Physiol 286:C426–32.

Solenov EI, Vetrivel L, Oshio K, Manley GT, Verkman AS (2002) Optical measurement of swelling and water transport in spinal cord slices from aquaporin null mice. J Neurosci Methods 113:85–90.

Somjen GG, Faas GC, Vreugdenhil M, Wadman WJ (1993) Channel shutdown: a response of hippocampal neurons to adverse environments. Brain Res 632:180–194.

Srinivasan R, Huang BS, Venugopal S, Johnston AD, Chai H, Zeng H, Golshani P, Khakh BS (2015) Ca2+ signaling in astrocytes from Ip3r2−/− mice in brain slices and during startle responses in vivo. Nat Neurosci 18.

Stockand JD, Shapiro MS eds. (2006) Ion Channels Methods and Protocols, Vol. 337. Humana Press Inc.

Stokum J a, Kurland DB, Gerzanich V, Simard JM (2014) Mechanisms of Astrocyte-Mediated Cerebral Edema. Neurochem Res.

Stout CE, Costantin JL, Naus CCG, Charles AC (2002) Intercellular calcium signaling in astrocytes via ATP release through connexin hemichannels. J Biol Chem 277:10482–10488.

Su G, Kintner DB, Flagella M, Shull GE, Sun D (2002a) Astrocytes from Na(+)-K(+)-Cl(-) cotransporter-null mice exhibit absence of swelling and decrease in EAA release. Am J Physiol Cell Physiol 282:C1147–C1160.

Su G, Kintner DB, Sun D (2002b) Contribution of Na+-K+-Cl- cotransporter to high-[K+]o -induced swelling and EAA release in astrocytes. Am J Physiol Cell Physiol 282:1136–1146.

Suter KJ, Smith BN, Dudek FE (1999) Electrophysiological Recording from Brain Slices. Methods 18:86–90.

Svoboda J, Sykova E (1991) Extracellular space volume changes in the rat spinal cord produced by nerve stimulation and peripheral injury. Brain Res 560:216–224.

Sykova E, Rothenberg S, Krekule I (1974) Changes of extracellular potassium concentration during spontaneous activity in the mesencephalic reticular formation of the rat. Brain Res 79:333–337.

Szatkowski M, Barbour B, Attwell D (1990) Non-vesicular release of glutamate from glial cells by reversed electrogenic glutamate uptake. Nature 349.

Takano T, Kang J, Jaiswal JK, Simon SM, Lin JH-C, Yu Y, Li Y, Yang J, Dienel G, Zielke HR, Nedergaard M (2005) Receptor-mediated glutamate release from volume sensitive channels in astrocytes. PNAS 102:16466–16471.

Talan M (1984) Body temperature of C57BL/6J mice with age. Exp Gerontol 19:25–29.

Tasleem RA, Chowdhary ND (2003) Fatal water intoxication. J Clin Pathol:803–804.

Tauck DL, Nadler JV (1985) Evidence of Functional Mossy Fiber Sprouting in Hippocampal Formation of Kainic Acid-Treated Rats. J Neurosci 5:1016–1022.

Taylor CP, Dudek FE (1984) Excitation of Hippocampal Pyramidal Cells by an Electrical Field Effect. J Neurophysiol 52.

Thrane AS, Rangroo Thrane V, Nedergaard M (2014) Drowning stars: reassessing the role of astrocytes in brain edema. Trends Neurosci 37:620–628.

Tian G-F, Azmi H, Takano T, Xu Q, Peng W, Lin J, Oberheim N, Lou N, Wang X, Zielke HR, Kang J, Nedergaard M (2005) An astrocytic basis of epilepsy. Nat Med 11:973–981.

Ting JT, Daigle TL, Chen Q, Feng G (2014) Acute brain slice methods for adult and aging animals: application of targeted patch clampanalysis and optogenetics Martina M, Taverna S, eds. Methods Mol Biol 1183:1–21.

Tovar KR, McGinley MJ, Westbrook GL (2013) Triheteromeric NMDA receptors at hippocampal synapses. J Neurosci 33:9150–9160.

Traynelis SF, Dingledine R (1988) Potassium-induced spontaneous electrographic seizures in the rat hippocampal slice. J Neurophysiol 59:259–276.

Traynelis SF, Dingledine R (1989) Role of extracellular space in hyperosmotic suppression of potassium-induced electrographic seizures. J Neurophysiol 61:927–938.

Trotter J, Karram K, Nishiyama A (2010) NG2 cells: Properties, progeny and origin. Brain Res Rev 63:72–82.

Unterberg a W, Stover J, Kress B, Kiening KL (2004) Edema and brain trauma. Neuroscience 129:1021–1029.

Vargova L, Sykova E (2014) Astrocytes and extracellular matrix in extrasynaptic volume transmission. Phil Trans R Soc B.

Voets T, Droogmans G, Raskin G, Eggermont J, Nilius B (1999) Reduced intracellular ionic strength as the initial trigger for activation of endothelial volume-regulated anion channels. Proc Natl Acad Sci 96:5298–5303.

Voigt J, Grosche A, Vogler S, Pannicke T, Hollborn M, Kohen L, Wiedemann P, Reichenbach A, Bringmann A (2015) Nonvesicular release of ATP from rat retinal glial (Müller) cells is differentially mediated in response to osmotic stress and glutamate. Neurochem Res 40:651–660.

Volman V, Bazhenov M, Sejnowski TJ (2013) Divide and conquer: functional segregation of synaptic inputs by astrocytic microdomains could alleviate paroxysmal activity following brain trauma. PLoS Comput Biol 9:e1002856.

Voss FK, Ullrich F, Munch J, Lazarow K, Lutter D, Mah N, Andrade-Navarro MA, Kries JP, Stauber T, Jentsch TJ (2014) Identification of LRRC8 Heteromers

as an Essential Component of the Volume-Regulated Anion Channel VRAC. Science (80-) 344:634–639.

Walther H, Lambert JD, Jones RS, Heinemann U, Hamon B (1986) Epileptiform activity in combined slices of the hippocampus, subiculum and entorhinal cortex during perfusion with low magnesium medium. Neurosci Lett 69:156–161.

Walz W ed. (2007) Patch-Clamp Analysis Advanced Techniques. Totowa: Humana Press Inc.

Walz W, Hertz L (1983) Intracellular Ion Changes of Astrocytes in Response to Extracellular Potassium. J Neurosci Res 423:411–423.

Walz W, Hinks EC (1986) A Transmembrane Sodium Cycle in Astrocytes. Brain Res 368:226–232.

Wang X-M, Bausch SB (2004) Effects of distinct classes of N-methyl-D-aspartate receptor antagonists on seizures, axonal sprouting and neuronal loss in vitro: suppression by NR2B-selective antagonists. Neuropharmacology 47:1008–1020.

Wang YU, Roman R, Lidofskyt SD, Fitz JG (1996) Autocrine signaling through ATP release represents a novel mechanism for cell volume regulation. Proc Natl Acad Sci 93:12020–12025.

Wasseff SK, Scherer SS (2011) Cx32 and Cx47 mediate oligodendrocyte:astrocyte and oligodendrocyte:oligodendrocyte gap junction coupling. Neurobiol Dis 42:506–513.

Wetherington J, Serrano G, Dingledine R (2008) Astrocytes in the epileptic brain. Neuron 58:168–178.

Wong RK, Traub RD, Miles R (1986) Cellular basis of neuronal synchrony in epilepsy. Adv Neurol 44:583–592.

Yamashiro M, Hasegawa H, Matsuda A, Kinoshita M, Matsumura O, Isoda K, Mitarai T (2013) A case of water intoxication with prolonged hyponatremia caused by excessive water drinking and secondary SIADH. Case Rep Nephrol Urol 3:147–152.

Yang M, Gao F, Liu H, Yu WH, Sun SQ (2009) Temporal changes in expression of aquaporin-3, -4, -5 and -8 in rat brains after permanent focal cerebral ischemia. Brain Res 1290:121–132.

Yao X, Derugin N, Manley GT, Verkman a S (2015) Reduced brain edema and infarct volume in aquaporin-4 deficient mice after transient focal cerebral ischemia. Neurosci Lett 584:368–372.

Ye Z-C, Wyeth MS, Baltan-Tekkok S, Ransom BR (2003) Functional hemichannels in astrocytes: a novel mechanism of glutamate release. J Neurosci 23:3588–3596.

Zador Z, Stiver S, Wang V, Manley GT (2009) Role of aquaporin-4 in cerebral edema and stroke. Handb Exp Pharmacol:159–170.

Zhang H, Cao HJ, Kimelberg HK, Zhou M (2011) Volume regulated anion channel currents of rat hippocampal neurons and their contribution to oxygen-and-glucose deprivation induced neuronal death. PLoS One 6:e16803.

Zhou N, Gordon GRJ, Feighan D, MacVicar B a (2010) Transient swelling, acidification, and mitochondrial depolarization occurs in neurons but not astrocytes during spreading depression. Cereb Cortex 20:2614–2624.

Chapter 2

Measuring Neuronal Activity in a Mouse Hippocampal Slice Preparation and General Methods

2.1 Preparation Of Acute Hippocampal Slices.

All animals and protocols used in these experiments were approved by the Institutional Animal Care and Use Committee (IACUC) of the University of California, Riverside and followed the approved protocols established by the American Veterinary Medical Association. Hippocampal slices were prepared from juvenile 15-to 18-day-old, or adult 2-to-5-month-old wild-type C57BL/6J mice (Jackson Laboratory, Bay Harbor, ME). Mice were deeply anesthetized under isoflurane and decapitated. Brains were removed and placed in an ice cold slicing buffer containing (in mM): 125 NaCl, 2.5 KCl, 3.8 $MgCl_2$, 1.25 NaH_2PO_4, 26 $NaHCO_3$ 25 glucose, 1.3 ascorbic acid, and 3.5 MOPS, bubbled with 5% CO_2 + 95% O_2 (Suter et al., 1999). Parasagittal hippocampal slices (350 μm) were prepared using a Leica VT 1200S Vibratome (Bannockburn, IL) and subsequently incubated for 45 minutes at 35°C in standard ACSF, which contained the following; (in mM): 125 NaCl, 2.5 KCl, 2.5 $CaCl_2$, 1.3 $MgCl_2$, 1.25 NaH_2PO_4, 26.0 $NaHCO_3$, and 15 glucose, oxygenated with 5% CO_2 + 95% O_2, (~300 - 303 mOsm). After recovery, slices were allowed to cool to room

temperature for a minimum of 15 minutes prior to transfer to a recoding chamber that was continuously perfused with oxygenated ACSF (1 mL/min) for electrophysiological recording. (in mM): 125 NaCl, 2.5 KCl, 3.8 $MgCl_2$, 1.25 NaH_2PO_4, 26 $NaHCO_3$ 25 glucose, 1.3 ascorbic acid, and 3.5 MOPS, bubbled with 5% CO_2 + 95% O_2

For adult experiments, slices were prepared as described above, but in a modified slicing buffer containing the following (in mM): 87 NaCl, 75 sucrose 2.5 KCl, 0.5 $CaCl_2$, 7 $MgCl_2$, 1.25 NaH_2PO_4, 25 $NaHCO_3$, 10 glucose, 1.3 ascorbic, acid, 0.1 kynurenic acid, 2.0 pyruvate, and 3.5 MOPS, bubbled with 5% CO_2 + 95% O_2. The adult slicing buffer was partially frozen to form a "slushy" solution for slice preparation. Drastically improved slice health was observed in adults via this method (Stockand and Shapiro, 2006). Slices were then incubated in an adult slicing buffer at 35°C for 45 minutes. Following recovery, slices were allowed to cool to room temperature for 15 minutes, before being transferred to room temperature standard ACSF and allowed to recover for an additional 20 to 30 minutes prior to electrophysiological recordings. To study the effect of swelling on neuronal excitability, acute hippocampal slices were chosen because they maintain neuronal and astrocytic communication in the majority of the neuronal networks. In addition, the hippocampus is one the main areas within the brain associated with seizures and epilepsy (Henshall and Meldrum, 2012)

2.2 Electrophysiology Instrumentation

For patch clamp experiments, a Multiclamp 700 B Microelectrode Amplifier was used with either an Axon Digidata 1550 or an Axon Digidata 1440A Digitizer and PClamp 10.4 Software (Molecular Devices, Sunnyvale, CA). Neurons in the CA1 region of hippocampus were identified by region, morphological characteristics, resting membrane potential and characteristic voltage-dependent currents using a voltage step protocol, then patch clamped using a borosilicate patch pipette. Patch pipettes were pulled from borosilicate glass capillaries and were 3.8-5.9 MΩ when filled with neuronal internal solution containing the following (in mM): 140 K-gluconate, 4 MgCl2, 0.4 EGTA, 4 Mg-ATP, 0.2 Na-GTP, 10 HEPES, and 10 phosphocreatine, pH 7.3 with KOH (Fiacco and McCarthy, 2004). Astrocytes in the CA1 stratum radiatum (s.r) were identified first by morphology and location, and second by their characteristic electrophysiological properties. Astrocytes exhibited a low input resistance, low resting potential (-78.0 ± 1.2 mV), and lack of voltage-gated conductances during a voltage step protocol. Astrocyte patch pipettes were pulled to a resistance of 5.5-8.9 MΩ when filled with astrocyte internal solution containing the following (in mM): 130 K-gluconate, 4 MgCl2, 10 HEPES, 10 glucose, 1.185 Mg-ATP, 10.55 phosphocreatine, and 0.1315 mg/ml creatine phosphokinase, pH 7.3 by KOH. Continuous recordings for both voltage and current clamp experiments were low-pass filtered at 2 kHz and digitized at 5 kHz. All experiments were conducted at room temperature (23-26 °C) unless otherwise stated. An electronic valve

controller (Warner instrument, Hampden CT) was used to bath-apply drugs during recordings.

2.3 General Methods

Neurons in the CA1 region of the hippocampus were identified and visualized using Differential Interference Contrast (DIC) optics based on their location and characteristic morphology. We chose to study neurons within the CA1 area of the hippocampus because this area is severely affected by epilepsy resulting in neuronal cell loss and astrocytic gliosis (Alarcon and Valentin, 2010). After neurons were visually located ~ 40 to 170 μM depth for patch clamp a pressure pipette filled with neuronal internal was then lowered into the slice and used to patch onto a cell. After patching onto a cell the current profile was obtained using voltage steps protocols for astrocytes and neurons. Cells that displayed both sodium and potassium currents were considered neurons, while only cells with a passive electrophysiological phenotype were considered to be astrocytes. Figure 2.1 is a schematic diagram illustrating a hippocampal slice with the patch pipette in place along with a patched neuron and representative voltage steps of an astrocyte and a neuron. In general, CA1 hippocampal neurons were patch clamped first in standard ACSF. For experimental conditions, 'normosmolar' ACSF (nACSF) was prepared in the same way as standard ACSF, but made Mg^{2+}-free by omission of $MgCl_2$. Normosmolar ACSF

also contained the same drugs as the hypoosmolar solutions, unless indicated otherwise. 'Hypoosmolar' ACSF (hACSF) was prepared by dilution of normosmolar ACSF with deionized water (%v/v) to 5, 10, 17, or 40% (285, 270, 249, and 180 mOsm) hypoosmolar to baseline. Upon attaining the whole-cell configuration, the normosmolar ACSF was perfused for 10 minutes to remove Mg^{2+} block from NMDA receptors and obtain a baseline recording of excitatory neuronal activity. This was followed by the application of hACSF up to three times for 5, 6, and 7 minutes, with equal wash periods in normosmolar ACSF in-between hACSF applications. In voltage-clamp experiments, neurons were held at -70 mV. For the K-gluconate-based internal solution, this holding potential is equal to the reversal potential for Cl^-, effectively eliminating contribution of IPSPs to the recorded currents. The process of repeatedly applying hACSF and recording neuronal currents and potentials was valuable both for discerning pharmacological effects, as well as, deciphering the integral and dynamic changes in neuronal excitability during cell swelling, water intoxication and cerebral edema. In the experimental conditions, a variety of electrophysiology techniques and antagonists were used to either block or enhance neuronal activity.

2.4 Application of hypoosmolar ACSF and swelling evokes a complex array of currents and potentials in CA1 pyramidal neurons within the hippocampus.

Water intoxication and cerebral edema can be fatal and occur quite rapidly within the brain, not only disrupting the water and ionic homeostasis, but also neuronal excitability and synchronization leading to seizures (Traynelis and Dingledine, 1989; Binder et al., 2004). Application of hypoosmolar ACSF in situ onto brain slices of the hippocampus, in turn, not only induces cell swelling, but also increases neuronal excitability through a number of potential mechanisms. Whole cell patch clamp electrophysiology provides us with the flexibility to record from neurons in either current clamp or voltage clamp. This technique allows for the recording of action potentials and EPSPs to a number of different types of currents, thereby elucidating the potential mechanisms of neuronal excitability.

While recording from CA1 neurons in voltage clamp mode, not only were EPSPs recorded, but also action potentials, both single action potentials and bursts of action potentials. EPSP's were defined as upper deflections greater than two times the average standard deviation above the mean baseline(Ellender et al., 2013). Complex spike bursts in pyramidal cells are considered to be discrete events from single action potentials often associated with synaptic plasticity within the hippocampus and synchronization of local neuronal networks, thus these events were examined separately (Harris et al., 2001). Detection of and defining bursts of action potential has been a long-standing challenge due to

their complexity and a variety of different methods have been proposed. Action potentials were defined as a burst by two of the most common parameters: 1) a large prolonged upward deflection (depolarization) from baseline (Kim and Connors, 1993; Helmchen et al., 1999; Larkum and Zhu, 2002); 2) falling within two standard error of the inter-spike interval distribution for all cells (Cocatre-Zilgien and Delcomyn, 1992; Shu et al., 2007). Figure 2.2 displays an interspike interval histogram with the action potentials involved in bursts shown in gray**.** The single action potentials are shown in black, along with representative traces of a single action potential and a burst of action potentials.

While a number of different currents were recorded under current clamp conditions, the main focus of our research, examined slow inward currents and their role in neuronal excitability during osmotic edema and swelling. Slow inward currents (SICs) have been observed spontaneously during normal physiological conditions, but are somewhat rare (Fellin et al., 2004). However, SICs are more often studied under the context of disease, such as cerebral edema, seizures and epilepsy and may play an important role in the generation of epileptiform activity (Noebels et al., 2012). SICs were identified and distinguished from AMPA currents and mEPSCs based on their slow kinetics. The hallmarks of SICs include; 1) resistance to TTX, 2) synchrony over short distances, at least 100 μm and 3) sensitive to blockade of NMDARs (Wetherington et al., 2008). I used criteria reported by (Angulo et al., 2004; Fellin et al., 2004, 2006a) to identify

currents as SICs. Specifically, these events had to have rise times slower than 10 ms and amplitudes ≥ 20 pA.

2.4 Analysis and Statistics

The analysis and basic protocol for all experiments was as follows: 1) Recordings were alternated between control and experimental conditions; 2) Each slice was only used once, and no more than 3 cells or 3 mice from the same litter were used per n for each experiment in order to avoid potential confounds of initial precipitating swelling effects on neurons and astrocytes, or litter specific abnormalities; 3) any recording in which access resistance changed by more than 20% was discarded.

The data analysis software Clampfit 10.4 (Molecular Devices, Sunnyvale, CA) was used to analyze the amplitude, frequency, and kinetics of the neuronal potentials and currents. Statistical analysis of the events was performed using the statistical program IBM SPSS Statistics 22. Unless otherwise stated, experiments involving one experimental group were analyzed using a repeated measures ANOVA to determine significance, followed by planned post hoc tests using the Student's t-test p-values and the Holm-Bonferroni correction or Tukey's HSD for multiple comparisons. For cross-comparisons between two experimental conditions, a split plot repeated measures ANOVA was used along with planned post hoc analysis tests using the Student's t-test. In instances where the assumptions of sphericity were violated during the repeated measures ANOVA

(via Mauchly's test) analysis was completed using the Greenhouse Geyser correction. Occasionally Friedman's test was used when the assumption of normality was violated, but only in the instance where one group was being tested. Statistical significance for the p-values is as follows (* = $p < .05$), (** = $p < .01$), and (*** = $p < .001$) with n = 8 to 11 cells in all experiments, always with equal number of cells per group, unless specified otherwise.

Figure 2.1

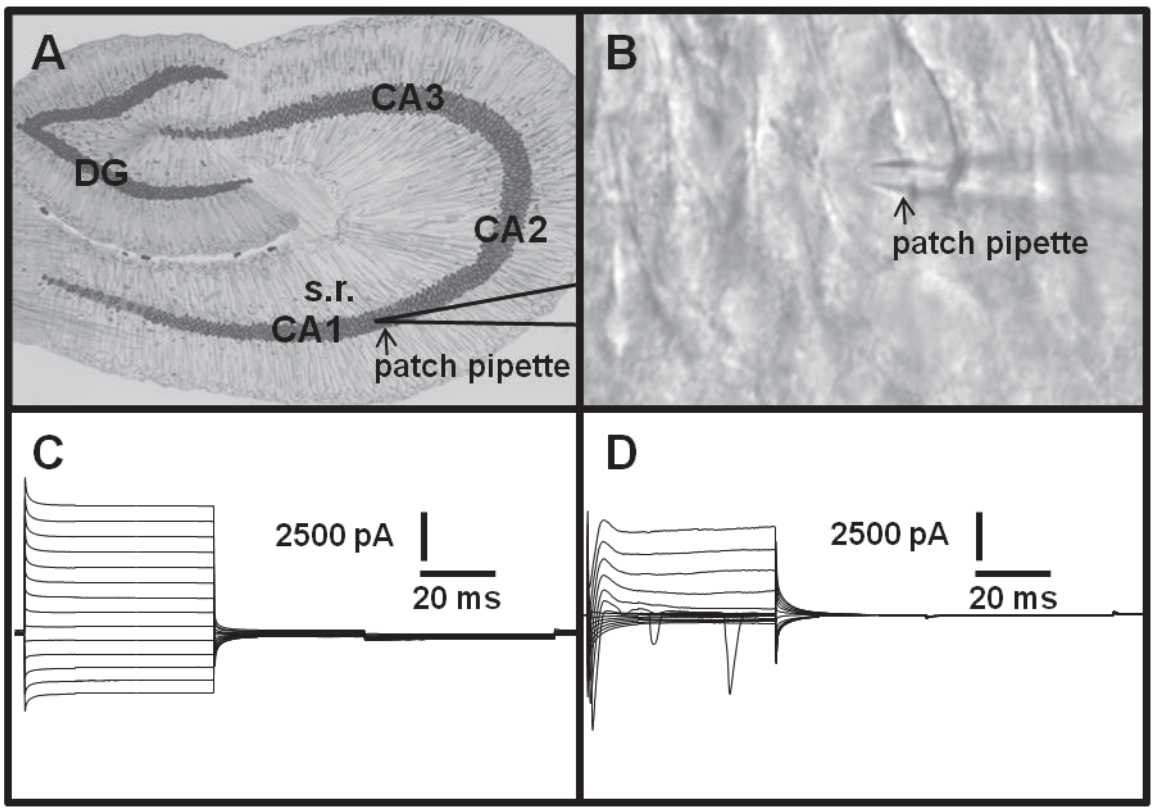

Figure 2.1: Diagram of hippocampus with patched neuron along with representative recordings of current profiles from an astrocyte and a neuron. Schematic of a parasagittal hippocampal slice showing the location of the neurons in the CA1 area being patch and the nearby s.r. area where astrocytes were recorded (A). Patch pipette attached to a pyramidal neuron in the CA1 area of the hippocampus from a brain slice (B). Representative recording from a passive astrocyte in the s.r. showing its current profile (C). Recording displaying the current profile from a CA1 pyramidal neuron (D).

Figure 2.2

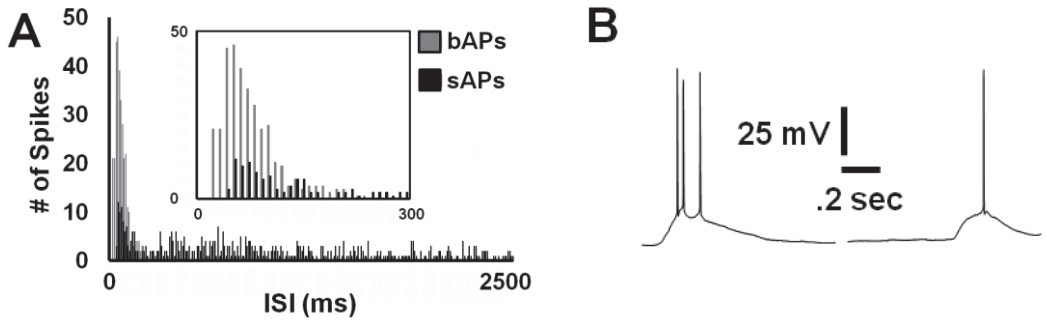

Figure 2.2: Single and bursts of action potentials classification. Interspike interval histogram of all the cells for an experimental group. ISIs for both single action potentials (black) and bursts of action potentials (gray) are shown. Insert: ISIs up to 300 ms (A). Representative burst of action potentials and single action potential from a CA1 pyramidal neuron in the hippocampus showing the characteristic prolonged depolarization of the burst (B).

References:

Abdullaev IF, Rudkouskaya A, Schools GP, Kimelberg HK, Mongin A a (2006) Pharmacological comparison of swelling-activated excitatory amino acid release and Cl- currents in cultured rat astrocytes. J Physiol 572:677–689.

Aghajanian GK, Rasmussen K (1989) Intracellular Studies in the Facial Nucleus Illustrating a Simple New Method for Obtaining Viable Motoneurons in Adult Rat Brain Slices. Synapse 338:331–338.

Akita T, Fedorovich S V, Okada Y (2011) Cellular Physiology and Biochemistr y Biochemistry Ca 2 + Nanodomain-Mediated Component of Swelling-Induced Volume-Sensitive Outwardly Rectifying Anion Current Triggered by Autocrine Action of ATP in Mouse Astrocytes. Cell Physiol Biochem.

Alarcon G, Valentin A (2010) Mesial temporal lobe epilepsy with hippocampal sclerosis. In: Atlas of Epilepsies. 1ed. (Panayiotopoulos CP, ed). SpringerLink.

Anderson CM, Swanson RA (2000) Astrocyte Glutamate Transport : Review of Properties , Regulation , and Physiological Functions. Glia 32:1–14.

Andrew RD, Fagan M, Ballyk B a, Rosen a S (1989a) Seizure susceptibility and the osmotic state. Brain Res 498:175–180.

Andrew RD, Fagan M, Ballyk B a, Rosen a S (1989b) Seizure susceptibility and the osmotic state. Brain Res 498:175–180.

Andrew RD, Labron MW, Boehnke SE, Carnduff L, Kirov S a (2007a) Physiological evidence that pyramidal neurons lack functional water channels. Cereb Cortex 17:787–802.

Andrew RD, Labron MW, Boehnke SE, Carnduff L, Kirov SA (2007b) Physiological Evidence That Pyramidal Neurons Lack Functional Water Channels. Cereb Cortex 17:787–802.

Andrew RD, Lobinowich ME, Osehobo EP (1997) Evidence against volume regulation by cortical brain cells during acute osmotic stress. Exp Neurol 143:300–312.

Andrew RD, MacVicar B a (1994) Imaging cell volume changes and neuronal excitation in the hippocampal slice. Neuroscience 62:371–383.

Angulo MC, Kozlov AS, Charpak S, Audinat E (2004) Glutamate released from glial cells synchronizes neuronal activity in the hippocampus. J Neurosci 24:6920–6927.

Arabadzisz D, Antal K, Parpan F, Emri Z, Fritschy J-M (2005) Epileptogenesis and chronic seizures in a mouse model of temporal lobe epilepsy are associated with distinct EEG patterns and selective neurochemical alterations in the contralateral hippocampus. Exp Neurol 194:76–90.

Araque A, Carmignoto G, Haydon PG, Oliet SHR, Robitaille R, Volterra A (2014) Gliotransmitters travel in time and space. Neuron 81:728–739.

Araque A, Sanzgiri RP, Parpura V, Haydon PG (1998) Calcium elevation in astrocytes causes an NMDA receptor-dependent increase in the frequency of miniature synaptic currents in cultured hippocampal neurons. J Neurosci 18:6822–6829.

Aronica E, Vliet EA Van, Mayboroda OA, Troost D, Lopes FH, Gorter JA (2000) Upregulation of metabotropic glutamate receptor subtype mGluR3 and mGluR5 in reactive astrocytes in a rat model of mesial temporal lobe epilepsy. 12:2333–2344.

Auzmendi J, González N, Girardi E (2008) The NMDAR Subunit NR2B Expression is Modified in Hippocampus after Repetitive Seizures. Neurochem Res 34:819–826.

Azouz R, Alroy G, Yaari Y (1997) Modulation of endogenous firing patterns by osmolarity in rat hippocampal neurones. :175–187.

Badaut J, Lasbennes F, Magistretti PJ, Regli L (2002) Aquaporins in brain: distribution, physiology, and pathophysiology. J Cereb Blood Flow Metab 22:367–378.

Baker DA, Xi Z, Shen H, Swanson CJ, Kalivas PW (2002) The Origin and Neuronal Function of In Vivo Nonsynaptic Glutamate. J Neurosci 22:9134–9141.

Ballyk BA, Quackenbush SJ, Andrew RD (1991) Osmotic Effects on the CA1 Neuronal Population in Hippocampal Slices with Special Reference to Glucose. J Neurophysiol 65.

Bardutzky J, Schwab S (2007) Antiedema therapy in ischemic stroke. Stroke 38:3084–3094.

Benfenati V, Caprini M, Dovizio M, Mylonakou MN, Ferroni S, Ottersen OP, Amiry-Moghaddam M (2011) An aquaporin-4/transient receptor potential vanilloid 4 (AQP4/TRPV4) complex is essential for cell-volume control in astrocytes. Proc Natl Acad Sci 108:2563–2568.

Bikson M, Hahn PJ, Fox JE, Jefferys JGR (2003) Depolarization block of neurons during maintenance of electrographic seizures. J Neurophysiol 90:2402–2408.

Binder DK, Auser CS, Words KEY (2006a) Functional Changes in Astroglial Cells in Epilepsy. 368:358–368.

Binder DK, Papadopoulos MC, Haggie PM, Verkman a S (2004) In vivo measurement of brain extracellular space diffusion by cortical surface photobleaching. J Neurosci 24:8049–8056.

Binder DK, Yao X, Zador Z, Sick TJ, Verkman AS (2006b) Increased Seizure Duration and Slowed Potassium Kinetics in Mice Lacking Aquaporin-4 Water Channels. 636:631–636.

Boulton AA, Baker GB, Walz W eds. (1992) Neuromethods Practical Cell Culture Techniques. Totowa, New Jersey: Humana Press Inc.

Bouzat P, Sala N, Payen J-F, Oddo M (2013) Beyond intracranial pressure: optimization of cerebral blood flow, oxygen, and substrate delivery after traumatic brain injury. Ann Intensive Care 3:23.

Bowens NH, Dohare P, Kuo Y, Mongin AA (2013) DCPIB , the Proposed Selective Blocker of Volume-Regulated Anion Channels , Inhibits Several Glutamate Transport Pathways in Glial Cells s. :22–32.

Campbell SL, Hablitz JJ (2004) Glutamate transporters regulate excitability in local networks in rat neocortex. Neuroscience 127:625–635.

Carey H V, Andrews MT, Martin SL (2003) Mammalian Hibernation : Cellular and Molecular Responses to Depressed Metabolism and Low Temperature. :1153–1181.

Chebabo SR, Hester M a, Aitken PG, Somjen GG (1995a) Hypotonic exposure enhances synaptic transmission and triggers spreading depression in rat hippocampal tissue slices. Brain Res 695:203–216.

Chebabo SR, Hester MA, Jing J, Aitken PG, Somjen GG (1995b) Interstitial space , electrical resistance and ion concentrations during hypotonia of rat hippocampal slices. J Physiol:685–697.

Cocatre-Zilgien JH, Delcomyn F (1992) Identification of bursts in spike trains. J Neurosci Methods 41:19–30.

Coles JA, Orkand RK (1983) Modification of potassium movement through the retina of the drone (Apis Mellifera) by glial uptake. J Physiol 340:157–174.

Collingridge GL (1995) The brain slice preparation : a tribute to the pioneer Henry Mcllfwain. 59:5–9.

Czeh G, Kriz N, Sykovat E (1981) Extracellular potassium accumulation in the frog spinal cord induced by stimulation of the skin and ventrolateral columns. J Physiol:57–72.

Danysz W, Parsons CG (1998) Glycine and N-Methyl-D-Aspartate Receptors: Physiological Significance and Possible Therapeutic Applications. Pharmacol Rev 50.

Delaney AJ, Power JM, Sah P (2012) Ifenprodil reduces excitatory synaptic transmission by blocking presynaptic P/Q type calcium channels. J Neurophysiol 107:1571–1575.

Desagher S, Glowinski J, Premont J (1997) Pyruvate Protects Neurons against Hydrogen Peroxide-Induced Toxicity. J Neurosci 17:9060–9067.

Diamond JS (2005) Deriving the Glutamate Clearance Time Course from Transporter Currents in CA1 Hippocampal Astrocytes : Transmitter Uptake Gets Faster during Development. 25:2906–2916.

Ding S, Fellin T, Zhu Y, Lee S-Y, Auberson YP, Meaney DF, Coulter D a, Carmignoto G, Haydon PG (2007) Enhanced astrocytic Ca2+ signals contribute to neuronal excitotoxicity after status epilepticus. J Neurosci 27:10674–10684.

Dingledine R, Borges K, Bowie D, Traynelis SF (1999) The glutamate receptor ion channels. Pharmacol Rev 51:7–61.

Dingledine R, Hynes MA, King GL (1986) Involvement of N-methyl-D-aspartate receptors in epileptiform bursting in the rat hippocampal slice. J Physiol 380:175–189.

Djukic B, Casper KB, Philpot BD, Chin L-S, McCarthy KD (2007) Conditional knock-out of Kir4.1 leads to glial membrane depolarization, inhibition of potassium and glutamate uptake, and enhanced short-term synaptic potentiation. J Neurosci 27:11354–11365.

Duan S, Anderson CM, Keung EC, Chen Y, Chen Y, Swanson RA (2003) P2X 7 Receptor-Mediated Release of Excitatory Amino Acids from Astrocytes. J Neurosci 23:1320–1328.

Dudek FE, Obenaus a, Tasker JG (1990) Osmolality-induced changes in extracellular volume alter epileptiform bursts independent of chemical synapses in the rat: importance of non-synaptic mechanisms in hippocampal epileptogenesis. Neurosci Lett 120:267–270.

Dudek FE, Patrylo PR, J.P. W (1999) Mechanisms of neuronal synchronization during epileptiform activity. Adv Neurol 79:699–708.

Duffy S, Labrie V, Roder JC (2008) D-serine augments NMDA-NR2B receptor-dependent hippocampal long-term depression and spatial reversal learning. Neuropsychopharmacology 33:1004–1018.

During MJ, D SD (1993) Extracellular hippocampal glutamate and spontaneous seizure in the conscious human brain. Lancet 341:1607–1610.

Eid T, Kovacs I, Spencer DD, Lanerolle NC De (2002) Novel expression of AMPA-receptor subunit GluR1 on mossy cells and CA3 pyramidal neurons in the human epileptogenic hippocampus. Eur J Neurosci 15.

Eid T, Lee T-SW, Thomas MJ, Amiry-Moghaddam M, Bjørnsen LP, Spencer DD, Agre P, Ottersen OP, de Lanerolle NC (2005) Loss of perivascular aquaporin 4 may underlie deficient water and K+ homeostasis in the human epileptogenic hippocampus. Proc Natl Acad Sci U S A 102:1193–1198.

Ellender TJ, Harwood J, Kosillo P, Capogna M, Bolam JP (2013) Heterogeneous properties of central lateral and parafascicular thalamic synapses in the striatum. J Physiol 591:257–272.

Elmslie KS, Yoshikami D (1985) Effects of Kynurenate on Root Potentials Evoked by Synaptic Activity and Amino Acids in the Frog Spinal Cord. Brain Res 330:265–272.

Fedorff S ed. (2012) Astrocytes Pt 3: Biochemistry, Phyisiology, and Pharmacology of Astrocytes, 3rd ed. Elsevier.

Fedoroff S, Vernadakis A eds. (1986) Astrocytes Development, Morphology, and Regional Specialization of Astrocytes. London: Academic Press Inc.

Fellin T, Gomez-Gonzalo M, Gobbo S, Carmignoto G, Haydon PG (2006a) Astrocytic glutamate is not necessary for the generation of epileptiform neuronal activity in hippocampal slices. J Neurosci 26:9312–9322.

Fellin T, Pascual O, Gobbo S, Pozzan T, Haydon PG, Carmignoto G (2004) Neuronal synchrony mediated by astrocytic glutamate through activation of extrasynaptic NMDA receptors. Neuron 43:729–743.

Fellin T, Pozzan T, Carmignoto G (2006b) Purinergic receptors mediate two distinct glutamate release pathways in hippocampal astrocytes. J Biol Chem 281:4274–4284.

Fernández M, Lao-Peregrín C, Martín ED (2010) Flufenamic acid suppresses epileptiform activity in hippocampus by reducing excitatory synaptic transmission and neuronal excitability. Epilepsia 51:384–390.

Fiacco T a, McCarthy KD (2004) Intracellular astrocyte calcium waves in situ increase the frequency of spontaneous AMPA receptor currents in CA1 pyramidal neurons. J Neurosci 24:722–732.

Fiacco TA, Agulhon C, Taves SR, Petravicz J, Casper KB, Dong X, Chen J, McCarthy KD (2007a) Selective stimulation of astrocyte calcium in situ does not affect neuronal excitatory synaptic activity. Neuron 54:611–626.

Fiacco TA, Agulhon C, Taves SR, Petravicz J, Casper KB, Dong X, Chen J, McCarthy KD (2007b) Selective Stimulation of Astrocyte Calcium In Situ Does Not Affect Neuronal Excitatory Synaptic Activity. Neuron 54:611–626.

Fishman RA (1975) Brain edema. N Engl J Med 293:706–711.

Flatman JA, Schwindt PC, Crill WE, Stafstrom CE (1983) Multiple actions of N-methyl-D-aspartate on cat neocortical neurons in vitro. Brain Res 266:169–173.

Fonnum F (1984) Glutamate: A Neurotransmitter in Mammalian Brain. J Neurochem.

Frasca A, Aalbers M, Frigerio F, Fiordaliso F, Salio M, Gobbi M, Cagnotto A, Gardoni F, Battaglia GS, Hoogland G, Di Luca M, Vezzani A (2011) Misplaced NMDA receptors in epileptogenesis contribute to excitotoxicity. Neurobiol Dis 43:507–515.

Fukuda a M, Pop V, Spagnoli D, Ashwal S, Obenaus a, Badaut J (2012) Delayed increase of astrocytic aquaporin 4 after juvenile traumatic brain injury: possible role in edema resolution? Neuroscience 222:366–378.

Gao X, Sakai K, Roberts RC, Ph D, Conley RR, Dean B, Tamminga CA (2000) Ionotropic Glutamate Receptors and Expression of N-Methyl-D-Aspartate Receptor Subunits in Subregions of Human Hippocampus: Effects of Schizophrenia. Am J Psychiatry 157:1141–1149.

Gill MB, Frausto S, Ikoma M, Sasaki M, Oikawa M, Sakai R, Swanson GT (2010) A series of structurally novel heterotricyclic alpha-amino-3-hydroxyl-5-methyl-4-isoxazole-propionate receptor-selective antagonists. Br J Pharmacol 160:1417–1429.

Gómez-Gonzalo M, Losi G, Chiavegato A, Zonta M, Cammarota M, Brondi M, Vetri F, Uva L, Pozzan T, de Curtis M, Ratto GM, Carmignoto G (2010) An

excitatory loop with astrocytes contributes to drive neurons to seizure threshold. PLoS Biol 8:e1000352.

Gonen T, Walz T (2006) The structure of aquaporins. Q Rev Biophys 39:361–396.

Gray WP, Sundstrom LR (1998) Kainic acid increases the proliferation of granule cell progenitors in the dentate gyrus of the adult rat. Brain Res:52–59.

Green JD (1969) The hippocampus. Physiol Rex 44:561–608.

Gunnarson E, Song Y, Kowalewski JM, Brismar H, Brines M, Cerami A, Andersson U, Zelenina M, Aperia A (2009) Erythropoietin modulation of astrocyte water permeability as a component of neuroprotection. Proc Natl Acad Sci U S A 106:1602–1607.

Gunnarson E, Zelenina M, Axehult G, Song Y, Bondar A, Krieger P, Brismar H, Zelenin S, Aperia A (2008) Identification of a molecular target for glutamate regulation of astrocyte water permeability. Glia 56:587–596.

Hackett PH, Roach RC (2001) High-altitude illness. N Engl J Med 345:107–114.

Haglund MM, Hochman DW (2005) Furosemide and mannitol suppression of epileptic activity in the human brain. J Neurophysiol 94:907–918.

Hamann S, Herrera-Perez JJ, Zeuthen T, Alvarez-Leefmans FJ (2010) Cotransport of water by the Na+-K+-2Cl(-) cotransporter NKCC1 in mammalian epithelial cells. J Physiol 588:4089–4101.

Han D, Sun M, He P-P, Wen L-L, Zhang H, Feng J (2015) Ischemic Postconditioning Alleviates Brain Edema After Focal Cerebral Ischemia Reperfusion in Rats Through Down-Regulation of Aquaporin-4. J Mol Neurosci.

Harris AZ, Pettit DL (2007) Extrasynaptic and synaptic NMDA receptors form stable and uniform pools in rat hippocampal slices. J Physiol 584:509–519.

Harris KD, Hirase H, Leinekugel X, Henze DA (2001) Temporal Interaction between Single Spikes and Complex Spike Bursts in Hippocampal Pyramidal Cells. 32:141–149.

Haskew-Layton RE, Rudkouskaya A, Jin Y, Feustel PJ, Kimelberg HK, Mongin A a (2008) Two distinct modes of hypoosmotic medium-induced release of excitatory amino acids and taurine in the rat brain in vivo. PLoS One 3:e3543.

Heinemann U, Franceschetti B, Hamon S, Konnerth A, Yaari Y (1985) Effects of anticonvulsants on spontaneous epileptiform activity which develops in the absence of chemical synaptic transmission in hippocampal slices. Brain Res 325:349–352.

Heinemann UWE, Lux HD (1977) Ceiling of stimulus induced rises in extracellular potassium concentraion in the cerebral cortex of cat. Brain Res 120:231–249.

Heldmaier G, Ruf T (1992) Body temperature and metabolic rate during natural hypothermia in endotherms. :696–706.

Helmchen F, Svoboda K, Denk W, Tank DW, Spring C, Harbor CS, York N (1999) In vivo dendritic calcium dynamics in deep-layer cortical pyramidal neurons.

Hemphill JC, Knudson MM, Derugin N, Morabito D, Manley GT (2001) Carbon dioxide reactivity and pressure autoregulation of brain tissue oxygen. Neurosurgery 48:377–384.

Henshall DC, Meldrum BS (2012) Cell death and survival mechanisms after single and repeated brief seizures. In: Jasper's basic mechanisms of the epilepsies. 4th edn. Bethesda, MD: Oxford University Press.

Hinterkeuser S, Schröder W, Hager G, Seifert G, Blümcke I, Elger CE, Schramm J, Steinhäuser C (2000) Astrocytes in the hippocampus of patients with temporal lobe epilepsy display changes in potassium conductances. Eur J Neurosci 12:2087–2096.

Hirrlinger PG, Wurm A, Hirrlinger J, Bringmann A, Reichenbach A (2008) Osmotic swelling characteristics of glial cells in the murine hippocampus, cerebellum, and retina in situ. J Neurochem 105:1405–1417.

Hirtz D, Thurman DJ, Mohamed M (2007) How common are the " common " neurologic disorders ?

Ho M-L, Rojas R, Eisenberg RL (2012) Cerebral edema. AJR Am J Roentgenol 199:W258–73.

Hsu MS, Lee DJ, Binder DK (2007) Potential role of the glial water channel aquaporin-4 in epilepsy. Neuron Glia Biol:287–297.

Huang R, Bossut DF, Somjen GG (1997) Enhancement of Whole Cell Synaptic Currents by Low Osmolarity and by Low [NaCl] in Rat Hippocampal Slices. :2349–2359.

Hubbard J a, Hsu MS, Fiacco T a, Binder DK (2013) Glial cell changes in epilepsy: overview of the clinical problem and therapeutic opportunities. Neurochem Int 63:638–651.

Hyzinski-García MC, Vincent MY, Haskew-Layton RE, Dohare P, Keller RW, Mongin A a (2011) Hypo-osmotic swelling modifies glutamate-glutamine cycle in the cerebral cortex and in astrocyte cultures. J Neurochem 118:140–152.

Igelmund P (1995) Modulation of synaptic transmission at low temperatures by hibernation related changes in ionic microenvironment in hippocampal slices of golden hamsters.pdf. Cryobiology 32:334–343.

Igelmund P, Heinemann U (1995) Synaptic transmission and paired-pulse behaviour of CA1 pyramidal cells in hippocampal slices from a hibernator at low temperature : importance of ionic environment. 689:9–20.

Jabs R, Seifert G, Steinhäuser C (2008) Astrocytic function and its alteration in the epileptic brain. Epilepsia 49 Suppl 2:3–12.

Jensen FE, Wang C, Stafstrom CE, Liu Z, Geary C, Stevens MC, Rakhade SN, Fitzgerald EF, Klein PM, Zhou C, Sun H, Richard L, Jensen FE, Jun HY, Yeom Y Il, Park SH, Kim KH, Shin H, Kim D (2015) Acute and Chronic Increases in Excitability in Rat Hippocampal Slices After Perinatal Hypoxia In Vivo Acute and Chronic Increases in Excitability in Rat Hippocampal Slices After Perinatal Hypoxia In Vivo. :73–81.

Jensen MS, Yaari Y (1988) The Relationshp Between Interictal and Ictal Paroxysms in an In Vitro Model o f rocal Hippocampal kpuepsy. :591–598.

Jensen MS, Yaari Y (1997) Role of Intrinsic Burst Firing , Potassium Accumulation , and Electrical Coupling in the Elevated Potassium Model of Hippocampal Epilepsy.

Jones RS, Heinemann U (1988) Synaptic and intrinsic responses of medial entorhinal cortical cells in normal and magnesium-free medium in vitro. J Neurophysiol 59:1476–1496.

Kahle KT, Gerzanich V, Simard JM (2010) Molecular mechanisms of microvascular failure in CNS injury - synergistic roles of NKCC1 and SUR1/TRPM4. J Neurosurg 113:622–629.

Kang N, Xu J, Xu Q, Nedergaard M, Kang J (2005a) Astrocytic Glutamate Release-Induced Transient Depolarization and Epileptiform Discharges in Hippocampal CA1 Pyramidal Neurons. J Neurophysiol 94:4121–4130.

Kang N, Xu J, Xu Q, Nedergaard M, Kang J (2005b) Astrocytic glutamate release-induced transient depolarization and epileptiform discharges in hippocampal CA1 pyramidal neurons. J Neurophysiol 94:4121–4130.

Kempski O, Staub F, Jansen M, Baethmann A (1990) Molecular mechanisms of glial cell swelling in acidosis. Adv Neurol 52:39–45.

Kettenmann H, Orkand RK, Schachner M (1983) Coupling among identified cells in mammalian nervous system cultures. J Neurosci 3:506–516.

Kilb W, Dierkes PW, Syková E, Vargová L, Luhmann HJ (2006) Hypoosmolar conditions reduce extracellular volume fraction and enhance epileptiform activity in the CA3 region of the immature rat hippocampus. J Neurosci Res 84:119–129.

Kim HG, Connors BW (1993) Apical Dendrites of the Neocortex : Correlation between Sodium- Spiking and Pyramidal Cell Morphology. 13.

Kimelberg HK (2004a) Water homeostasis in the brain: basic concepts. Neuroscience 129:851–860.

Kimelberg HK (2004b) Increased release of excitatory amino acids by the actions of ATP and peroxynitrite on volume-regulated anion channels (VRACs) in astrocytes. 45:511–519.

Kimelberg HK (2004c) The problem of astrocyte identity. Neurochem Int 45:191–202.

Kimelberg HK (2005) Astrocytic swelling in cerebral ischemia as a possible cause of injury and target for therapy. Glia 50:389–397.

Kimelberg HK, Biddlecome S, S BR (1979a) SITS-inhibitable Cl- transport and Na+-dependent H+ production in primary astroglial cultures. Brain Res 173:11–124.

Kimelberg HK, Bourke RS (1982) Chemical and Cellular Architecture (Lajtha A, ed). Springer.

Kimelberg HK, Bowman C, Biddlecome S, Bourke RS (1979b) Cation transport and membrane potential properties of primary astroclial cultures form neonatl rat brains. Brain Res 177:533–550.

Kimelberg HK, Macvicar BA, Sontheimer H (2006) Anion Channels in Astrocytes : Biophysics , Pharmacology , and Function. 757:747–757.

Klatzo I (1967) Neuropathological aspects of brain edema. J Neuropathol Exp Neurol 26:1–14.

Kofuji P, Newman E a (2004) Potassium buffering in the central nervous system. Neuroscience 129:1045–1056.

Korn SJ, Giacchino JL, Chamberlin NL, Dingledine R (1987) Epileptiform Burst Activity Induced by Potassium in the Hippocampus and its Regulation by GABA-Mediated Inhibition. J Neurophysiol 57.

Kozler P, Pokorný J (2014) CT density decrease in water intoxication rat model of brain oedema. 35:608–612.

Kozler P, Riljak V, Pokorný J (2013) Both Water Intoxication and Osmotic BBB Disruption Increase Brain Water Content in Rats. 62.

Kozlov a S, Angulo MC, Audinat E, Charpak S (2006a) Target cell-specific modulation of neuronal activity by astrocytes. PNAS 103:10058–10063.

Kozlov AS, Angulo MC, Audinat E, Charpak S (2006b) Target cell-specific modulation of neuronal activity by astrocytes. PNAS 103.

Kriz N, Sykova E, Ujec E, Vyklicky L (1974) Changes of extracellular potassium concentration induced by neuronal activity in the spinal cord of the cat. J Paediatr Child Heal:1–15.

Lanerolle NC De, Eid T, Campe G Von, Kovacs I, Spencer DD, Brines M (1998) Glutamate receptor subunits GluR1 and GluR2/3 distribution shows reorganization in the human epileptogenic hippocampus. Eur J Neurosci 10:1687–1703.

Larkum ME, Zhu JJ (2002) Signaling of Layer 1 and Whisker-Evoked Ca 2 ⁒ and Na ⁒ Action Potentials in Distal and Terminal Dendrites of Rat Neocortical Pyramidal Neurons In Vitro and In Vivo. 22:6991–7005.

Lassmann H, Petsche U, Kitz K, Baran H, Sperk G, Seitelberger F, Hornykiewicz O (1984) The role of brain edema in epileptic brain damage induced by systemic kainic acid injection. Neuroscience 13:691–704.

Le Meur K, Galante M, Angulo MC, Audinat E (2007) Tonic activation of NMDA receptors by ambient glutamate of non-synaptic origin in the rat hippocampus. J Physiol 580:373–383.

Lee TS, Eid T, Mane S, Kim JH, Spencer DD, Ottersen OP, De Lanerolle NC (2004) Aquaporin-4 is increased in the sclerotic hippocampus in human temporal lobe epilepsy. Acta Neuropathol 108:493–502.

Lehmenkühler A, Syková E, Svoboda J, Zilles K, Nicholson C (1993) Extracellular space parameters in the rat neocortex and subcortical white

matter during postnatal development determined by diffusion analysis. Neuroscience 55:339–351.

Lin S-C, Bergles DE (2002) Physiological characteristics of NG2-expressing glial cells. J Neurocytol 31:537–549.

Liu H, Tashmukhamedov BA, Inoue H, Okada Y (2006) Roles of Two Types of Anion Channels in Glutamate Release from Mouse Astrocytes Under Ischemic or Osmotic Stress. 357:343–357.

Liu SJ, Cull-candy SG (2000) Synaptic activity at calcium- permeable AMPA receptors induces a switch in receptor subtype. Nature 405:1–5.

Lloyd KG, Bossi L, Morselli C, Rougier M, Loiseau H (1986) Alterations in human epilepsy. Adv Neurol 44:1033–1044.

Lynn BD, Tress O, May D, Willecke K, Nagy JI (2011) Ablation of connexin30 in transgenic mice alters expression patterns of connexin26 and connexin32 in glial cells and leptomeninges. Eur J Neurosci 34:1783–1793.

MacAulay N, Hamann S, Zeuthen T (2004) Water transport in the brain: role of cotransporters. Neuroscience 129:1031–1044.

MacVicar BA (1984) Voltage-dependent calcium channels in glial cells. Science (80-):1345–1347.

Maeno E, Ishizaki Y, Kanaseki T, Hazama A, Okada Y (2000) Normotonic cell shrinkage because of disordered volume regulation is an early prerequisite to apoptosis. PNAS.

Mahanty NK, Sah P (1998) Calcium-permeable AMPA receptors mediate long-term potentiation in interneurons in the amygdala. Nature 394:683–687.

Manley GT, Fujimura M, Ma T, Noshita N, Filiz F, Bollen a W, Chan P, Verkman a S (2000) Aquaporin-4 deletion in mice reduces brain edema after acute water intoxication and ischemic stroke. Nat Med 6:159–163.

Mares P, Mikulecká A (2009) Different effects of two N-methyl-D-aspartate receptor antagonists on seizures, spontaneous behavior, and motor performance in immature rats. Epilepsy Behav 14:32–39.

Mayer ML, Westbrook GL, Guthrie PB (1984) Voltage-dependent block by Mg2+ of NMDA responses in spinal cord neurones. Nature 309:261–263.

Mccarty NA, O'Neil RG (1992) Calcium Signaling in Cell Volume Regulation. Physiol Rev 72.

McCool BA, Lovinger DM (1995) Ifenprodil Inhibition of the 5-Hydroxytryptamine3 Receptor. Neuropharmacology 34:621–629.

Mccormick DA, Contreras D (2001) On the cellular and network bases of epileptic seizures. Annu Rev Physiol 63:815–846.

Meldrum BS (2000) Glutamate and Glutamine in the Brain Glutamate as a Neurotransmitter in the Brain : Review of Physiology and Pathology 1. 8:1007–1015.

Meldrum BS, Akbar MT, Chapman AG (1999) Glutamate receptors and transporters in genetic and acquired models of epilepsy. 36:189–204.

Miller RH, Raff MC (1984) Fibrous and protoplasmic astrocytes are biochmically and developmentally distinct. J Neurosci 4:585–592.

Mongin AA, Aksentsev SL, Orlov SN, Kyacheva ZB, Mezen NI, Fedulov AS, Konev SV (1996) Swelling-induced activation of Na+, K+, 2Cl cotransport in C6 glioma cells: kinetic properties and intracellular signaling mechanisms. Biochim Biophys Acta:229–236.

Mongin AA, Kimelberg HK (2005) ATP regulates anion channel-mediated organic osmolyte release from cultured rat astrocytes via multiple Ca2+-sensitive mechanisms. Am J Physiol Cell Physiol:204–213.

Mongin AA, Orlov SN (2001) Mechanisms of cell volume regulation and possible nature of the cell volume sensor. Pathophysiology 8:77–88.

Montero TD, Orellana J a (2015) Hemichannels: new pathways for gliotransmitter release. Neuroscience 286:45–59.

Mortazavi MM, Romeo AK, Deep A, Griessenauer CJ, Shoja MM, Tubbs RS, Fisher W (2012) Hypertonic saline for treating raised intracranial pressure: literature review with meta-analysis. J Neurosurg 116:210–221.

Mosley C a, Myers SJ, Murray EE, Santangelo R, Tahirovic Y a, Kurtkaya N, Mullasseril P, Yuan H, Lyuboslavsky P, Le P, Wilson LJ, Yepes M, Dingledine R, Traynelis SF, Liotta DC (2009) Synthesis, structural activity-relationships, and biological evaluation of novel amide-based allosteric binding site antagonists in NR1A/NR2B N-methyl-D-aspartate receptors. Bioorg Med Chem 17:6463–6480.

Murtha L a, McLeod DD, Pepperall D, McCann SK, Beard DJ, Tomkins AJ, Holmes WM, McCabe C, Macrae IM, Spratt NJ (2015) Intracranial pressure elevation after ischemic stroke in rats: cerebral edema is not the only cause, and short-duration mild hypothermia is a highly effective preventive therapy. J Cereb Blood Flow Metab 35:592–600.

Nagelhus EA, Mathiisen TM, Ottersen OP (2002) Aquaporin-4 in the central nervous system: Cellular and subcellular distribution and coexpression with KIR4.1. Neuroscience 112:921–934.

Nakanishi S (1994) Metabotropic Glutamate Receptors: Synaptic Transmission, Modulation, and Plasticity. Neuron 13:1031–1037.

Neusch C, Papadopoulos N, Müller M, Maletzki I, Winter SM, Hirrlinger J, Handschuh M, Bähr M, Richter DW, Kirchhoff F, Hülsmann S (2006) Lack of the Kir4.1 channel subunit abolishes K+ buffering properties of astrocytes in the ventral respiratory group: impact on extracellular K+ regulation. J Neurophysiol 95:1843–1852.

Nicchia GP, Frigeri A, Liuzzi GM, Svelto M (2003) Inhibition of aquaporin-4 expression in astrocytes by RNAi determines alteration in cell morphology, growth, and water transport and induces changes in ischemia-related genes. FASEB 17:1508–1510.

Nilius B, Droogmans G (2003) Amazing chloride channels: an overview. Acta Physio 177:119–147.

Nilius B, Droogmans GUY (2001) Ion Channels and Their Functional Role in Vascular Endothelium. Physiol Rev 81.

Nilius B, Eggermont J, Voets T, Buyse G, Manolopoulos V, Droogmans GUY (1997) Properties of volume-regulated anion channels in mammalian cells. Prog Biophys Mol Biol 68:69–119.

Nilius B, Oike M, Zahradnik I, Droogmans G (1994) Activation of a C1- Current by Hypotonic Volume Increase in Human Endothelial Cells. J Gen Physiol:787–805.

Nilius B, Prenen J, Droogmans G (1998) Modulation of volume-regulated anion channels by extra- and intracellular pH. J Physiol 9:742–748.

Noebels J, Avoli M, Rogawski M, Olsen R, Delgado-Escueta A eds. (2012) Jasper's Basic Mechanisms of the Epilepsies. Oxford University Press.

Oberheim NA, Wang X, Goldman S, Nedergaard M (2006) Astrocytic complexity distinguishes the human brain. Trends Neurosci 29:547–553.

Orkand RK, Nicholls JG, Kuffler SW (1966) Effect of nerve impulses on the membrane potential of glia cells in the central nervous system of amphibia. J Neurophysiol 29:788–806.

Oshio K, Binder DK, Yang B, Schecter S, Verkman a S, Manley GT (2004) Expression of aquaporin water channels in mouse spinal cord. Neuroscience 127:685–693.

Ozturk SS, Hu W eds. (2005) Cell culture technology for pharmaceutical and cell-based therapies. CRC Press.

Paoletti P, Ascher P (1994) Mechanosensitivity of NMDA Receptors in Cultured Mouse Central Neurons. Neuron 13:645–655.

Papadopoulos MC, Verkman AS (2007a) Aquaporin-4 and brain edema. Pediatr Nephrol 22:778–784.

Papadopoulos MC, Verkman AS (2007b) Aquaporin-4 and brain edema. Pediatr Nephrol 22:778–784.

Parpura V, Haydon PG (2000) Physiological astrocytic calcium levels stimulate glutamate release to modulate adjacent neurons. PNAS 97:8629–8634.

Pasantes-Morales H, Franco R, Torres-Marquez E, Hernández-Fonseca K, Ortega A (2000) Amino Acid Osmolytes in Regulatory Volume Decrease and Isovolumetric Regulation in Brain Cells: Contribution and Mechanisms. Cell Physiol Biochem:361–370.

Pasti L, Volterra A, Pozzan T, Carmignoto G (1997) Intracellular Calcium Oscillations in Astrocytes : A Highly Plastic , Astrocytes In Situ. 17:7817–7830.

Pawlak R, Melchor JP, Matys T, Skrzypiec AE, Strickland S (2005) Ethanol-withdrawal seizures are controlled by tissue plasminogen activator via modulation of NR2B-containing NMDA receptors. 102:443–448.

Pedersen SF, Klausen TK, Nilius B (2015) The identification of a volume-regulated anion channel: an amazing Odyssey. Acta Physiol (Oxf):1–14.

Petravicz J, Fiacco T a, McCarthy KD (2008) Loss of IP3 receptor-dependent Ca2+ increases in hippocampal astrocytes does not affect baseline CA1 pyramidal neuron synaptic activity. J Neurosci 28:4967–4973.

Petroff OAC, Errante LD, Rothman DL, Kim JH, Spencer DD (2002) Glutamate – glutamine Cycling in the Epileptic Human Hippocampus. Epilepsia 43:703–710.

Porter JT, McCarthy KD (1996) Hippocampal astrocytes in situ respond to glutamate released from synaptic terminals. J Neurosci 16:5073–5081.

Qiu Z, Dubin AE, Mathur J, Tu B, Reddy K, Miraglia LJ, Reinhardt J, Orth AP, Patapoutian A (2014) SWELL1, a Plasma Membrane Protein, Is an Essential Component of Volume-Regulated Anion Channel. Cell 157:447–458.

Radojevic N, Bjelogrlic B, Aleksic V, Rancic N, Samardzic M, Petkovic S, Savic S (2012) Forensic aspects of water intoxication: four case reports and review of relevant literature. Forensic Sci Int 220:1–5.

Ramos-mandujano G, Vazquez-Juarez E, Hernandez-Benitez R, Pasantes-Moreales H (2007) Thrombin Potently Enhances Swelling-Sensitive Glutamate Efflux from Cultured Astrocytes. Glia:917–925.

Rauner C, Köhr G (2011) Triheteromeric NR1/NR2A/NR2B receptors constitute the major N-methyl-D-aspartate receptor population in adult hippocampal synapses. J Biol Chem 286:7558–7566.

Risher WC, Andrew RD, Kirov S a (2009a) Real-time passive volume responses of astrocytes to acute osmotic and ischemic stress in cortical slices and in vivo revealed by two-photon microscopy. Glia 57:207–221.

Risher WC, Andrew RD, Kirov SA (2009b) Real-Time Passive Volume Responses of Astrocytes to Acute Osmotic and Ischemic Stress in Cortical Slices and In Vivo Revealed by Two-Photon Microscopy. 221:207–221.

Roper SN, Obenaus a, Dudek FE (1992) Osmolality and nonsynaptic epileptiform bursts in rat CA1 and dentate gyrus. Ann Neurol 31:81–85.

Rosen AS, Andrew RD (1990) Osmotic effects upon excitability in rat neocortical slices. Neuroscience 38:579–590.

Rossi DJ, Oshima T, Attwell D (2000) Glutamate release in severe brain ischaemia is mainly by reversed uptake. Nature 403:1–6.

Rossi S, Zanier ER, Mauri I, Columbo A, Stocchetti N (2001) Brain temperature , body core temperature , and intracranial pressure in acute cerebral damage. Neurol Neurosurg Psychiatry 71:448–454.

Rungta RL, Choi HB, Tyson JR, Malik A, Dissing-Olesen L, Lin PJC, Cain SM, Cullis PR, Snutch TP, MacVicar BA (2015) The Cellular Mechanisms of Neuronal Swelling Underlying Cytotoxic Edema. Cell 161:610–621.

Sabirov RZ, Prenen J, Tomita T, Droogmans G, Nilius B (2000) Reduction of ionic strength activates single volume-regulated anion channels (VRAC) in endothelial cells. Pflugers Arch:315–320.

Saly V, Andrew RD (1993) CA3 neuron excitation and epileptiform discharge are sensitive to osmolality. J Neurophysiol 69:2200–2208.

Schwartzkroin P a, Baraban SC, Hochman DW (1998a) Osmolarity, ionic flux, and changes in brain excitability. Epilepsy Res 32:275–285.

Schwartzkroin P a., Baraban SC, Hochman DW (1998b) Osmolarity, ionic flux, and changes in brain excitability. Epilepsy Res 32:275–285.

Shelton MK, McCarthy KD (1999) Mature hippocampal astrocytes exhibit functional metabotropic and ionotropic glutamate receptors in situ. Glia 26:1–11.

Shen Y, Linden DJ (2005) Long-term potentiation of neuronal glutamate transporters. Neuron 46:715–722.

Shigetomi E, Bowser DN, Sofroniew M V, Khakh BS (2008) Two Forms of Astrocyte Calcium Excitability Have Distinct Effects on NMDA Receptor-Mediated Slow Inward Currents in Pyramidal Neurons. 28:6659–6663.

Shu Y, Duque A, Yu Y, Haider B, Mccormick DA (2007) Properties of Action-Potential Initiation in Neocortical Pyramidal Cells : Evidence From Whole Cell Axon Recordings. :746–760.

Siegel AJ (2015) Fatal Water Intoxication and Cardiac Arrest in Runners during Marathons: Prevention and Treatment Based on Validated Clinical Paradigms. Am J Med.

Sofroniew M V, Vinters H V (2010) Astrocytes: biology and pathology. Acta Neuropathol 119:7–35.

Solenov E, Watanabe H, Manley GT, Verkman a S (2004) Sevenfold-reduced osmotic water permeability in primary astrocyte cultures from AQP-4-deficient mice, measured by a fluorescence quenching method. Am J Physiol Cell Physiol 286:C426–32.

Solenov EI, Vetrivel L, Oshio K, Manley GT, Verkman AS (2002) Optical measurement of swelling and water transport in spinal cord slices from aquaporin null mice. J Neurosci Methods 113:85–90.

Somjen GG, Faas GC, Vreugdenhil M, Wadman WJ (1993) Channel shutdown: a response of hippocampal neurons to adverse environments. Brain Res 632:180–194.

Srinivasan R, Huang BS, Venugopal S, Johnston AD, Chai H, Zeng H, Golshani P, Khakh BS (2015) Ca2+ signaling in astrocytes from Ip3r2−/− mice in brain slices and during startle responses in vivo. Nat Neurosci 18.

Stockand JD, Shapiro MS eds. (2006) Ion Channels Methods and Protocols, Vol. 337. Humana Press Inc.

Stokum J a, Kurland DB, Gerzanich V, Simard JM (2014) Mechanisms of Astrocyte-Mediated Cerebral Edema. Neurochem Res.

Stout CE, Costantin JL, Naus CCG, Charles AC (2002) Intercellular calcium signaling in astrocytes via ATP release through connexin hemichannels. J Biol Chem 277:10482–10488.

Su G, Kintner DB, Flagella M, Shull GE, Sun D (2002a) Astrocytes from Na(+)-K(+)-Cl(-) cotransporter-null mice exhibit absence of swelling and decrease in EAA release. Am J Physiol Cell Physiol 282:C1147–C1160.

Su G, Kintner DB, Sun D (2002b) Contribution of Na+-K+-Cl- cotransporter to high-[K+]o -induced swelling and EAA release in astrocytes. Am J Physiol Cell Physiol 282:1136–1146.

Suter KJ, Smith BN, Dudek FE (1999) Electrophysiological Recording from Brain Slices. Methods 18:86–90.

Svoboda J, Sykova E (1991) Extracellular space volume changes in the rat spinal cord produced by nerve stimulation and peripheral injury. Brain Res 560:216–224.

Sykova E, Rothenberg S, Krekule I (1974) Changes of extracellular potassium concentration during spontaneous activity in the mesencephalic reticular formation of the rat. Brain Res 79:333–337.

Szatkowski M, Barbour B, Attwell D (1990) Non-vesicular release of glutamate from glial cells by reversed electrogenic glutamate uptake. Nature 349.

Takano T, Kang J, Jaiswal JK, Simon SM, Lin JH-C, Yu Y, Li Y, Yang J, Dienel G, Zielke HR, Nedergaard M (2005) Receptor-mediated glutamate release from volume sensitive channels in astrocytes. PNAS 102:16466–16471.

Talan M (1984) Body temperature of C57BL/6J mice with age. Exp Gerontol 19:25–29.

Tasleem RA, Chowdhary ND (2003) Fatal water intoxication. J Clin Pathol:803–804.

Tauck DL, Nadler JV (1985) Evidence of Functional Mossy Fiber Sprouting in Hippocampal Formation of Kainic Acid-Treated Rats. J Neurosci 5:1016–1022.

Taylor CP, Dudek FE (1984) Excitation of Hippocampal Pyramidal Cells by an Electrical Field Effect. J Neurophysiol 52.

Thrane AS, Rangroo Thrane V, Nedergaard M (2014) Drowning stars: reassessing the role of astrocytes in brain edema. Trends Neurosci 37:620–628.

Tian G-F, Azmi H, Takano T, Xu Q, Peng W, Lin J, Oberheim N, Lou N, Wang X, Zielke HR, Kang J, Nedergaard M (2005) An astrocytic basis of epilepsy. Nat Med 11:973–981.

Ting JT, Daigle TL, Chen Q, Feng G (2014) Acute brain slice methods for adult and aging animals: application of targeted patch clampanalysis and optogenetics Martina M, Taverna S, eds. Methods Mol Biol 1183:1–21.

Tovar KR, McGinley MJ, Westbrook GL (2013) Triheteromeric NMDA receptors at hippocampal synapses. J Neurosci 33:9150–9160.

Traynelis SF, Dingledine R (1988) Potassium-induced spontaneous electrographic seizures in the rat hippocampal slice. J Neurophysiol 59:259–276.

Traynelis SF, Dingledine R (1989) Role of extracellular space in hyperosmotic suppression of potassium-induced electrographic seizures. J Neurophysiol 61:927–938.

Trotter J, Karram K, Nishiyama A (2010) NG2 cells: Properties, progeny and origin. Brain Res Rev 63:72–82.

Unterberg a W, Stover J, Kress B, Kiening KL (2004) Edema and brain trauma. Neuroscience 129:1021–1029.

Vargova L, Sykova E (2014) Astrocytes and extracellular matrix in extrasynaptic volume transmission. Phil Trans R Soc B.

Voets T, Droogmans G, Raskin G, Eggermont J, Nilius B (1999) Reduced intracellular ionic strength as the initial trigger for activation of endothelial volume-regulated anion channels. Proc Natl Acad Sci 96:5298–5303.

Voigt J, Grosche A, Vogler S, Pannicke T, Hollborn M, Kohen L, Wiedemann P, Reichenbach A, Bringmann A (2015) Nonvesicular release of ATP from rat retinal glial (Müller) cells is differentially mediated in response to osmotic stress and glutamate. Neurochem Res 40:651–660.

Volman V, Bazhenov M, Sejnowski TJ (2013) Divide and conquer: functional segregation of synaptic inputs by astrocytic microdomains could alleviate paroxysmal activity following brain trauma. PLoS Comput Biol 9:e1002856.

Voss FK, Ullrich F, Munch J, Lazarow K, Lutter D, Mah N, Andrade-Navarro MA, Kries JP, Stauber T, Jentsch TJ (2014) Identification of LRRC8 Heteromers

as an Essential Component of the Volume-Regulated Anion Channel VRAC. Science (80-) 344:634–639.

Walther H, Lambert JD, Jones RS, Heinemann U, Hamon B (1986) Epileptiform activity in combined slices of the hippocampus, subiculum and entorhinal cortex during perfusion with low magnesium medium. Neurosci Lett 69:156–161.

Walz W ed. (2007) Patch-Clamp Analysis Advanced Techniques. Totowa: Humana Press Inc.

Walz W, Hertz L (1983) Intracellular Ion Changes of Astrocytes in Response to Extracellular Potassium. J Neurosci Res 423:411–423.

Walz W, Hinks EC (1986) A Transmembrane Sodium Cycle in Astrocytes. Brain Res 368:226–232.

Wang X-M, Bausch SB (2004) Effects of distinct classes of N-methyl-D-aspartate receptor antagonists on seizures, axonal sprouting and neuronal loss in vitro: suppression by NR2B-selective antagonists. Neuropharmacology 47:1008–1020.

Wang YU, Roman R, Lidofskyt SD, Fitz JG (1996) Autocrine signaling through ATP release represents a novel mechanism for cell volume regulation. Proc Natl Acad Sci 93:12020–12025.

Wasseff SK, Scherer SS (2011) Cx32 and Cx47 mediate oligodendrocyte:astrocyte and oligodendrocyte:oligodendrocyte gap junction coupling. Neurobiol Dis 42:506–513.

Wetherington J, Serrano G, Dingledine R (2008) Astrocytes in the epileptic brain. Neuron 58:168–178.

Wong RK, Traub RD, Miles R (1986) Cellular basis of neuronal synchrony in epilepsy. Adv Neurol 44:583–592.

Yamashiro M, Hasegawa H, Matsuda A, Kinoshita M, Matsumura O, Isoda K, Mitarai T (2013) A case of water intoxication with prolonged hyponatremia caused by excessive water drinking and secondary SIADH. Case Rep Nephrol Urol 3:147–152.

Yang M, Gao F, Liu H, Yu WH, Sun SQ (2009) Temporal changes in expression of aquaporin-3, -4, -5 and -8 in rat brains after permanent focal cerebral ischemia. Brain Res 1290:121–132.

Yao X, Derugin N, Manley GT, Verkman a S (2015) Reduced brain edema and infarct volume in aquaporin-4 deficient mice after transient focal cerebral ischemia. Neurosci Lett 584:368–372.

Ye Z-C, Wyeth MS, Baltan-Tekkok S, Ransom BR (2003) Functional hemichannels in astrocytes: a novel mechanism of glutamate release. J Neurosci 23:3588–3596.

Zador Z, Stiver S, Wang V, Manley GT (2009) Role of aquaporin-4 in cerebral edema and stroke. Handb Exp Pharmacol:159–170.

Zhang H, Cao HJ, Kimelberg HK, Zhou M (2011) Volume regulated anion channel currents of rat hippocampal neurons and their contribution to oxygen-and-glucose deprivation induced neuronal death. PLoS One 6:e16803.

Zhou N, Gordon GRJ, Feighan D, MacVicar B a (2010) Transient swelling, acidification, and mitochondrial depolarization occurs in neurons but not astrocytes during spreading depression. Cereb Cortex 20:2614–2624.

Chapter 3

Osmotic edema rapidly evokes excitatory slow inward currents in neurons.

Abstract

Cerebral edema affects millions of people worldwide and is associated with a plethora of diseases, disorders, and conditions such as traumatic brain injury, stroke, cardiac arrest, autism and epilepsy. Edema is characterized by swelling of the brain tissue, increased intracranial pressure, reduced cerebral blood flow and can result in seizures, cerebral herniation and death. Treatments for these conditions are often limited or ineffective, substantiating the need to further understand the cellular contributions and mechanisms involved during different types of edema (Zador et al., 2009; Stokum et al., 2014; Murtha et al., 2015; Yao et al., 2015). It has been known for some time that cell swelling and reduction of the extracellular space can lead to increases in neuronal excitability and even to seizures *in vitro* and *in vivo* (Traynelis and Dingledine, 1989; Binder et al., 2004). However, the identity of the cell types undergoing volume increases and the mechanisms leading to increased neuronal excitability remain unclear. Using electrophysiological whole-cell patch clamp techniques, neuronal currents were recorded in CA1 pyramidal neurons during application of hypoosmolar ACSF (hACSF) in acutely isolated hippocampal slices from mice. Hypoosmolar ACSF evoked NMDA receptor-driven slow inward currents (SICs) in neurons,

which initiated after about 1 minute of hACSF application. Neuronal excitability increased as osmolarity decreased in a dose-dependent manner. Even 5% reductions in osmolarity were sufficient to significantly increase neuronal excitability. SICs were re-evokable with successive hACSF applications. Excitability in CA1 neurons remained elevated during hypoosmolar insult even when AMAP receptors were blocked by NBQX, an AMPAR antagonist. Neuronal excitability was also increased during application of hACSF while blocking both APs and AMPA receptors. Blocking neuronal receptors with the AP5, and NMDA receptor antagonist significantly reduced neuronal excitability during hACSF application. Taken together, these results indicate that both mild and moderate osmotic insults are capable of increasing neuronal excitability, within minutes, through a combination of synaptic and non-synaptic activation of glutamate receptors.

Introduction

Osmotic edema, is a type of cellular edema which results from the dilution of the ions within the body, and subsequently changes the delicate homeostasis of the body and the brain. In addition, osmotic edema possesses elements of both vasogenic edema, via entry of water into the brain, and cytotoxic edema, via intracellular swelling of cells (Risher et al., 2009; Ho et al., 2012; Kozler et al., 2013) making it an ideal model to examine cerebral edema. Depending on the type and severity, edemas are capable of disrupting the homeostatic levels within

the brain, swelling brain tissue, increasing intracranial pressure, reducing cerebral blood flow, inducing hyperexcitability, seizures and can even result in cerebral herniation and death (Fishman, 1975; Tasleem and Chowdhary, 2003; Unterberg et al., 2004; Ho et al., 2012). However, the molecular mechanisms by which the brain swells and neuronal excitability increases may be different depending on the specific type of edema and are not fully understood (Manley et al., 2000; Stokum et al., 2014; Han et al., 2015; Rungta et al., 2015; Yao et al., 2015) substantiating the necessity for further research in this area.

One hallmark of many different types of cerebral edema including water intoxication is an increase in brain activity following the initial swelling of the brain tissue (Traynelis and Dingledine, 1989; Binder et al., 2004). This increase in neuronal excitability can then lead to synchronization of neuronal networks and seizures within the brain (Saly and Andrew, 1993; Mccormick and Contreras, 2001). Neurons within a local network have been shown to be synchronized by slow inward currents (SICs), also sometimes referred to as slowly decaying transient inward currents, or STCs (Kang et al., 2005) within the hippocampus, and are thought to be produced by astrocytic glutamate binding to neuronal NMDA receptors (Angulo et al., 2004; Fellin et al., 2004; Kang et al., 2005). SICs have been implicated in the hypersynchronous discharge characterizing the ictal portion of an epileptic seizure and are seen across several seizure and epilepsy models (Fellin et al., 2004, 2006; Kang et al., 2005; Tian et al., 2005; Gómez-

Gonzalo et al., 2010). However the mechanisms by which SICs are produced, modulated, and synchronize neuronal activity during cellular edema leading to hyperexcitability and seizures is limited. In this chapter we examine the changes in SICs contributing to neuronal excitability during the beginning stages of cellular swelling produced by osmotic insult in the CA1 area of acute hippocampal slices from mice.

Results

AMPA receptors contribute to neuronal excitability during hypoosmolar stress.

Since a reduction in the extracellular space has been shown to precede epileptic activity, it was first decided to measure neuronal activity under basal hypoosmolar conditions in order to get an idea of overall neuronal excitability during hypoosmolar stress. Experiments were performed as outlined in chapter 2. After establishing a 10-minute baseline in normosmolar ACSF, a mild 17% hACSF was applied three times, in succession, alternating with equal-length wash periods in nACSF (Figure 3.1 A, 17% hACSF, top recording). To determine the relative contribution of AMPA receptors to neuronal activity during a mild osmotic stress, the 17% hACSF experiment was repeated with the inclusion of 10 μM NBQX, an AMPA receptor antagonist, in both the hACSF and nACSF (Figure 3.1 A, 17% +NBQX, middle recoding), and then compared to the 17%

hACSF experiment. Additionally, we wanted to examine the relative contribution of neuronal firing of action potentials to neuronal activity during osmotic stress. To this end, the 17% hACSF experiment was repeated a third time with the inclusion of 1 μM tetrodotoxin, (TTX) a voltage-gated sodium channel blocker along with NBQX in the nACSF and hACSF (Figure 3.1 A, 17% +TTX, bottom recording) then compared to the 17% hACSF plus NBQX experiment. Slow inward currents (SICs) were measured and analyzed for all of the experiments. The frequency of SICs significantly decreased due to blockade of AMPA receptors in the baseline and all three hypoosmolar applications (Table 3.1 and Figure 3.1 B). However, blockade of action potentials by TTX did not affect the frequency of SICs, suggesting that the majority of the activity was due to action potential independent sources. Kinetics of SICs are typically analyzed by researchers, and are useful for classifying these currents as SICs (Angulo et al., 2004; Fellin et al., 2004).The absolute amplitude of the SICs was also similar for all three groups, indicating a similar degree of activation (Table 3.1 and Figure 3.1 C). The time to evoke SICs, occurred within approximately 1 to 2 minutes after application of hACSF in all of the conditions (Figure 3.1 D). Surprisingly, SIC rise time was similar across all experimental groups even though AMPA currents, which are faster than NMDA currents, are contributing to the SICs in the 17% hACSF experiment (Table 3.1 and Figure 3.1 E). Decay Tau of SICs was significantly longer while blocking AMPA receptors during the 2nd and 3rd application possibly indicating some sort of modulation of AMPA or NMDA

receptors during osmotic stress or NMDARs playing a larger role during the 1st 17% hACSF condition (Table 3.1 and Figure 3.1 F).

After analyzing SICs between experimental groups, they were also compared within each experiment, comparing baseline activity to the three repeated hACSF applications. The frequency of SICs in the 17% hACSF experiment significantly increased during the 1st, 2nd, and 3rd mild osmotic insult compared to the baseline activity (Table 3.1 and Figure 3.1 B). Furthermore, frequency increased in the 2nd and 3rd hACSF applications compared to the 1st application, and increased in the 3rd application compared to the 2nd application (Figure 3.1 B). This data indicates that mild osmotic insult is capable of increasing neuronal excitability whenever it is applied. In addition, neuronal excitability is actually increasing over time with each consecutive hACSF application, implying an inherent increase in tissue excitability. Mild osmotic insult in the presence of NBQX increased the SIC frequency independent of AMPA receptor activation during all three hACSF applications, although the level of significance in the 2nd application period was slightly lower than the other two (Figure 3.1 B). Additionally, SIC frequency in the 3rd application increased compared to the 1st application, possibly indicating an overall increase in tissue excitability over time due to mild osmotic insult (Figure 3.1 B). SICs frequency remained elevated while blocking AMPA receptors, and inhibiting action potentials during all three hACSF applications. The 3rd application was significantly larger than the 2nd application, similar to the other experiments

(Figure 3.1 B). The data suggests that glutamate released during neuronal firing of action potentials, has little to no effect on the overall frequency of SICs during mild osmotic stress. A general trend was observed for SIC amplitude, repeated applications of mild osmotic stress decreased amplitude for all three experimental groups (Table 3.1). For the 17% hACSF group, SIC amplitude decreased in both the 2nd and 3rd hACSF application compared to the 1st; the 3rd application was also significantly smaller compared to the 2nd application (Figure 3.1 C). While blocking of AMPA receptors, amplitude in the 3rd application decreased compared to the 1st and 2nd hACSF applications, indicating an AMPA-independent decrease in amplitude during mild osmotic stress (Figure 3.1 C). Amplitude also significantly decreased in the 3rd application compared to the 1st application when blocking AMPARs and neuronal action potentials, lending support to the idea that glutamate released during neuronal firing of action potentials, under mild osmotic stress may have a limited role in SICs (Figure 3.1 C). Within the 17% hACSF experiment rise time became significantly faster for SICs in the 2nd and 3rd hACSF application compared to the 1st application (Table 3.1 and Figure 3.1 E). However, while blocking AMPARs only the 3rd osmotic stress was significantly faster than the 1st osmotic stress (Figure 3.1 E) . This data suggests that the observable decrease in rise time could potentially be due to some sort modulation of both AMPARs and NMDARs during osmotic stress. Rise time followed a similar trend as the other experiments while blocking neuronal firing SIC rise time was significantly

faster in the 2nd and 3rd applications from the 1st application (Figure 3.1 E). Decay tau decreased from the 1st application to the 2nd and 3rd in the 17% hACSF experiment (Figure 3.1 F). While blocking neuronal firing of action potentials decay tau also significantly decreased in the 2nd and 3rd hACSF applications compared to the 1st application. Overall this data suggests that tissue excitability is changing over time during mild osmotic stress. Both AMPA receptors and NMDA receptors appear to be playing a role in neuronal excitability during mild osmotic stress and potentially may be modulated in some way during this time.

Mild and moderate osmotic stress increases neuronal slow inward currents in neurons above normosmolar controls.

Magnesium was omitted from both normosmolar and hACSF solutions, in the majority of our experiments, in order to remove the magnesium block from NMDA receptors and record SICs. However, in some preparations, low-Mg^{2+} or Mg^{2+}-free solutions alone increase neuronal excitability to the point of seizure activity, and have been frequently used to record excitotoxicity, seizures, and epilepsy (Walther et al., 1986; Jones and Heinemann, 1988). Since our normosmolar ACSF (nACSF) is Mg^{2+}-free, some of the short-term, and potentially long-term changes in neuronal excitability during repeated applications of hACSF could be related to the lack of Mg^{2+} alone. To ensure that the changes in neuronal excitability were due to osmotic stress and not simply an

effect of long-term exposure to the Mg^{2+}-free ACSF was an important consideration. In a control experiment, SICs were recorded from CA1 neurons during long-term continuous application of nACSF (Figure 3.2 A, top trace) then compared to mild, (17% hACSF, Figure 3.2 A, middle trace) and moderate, (40% hACSF, Figure 3.2 A, bottom trace) osmotic stress. Both the normosmolar and hypoosmolar ACSFs contained 1 μM TTX to block neuronal action potentials and 10 μM NBQX to block AMPA receptors in order to match conditions used previously in recordings of SICs in neurons (Fellin et al., 2006; Fiacco et al., 2007). SICs evoked during each period of hACSF were compared to those at equal time points in our control experiment. The nACSF condition alone exhibited the same general trend described by previous researchers of a gradual increase in synaptic noise, baseline current and frequency of NMDA mEPSCs (Tian et al., 2005; Fiacco et al., 2007; Le Meur et al., 2007; Jensen et al., 2015). At nACSF time points 2 and 3 (corresponding to the 2nd and 3rd hACSF applications in experimental conditions), SIC frequency significantly increased compared to the baseline (2nd: $p < 0.01$ and 3rd: $p < 0.01$) as well as the 1st time point (2nd: $p < 0.05$ and 3rd: $p < 0.01$, data not shown) (Table 3.2). SIC frequency was significantly increased during both mild and moderate osmotic insults at all hACSF application time points as compared to the equivalent time points in nACSF controls, with the exception of the 2nd application of 17% hACSF (Table 3.2 and Figure 3.2 B). Thus, the overall increase in SICs during hACSF application is not accounted for by the removal of Mg^{2+} alone. Rather, osmotic

stress significantly increases excitability in CA1 pyramidal neurons through the generation of SICs.

Absolute amplitudes of the SICs evoked in 17% and 40% hACSF ranged from 20.06 to 609.74 pA and 20.03 to 901.79 pA, respectively. On average, these amplitudes were larger than those occurring spontaneously in the nACSF control during the 1st and 2nd application time periods (Table 3.2 and Figure 3.2 C). Amplitudes of SICs evoked in hACSF were not significantly different from control amplitudes by the 3rd application (Figure 3.2 C). The large amplitudes of many SICs, in some cases several hundred pA, are likely sufficient to drive neurons above threshold for firing action potentials, a hypothesis tested in subsequent experiments (chapter 4). Analysis of rise times indicated that SICs occurring in either the 17% or 40% hACSF were significantly slower than SICs observed in the nACSF controls (Figure 3.2 D). The decay taus of SICs were significantly longer on average compared to control for both hACSF doses at all application time points, with the exception of the 2nd application time point for 17% hACSF (Figure 3.2 E). Interestingly, the 2nd application time point for 17% hACSF was also the only time point in which we observed no increase in SIC frequency over baseline (Figure 3.2 B). Analysis of the kinetics over time suggests that the SICs evoked in mild and moderate hypoosmolar conditions are a heterogeneous population, with different types becoming more prominent over the repeated applications of hACSF.

It should be noted that in addition to the above between-group comparisons of hACSF with control, SICs were also analyzed within-group for each of the three individual conditions to examine if there were any changes across the repeated application periods compared to the baseline period in normosmolar ACSF. For both 17% and 40% hACSF, frequency of SICs increased significantly in all application periods, although the level of significance in the 2nd application period was slightly lower than the significance level for the 1st and 3rd application periods compared to baseline. Frequency for the normosmolar ACSF condition was significantly increased in the 2nd and 3rd application time point compared to the baseline and 1st time point, as previously stated. Thus the Mg^{2+}-Free solution alone is increasing neuronal excitability over time and by ~ 20 minutes neuronal excitability has significantly increased over the normal neuronal excitability, which is consistent with what other researcher have found in magnesium-free solutions (Walther et al., 1986; Jones and Heinemann, 1988; Tian et al., 2005). However, the removal of Mg^{2+} alone does not account for the overall increase in SICs during hACSF application. Amplitude decreased from the 1st application to the 3rd application for both the 17% and 40% hACSF groups. For the 40% hACSF only, amplitude also decreased from the 2nd to the 3rd period. Rise time and decay tau also decreased significantly from the 1st application to the 2nd and 3rd application but only the 17% hACSF experiment. No other changes were observed in the SIC kinetics for the 17% or 40% hACSF experiments.

Hypoosmolar ACSF increases neuronal SICs in a dose-dependent manner

Next, we wanted to determine if there is a threshold of hACSF to evoke SICs (i.e. if they are “all-or-none”), and to see if there is a dose-response relationship between reductions in solution osmolarity and SICs. To this end, we recorded whole-cell neuronal currents in normosmolar ACSF for a 10-minute baseline, followed by a 5-minute application of 5%, 10%, 17% or 40% hACSF, before returning again to normosmolar ACSF. SICs were analyzed over the 5-minute evoke period (Figure 3.3 A, grey box) and compared to baseline and across osmolarity conditions. We observed SICs in all the conditions, including (rarely) during the normosmolar ACSF baseline condition (Figure 3.3 B). SIC frequency significantly increased in all the hACSF concentrations even in 5% hACSF compared to baseline (Figure 3.3 C). SIC frequency increased significantly as osmolarity decreased, indicating a clear dose effect of hACSF on neuronal excitability (Figure 3.3 C, D). The resulting linear regression had an R^2 = 0.6136 and can be described as follows y = 0.0948x + 0.4472, where, y is the frequency of SICs per minute and x is the percent decrease in osmolarity. These data suggest that even the smallest reductions in osmolarity are sufficient to increase neuronal excitatory currents independently of neuronal firing, and that this activity increase is strongly dose-dependent. Although rare, the presence of SICs during the baseline period prior to application of hACSF suggests that SICs are a graded phenomenon with no threshold for their initiation.

Neuronal SICs increase in frequency at physiological temperature during osmotic stress.

Temperature plays an important role in cell excitability and metabolism. The extracellular ionic environment has been shown to be modulated by changes in temperature, thus affecting synaptic transmission (Igelmund and Heinemann, 1995). As temperature decreases, cellular metabolism slows down, and neurons become less excitable and completely inhibited at very low temperatures (Heldmaier and Ruf, 1992; Igelmund, 1995; Igelmund and Heinemann, 1995; Carey et al., 2003). In addition, cellular swelling may be effected by temperature as previous studies have determined that as brain temperature increases, intracranial pressure increases and vise versa (Rossi et al., 2001). The previous experiments it this chapter were all conducted at room temperature and although SICs frequency increased during osmotic stress it could potentially be an underestimation of actual neuronal excitability under physiological conditions.

To investigate the temperature sensitivity of neuronal excitability under mild hypoosmolar stress SICs from CA1 pyramidal neurons were recorded during a 17% hACSF plus TTX and NBQX osmotic stress at room temperature (22.74 ± 0.23 °C) and physiological temperature ~ 37 °C for C57BL/6J mice (36.95 ± 0.07 °C) (Talan, 1984). Frequency of SICs/minute was significantly increased at physiological temperature compared to room temperature during all three hACSF applications (Table 3.3 and Figure 3.4 A). SIC frequency within each experiment also significantly increased from baseline conditions to the three hACSF

applications for neurons at room temperature and physiological. Absolute amplitude was similar for both room temperature and physiological temperature. However, within group analysis revealed that amplitude decreased in the 3rd hACSF application compared to the 1st application for the cells at room temperature while amplitude for both the 2nd and 3rd hACSF applications were reduced compared to the 1st application under physiological temperatures (Table 3.3 and Figure 3.4 B). The reduction in amplitude during the repeated osmotic insults could indicate some temperature dependent modulatory mechanism to reduce overall neuronal excitability during osmotic insult. Rise time of SICs was significantly faster at physiological temperature than room temperature during all three hACSF applications (Table 3.3 and Figure 3.4 C). Furthermore for room temperature rise time became faster in the 2nd and 3rd hACSF applications compared to the 1st application. Interestingly, rise time for SICs at physiological temperature was slightly different, while still becoming faster in the 2nd and 3rd hACSF applications compared to the 1st application, it appears to have rebounded in the 3rd application unlike SIC rise time in 3rd application from the room temperature neurons which became faster (Figure 3.4 C). Decay tau of neuronal SICs was significantly longer in the room temperature neurons compared to the neurons at physiological temperature but only for the 1st hACSF application (Table 3.3 and Figure 3.4 D). For SICs recorded from neurons at physiological temperature, no significant change was observed in the decay tau over the three hACSF applications however, decay tau of SICs within the room

temperature cells were faster in the 2nd and 3rd application compared to the 1st application of hACSF (Figure 3.4 D). The results from these experiments suggest that SIC activity at room temperature is an underestimation of the actual SIC activity that would be observed in more physiological conditions.

Neuronal slow inward currents in hACSF are NMDA receptor-dependent and partially non-synaptic

Swelling of brain tissue and subsequent reduction of the extracellular space can increase the ambient glutamate concentration, increasing the likelihood that this non-synaptic glutamate would bind to extrasynaptic receptors. Previous work has shown that SICs evoked by various stimuli may be driven by non-synaptic sources of glutamate (Angulo et al., 2004; Fellin et al., 2004; Kozlov et al., 2006; Fiacco et al., 2007). Along these lines we chose to examine how non-synaptic sources of glutamate influenced excitability in hACSF conditions. Synaptic transmission in the slices was abolished by first incubating slices for 2 hours in bafilomycin A1 (4 μM), an inhibitor of the vacuolar H^+-ATPase responsible for loading synaptic vesicles, prior to recording activity in hACSF; 1 μM bafilomycin A1 (baf) was included in the ACSF during neuronal recordings. Despite the lack of vesicular neurotransmitter release, excitability was still elevated by 17% hACSF +TTX +NBQX +baf (Figure 3.5 A, top trace). Recordings in voltage clamp revealed that the most potent effect of bafilomycin was on SIC frequency in hACSF which was reduced by 40% in the 1st

application, 73% in the 2nd, and 67% in the 3rd hACSF application (Table 3.4 and Figure 3.5 B). In all cases, addition of the NMDA antagonist AP5 (50 μM) virtually eliminated the activity still present in bafilomycin during all hACSF applications, providing further evidence that NMDA receptor activation is necessary for the observed hACSF-induced changes in excitability (Figure 3.5 B). The effect of bafilomycin on SIC frequency suggests that vesicular glutamate release may increase SIC frequency and/or severity.

Hypoosmolar challenge evokes large excitatory slow inward currents in neurons that correlate with real-time volume changes in astrocytes

In a subset of experiments, we examined the immediate timecourse of effects before, during, and after osmotic edema on spontaneous neuronal excitability and real-time astrocyte volume changes in the hippocampus. We hypothesized that during osmotic edema SICs would increase in frequency as astrocyte volume expanded. After osmotic edema, during the "wash," astrocyte volume would decrease and neuronal SICs would be reduced or inhibited. SICs were recorded during mild or moderate stress. Following the hACSF application, the solution was switched back to nACSF for a 5-minute “wash” period. All solutions also contained 1 μM TTX and 10 μM NBQX. Application of 17% or 40% hACSF produced a positive shift in holding current (27.92 ± 3.92 pA in 17%; 42.17 ± 2.34 pA in 40%) and evoked large excitatory SICs within one minute of hACSF application (Figure 3.6 A). Occurrence of SICs over the baseline period

was either nonexistent or extremely infrequent (5/10 cells in 17% hACSF, 7/10 cells in 40% hACSF) (Figure 3.6 B). Frequency of SICs peaked approximately 2 minutes into hACSF treatment regardless of dose, and correspondingly diminished to baseline approximately 2-3 minutes into the wash period (Figure 3.6 B & C). Frequency of SICs evoked in 40% hACSF remained marginally but significantly elevated during the wash period. On average, SICs evoked in hACSF had large amplitudes, which declined significantly over the wash period (Table 3.5 and Figure 3.6 D & E). Kinetics of SICs evoked in hACSF were significantly slower than SICs occurring over the wash periods (Table 3.3 and Figure 3.6 F & G). Rise times of SICs in the moderate osmotic insult were significantly faster compared to mild osmotic stress, but were slower during the wash period. These findings suggest that slow inward currents are one of the first events occurring during acute osmotic edema to increase neuronal excitability.

The slow kinetics of SICs observed in hACSF support the notion that hACSF slowed glutamate diffusion through a compressed extracellular space. If this is the case, we would expect to observe significant cellular edema within 2 minutes of hACSF application (when SIC frequency peaks). Astrocytes in particular are capable of swelling during long periods of reduced osmolarity and have been reported to swell selectively in such conditions (Andrew et al., 2007; Risher et al., 2009). Examination of astrocyte volume in our conditions (by another graduate student in the lab, Tom Murphy) revealed that hACSF induced rapid swelling of astrocytes within the first minute of hACSF application (Figure

3.6 H & I). Astrocyte volume increased most rapidly over the first 1-2 minutes after exposure to hACSF. This time course closely mirrored the frequency and amplitude distributions of SICs (Figure 3.6 C & E), suggesting that astrocyte swelling may be important for reduction of the ECS and generation of SICs in the early stages of osmotic edema.

Discussion

Cellular swelling underlies one of two forms of cerebral edema, which is defined by excess accumulation of fluid in brain tissue. Common to virtually all neurological disorders and disease is toxicity and cell death brought on by increased and unchecked neuronal excitability. Studies suggest that osmotic edema contributes significantly to excitability of neurons in pathological conditions; so much so that cell swelling precedes the onset of seizures (Traynelis and Dingledine, 1988; Andrew et al., 1989; Rosen and Andrew, 1990; Binder et al., 2004). Despite the importance of cellular edema to brain pathology, the specific effects of acute cell swelling on neuronal excitability have not been clearly delineated. Here we demonstrate that one of the first effects of acute osmotic stress in hippocampal CA1 neurons are NMDA receptor dependent slow inward currents. Even small changes in osmolarity are sufficient to significantly elevate excitability of CA1 pyramidal neurons. Osmotic insult and is slow inward currents within approximately one minute in hACSF solution. Furthermore, SICs are elicited by both mild and moderate osmotic stress along the same timescale

as astrocytic swelling. SICs are NMDA-dependent, however, mild osmotic stress and action potentials evoked in neurons do not require activation of AMPA receptors, and may be largely nonsynaptic in origin. However, the frequency of SICs significantly decreased due to blockade of AMPA receptors in the baseline and all three repeated hypoosmolar applications. This indicates that AMPA receptors were also activate during mild osmotic stress, as other researchers have observed in different models of edema (Traynelis and Dingledine, 1988; Tian et al., 2005; Risher et al., 2009; Zhou et al., 2010), Physiological temperature, not surprisingly, increased SIC frequency compared to room temperature during all three hACSF applications. All studies of SICs, regardless of proposed mechanism, have found that they are mediated by NMDA receptors. In the present study, we also observed that NMDA receptors are responsible for SICs as they are, blocked by both DL-AP5.

Neuronal slow inward currents are a particularly interesting case of excitability to study in osmotic challenge because they are NMDA-dependent, TTX-independent, and have been suggested to originate from astrocytic glutamate release (Angulo et al., 2004; Fellin et al., 2004; Kozlov et al., 2006). It has been debated whether such currents represent normal or pathological activity (Angulo et al., 2004; Tian et al., 2005; Wetherington et al., 2008). In support of the latter interpretation, we found an approximately linear relationship between reductions in osmolarity and SIC frequency; even 5% hypoosmotic stress was sufficient to generate a significant increase in SICs. Rise time and

decay tau of SICs were both significantly longer during application of 17% or 40% hACSF compared to baseline. Interestingly, the kinetics of SICs evoked by repeated hACSF applications were not static. Rather, they tended to become shorter in subsequent hACSF applications. Amplitude of SICs also increased substantially in the 1st evoke with hACSF, but declined to baseline levels by the 3rd application; however, SIC frequency remained elevated.

Overall, the changes in SICs during cell swelling demonstrate that osmotic edema is a dynamic process, with several possible avenues to explore in regard to underlying mechanisms. Our findings suggest that increases in neuronal excitability may have two distinct components: an "acute" phase, and a "chronic" phase. The "acute" phase occurs during the first application of hACSF and is dominated by large, frequent currents with slow rise times and decay taus. These events may be induced by GluN2D subunit-containing NMDA receptors in juvenile mice. The "chronic" phase, occurring during 2nd and 3rd period of cell swelling, is characterized by a more moderate increase in SIC frequency and slightly faster rise times which may represent activity through GluN2A subunit NMDA receptors. Such changes could occur through changes in NMDA receptor channel opening probability, receptor subunit composition or internalization of receptors (Meldrum et al., 1999; Pawlak et al., 2005; Auzmendi et al., 2008). These phases could also reflect changes in extracellular glutamate concentration. Neuronal and astrocytic glutamate sources may become depleted

during the acute phase with insufficient time between subsequent hACSF applications for these stores to replenish.

As observed in other studies, hACSF induced a rapid and significant increase in astrocyte volume. However, the degree of swelling we observed was smaller compared to earlier studies. Risher et al (2009) observed an astrocyte volume increase of approximately 12.8% after 5 minutes of -40 mOsm ACSF (approximately 14% hypoosmolar from baseline). In contrast, we observed a similar degree of astrocyte swelling only in 40% hypoosmolar ACSF. Seventeen percent hACSF produced only a 5% increase in astrocyte volume in the present study, less than half what was reported by Risher et al, despite being a more mild osmotic stress. Minor differences in methodology could partially account for these discrepancies. For example, Risher and colleagues worked at physiological temperature and used a more rapid solution exchange rate, which would likely speed up the volume response of astrocytes. By contrast, Hirrlinger et al (2008), who used an exchange rate and temperature similar to ours, observed little or no volume increase within the first 5-7 minutes of a 35% hypoosmotic challenge. Differences in analytical methods also cannot be ruled out. We have observed that the measurements of cell soma size are extremely sensitive to the type of automated thresholding method applied. We chose the method used in the current study because it provided the most accurate and consistent representation of volume changes in the cell soma. Certain other

thresholding methods (for example, "default") often produce measurements more in line with Risher and colleagues. Finally, inclusion of TTX in our conditions may have inhibited astrocyte swelling. By blocking neuronal firing we also inhibited the majority of neurotransmitter release, to which astrocytes are normally responsive owing to their complement of metabotropic receptor types (Porter and McCarthy, 1996; Shelton and McCarthy, 1999). The Gq family of metabotropic receptors is reported to target a phosphorylation site on AQP4 and increase astrocyte water permeability accordingly (Gunnarson et al., 2008, 2009).

Overall, these findings carry important implications for understanding the early events triggering excitotoxicity in the diseased or damage brain. Future studies will focus on understanding the specific contributions of astrocytes vs. neurons to acute excitability increases triggered by cellular edema.

Figure 3.1

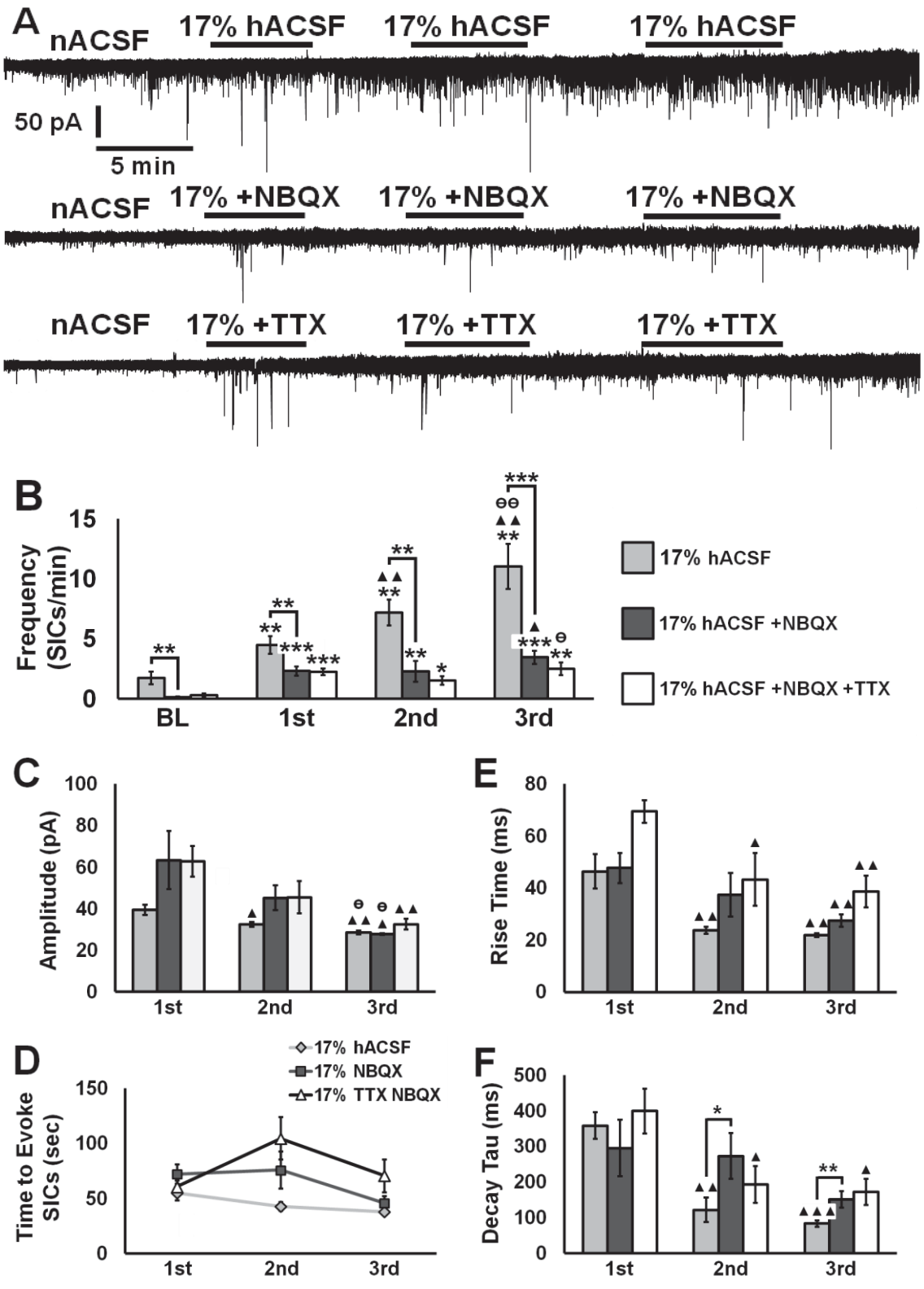
A
nACSF
17% hACSF
17% hACSF
17% hACSF
50 pA
5 min
nACSF
17% +NBQX
17% +NBQX
17% +NBQX
nACSF
17% +TTX
17% +TTX
17% +TTX
B
Frequency (SICs/min)
15
10
5
0
BL
1st
2nd
3rd
17% hACSF
17% hACSF +NBQX
17% hACSF +NBQX +TTX
C
Amplitude (pA)
100
80
60
40
20
0
1st
2nd
3rd
E
Rise Time (ms)
80
60
40
20
0
1st
2nd
3rd
D
17% hACSF
17% NBQX
17% TTX NBQX
Time to Evoke SICs (sec)
150
100
50
0
1st
2nd
3rd
F
Decay Tau (ms)
500
400
300
200
100
0
1st
2nd
3rd

Figure 3.1 AMPA receptors contribute to neuronal excitability during hypoosmolar stress. Asterisks directly above columns indicate significance to the baseline (BL) while the triangles indicate significance to the 1st application, the theta symbol represents significance to the 2nd application, and asterisks above the bars comparing groups indicate a difference between groups. Recordings from CA1 pyramidal neurons in the hippocampus during repeated hypoosmolar application; 17% hACSF (top), 17% hACSF with NBQX (10 μM) (middle), and 17% hACSF with TTX (1 μM) and NBQX (bottom) (A). Application of hACSF increased the frequency of SICs in all of the conditions compared to baseline. In addition, blockade of AMPA receptors with NBQX significantly decreased neuronal excitability due to hypoosmolar stress in the baseline, 1st, 2nd, and 3rd 17% hACSF application compared to 17% hACSF alone (B). Amplitude of SIC like currents decreased from the 1st application of 17% hACSF to the 3rd application in all conditions, while the 2nd application in the 17% hACSF condition alone was reduced compared to the 1st application. Furthermore, amplitude decreased in the 3rd application of both the 17% hACSF, and 17% hACSF plus NBQX compared to the 2nd application of hACSF (C). The time to evoke SIC like currents was similar in all of the hACSF conditions (D). Rise time of SIC like currents was faster in the 2nd application compared to the 1st application for both the 17% hACSF and 17% hACSF with TTX and NBQX condition compared to the 1st application. However rise time was significantly faster for all the hACSF conditions in the 3rd application of hACSF compared to the 1st application (E). Decay Tau was significantly faster in the 2nd application and 3rd application of hACSF compared to the 1st application for both the 17% hACSF, and 17% hACSF with TTX and NBQX condition. In addition, decay tau of SICs was significantly slower in the 17% hACSF plus NBQX condition compared to the 17% hACSF condition in both the 2nd and 3rd application of hACSF (F). Statistical significance for all figures (*$p < 0.05$), and (**$p < 0.01$), and (***$p < .001$) same for triangles and theta; n = 9 to 10 cells per group.

Table 3.1

Frequency (SICs/min)				
Group	Baseline	1st App	2nd App	3rd App
17% hACSF	1.75 ± 0.53	4.48 ± 0.74	7.20 ± 1.08	11.06 ± 1.88
17% +NBQX	0.15 ± 0.07	2.32 ± 0.38	2.30 ± 0.85	3.47 ± 0.54
17% +NBQX +TTX	0.29 ± 0.14	2.25 ± 0.26	1.55 ± 0.36	2.52 ± 0.53
Amplitude (pA)				
Group	Baseline	1st App	2nd App	3rd App
17% hACSF	35.84 ± 7.02	39.49 ± 2.47	32.4 ± 1.2	28.63 ± 0.96
17% +NBQX	29.01 ± 6.99	63.42 ± 13.89	45.24 ± 5.93	27.77 ± 0.43
17% +NBQX +TTX	36.16 ± 12.1	62.86 ± 7.37	45.51 ± 7.82	32.49 ± 2.59
Time to Evoke (sec)				
Group	Baseline	1st App	2nd App	3rd App
17% hACSF		55.04 ± 6.68	42.95 ± 3.85	38.13 ± 2.45
17% +NBQX		72.1 ± 8.8	75.86 ± 16.94	45.76 ± 6.09
17% +NBQX +TTX		60.63 ± 5.74	104.52 ± 19.29	70.58 ± 14.87
Rise Time (ms)				
Group	Baseline	1st App	2nd App	3rd App
17% hACSF	14.31 ± 3.12	46.35 ± 6.65	23.65 ± 1.36	21.83 ± 0.66
17% +NBQX	4.46 ± 2.4	47.67 ± 5.72	37.37 ± 8.39	27.48 ± 2.38
17% +NBQX +TTX	20.85 ± 10.92	69.46 ± 4.35	43.31 ± 10.22	38.69 ± 6.10
Decay Tau (ms)				
Group	Baseline	1st App	2nd App	3rd App
17% hACSF	44.13 ± 16.28	358.21 ± 37.52	122.2 ± 35.04	83.56 ± 8.61
17% +NBQX	11.47 ± 8.62	295.62 ± 79.03	273.23 ± 64.76	150.81 ± 23.34
17% +NBQX +TTX	242.77 ± 156.08	398.99 ± 62.78	193.66 ± 51.46	172.86 ± 36.84

Table 3.1: Frequency and kinetics of SICs, contributions of mild osmotic stress, AMPA receptors, and neuronal firing of action potentials. Numbers indicate mean plus SE for SIC frequency, amplitude, time to evoke, rise time and decay tau during baseline activity and three repeated applications of hACSF for three experimental conditions including; 17% hACSF, 17% hACSF +NBQX, and 17% hACSF +NBQX +TTX.

Figure 3.2

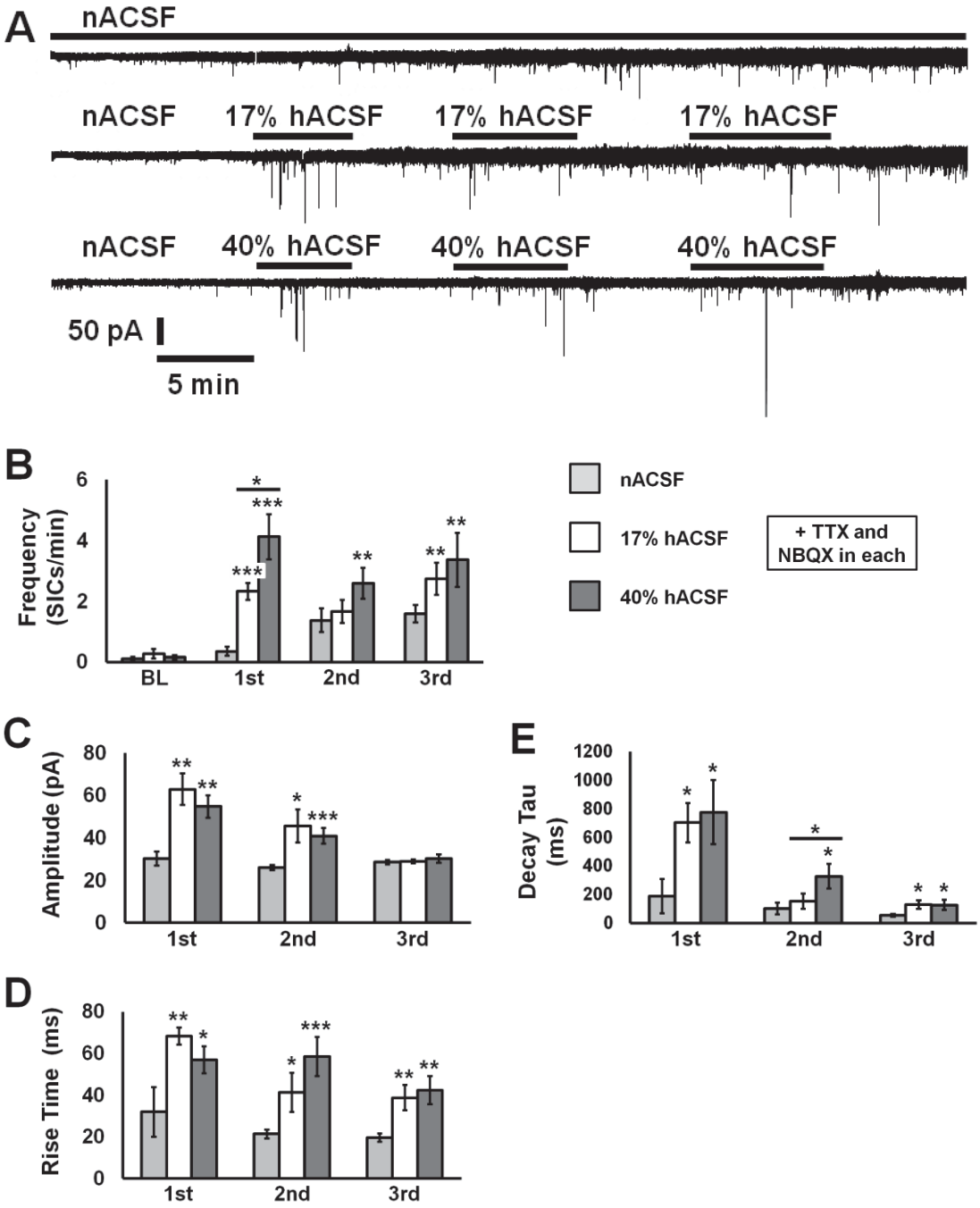
A
nACSF
nACSF
17% hACSF
17% hACSF
17% hACSF
nACSF
40% hACSF
40% hACSF
40% hACSF
50 pA
5 min
B
Frequency (SICs/min)
BL
1st
2nd
3rd
nACSF
17% hACSF
40% hACSF
+ TTX and NBQX in each
C
Amplitude (pA)
D
Rise Time (ms)
E
Decay Tau (ms)

Figure 3.2: Large neuronal SICs are evoked in hypoosmolar conditions. Whole-cell voltage clamp recordings of neuronal excitatory currents in TTX (1 μM) and NBQX (10 μM) in normosmolar ACSF throughout (A, top); plus the effect of 17% hACSF (A, middle) or 40% hACSF (A, bottom). Frequency of SICs increased during the 1st and 3rd application of 17% hACSF compared to normosmolar ACSF, while in 40% hACSF, SICs increased during the 1st, 2nd and 3rd applications compared to the same time period in normosmolar ACSF (B). Amplitude of SICs was significantly larger in the 1st and 2nd applications of 17% and 40% hACSF compared to normosmolar ACSF (C). Rise time of SICs was slower in both hACSF conditions compared to normosmolar ACSF during all three time periods (D). Decay tau of SICs evoked in 17% and 40% hACSF were significantly slower across all application time points compared to normosmolar ACSF, with the exception of the second application of 17% hACSF (E). Note, only comparisons between groups are displayed. Statistical significance for all figures (*$p < 0.05$), (**$p < 0.01$) (***$p < 0.001$); n = 4 to 10 cells per group.

Table 3.2

Frequency (SICs/min)				
Group	**Baseline**	**1st App**	**2nd App**	**3rd App**
nACSF	0.11 ± 0.07	0.36 ± 0.16	1.37 ± 0.39	1.59 ± 0.29
17% hACSF	0.27 ± 0.16	2.33 ± 0.28	1.66 ± 0.38	2.75 ± 0.53
40% hACSF	0.16 ± 0.08	4.13 ± 0.74	2.59 ± 0.51	3.36 ± 0.89
Amplitude (pA)				
Group	**Baseline**	**1st App**	**2nd App**	**3rd App**
nACSF		30.18 ± 3.35	26.08 ± 1.18	28.55 ± 1.00
17% hACSF		62.86 ± 7.37	45.51 ± 7.82	28.88 ± 0.93
40% hACSF		54.73 ± 5.25	40.90 ± 3.70	30.26 ± 1.95
Rise Time (ms)				
Group	**Baseline**	**1st App**	**2nd App**	**3rd App**
nACSF		31.9 ± 11.99	21.32 ± 2.05	19.5 ± 1.98
17% hACSF		68.24 ± 4.07	41.25 ± 9.37	38.69 ± 6.10
40% hACSF		56.94 ± 6.48	58.37 ± 9.36	42.27 ± 6.69
Decay Tau (ms)				
Group	**Baseline**	**1st App**	**2nd App**	**3rd App**
nACSF		189.18 ± 120.16	100.3 ± 41.18	52.68 ± 10.55
17% hACSF		701.91 ± 138.32	151.31 ± 52.10	128.8 ± 30.67
40% hACSF		775.1 ± 224.8	326.23 ± 86.34	125.99 ± 34.31

Table 3.2: Mean and SE for frequency, amplitude, rise time and decay tau of SICs during a continuous application nACSF, mild, and moderate osmotic stress.

Figure 3.3:

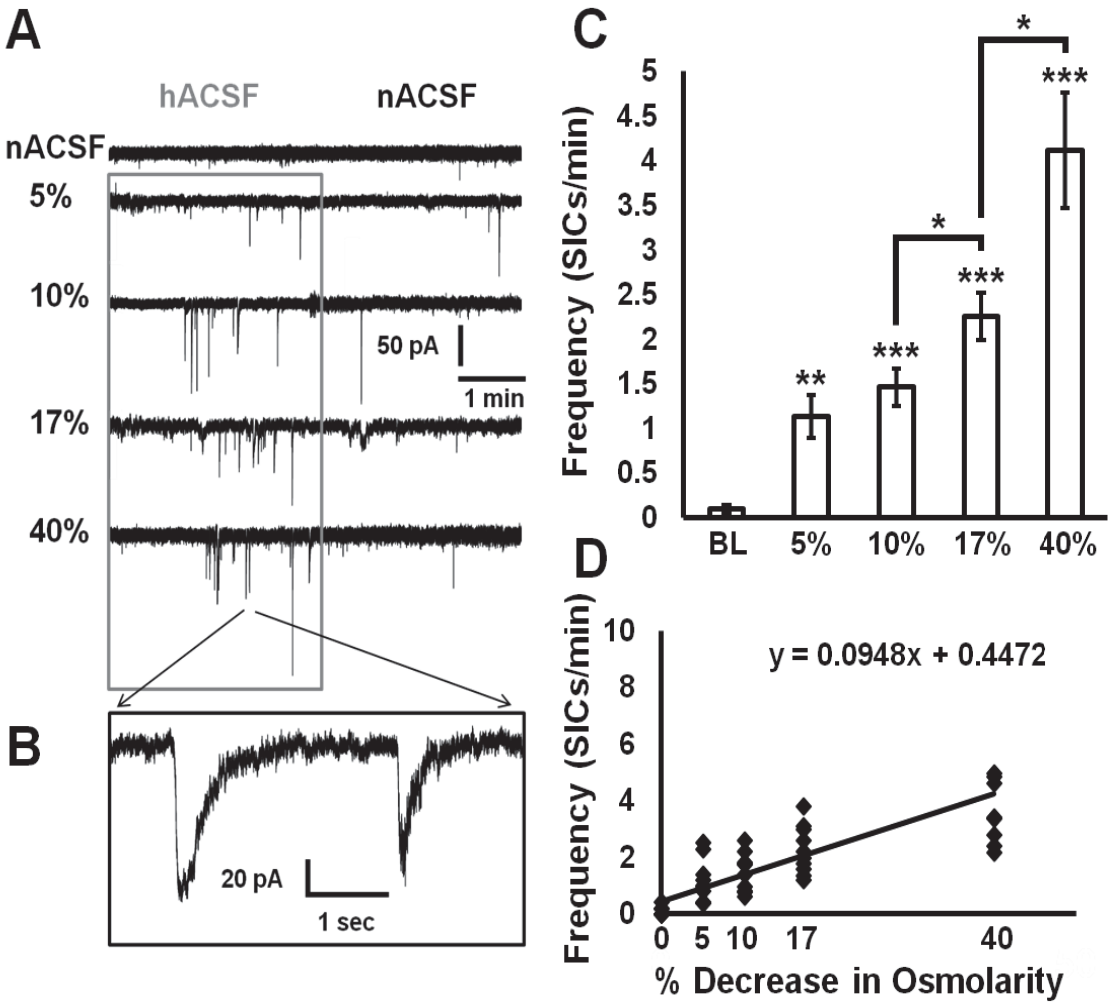

Figure 3.3: Hypoosmolar ACSF increases neuronal SICs in a dose-dependent manner. Electrophysiological whole-cell recordings of SICs from neurons over the same time course (10 minutes) in nACSF, as well as 5, 10, 17, and 40% hACSF (gray box) (5 minutes) followed by the 5 minute wash period in nACSF (A). Representative trace from the 40% hACSF, demonstrating the characteristic size and timecourse of SICs evoked during hACSF application (B). Frequency of SICs per minute was significantly elevated over baseline during a 5 minute application of 5, 10, 17, and 40% hACSF (C). Scatter plot of frequency of SICs per minute for each cell as osmolarity decreased demonstrates a near linear dose-response relationship (R^2 = .6123) between hypoosmolarity and neuronal excitability (D). (*$p < 0.05$; **$p < 0.01$; and ***$p < 0.001$); n = 10 cells per group.

Figure 3.4

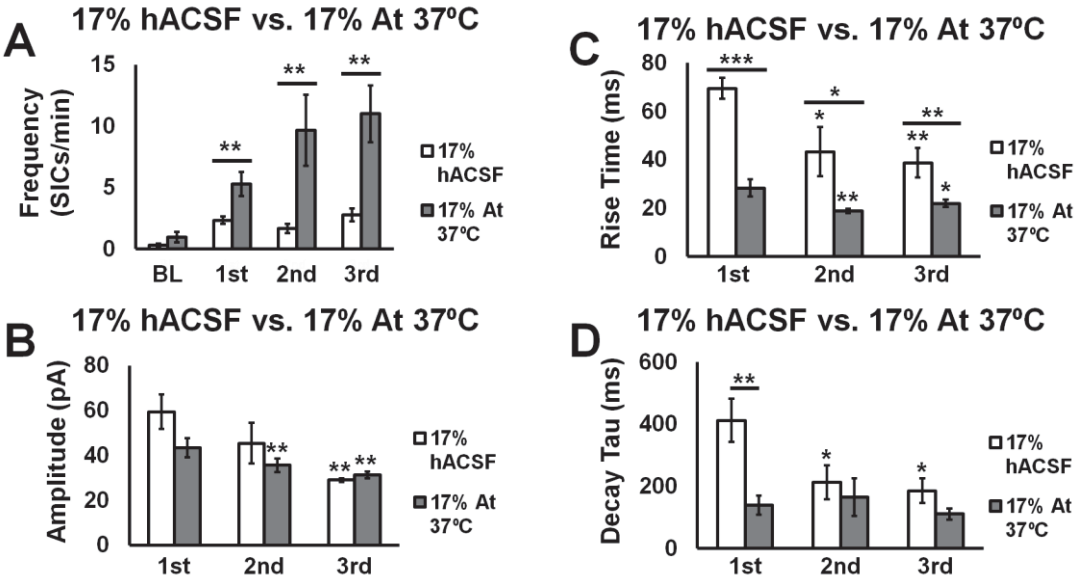

Figure 3.4: Neuronal excitability at physiological and room temperature during osmotic stress. Frequency of SICs increases significantly for the 1st, 2nd, and 3rd hACSF applications under physiological condition compared to room temperature (A). The absolute amplitude of SICs was similar under physiological and room temperature, however amplitude decreased within both room temperature and physiological temperature in the 3rd hACSF application compared to the 1st. In addition, amplitude of SICs also decreased in the 2nd hACSF application compared to the 1st, but only in the neurons at physiological temperature (B). The rise time of neuronal SICs, at physiological temperature was significantly faster than the rise time at room temperature during all three hACSF applications. Rise time of SICs also became significantly faster in the 2nd and 3rd hACSF applications compared to the 1st application for both the room temperature and physiological temperature experiments (C). The neurons exposed to osmotic stress at physiological temperature had a significantly faster decay tau for SIC than the neurons at room temperature, but only during the 1st application of hACSF. Interestingly, decay tau within the room temperature cells decreased in the 2nd and 3rd application compared to the 1st application of hACSF, however no significant change was observed in the decay tau for SICs within the neurons recorded at physiological temperature (D). (*$p < 0.05$; **$p < 0.01$, and ***$p < 0.001$); n = 8-9 cells per group.

Table 3.3

Frequency (SICs/min)				
Group	**Baseline**	**1st App**	**2nd App**	**3rd App**
17% hACSF	0.27 ± 0.16	2.33 ± 0.28	1.66 ± 0.38	2.75 ± 0.53
17% At 37 ºC	0.95 ± 0.42	5.26 ± 0.98	9.64 ± 2.89	10.99 ± 2.31
Amplitude (pA)				
Group	**Baseline**	**1st App**	**2nd App**	**3rd App**
17% hACSF		59.37 ± 7.77	45.30 ± 9.02	28.88 ± 0.93
17% At 37 ºC		43.39 ± 4.27	35.51 ± 2.96	31.25 ± 1.61
Rise Time (ms)				
Group	**Baseline**	**1st App**	**2nd App**	**3rd App**
17% hACSF		69.46 ± 4.35	43.31 ± 10.22	38.69 ± 6.10
17% At 37 ºC		28.27 ± 3.57	18.69 ± 0.85	21.93 ± 1.59
Decay Tau (ms)				
Group	**Baseline**	**1st App**	**2nd App**	**3rd App**
17% hACSF		411.43 ± 69.78	211.62 ± 54.68	185.27 ± 39.33
17% At 37 ºC		139.70 ± 30.72	164.31 ± 60.36	110.22 ± 17.00

Table 3.3: Neuronal SICs during mild osmotic stress at room and physiological temperature. Mean and SE for SIC frequency, amplitude, rise time, and decay tau before and during 3 repeated applications of mild osmotic stress at room and physiological temperature.

Figure 3.5

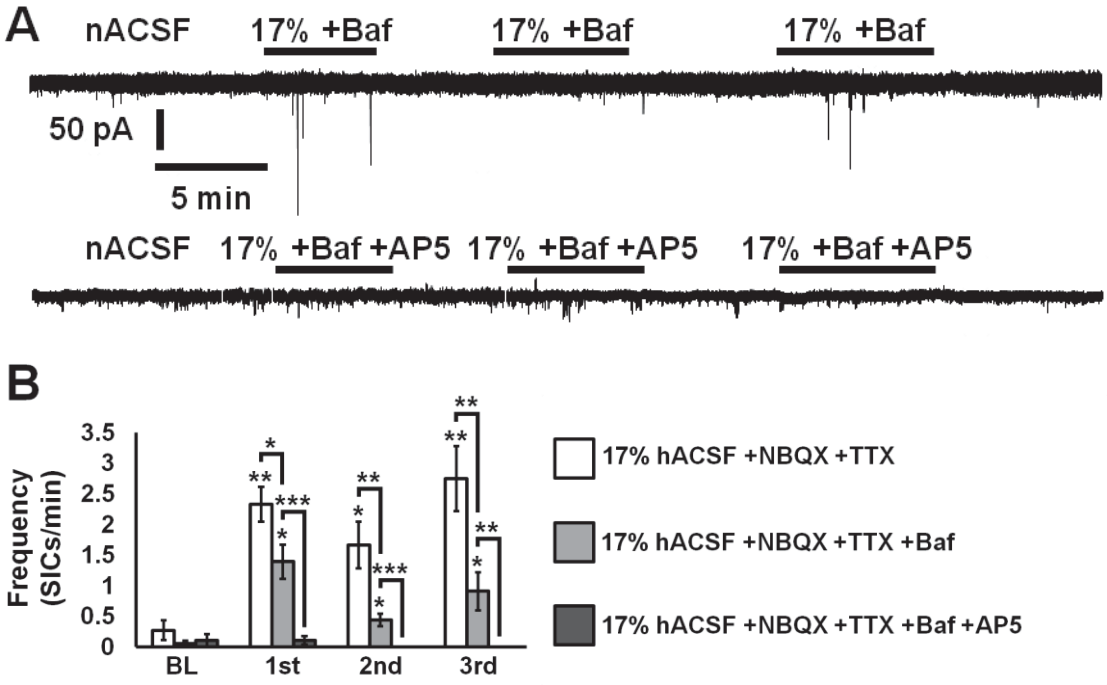

Figure 3.5 Synaptic and non-synaptic components of SICs during osmotic edema. Voltage clamp recordings of neuronal membrane currents in bafilomycin (A, upper trace) and bafilomycin (baf) + 50 μM AP5 (A, lower trace). The nACSF always contained the same concentrations of NBQX (10 μM), TTX (1 μM), baf and AP5 as the 17% hACSF condition. Frequency of SICs was also significantly elevated non-synaptically in all three hACSF applications but not quite to the extent observed with synaptic activity intact (B). SICs were nearly completely blocked by AP5. The data suggest that some portion of SICs may be due to activation of postsynaptic NMDARs. (*$p < 0.05$; **$p < 0.01$; and ***$p < 0.001$); n = 9 cells per group.

Table 3.4

Frequency (SICs/min)				
Group	**Baseline**	**1st App**	**2nd App**	**3rd App**
17% +NBQX +TTX	0.27 ± 0.16	2.33 ± 0.28	1.66 ± 0.38	2.75 ± 0.53
17% +NBQX +TTX +baf	0.05 ± 0.05	1.39 ± 0.28	0.44 ± 0.10	0.91 ± 0.31
17% +NBQX +TTX +baf +AP5	0.11 ± 0.11	0.11 ± 0.07	0 ± 0	0 ± 0

Table 3.4: Mean and SE for frequency of SICs during mild osmotic stress while blocking vesicular release of neurotransmitters, and NMDA receptors.

Figure 3.6

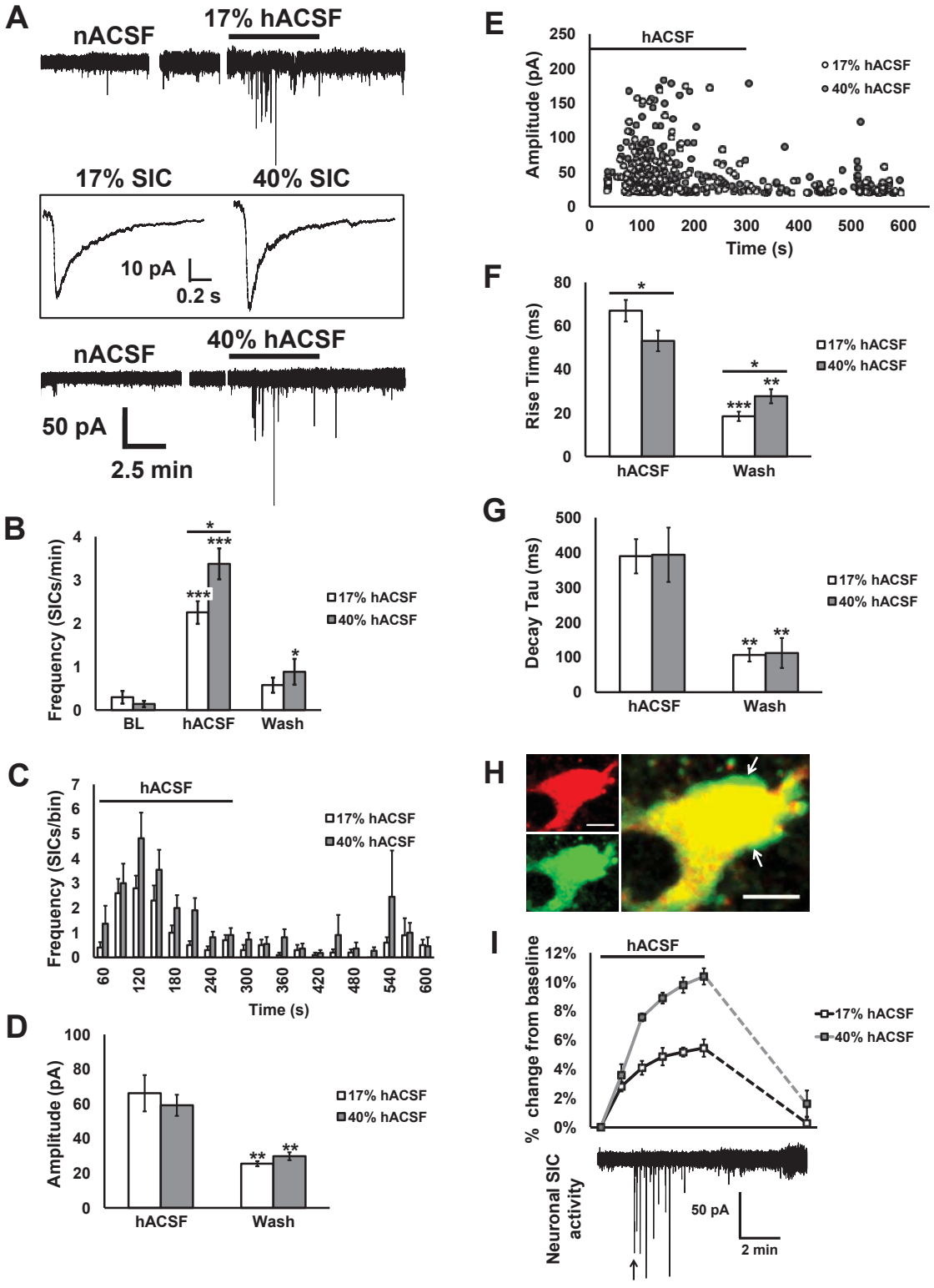
A
nACSF
17% hACSF
17% SIC
40% SIC
10 pA
0.2 s
nACSF
40% hACSF
50 pA
2.5 min
B
Frequency (SICs/min)
BL
hACSF
Wash
17% hACSF
40% hACSF
C
hACSF
Frequency (SICs/bin)
Time (s)
17% hACSF
40% hACSF
D
Amplitude (pA)
hACSF
Wash
17% hACSF
40% hACSF
E
hACSF
Amplitude (pA)
Time (s)
17% hACSF
40% hACSF
F
Rise Time (ms)
hACSF
Wash
17% hACSF
40% hACSF
G
Decay Tau (ms)
hACSF
Wash
17% hACSF
40% hACSF
H
I
hACSF
% change from baseline
17% hACSF
40% hACSF
Neuronal SIC activity
50 pA
2 min

Figure 3.6: Large neuronal SICs are evoked by hypoosmolar ACSF and occur during astrocyte volume increases. (A) Whole-cell voltage clamp recordings of neuronal excitatory currents in TTX (1 μM) and NBQX (10 μM) in normosmolar ACSF (nACSF; baseline condition) and in 17% or 40% hypoosmolar ACSF (hACSF). Switch from normosmolar to hACSF evoked SICs in neurons within approximately 60 seconds on average. Note that most SICs were evoked within the first few minutes of hACSF application. SICs evoked during hACSF application are averaged and shown in the inset for each condition. (B) Summary histogram of SIC frequency during hACSF application compared to the baseline and wash period. SICs continued to occur during the wash period but at a much lower rate. Frequency of SICs was greater in 40% compared to 17% hACSF. (C) Frequency of SICs analyzed in 30s bins over the hACSF and wash periods indicates that most SICs occur in the early part of the hACSF application, peak at about 120s and gradually decline. SICs occurring during the wash period were more variable. (D) There was no difference in the amplitude of SICs on average between 17% and 40% hACSF. Amplitudes of SICs in both conditions were significantly larger compared to SICs occurring over the wash period. (E) Scatter plot of amplitudes of all SICs occurring during the hACSF and wash periods reveals that most large amplitude SICs occurred during osmotic challenge, although overall amplitudes were highly variable. (F, G) SICs occurring during hACSF application had very slow kinetics, with rise times of 50-60 ms and decay taus around 380 ms. These kinetics were significantly slower compared to SICs occurring over the wash period. (H) Baseline images of astrocytes loaded with fluorescent dextran, after 10-minutes in normosmolar ACSF (upper left panel) and 5-minutes in 40% hACSF (lower left panel). Right panel is overlay, with arrows indicating regions of the astrocyte soma with expanded volume. Images are pseudo-colored to differentiate between nACSF and hACSF conditions. (I) Volume changes in astrocytes quantified as percent change from baseline in one minute intervals. Significant increase in astrocyte volume occurred within one minute in both 17% and 40% hACSF. Astrocyte volume continued to rise throughout the 5-minute application of hACSF, and recovered to baseline after a 5-minute wash period in nACSF. Note that astrocyte volume increases initiated prior to SICs evoked in adjacent neurons, and that SICs occur *while astrocyte volume is increasing*. (*$p < 0.05$; **$p < 0.01$, and ***$p < 0.001$); Neurons, n = 10 cells per group; Astrocytes, n = 7-8 cells per group. Scale bars, 5 μm.

Table 3.5

Frequency (SICs/min)			
Group	**Baseline**	**hACSF**	**Wash**
17% hACSF	0.29 ± 0.14	2.25 ± 0.26	0.57 ± 0.17
40% hACSF	0.14 ± 0.07	3.37 ± 0.36	0.88 ± 0.30
Amplitude (pA)			
Group	**Baseline**	**hACSF**	**Wash**
17% hACSF		66.15 ± 10.49	25.53 ± 1.50
40% hACSF		59.19 ± 6.09	29.82 ± 2.26
Rise Time (ms)			
Group	**Baseline**	**hACSF**	**Wash**
17% hACSF		67.01 ± 4.96	18.49 ± 2.16
40% hACSF		53.14 ± 4.75	27.70 ± 3.25
Decay Tau (ms)			
Group	**Baseline**	**hACSF**	**Wash**
17% hACSF		389.47 ± 49.02	106.92 ± 18.73
40% hACSF		393.61 ± 77.85	112.41 ± 42.99

Table 3.5: Neuronal excitability before, during, and after mild or moderate osmotic stress. SIC frequency, amplitude, rise time, and decay tau before, during a 17% or 40% hACSF application, and after hACSF applications, all numbers are mean ± SE.

References

Andrew RD, Fagan M, Ballyk B a, Rosen a S (1989) Seizure susceptibility and the osmotic state. Brain Res 498:175–180.

Andrew RD, Labron MW, Boehnke SE, Carnduff L, Kirov SA (2007) Physiological Evidence That Pyramidal Neurons Lack Functional Water Channels. Cereb Cortex 17:787–802.

Andrew RD, MacVicar B a (1994) Imaging cell volume changes and neuronal excitation in the hippocampal slice. Neuroscience 62:371–383.

Angulo MC, Kozlov AS, Charpak S, Audinat E (2004) Glutamate released from glial cells synchronizes neuronal activity in the hippocampus. J Neurosci 24:6920–6927.

Auzmendi J, González N, Girardi E (2008) The NMDAR Subunit NR2B Expression is Modified in Hippocampus after Repetitive Seizures. Neurochem Res 34:819–826.

Azouz R, Alroy G, Yaari Y (1997) Modulation of endogenous firing patterns by osmolarity in rat hippocampal neurones. :175–187.

Balestrino M, Young J, Aitken P (1999) Block of (Na+,K+)ATPase with ouabain induces spreading depression-like depolarization in hippocampal slices. Brain Res 838:37–44.

Binder DK, Papadopoulos MC, Haggie PM, Verkman a S (2004) In vivo measurement of brain extracellular space diffusion by cortical surface photobleaching. J Neurosci 24:8049–8056.

Carey H V, Andrews MT, Martin SL (2003) Mammalian Hibernation : Cellular and Molecular Responses to Depressed Metabolism and Low Temperature. :1153–1181.

Fellin T, Gomez-Gonzalo M, Gobbo S, Carmignoto G, Haydon PG (2006) Astrocytic glutamate is not necessary for the generation of epileptiform neuronal activity in hippocampal slices. J Neurosci 26:9312–9322.

Fellin T, Pascual O, Gobbo S, Pozzan T, Haydon PG, Carmignoto G (2004) Neuronal synchrony mediated by astrocytic glutamate through activation of extrasynaptic NMDA receptors. Neuron 43:729–743.

Fiacco TA, Agulhon C, Taves SR, Petravicz J, Casper KB, Dong X, Chen J, McCarthy KD (2007) Selective Stimulation of Astrocyte Calcium In Situ Does Not Affect Neuronal Excitatory Synaptic Activity. Neuron 54:611–626.

Fishman RA (1975) Brain edema. N Engl J Med 293:706–711.

Gómez-Gonzalo M, Losi G, Chiavegato A, Zonta M, Cammarota M, Brondi M, Vetri F, Uva L, Pozzan T, de Curtis M, Ratto GM, Carmignoto G (2010) An excitatory loop with astrocytes contributes to drive neurons to seizure threshold. PLoS Biol 8:e1000352.

Gunnarson E, Song Y, Kowalewski JM, Brismar H, Brines M, Cerami A, Andersson U, Zelenina M, Aperia A (2009) Erythropoietin modulation of astrocyte water permeability as a component of neuroprotection. Proc Natl Acad Sci U S A 106:1602–1607.

Gunnarson E, Zelenina M, Axehult G, Song Y, Bondar A, Krieger P, Brismar H, Zelenin S, Aperia A (2008) Identification of a molecular target for glutamate regulation of astrocyte water permeability. Glia 56:587–596.

Han D, Sun M, He P-P, Wen L-L, Zhang H, Feng J (2015) Ischemic Postconditioning Alleviates Brain Edema After Focal Cerebral Ischemia Reperfusion in Rats Through Down-Regulation of Aquaporin-4. J Mol Neurosci.

Haskew-Layton RE, Rudkouskaya A, Jin Y, Feustel PJ, Kimelberg HK, Mongin A a (2008) Two distinct modes of hypoosmotic medium-induced release of excitatory amino acids and taurine in the rat brain in vivo. PLoS One 3:e3543.

Heldmaier G, Ruf T (1992) Body temperature and metabolic rate during natural hypothermia in endotherms. :696–706.

Hirrlinger PG, Wurm A, Hirrlinger J, Bringmann A, Reichenbach A (2008) Osmotic swelling characteristics of glial cells in the murine hippocampus, cerebellum, and retina in situ. J Neurochem 105:1405–1417.

Ho M-L, Rojas R, Eisenberg RL (2012) Cerebral edema. AJR Am J Roentgenol 199:W258–73.

Hyzinski-García MC, Vincent MY, Haskew-Layton RE, Dohare P, Keller RW, Mongin A a (2011) Hypo-osmotic swelling modifies glutamate-glutamine cycle in the cerebral cortex and in astrocyte cultures. J Neurochem 118:140–152.

Igelmund P (1995) Modulation of synaptic transmission at low temperatures by hibernation related changes in ionic microenvironment in hippocampal slices of golden hamsters.pdf. Cryobiology 32:334–343.

Igelmund P, Heinemann U (1995) Synaptic transmission and paired-pulse behaviour of CA1 pyramidal cells in hippocampal slices from a hibernator at low temperature : importance of ionic environment. 689:9–20.

Jarvis CR, Anderson TR, Andrew RD (2001) Anoxic depolarization mediates acute damage independent of glutamate in neocortical brain slices. Cereb Cortex 11:249–259.

Jensen FE, Wang C, Stafstrom CE, Liu Z, Geary C, Stevens MC, Rakhade SN, Fitzgerald EF, Klein PM, Zhou C, Sun H, Richard L, Jensen FE, Jun HY, Yeom Y Il, Park SH, Kim KH, Shin H, Kim D (2015) Acute and Chronic Increases in Excitability in Rat Hippocampal Slices After Perinatal Hypoxia In Vivo Acute and Chronic Increases in Excitability in Rat Hippocampal Slices After Perinatal Hypoxia In Vivo. :73–81.

Jones RS, Heinemann U (1988) Synaptic and intrinsic responses of medial entorhinal cortical cells in normal and magnesium-free medium in vitro. J Neurophysiol 59:1476–1496.

Kang N, Xu J, Xu Q, Nedergaard M, Kang J (2005) Astrocytic glutamate release-induced transient depolarization and epileptiform discharges in hippocampal CA1 pyramidal neurons. J Neurophysiol 94:4121–4130.

Kozler P, Riljak V, Pokorný J (2013) Both Water Intoxication and Osmotic BBB Disruption Increase Brain Water Content in Rats. 62.

Kozlov a S, Angulo MC, Audinat E, Charpak S (2006) Target cell-specific modulation of neuronal activity by astrocytes. PNAS 103:10058–10063.

Le Meur K, Galante M, Angulo MC, Audinat E (2007) Tonic activation of NMDA receptors by ambient glutamate of non-synaptic origin in the rat hippocampus. J Physiol 580:373–383.

Manley GT, Fujimura M, Ma T, Noshita N, Filiz F, Bollen a W, Chan P, Verkman a S (2000) Aquaporin-4 deletion in mice reduces brain edema after acute water intoxication and ischemic stroke. Nat Med 6:159–163.

Mccormick DA, Contreras D (2001) On the cellular and network bases of epileptic seizures. Annu Rev Physiol 63:815–846.

Meldrum BS, Akbar MT, Chapman AG (1999) Glutamate receptors and transporters in genetic and acquired models of epilepsy. 36:189–204.

Murtha L a, McLeod DD, Pepperall D, McCann SK, Beard DJ, Tomkins AJ, Holmes WM, McCabe C, Macrae IM, Spratt NJ (2015) Intracranial pressure elevation after ischemic stroke in rats: cerebral edema is not the only cause,

and short-duration mild hypothermia is a highly effective preventive therapy. J Cereb Blood Flow Metab 35:592–600.

Pawlak R, Melchor JP, Matys T, Skrzypiec AE, Strickland S (2005) Ethanol-withdrawal seizures are controlled by tissue plasminogen activator via modulation of NR2B-containing NMDA receptors. 102:443–448.

Porter JT, McCarthy KD (1996) Hippocampal astrocytes in situ respond to glutamate released from synaptic terminals. J Neurosci 16:5073–5081.

Risher WC, Andrew RD, Kirov S a (2009) Real-time passive volume responses of astrocytes to acute osmotic and ischemic stress in cortical slices and in vivo revealed by two-photon microscopy. Glia 57:207–221.

Rosen AS, Andrew RD (1990) Osmotic effects upon excitability in rat neocortical slices. Neuroscience 38:579–590.

Rossi S, Zanier ER, Mauri I, Columbo A, Stocchetti N (2001) Brain temperature , body core temperature , and intracranial pressure in acute cerebral damage. Neurol Neurosurg Psychiatry 71:448–454.

Rungta RL, Choi HB, Tyson JR, Malik A, Dissing-Olesen L, Lin PJC, Cain SM, Cullis PR, Snutch TP, MacVicar BA (2015) The Cellular Mechanisms of Neuronal Swelling Underlying Cytotoxic Edema. Cell 161:610–621.

Saly V, Andrew RD (1993) CA3 neuron excitation and epileptiform discharge are sensitive to osmolality. J Neurophysiol 69:2200–2208.

Schwartzkroin P a., Baraban SC, Hochman DW (1998) Osmolarity, ionic flux, and changes in brain excitability. Epilepsy Res 32:275–285.

Shelton MK, McCarthy KD (1999) Mature hippocampal astrocytes exhibit functional metabotropic and ionotropic glutamate receptors in situ. Glia 26:1–11.

Stokum J a, Kurland DB, Gerzanich V, Simard JM (2014) Mechanisms of Astrocyte-Mediated Cerebral Edema. Neurochem Res.

Taber KH, Lin CT, Liu JW, Thalmann RH, Wu JY (1986) Taurine in hippocampus: localization and postsynaptic action. Brain Res 386:113–121.

Talan M (1984) Body temperature of C57BL/6J mice with age. Exp Gerontol 19:25–29.

Tasleem RA, Chowdhary ND (2003) Fatal water intoxication. J Clin Pathol:803–804.

Tian G-F, Azmi H, Takano T, Xu Q, Peng W, Lin J, Oberheim N, Lou N, Wang X, Zielke HR, Kang J, Nedergaard M (2005) An astrocytic basis of epilepsy. Nat Med 11:973–981.

Toorn A Van Der, Sykovh E, Dijkhuizen RM, Vofisek I, Vargovh L, Skobisovh E, Campagne MVL, Reese T, Nicolay K (1996) Dynamic Changes in Water ADC , Energy Metabolism , Extracellular Space Volume , and Tortuosity in Neonatal Rat Brain During Global Ischemia. MRM 36:52–60.

Traynelis SF, Dingledine R (1988) Potassium-induced spontaneous electrographic seizures in the rat hippocampal slice. J Neurophysiol 59:259–276.

Traynelis SF, Dingledine R (1989) Role of extracellular space in hyperosmotic suppression of potassium-induced electrographic seizures. J Neurophysiol 61:927–938.

Tuz K, Ordaz B, Vaca L, Quesada O, Pasantes-Morales H (2001) Isovolumetric regulation mechanisms in cultured cerebellar granule neurons. J Neurochem 79:143–151.

Unterberg a W, Stover J, Kress B, Kiening KL (2004) Edema and brain trauma. Neuroscience 129:1021–1029.

Walther H, Lambert JD, Jones RS, Heinemann U, Hamon B (1986) Epileptiform activity in combined slices of the hippocampus, subiculum and entorhinal cortex during perfusion with low magnesium medium. Neurosci Lett 69:156–161.

Wetherington J, Serrano G, Dingledine R (2008) Astrocytes in the epileptic brain. Neuron 58:168–178.

Yao X, Derugin N, Manley GT, Verkman a S (2015) Reduced brain edema and infarct volume in aquaporin-4 deficient mice after transient focal cerebral ischemia. Neurosci Lett 584:368–372.

Zador Z, Stiver S, Wang V, Manley GT (2009) Role of aquaporin-4 in cerebral edema and stroke. Handb Exp Pharmacol:159–170.

Zhou N, Gordon GRJ, Feighan D, MacVicar B a (2010) Transient swelling, acidification, and mitochondrial depolarization occurs in neurons but not astrocytes during spreading depression. Cereb Cortex 20:2614–2624.

Chapter 4

Osmotic stress evokes action potentials and excitatory potentials in CA1 pyramidal neurons of the hippocampus

Abstract

In the previous chapter evidence was provided that osmotic insults are capable of increasing neuronal excitability through activation of AMPARs and NMDARs. In this chapter I propose that this non-synaptic source of glutamate activates neuronal receptors and produces enhanced neuronal excitability in the form of increased EPSPs, APs, and burst firing. Action potentials and EPSPs were measured in current clamp mode in CA1 pyramidal neurons using whole-cell patch clamp electrophysiological techniques. Like SICs, EPSPs, APs and bursting APs were re-evokable and also occurred within ~1 minute of hACSF application. In current clamp recordings, both mild and moderate osmotic insult evoked neuronal action potentials, burst firing, and EPSPs in the absence or presence of the AMPA receptor antagonist NBQX. Furthermore, increased subthreshold EPSPs and neuronal APs were observed in the presence of Mg^{2+}, suggesting that shifts in osmolarity induce increases in neuronal excitability under more physiological conditions.

After abolishing all spontaneous vesicular transmitter release by incubation of hippocampal slices in bafilomycin A1, mild osmotic insult

significantly increased action potentials, burst firing, and EPSPs in CA1 pyramidal neurons. Furthermore, these potentials of non-synaptic origin were due to activation of NMDA receptors, as they were significantly reduced in the presence of AP5. According to our data, both moderate and severe osmotic insults are capable of increasing neuronal firing of action potentials and burst firing within minutes, which ultimately may lead to synchronization of local neuronal networks, seizures and epilepsy. These findings may have important implications for the treatment of numerous conditions associated with cellular edema and excitotoxicity including stroke, ischemia, traumatic brain injury, hyponatremia, Alzheimer's disease, inflammatory diseases, and epilepsy.

Introduction

Osmotic edema is a condition characterized by the accumulation of an excessive amount of fluid buildup within the brain resulting in swelling of the tissue. Previous research has shown that before the initiation of a seizure there is a reduction of the extracellular space (Traynelis and Dingledine, 1989; Binder et al., 2004). In addition, changes in ionic homeostasis and osmolarity result in alterations in neuronal excitability, which may in turn lead to local synchronization of neuronal firing and seizure generation (Schwartzkroin et al., 1998). In chapter 3 I demonstrated that mild and moderate osmotic insult was capable of increasing neuronal excitability by producing SICs through activation of NMDA receptors. In our recordings of neuronal currents in the previous chapter, neurons

were voltage clamped at a holding potential of -70 mV and synaptic transmission in the slice was suppressed by TTX and AMPA receptor antagonists. While these conditions are ideal to isolate neuronal SICs, they do not mimic very well the physiological condition in which neuronal membrane potential can change and AMPA receptors can influence neuronal excitability. Furthermore, while the amplitudes of many SICs seem large enough to depolarize neurons above firing threshold, it was important for us to test this possibility.

The hippocampus is particularly prone to epileptic activity, and has a low seizure threshold (Green, 1969). Previous studies have found a contribution of hypoosmolarity to the generation and strength of seizure-like activity in hippocampal slices (Andrew et al., 1989; Ballyk et al., 1991; Saly and Andrew, 1993). However, these studies examined the effects of osmotic edema only on evoked neuronal activity 10-20 minutes after osmotic challenge. To complement this earlier work, the effects of acute osmotic edema on neuronal excitability in CA1 pyramidal neurons in the hippocampus were examined. Postsynaptic potentials (PSPs), EPSPs and APs were recorded as measure of neuronal excitability during acute osmotic stress, and classified action potentials as single action potentials or bursts of action potentials, which are indicative of neuronal synchronization.

Results

Mild osmotic stress evokes action potentials and excitatory potentials in CA1 pyramidal neurons that persist when AMPA receptors are blocked

To examine the effects of acute osmotic edema on neuronal excitability in CA1 pyramidal neurons in the hippocampus, I measured PSPs during osmotic stress. The effects of a 17% hACSF on APs and EPSPs were examined during repeated hACSF applications (Figure 4.1 A). First, I found that the frequency of APs, bursts of APs, and EPSPs increased significantly in response to the osmotic stress. The frequency of APs significantly increased in the 1st hACSF application compared to the baseline (Figure 4.1 D and Table 4.1). Interestingly, osmotic insult increased bursting during all three hACSF applications (Figure 4.1 E and Table 4.1). The frequency of EPSPs followed a similar trend as bursting activity, and was significantly elevated during all three hACSF applications compared to baseline (Figure 4.1 G and Table 4.1). These results indicate that acute mild osmotic insult is capable of increasing action potentials, burst firing, and EPSPs. To examine the contribution of AMPA receptors specifically to the observed increase in neuronal excitability during osmotic stress, I replicated these experiments in the presence of 10 μM NBQX (Figure 4.1 B). Neuronal excitability was still significantly elevated in the presence of NBQX during osmotic insult. During the blockade of AMPA receptors, action potential frequency increased during the 1st application of hACSF + NBQX (Figure 4.1D

and Table 4.1). Furthermore, bursting activity was elevated independent of AMPA receptor activation during the 1st osmotic insult (Figure 4.1 E and Table 4.1). Frequency of EPSPs also increased independent of AMPA receptor activation during all three hACSF applications (Figure 4.1 G and Table 4.1). During osmotic insult the percentage of neurons firing single action potentials and bursts of APs increased the most during the first hACSF application, with around 90% of the neurons exhibiting bursting activity (Figure 4.1 C). The number of action potentials per burst was similar during both the 17% hACSF and 17% hACSF +NBQX, averaging ~ 4 APs/burst (Figure 4.1 F). Similar to the number of action potentials per burst, no significant difference was found in the frequency of APs, bursts, or EPSPs between 17% hACSF and 17% hACSF + NBQX. These data suggest that AMPA receptor activation is not required for the majority of the APs and EPSPs evoked by mild osmotic insult. This result was somewhat surprising given the known role of AMPA receptors in neuronal depolarization and excitability.

Moderate osmotic stress evokes APs, busting activity and EPSPs in CA1 pyramidal neurons that persist when AMPA receptors are blocked

Next, the effects of moderate osmotic stress and AMPA receptor activation on neuronal excitability (Figure 4.2 A & B) were examined. All neurons exhibited bursting activity during the 40% hACSF application with or without NBQX (Figure 4.2 C). The frequency of APs significantly increased during 1st

and 2nd hACSF applications for both groups compared to the baseline activity (Figure 4.2 D and Table 4.2). Bursting activity followed a similar trend of increasing in both the 1st and 2nd hACSF applications, regardless of whether AMPA receptors were blocked or not (Figure 4.2 E and Table 4.2). Similar to the mild osmotic insult, the average number of APs/burst was ~ 4 during moderate osmotic stress (Figure 4.2 F and Table 4.2). Frequency of EPSPs also increased in 40% hACSF ± NBQX during the 1st and 2nd hACSF applications. However, like mild osmotic insult, the increase in neuronal activity during moderate osmotic insult appears to be mainly independent of AMPA receptor activation.

Effects of mild osmotic edema on neuronal excitability before, during and after insult

Similar to experiments in Chapter 3 measuring slow inward currents, in a subset of experiments neuronal excitability before, during, and after a single application of 17% hACSF was examined. This confirmed the positive shift in holding current observed in voltage-clamp recordings, application of 17% hACSF rapidly hyperpolarized the membrane potential of CA1 pyramidal neurons by 3.69 ± 0.51 mV. Despite hyperpolarizing neuronal resting V_m, action potentials and EPSPs were evoked by 17% hACSF (Figure 4.3 A, upper traces), as well as in 17% hACSF + NBQX (10 μM; lower traces). I analyzed APs and bursts based on criterion outline in Chapter 2. Similar to our observations of SICs, few neurons generated either sAPs or bAPs in normosmolar ACSF, but exhibited a dramatic

increase in both types of APs during hACSF application (Figure 4.3 C). Total AP frequency was elevated significantly above baseline during the hACSF application for both the 17% hACSF and 17% hACSF + NBQX groups, then declined significantly after return to nACSF (Figure 4.3 D and Table 4.3). In addition, bAPs were also enhanced in both groups by mild osmotic stress (Figure 4.3 E). Bursts of APs dropped back down during the wash period to near baseline levels. Reduced frequency of bursts during the wash period was accompanied by a significant decrease in the number of APs within each burst (Figure 4.3 F and Table 4.3). Addition of NBQX did not affect bAP frequency or properties, and was only effective in reducing EPSP frequency (Figure 4.3 G and Table 4.3). Reduction of EPSPs by NBQX is not surprising given the large increase in network activity and incoming APs into the recorded cell. These findings suggest that the generation of APs themselves is largely independent of AMPA receptor activation, while synaptic AMPAR activity increases as a result of the elevated APs evoked by osmotic edema.

Based upon observations that 40% hACSF evoked a significantly greater frequency of SICs compared to 17% hACSF (Chapter 3), it was reasoned that APs and EPSPs would also increase in a similar manner and with similar dependence (or lack thereof) on AMPA receptors. This was tested by replicating the above experiments using 40% hACSF, once again, in both the presence and absence of NBQX (Figure 4.4 A). Switching to 40% hACSF caused neurons to hyperpolarize nearly twice as much as 17% hACSF (-7.35 ± 0.91 mV vs. -3.69

mV for 17%). As before, the number of neurons displaying bAPs jumped from less than half at baseline, up to 100% during application of 40% hACSF (Figure 4.4 B and Table 4.4). This dose of hACSF also increased the number of cells displaying sAPs, reaching 100% participation in the absence of NBQX. The percentage of neurons in which APs were evoked diminished over the wash period. Total AP frequency in 40% hACSF ± NBQX was 3-4 times higher than in 17% hACSF ± NBQX, and once again significantly decreased during the wash period (Figure 4.4 C). Much more pronounced was the effect of NBQX on bAP activity in the 40% vs. the 17% hACSF (Figure 4.4 D and Table 4.4). Although burst frequency was significantly higher in 40% hACSF + NBQX and remained elevated over the wash period, NBQX inhibited the hACSF-induced increase by more than 50% and also reduced burst frequency to baseline levels after hACSF washout. Interestingly, despite the significant effect of NBQX on bAP frequency in 40% hACSF, NBQX did not alter the number of spikes per burst (Figure 4.4 E). EPSP activity in 40% hACSF ± NBQX closely followed the pattern established in 17% hACSF (Figure 4.4 F). Blocking AMPA receptors reduced EPSPs by about 50% in all conditions. In sum, the observed excitability changes in 17% and 40% hACSF suggest that AMPA receptor activation is not required for the increase in APs evoked by hACSF, but AMPA receptors may play a larger role in contributing to the frequency of bursting activity as hypoosmolar conditions become more extreme.

Differential effects of NBQX on bursts of action potentials between 17% and 40% hACSF suggested that AMPA receptors influence neuronal excitability only at moderate reductions in osmolarity. However, AMPA receptors also normally play an important role in NMDA receptor activation, as they are the physiological means by which the synaptic membrane depolarizes sufficiently to remove magnesium block. Since our normosmolar ACSF and hACSFs contain 0 mM Mg^{2+}, it could be argued that AMPA receptors play a more important role when Mg^{2+} is closer to physiological levels. To address this, I repeated the previous 40% hACSF experiments using normosmolar ACSF containing physiological Mg^{2+} (1.3 mM), and hACSF made by dilution of the same. Inclusion of Mg^{2+} suppressed overall activity considerably (Figure 4.5 A). However, application of hACSF ± NBQX still evoked sAPs, bAPs, and EPSPs in the presence of Mg^{2+} that were significantly elevated over baseline and wash periods (Figure 4.5 A and Table 4.5). Compared to recordings in Mg^{2+}-free hACSF (with or without NBQX), neurons in hACSF containing Mg^{2+} exhibited significantly fewer APs (Figure 4.5 B) and bursts (Figure 4.5 C and Table 4.5). Baseline and wash APs were completely abolished by the addition of Mg^{2+}. As would be expected, Mg^{2+} reduced baseline EPSP activity by more than half of that observed in Mg^{2+}-free hACSF or Mg^{2+}-free hACSF + NBQX (Figure 4.5 D). Inclusion of Mg^{2+} inhibited the increased EPSP frequency observed during the wash period. Frequency of EPSPs in Mg^{2+} was also suppressed by NBQX at all time points. Taken together, these data suggest that the relative contribution of

AMPA receptors to hACSF-induced excitability is similar in the presence or absence of Mg^{2+}, and that Mg^{2+} has a much more significant effect overall in reducing APs and bAPs than did NBQX. These findings point to a significant role for NMDA receptors in the generation of APs by osmotic edema, which were tested more specifically in the following experiments.

Neuronal excitability increases in hACSF are NMDA receptor-dependent and predominantly nonsynaptic

Swelling of brain tissue and subsequent reduction of the extracellular space can increase the ambient glutamate concentration, increasing the likelihood that non-synaptic glutamate binds extrasynaptic receptors. Previous work has shown that SICs evoked by various stimuli may be driven by non-synaptic sources of glutamate (Angulo et al., 2004; Fellin et al., 2004; Kozlov et al., 2006; Fiacco et al., 2007). It was decided to more closely examine how non-synaptic sources of glutamate influence excitability of neurons by osmotic edema in this model. Synaptic transmission in slices was abolished by incubating slices in Bafilomycin A1 (4 μM), an inhibitor of the vacuolar H^+-ATPase responsible for loading synaptic vesicles, prior to recording activity in hACSF. Despite abolishing vesicular neurotransmitter release, excitability was still elevated by 17% hACSF + NBQX (Figure 4.6 A). In fact, blocking synaptic transmission had no effect on the total frequency of APs (Figure 4.6 B and Table 4.6) or on the frequency of bursts evoked by 17% hACSF (Figure 4.6 C and Table 4.6). Frequency of

EPSPs was mildly but noticeably reduced by bafilomycin, and was not significantly different from either 17% hACSF without bafilomycin, or its own baseline (Figure 4.6 D). In all cases, addition of the NMDA receptor antagonist DL-AP5 (50 μM) virtually eliminated the activity present in bafilomycin, providing further evidence that NMDA receptor activation (but not vesicular glutamate release) is necessary for the observed hACSF-induced changes in neuronal excitability. However, the effect of bafilomycin on the frequency of SICs suggests that vesicular glutamate release may modulate frequency and/or severity of SICs.

Discussion

Osmotic edema is a condition characterized by cell swelling (Andrew et al., 2007; Risher et al., 2009). In addition, changes in ionic homeostasis and osmolarity result in alterations in neuronal excitability, which may in turn lead to local synchronization of neuronal firing and seizure generation Previous research has shown that during osmotic edema there is an increase in neuronal excitability (Rosen and Andrew, 1990; Huang et al., 1997). The mechanisms underlying swelling and seizure generation are poorly understood, but the role of astrocytes has recently come to the forefront. Astrocytes have an integral role in maintaining the ionic homeostasis in the extracellular space through the uptake of potassium (K^+), glutamate, and water thereby regulating neuronal excitability.

In pioneering work, it was found that evoked population spikes, field potentials, and whole-cell evoked EPSCs were enhanced in hypoosmolar artificial cerebrospinal fluid (hACSF) (Andrew et al., 1989; Chebabo et al., 1995; Huang et al., 1997). Excitability of individual CA1 pyramidal neurons remained stable, as gauged by resting membrane potential, cell input resistance and action potential (AP) threshold (Andrew et al., 1989; Ballyk et al., 1991). It was concluded that a combination of non-synaptic, electrical field effects and enhanced chemical synaptic transmission increased the excitability of the population of CA1 pyramidal neurons (Ballyk et al., 1991; Huang et al., 1997). Both effects can be explained by a concomitant reduction of the extracellular space (ECS): During cell swelling, increased tissue resistance enhances the voltage across neuronal membranes (Andrew et al., 1989), while also elevating the concentration of ambient neurotransmitter molecules in the vicinity of ligand-gated ion channels (Huang et al., 1997). A limitation of these studies was that effects on spontaneous neuronal activity were not measured, and evoked recordings were performed only after several minutes in reduced osmolarity conditions.

Here evidence is provided that acute mild and moderate osmotic insult increased action potentials, bursts activity, and subthreshold synaptic potentials. In agreement with literature on cerebral edema (Rosen and Andrew, 1990; Andrew and MacVicar, 1994; Azouz et al., 1997; Schwartzkroin et al., 1998b), I observed significant increases in neuronal excitability upon acute application of

mild (17%) or moderate (40%) hypoosmolar ACSF. Within minutes, both doses caused spontaneous EPSP frequency, AP and bAP frequency recorded in CA1 pyramidal neurons to increase significantly over baseline, in most cases recurring upon successive hACSF applications. Surprisingly, action potential frequency tended to decrease during the 2nd and 3rd applications, an inverse relationship to EPSP frequency. AMPA receptor activation was not required for APs, bAPs, or EPSPs induced by mild osmotic stress in acute hippocampal slices. In the present study, I also observed that NMDA receptors are responsible for APs, bAPs and EPSPs, as they are blocked by both DL.

I found little evidence for the involvement of AMPA receptors (AMPARs) in frequency of EPSPs, APs or bursting activity during osmotic edema. Action potentials, bursts and EPSPs appeared to be sensitive almost exclusively to concentrations of Mg^{2+} in the bath. Blocking AMPA receptors with NBQX did not result in a significant reduction in APs, bursts, or EPSP, suggesting they mainly NMDA receptor-dependent. The lack of AMPAR involvement is suggestive of a non-synaptic phenomenon, as AMPARs do not form functional extrasynaptic pools. This is in agreement with previous studies suggesting that osmotic excitability changes are a non-synaptic phenomenon (Traynelis & Dingledine 1989; Fiacco et al. 2007). It should be noted however that I have observed, (Chapter 3) that there does appear to be some activation of fast 'AMPA like currents' during osmotic stress.

The shift in excitatory potential distributions during successive applications of hACSF could be due to a number of possibilities. The hyperpolarization during hACSF application or the rate at which the neurons hyperpolarize could also account for a portion of the decreased excitability during repeated hACSF treatments. Another possibility for the decreased excitability in subsequent exposures to hACSF could be a result of less glutamate available for neurons to release during firing, and/or diminished intracellular glutamate stores in astrocytes that have insufficient time to recover to baseline levels between applications of hACSF. Along these lines there is some evidence to suggest that hypoosmolar cell swelling and excitability may modulate the glutamate-glutamine cycle, resulting in decreased glutamate levels (Hyzinski-García et al., 2011). Therefore, there may be a compensatory or modulatory response occurring within neurons and/or astrocytes after the initial bout of osmotic stress in order to reduce the excitatory effect of further osmotic reduction on neurons and help prevent runaway excitation and damage to neurons or astrocytes.

Figure 4.1

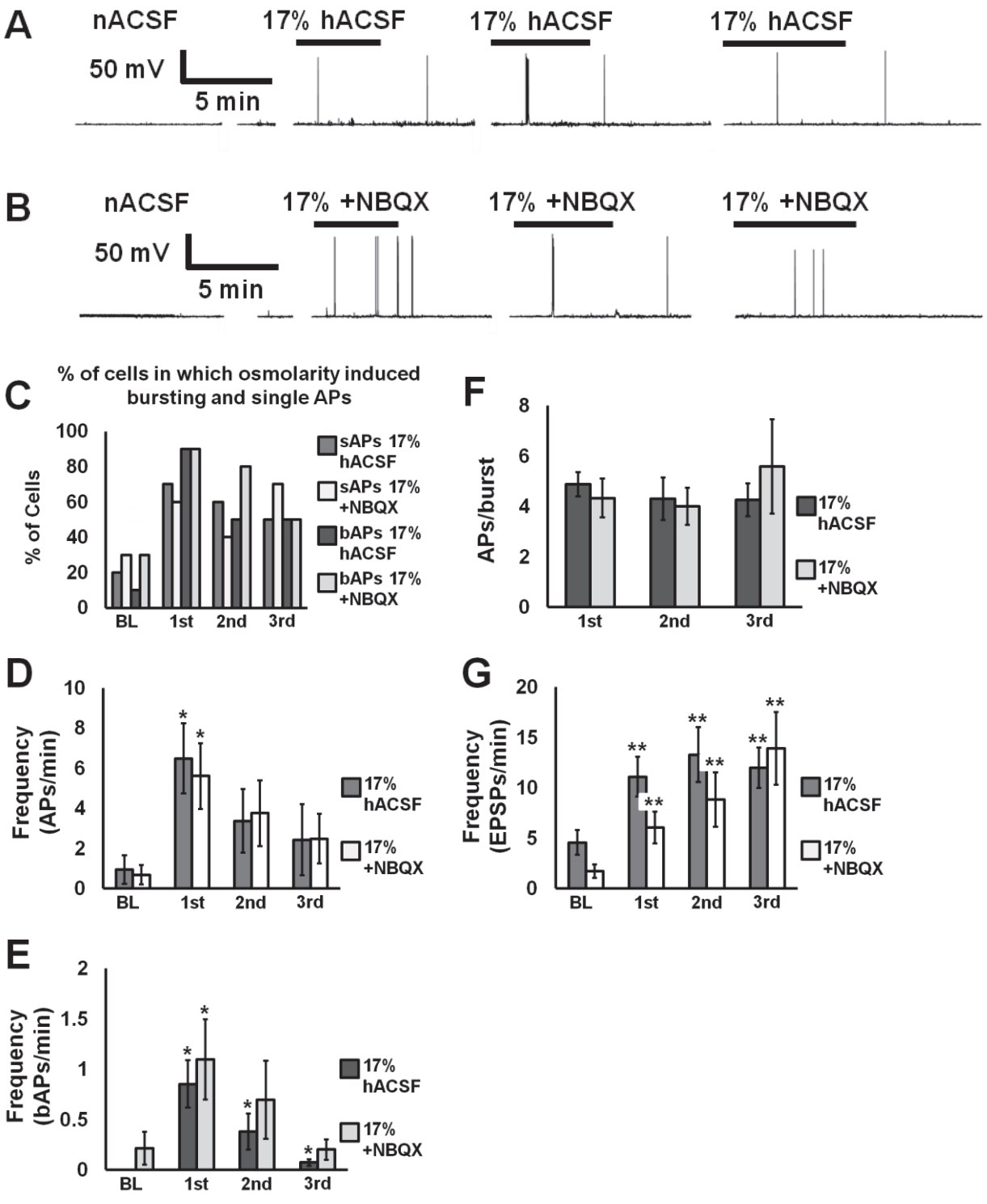
A
nACSF
17% hACSF
17% hACSF
17% hACSF
50 mV
5 min
B
nACSF
17% +NBQX
17% +NBQX
17% +NBQX
50 mV
5 min
C
% of cells in which osmolarity induced bursting and single APs
% of Cells
100
80
60
40
20
0
BL
1st
2nd
3rd
sAPs 17% hACSF
sAPs 17% +NBQX
bAPs 17% hACSF
bAPs 17% +NBQX
F
APs/burst
8
6
4
2
0
1st
2nd
3rd
17% hACSF
17% +NBQX
D
Frequency (APs/min)
10
8
6
4
2
0
BL
1st
2nd
3rd
17% hACSF
17% +NBQX
G
Frequency (EPSPs/min)
20
15
10
5
0
BL
1st
2nd
3rd
17% hACSF
17% +NBQX
E
Frequency (bAPs/min)
2
1.5
1
0.5
0
BL
1st
2nd
3rd
17% hACSF
17% +NBQX

Figure 4.1: AMPA receptor activation is not required for APs or EPSPs induced by mild osmotic stress in acute hippocampal slices. Representative whole-cell neuronal recordings during 17% hACSF (A) and 17% +NBQX (B). (C) The percentage of cells exhibiting single and bursting APs was greater in both hACSF groups compared to baseline. Bursting occurred in 90% of CA1 pyramidal neurons in the 1st hACSF application then decreased in both groups in the 2nd and 3rd applications. (D) The frequency of APs significantly increased during the 1st hACSF application in both groups compared to baseline. (E) The frequency of bAPs significantly increased during the 1st hACSF application in both groups compared to baseline, but remained significantly elevated in the17% hACSF group only in the 2nd and 3rd hACSF applications compared to baseline. (F) The number of AP/burst was similar for both groups. (G) EPSP frequency increased in all three hACSF applications over baseline activity in both of the groups. The presence of NBQX did not significantly change neuronal excitability during the application of the 17% hACSF compared to the 17% +NBQX for any of the measures. Statistical significance for all figures (* = $p < .05$), and (** = $p < .01$). n = 9 cells for all groups with the exception of APs/burst, n = 5.

Table 4.1

Frequency (APs/min)				
Group	**Baseline**	**1st App**	**2nd App**	**3rd App**
17% hACSF	0.95 ± 0.71	6.49 ± 1.75	3.38 ± 1.58	2.44 ± 1.78
17% +NBQX	0.70 ± 0.49	5.62 ± 1.64	3.76 ± 1.63	2.49 ± 1.23
% of Cells in Which Osmolarity Induced sAPs				
Group	**Baseline**	**1st App**	**2nd App**	**3rd App**
17% hACSF	20	70	60	50
17% +NBQX	30	60	40	70
% of Cells in Which Osmolarity Induced bAPs				
Group	**Baseline**	**1st App**	**2nd App**	**3rd App**
17% hACSF	10	90	50	50
17% +NBQX	30	90	80	50
Frequency (bAPs/min)				
Group	**Baseline**	**1st App**	**2nd App**	**3rd App**
17% hACSF	0 ± 0	0.85 ± 0.23	0.38 ± 0.18	0.08 ± 0.03
17% +NBQX	0.22 ± 0.16	1.10 ± 0.40	0.70 ± 0.39	0.20 ± 0.10
# of APs/burst				
Group	**Baseline**	**1st App**	**2nd App**	**3rd App**
17% hACSF		4.89 ± 0.49	4.31 ± 0.85	4.27 ± 0.66
17% +NBQX		4.34 ± 0.77	4.40 ± 0.76	5.59 ± 1.87
Frequency (EPSPs/min)				
Group	**Baseline**	**1st App**	**2nd App**	**3rd App**
17% hACSF	4.59 ± 1.22	11.11 ± 1.99	13.31 ± 2.73	11.99 ± 2.00
17% +NBQX	1.73 ± 0.66	6.06 ± 1.57	8.86 ± 2.71	13.93 ± 3.63

Table 4.1: Contributions of AMPA receptors to neuronal excitability during mild osmotic stress. Mean and SE for the frequency of APs/min, frequency of bAPs/min, number of APs/burst, and frequency of EPSPs/min. Percentage of cells that responded to the 17% hACSF and 17% +NBQX during repeated applications with either sAPs or bAPs.

Figure 4.2

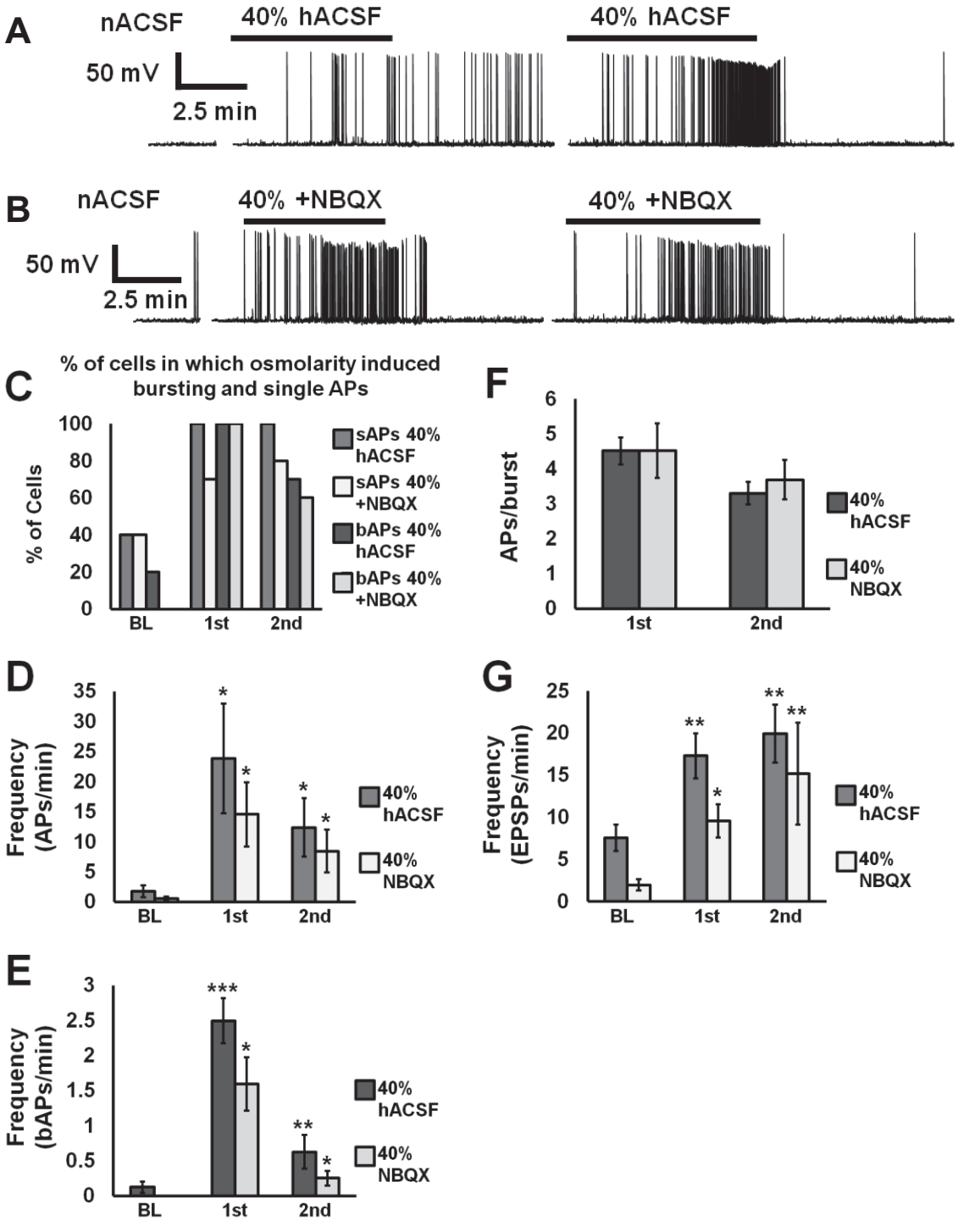
A
nACSF
40% hACSF
40% hACSF
50 mV
2.5 min
B
nACSF
40% +NBQX
40% +NBQX
50 mV
2.5 min
C
% of cells in which osmolarity induced bursting and single APs
% of Cells
100
80
60
40
20
0
BL
1st
2nd
sAPs 40% hACSF
sAPs 40% +NBQX
bAPs 40% hACSF
bAPs 40% +NBQX
F
APs/burst
6
5
4
3
2
1
0
1st
2nd
40% hACSF
40% NBQX
D
Frequency (APs/min)
35
30
25
20
15
10
5
0
BL
1st
2nd
40% hACSF
40% NBQX
G
Frequency (EPSPs/min)
25
20
15
10
5
0
BL
1st
2nd
40% hACSF
40% NBQX
E
Frequency (bAPs/min)
3
2.5
2
1.5
1
0.5
0
BL
1st
2nd
40% hACSF
40% NBQX

Figure 4.2: AMPA receptor activation is not required for APs, bAPs, or EPSPs induced by moderate osmotic stress. Whole-cell patch-clamp recording from neurons in the CA1 area of the hippocampus during 40% hACSF (A) and 40% +NBQX (B). (C) The percentage of cells exhibiting single and bursting APs was greater in both groups compared to baseline. Bursting occurred in 100% of CA1 pyramidal neurons in the 1st hACSF application then decreased in the 2nd application. (D) AP frequency increased during the 1st and 2nd hACSF applications for both groups compared to baseline. (E) The frequency of bAPs significantly increased during the 1st and 2nd moderate osmotic insult in both groups compared to baseline (F) APs/burst was similar for both groups. (G) EPSP frequency increased in both of the hACSF applications compared to baseline activity in the 40% hACSF and 40% +NBQX groups. The presence of NBQX did not significantly change neuronal excitability during the application of the 40% hACSF compared to the 40% +NBQX for any of the measures. Statistical significance for all figures (* = $p < .05$), (** = $p < .01$) (*** = $p < .001$). n = 8-10 cells for all groups, with the exception of APs/burst, n = 5.

Table 4.2

Frequency (APs/min)			
Group	Baseline	1st App	2nd App
40% hACSF	1.74 ± 0.99	23.85 ± 9.11	12.34 ± 4.84
40% +NBQX	0.54 ± 0.32	14.52 ± 5.30	8.40 ± 3.57
% of Cells in Which Osmolarity Induced sAPs			
Group	Baseline	1st App	2nd App
40% hACSF	40	100	100
40% +NBQX	40	70	80
% of Cells in Which Osmolarity Induced bAPs			
Group	Baseline	1st App	2nd App
40% hACSF	20	100	70
40% +NBQX	0	100	60
Frequency (bAPs/min)			
Group	Baseline	1st App	2nd App
40% hACSF	0.12 ± 0.08	2.49 ± 0.32	0.62 ± 0.24
40% +NBQX	0 ± 0	1.59 ± 0.38	0.25 ± 0.10
# of APs/burst			
Group	Baseline	1st App	2nd App
40% hACSF		4.51 ± 0.39	3.3 ± 0.32
40% +NBQX		4.52 ± 0.78	3.69 ± 0.57
Frequency (EPSPs/min)			
Group	Baseline	1st App	2nd App
40% hACSF	7.56 ± 1.58	17.27 ± 2.66	19.91 ± 3.43
40% +NBQX	1.94 ± 0.68	9.53 ± 1.98	15.14 ± 6.05

Table 4.2: Contributions of AMPA receptors to neuronal excitability during moderate osmotic stress. Mean and SE for the frequency of APs/min, frequency of bAPs/min, number of APs/burst, and frequency of EPSPs/min. Percentage of cells that responded to the 17% hACSF and 17% +NBQX during repeated applications with either sAPs or bAPs.

Figure 4.3

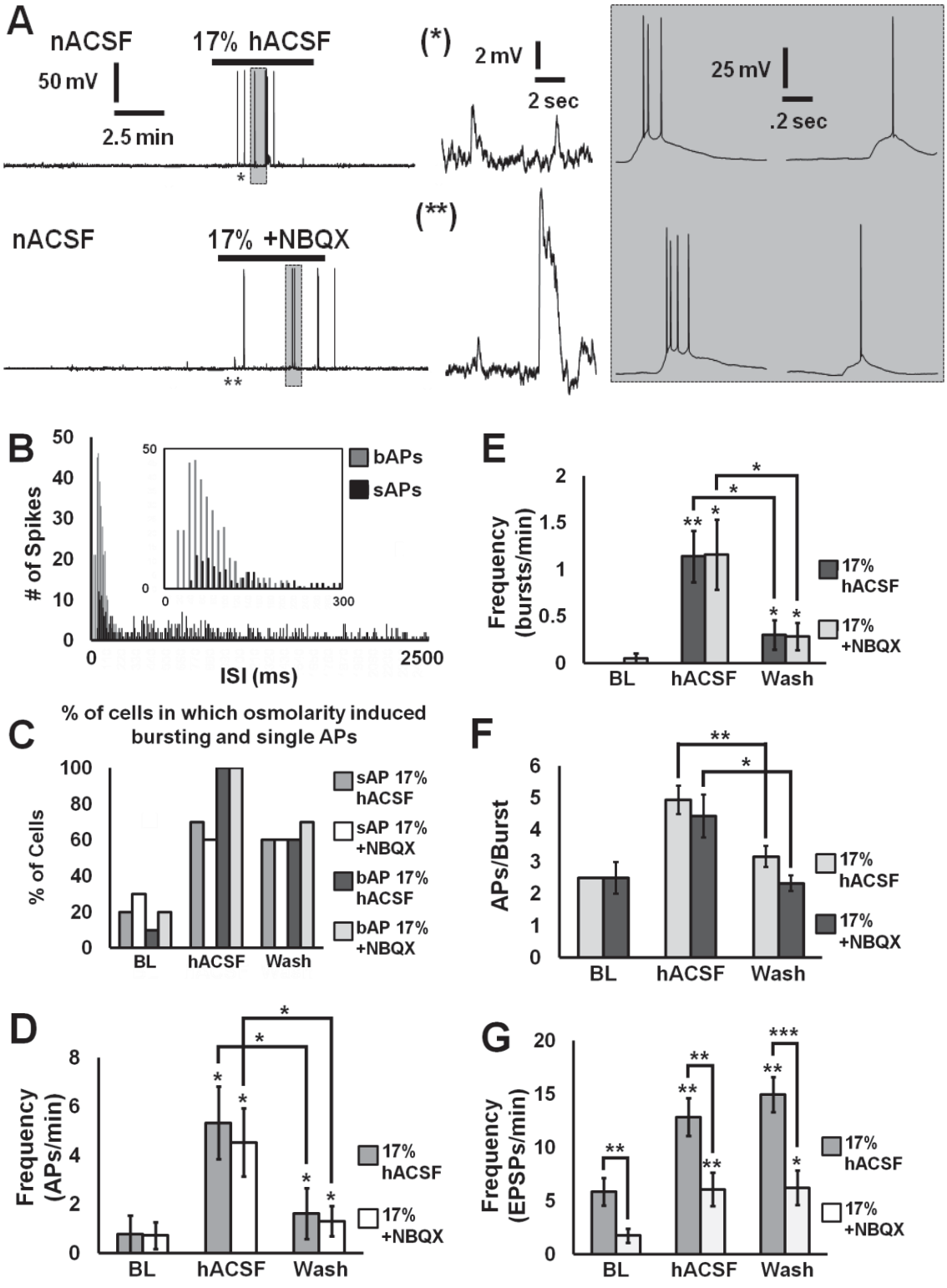
A
nACSF
17% hACSF
50 mV
2.5 min
(*)
2 mV
2 sec
25 mV
.2 sec
nACSF
17% +NBQX
(**)
B
# of Spikes
ISI (ms)
bAPs
sAPs
C
% of cells in which osmolarity induced bursting and single APs
% of Cells
sAP 17% hACSF
sAP 17% +NBQX
bAP 17% hACSF
bAP 17% +NBQX
BL
hACSF
Wash
D
Frequency (APs/min)
17% hACSF
17% +NBQX
E
Frequency (bursts/min)
F
APs/Burst
G
Frequency (EPSPs/min)

Figure 4.3: 17% hACSF evokes neuronal action potentials and increased bursting activity that is independent of AMPA receptor activation (A) Current clamp recording of neuronal membrane potential in nACSF (baseline period) followed by 17% hACSF without NBQX (upper traces) and in 10 μM NBQX (lower traces). Asterisks mark expanded traces of EPSPs (middle panels), while shaded boxes indicate expanded traces of single APs and bursting activity (right panels). 17% hACSF evoked APs independent of AMPA receptors. (B) Plotting interspike interval into 10 ms bins revealed that most bursting activity correlated with the highest frequency of APs, but that single APs could also occur at high frequency and were more uniform in their distribution. (C) The percentage of cells exhibiting single and bursting APs was much greater in the hACSF condition compared to baseline. Bursting occurred in100% of CA1 pyramidal neurons in hACSF compared to only 10-20% in nACSF. The percentage of cells in which reduced osmolarity induced bursting and single APs was almost the same in 10 μM NBQX, indicating that AMPA receptors did not participate in the effect. (D and E) While spontaneous APs and bursting activity were infrequent in control conditions, 17% hACSF and 17% hACSF + NBQX evoked frequent APs and bursts. Frequency of APs and bursts declined significantly during the wash period but were still significantly elevated compared to baseline. (F) The number of action potentials within a burst was higher on average in 17% hACSF compared to baseline and wash periods. (G) NBQX reduced by approximately half the frequency of subthreshold EPSPs. Although EPSPs were partially blocked by NBQX, this did not affect the ability of 17% hACSF to evoke single and bursting APs in CA1 pyramidal cells. (*$p < 0.05$; **$p < 0.01$; and ***$p < 0.001$); n = 8 to 10 cells per group.

Table 4.3

Frequency (APs/min)			
Group	**Baseline**	**hACSF**	**Wash**
17% hACSF	0.78 ± 0.78	5.33 ± 1.49	1.62 ± 1.05
17% +NBQX	0.73 ± 0.55	4.53 ± 1.40	1.31 ± 0.62
% of Cells in Which Osmolarity Induced sAPs			
Group	**Baseline**	**hACSF**	**Wash**
17% hACSF	20	70	60
17% +NBQX	30	60	60
% of Cells in Which Osmolarity Induced bAPs			
Group	**Baseline**	**hACSF**	**Wash**
17% hACSF	10	100	60
17% +NBQX	20	100	70
Frequency (bAPs/min)			
Group	**Baseline**	**hACSF**	**Wash**
17% hACSF	0 ± 0	1.14 ± 0.28	0.30 ± 0.16
17% +NBQX	0.05 ± 0.05	1.16 ± 0.37	0.29 ± 0.15
# of APs/burst			
Group	**Baseline**	**hACSF**	**Wash**
17% hACSF	2.5 ± -.-	4.94 ± 0.44	3.16 ± 0.33
17% +NBQX	2.5 ± 0.5	4.43 ± 0.68	2.32 ± 0.24
Frequency (EPSPs/min)			
Group	**Baseline**	**hACSF**	**Wash**
17% hACSF	5.84 ± 1.27	12.84 ± 1.78	14.94 ± 1.65
17% +NBQX	1.73 ± 0.66	6.06 ± 1.57	6.22 ± 1.62

Table 4.3: AMPA receptor contributions to neuronal excitability before, during and after mild osmotic insult. Mean and SE for frequency of APs, bAPs, and EPSPs along with the average number of APs/burst, and the percentage of cells in which osmolarity induced sAPs or bAPs before, during, and after mild osmotic stress.

Figure 4.4

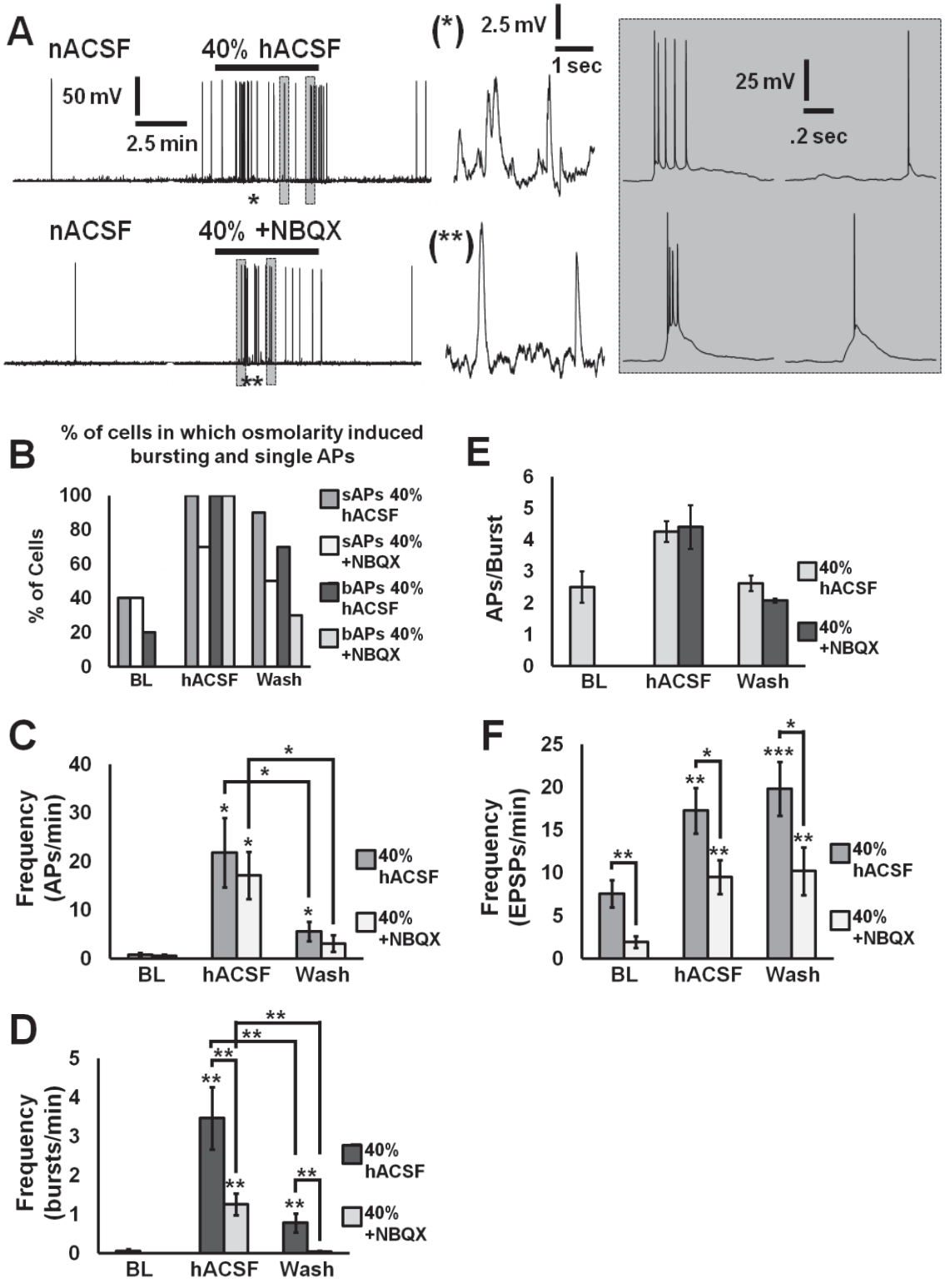
A
nACSF
40% hACSF
50 mV
2.5 min
*
nACSF
40% +NBQX
**
(*)
2.5 mV
1 sec
(**)
25 mV
.2 sec
B
% of cells in which osmolarity induced bursting and single APs
% of Cells
100
80
60
40
20
0
BL
hACSF
Wash
sAPs 40% hACSF
sAPs 40% +NBQX
bAPs 40% hACSF
bAPs 40% +NBQX
E
APs/Burst
6
5
4
3
2
1
0
BL
hACSF
Wash
40% hACSF
40% +NBQX
C
Frequency (APs/min)
40
30
20
10
0
BL
hACSF
Wash
40% hACSF
40% +NBQX
F
Frequency (EPSPs/min)
25
20
15
10
5
0
BL
hACSF
Wash
40% hACSF
40% +NBQX
D
Frequency (bursts/min)
5
4
3
2
1
0
BL
hACSF
Wash
40% hACSF
40% +NBQX

Figure 4.4: 40% hACSF evokes neuronal action potentials and increased bursting activity that is partly dependent on AMPA receptor activation (A) Whole cell current-clamp recordings of neuronal action potentials and EPSPs in normosmolar ACSF (baseline) followed by 40% hACSF (upper traces) or 40% hACSF + 10 μM NBQX (lower traces). Asterisks mark location of expanded traces of EPSPs (middle panels), while shaded boxes mark expanded traces of APs (right panels). Note the combination of single APs and bursting activity evoked by hACSF ± NBQX. (B) Nearly all CA1 pyramidal cells fired APs and displayed bursting activity in hACSF, while less than half the cells fired APs over the baseline period where bursting was rare. The percentage of cells with APs and bursts declined during the wash period. (C & D) Frequency of APs and bursting activity significantly increased during application of 40% hACSF compared to baseline and wash periods. NBQX did not affect the frequency of single APs evoked by hACSF (C) but it did significantly reduce bursting activity (D). (E) The number of APs per burst was higher during hACSF application compared to baseline and wash periods, although the number of cells exhibiting bursts over the baseline and wash periods was too low to run statistics. (F) Frequency of EPSPs was significantly elevated in 40% hACSF and wash periods over baseline, and reduced significantly in all conditions by NBQX. The AMPA receptor dependent synaptic activity is not surprising given the frequency of APs occurring in the network onto the recorded cell. (*$p < 0.05$; **$p < 0.01$; and ***$p < 0.001$); n = 9 to 10 cells per group.

Table 4.4

Frequency (APs/min)			
Group	**Baseline**	**hACSF**	**Wash**
40% hACSF	0.75 ± 0.44	21.81 ± 7.13	5.61 ± 2.00
40% +NBQX	0.54 ± 0.32	17.09 ± 4.86	3.13 ± 1.75
% of Cells in Which Osmolarity Induced sAPs			
Group	**Baseline**	**hACSF**	**Wash**
40% hACSF	40	100	90
40% +NBQX	40	70	50
% of Cells in Which Osmolarity Induced bAPs			
Group	**Baseline**	**hACSF**	**Wash**
40% hACSF	20	100	70
40% +NBQX	0	100	30
Frequency (bAPs/min)			
Group	**Baseline**	**hACSF**	**Wash**
40% hACSF	0.05 ± 0.05	3.47 ± 0.80	0.78 ± 0.24
40% +NBQX	0 ± 0	1.55 ± 0.34	0.24 ± 0.20
# of APs/burst			
Group	**Baseline**	**hACSF**	**Wash**
40% hACSF	2.5 ± 0.5	4.26 ± 0.33	2.62 ± 0.25
40% +NBQX		4.41 ± 0.70	2.07 ± 0.07
Frequency (EPSPs/min)			
Group	**Baseline**	**hACSF**	**Wash**
40% hACSF	7.56 ± 1.58	17.27 ± 2.66	19.81 ± 3.14
40% +NBQX	1.94 ± 0.68	9.53 ± 1.98	10.21 ± 2.78

Table 4.4: AMPA receptor contributions to neuronal excitability before, during and after moderate osmotic insult. Mean and SE for frequency of APs, bAPs, and EPSPs along with the average number of APs/burst, and the percentage of cells in which osmolarity induced sAPs or bAPs before, during, and after moderate osmotic stress.

Figure 4.5

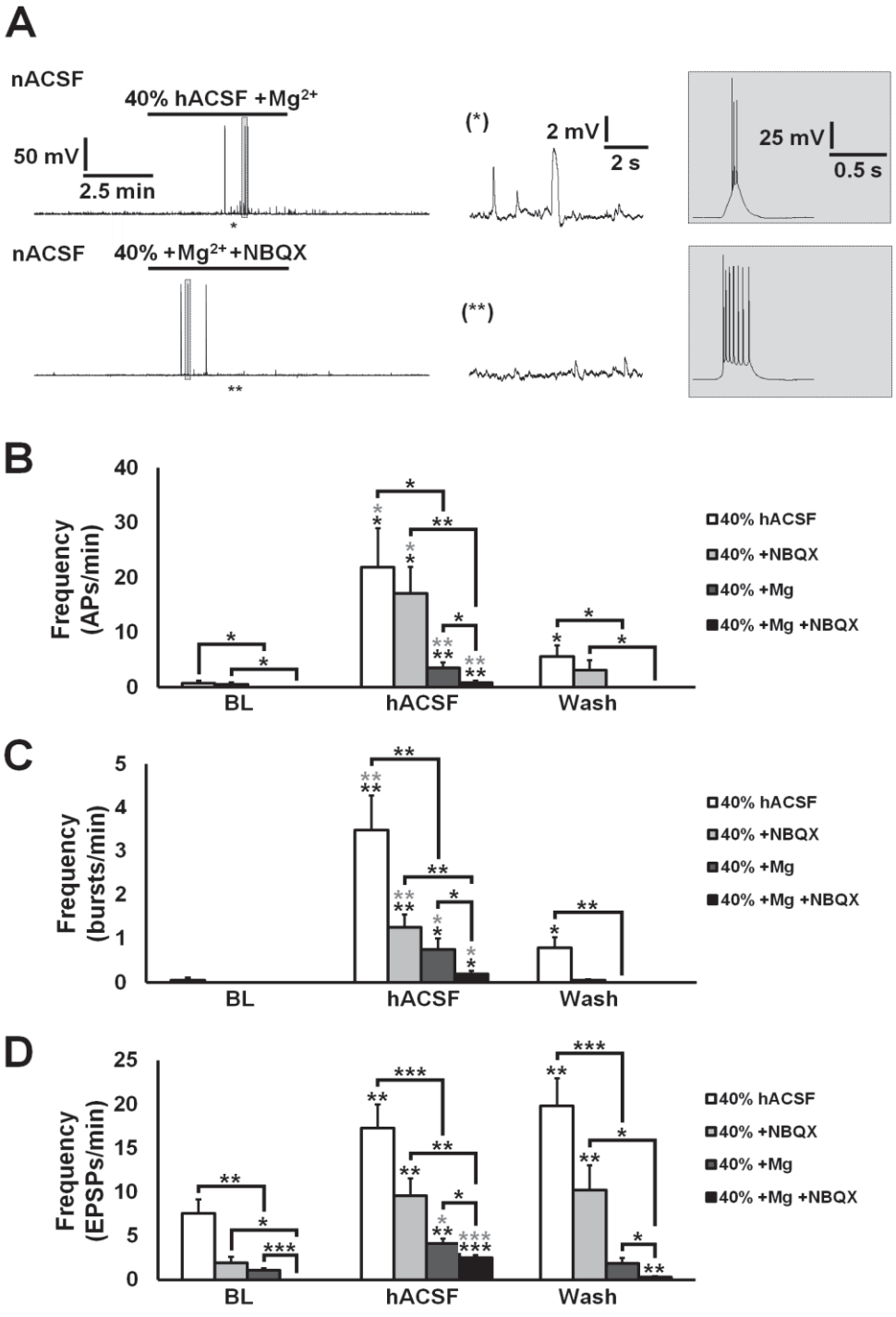
A
nACSF
40% hACSF +Mg2+
50 mV
2.5 min
(*)
2 mV
2 s
25 mV
0.5 s
nACSF
40% +Mg2+ +NBQX
(**)
B
Frequency (APs/min)
40
30
20
10
0
BL
hACSF
Wash
40% hACSF
40% +NBQX
40% +Mg
40% +Mg +NBQX
C
Frequency (bursts/min)
5
4
3
2
1
0
BL
hACSF
Wash
40% hACSF
40% +NBQX
40% +Mg
40% +Mg +NBQX
D
Frequency (EPSPs/min)
25
20
15
10
5
0
BL
hACSF
Wash
40% hACSF
40% +NBQX
40% +Mg
40% +Mg +NBQX

Figure 4.5: Neuronal action potentials and EPSPs evoked by hACSF in increasingly physiological conditions (A) Representative current clamp recordings of neuronal membrane potential in 40% hACSF with Mg^{2+} (diluted to approx. 0.7 mM; upper traces) and 40% hACSF plus 10 μM NBQX (lower traces). Asterisks below each trace mark location of expanded EPSPs (middle panels), while shaded boxes mark location of expanded APs (right panels). (B) Frequency of total action potentials (single plus bursts) was significantly elevated over baseline (black asterisks) and wash periods (grey asterisks) in all conditions. Addition of Mg^{2+} reduced the frequency of APs overall, indicating the role for NMDARs. Note, however, that NMDARs were still activated significantly by hACSF with Mg^{2+} present. (C) Examination of bursts alone revealed very similar results as total APs. Bursting activity was significantly elevated over baseline in all conditions (black asterisks) and remained elevated compared to the wash period (grey asterisks). (D) Frequency of EPSPs was reduced in a stepwise fashion with addition of NBQX, Mg^{2+}, and NBQX + Mg^{2+}. Presence of Mg^{2+} alone had a greater effect on reducing EPSP frequency compared to addition of NBQX alone, indicated a greater role for NMDARs over AMPARs. (*$p < 0.05$; **$p < 0.01$; and ***$p < 0.001$); n = 8 to 10 cells per group.

Table 4.5

Frequency (APs/min)			
Group	**Baseline**	**hACSF**	**Wash**
40% hACSF	0.75 ± 0.44	21.81 ± 7.13	5.61 ± 2.00
40% +NBQX	0.54 ± 0.32	17.09 ± 4.86	3.13 ± 1.75
40% +Mg	0 ± 0	3.53 ± 1.01	0 ± 0
40% +Mg + NBQX	0 ± 0	0.79 ± 0.42	0 ± 0
Frequency (bAPs/min)			
Group	**Baseline**	**hACSF**	**Wash**
40% hACSF	0.05 ± 0.05	3.47 ± 0.80	0.78 ± 0.24
40% +NBQX	0 ± 0	1.55 ± 0.34	0.24 ± 0.20
40% +Mg	0 ± 0	0.74 ± 0.25	0 ± 0
40% +Mg + NBQX	0 ± 0	0.19 ± 0.07	0 ± 0
Frequency (EPSPs/min)			
Group	**Baseline**	**hACSF**	**Wash**
40% hACSF	7.56 ± 1.58	17.27 ± 2.66	19.81 ± 3.14
40% +NBQX	1.94 ± 0.68	9.53 ± 1.98	10.21 ± 2.78
40% +Mg	1.09 ± 0.23	4.10 ± 0.55	1.86 ± 0.63
40% +Mg + NBQX	0 ± 0	2.47 ± 0.34	0.32 ± 0.08

Table 4.5: APs, bAPs, and EPSPs before, during, and after moderate osmotic stress, contributions of Mg^{2+} and NBQX. Frequency of APs, bAPs, and EPSPs before, during a 40% hACSF application, and after hACSF applications, with or without Mg^{2+} and NBQX, all numbers are mean ± SE.

Figure 4.6

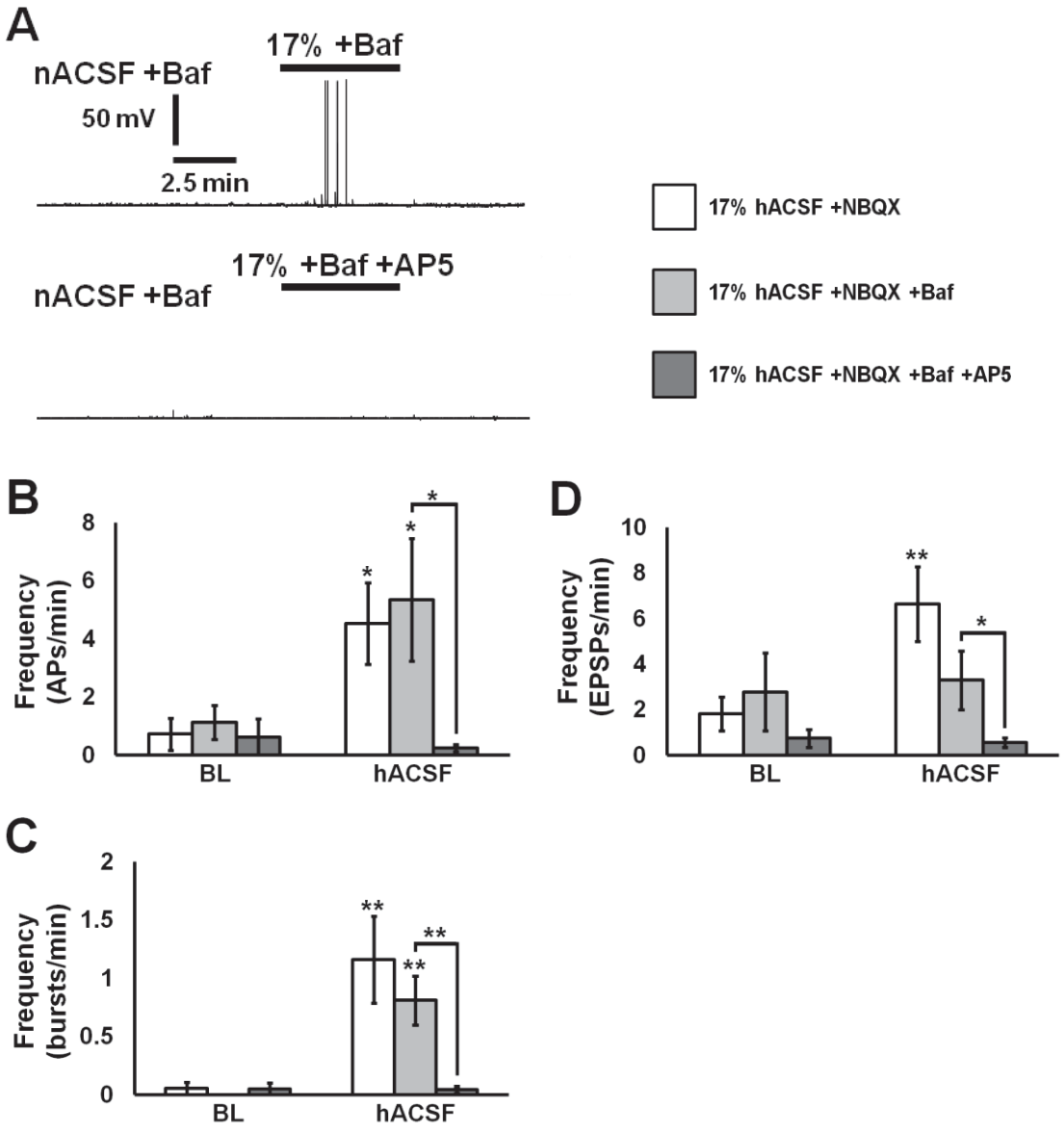
A
17% +Baf
nACSF +Baf
50 mV
2.5 min
17% +Baf +AP5
nACSF +Baf
17% hACSF +NBQX
17% hACSF +NBQX +Baf
17% hACSF +NBQX +Baf +AP5
B
Frequency (APs/min)
BL
hACSF
C
Frequency (bursts/min)
BL
hACSF
D
Frequency (EPSPs/min)
BL
hACSF

Figure 4.6: Action potentials evoked by osmotic edema are non-synaptic and NMDA receptor-dependent (A) Current-clamp (left traces) recordings of neuronal membrane potentials in bafilomycin (upper panels) and bafilomycin (baf) + 50 μM AP5 (lower panels). NBQX and baf were present throughout. Application of 17% hACSF evoked APs independent of synaptic activity and were blocked by the NMDA receptor antagonist. (B) Summary histogram indicating that APs remained significantly elevated on average in baf compared to baseline, and equal to the frequency of APs in hACSF without baf. AP5 nearly completely abolished APs. (C) Blockade of quantal vesicular release did not reduce bursting activity compared to bursts evoked with spontaneous vesicular release intact. Bursting activity was also completely blocked by AP5. (D) Not surprisingly, baf reduced the occurrence of EPSPs, which were no longer significantly elevated over baseline compared to the recordings performed without baf. AP5 significantly reduced the frequency of EPSPs, indicating that many of them are NMDA receptor-dependent. (*$p < 0.05$; and **$p < 0.01$); n = 8 to 10 cells per group.

Table 4.6

Frequency (APs/min)		
Group	**Baseline**	**hACSF**
17% +NBQX	0.73 ± 0.55	4.53 ± 1.4
17% +Baf	1.13 ± 0.59	5.34 ± 2.11
17% +Baf +AP5	0.63 ± 0.63	0.25 ± 0.13
Frequency (bAPs/min)		
Group	**Baseline**	**hACSF**
17% +NBQX	0.05 ± 0.05	1.16 ± 0.37
17% +Baf	0 ± 0	0.81 ± 0.21
17% +Baf +AP5	0.05 ± 0.05	0.04 ± 0.03
Frequency (EPSPs/min)		
Group	**Baseline**	**hACSF**
17% +NBQX	1.83 ± 0.74	6.64 ± 1.65
17% +Baf	2.78 ± 1.7	3.3 ± 1.29
17% +Baf +AP5	0.75 ± 0.4	0.55 ± 0.21

Table 4.6: Frequency of APs, bAPs, and EPSPs, contributions of vesicular release, and NMDA receptors during mild osmotic stress. Numbers indicate mean plus SE for frequency of APs, bAPs, and EPSPs, during baseline activity and a 17% hACSF application for three experimental conditions including; 17% hACSF +NBQX, 17% hACSF +NBQX +baf, and 17% hACSF +NBQX +baf +AP5.

References

Andrew RD, Fagan M, Ballyk B a, Rosen a S (1989) Seizure susceptibility and the osmotic state. Brain Res 498:175–180.

Angulo MC, Kozlov AS, Charpak S, Audinat E (2004) Glutamate released from glial cells synchronizes neuronal activity in the hippocampus. J Neurosci 24:6920–6927.

Ballyk BA, Quackenbush SJ, Andrew RD (1991) Osmotic Effects on the CA1 Neuronal Population in Hippocampal Slices with Special Reference to Glucose. J Neurophysiol 65.

Binder DK, Papadopoulos MC, Haggie PM, Verkman a S (2004) In vivo measurement of brain extracellular space diffusion by cortical surface photobleaching. J Neurosci 24:8049–8056.

Fellin T, Gomez-Gonzalo M, Gobbo S, Carmignoto G, Haydon PG (2006) Astrocytic glutamate is not necessary for the generation of epileptiform neuronal activity in hippocampal slices. J Neurosci 26:9312–9322.

Fellin T, Pascual O, Gobbo S, Pozzan T, Haydon PG, Carmignoto G (2004) Neuronal synchrony mediated by astrocytic glutamate through activation of extrasynaptic NMDA receptors. Neuron 43:729–743.

Fiacco TA, Agulhon C, Taves SR, Petravicz J, Casper KB, Dong X, Chen J, McCarthy KD (2007) Selective stimulation of astrocyte calcium in situ does not affect neuronal excitatory synaptic activity. Neuron 54:611–626.

Green JD (1969) The hippocampus. Physiol Rex 44:561–608.

Kozlov AS, Angulo MC, Audinat E, Charpak S (2006) Target cell-specific modulation of neuronal activity by astrocytes. PNAS 103.

Saly V, Andrew RD (1993) CA3 neuron excitation and epileptiform discharge are sensitive to osmolality. J Neurophysiol 69:2200–2208.

Schwartzkroin P a, Baraban SC, Hochman DW (1998) Osmolarity, ionic flux, and changes in brain excitability. Epilepsy Res 32:275–285.

Traynelis SF, Dingledine R (1989) Role of extracellular space in hyperosmotic suppression of potassium-induced electrographic seizures. J Neurophysiol 61:927–938.

Chapter 5

Osmotic insults in adult mice compared to juveniles and during the development of epilepsy

Abstract

Epilepsy is one of the major public health concerns throughout the world today. It is the 4th most common neurological problem, behind migraine, stroke, and Alzheimer's disease (Hirtz et al., 2007), all of which are associated with cerebral edema. The mechanisms underlying seizure generation are poorly understood and these mechanisms may vary depending on differences in age and on the type of epilepsy. The goal of the research in this chapter was twofold: 1) determine if there were changes in neuronal excitability between juvenile (P15- to P21-day-old) and adult (2- to 5-month-old) mice due to osmotic insult; 2) examine the degree of neuronal excitability in adults due to osmotic stress in a model of epilepsy.

Application of hACSF was capable of increasing SICs in both juvenile and adult mice. Both mild and moderate hypoosmolar insults evoked NMDA receptor-driven slow inward currents (SICs) in neurons from adults, which, like juveniles, initiated within ~1 minute of hACSF application. Adult SICs during the mild 17% hACSF osmotic stress showed a 2-fold increase in frequency of SICs/minute compared to juveniles. The moderate 40% hACSF osmotic stress in adults had a

3-fold increase in SICs/minute compared to juveniles. In addition, hypoosmolar insults induced neuronal firing of action potentials (APs), burst firing, and EPSPs independent of AMPA receptor activation in adults similar to juveniles. The frequency of bursts/minute was significantly increased in adult slices compared to juveniles during the 1st application of a moderate osmotic insult. In addition, the number of APs/burst in the 2nd application of the moderate osmotic stress decreased in adults compared to the 1st application, and it was significantly lower than juveniles in the 2nd application. Overall the results from these experiments indicate that there are differences in neuronal excitability in adult animals compared to juveniles during osmotic insult.

To examine the degree of neuronal excitability during osmotic stress in a model of epilepsy intrahippocampal (IH) kainic acid (KA) injected mice were compared to normal (saline injected control) adult mice during the pathogenesis of the disease. SICs from IH KA mice had significantly slower rise times than the saline injected controls during a mild osmotic stress at 7-days post-injection, possibly indicating a change in NMDA subunit composition during the early development of epilepsy. The findings in these experiments may contribute to a better understanding of cerebral edema and seizures in juvenile and adult mice as well as during development and the pathogenesis of epilepsy.

Introduction

Swelling of brain cells (cellular edema) is a principal component of numerous brain disorders including ischemia, cortical spreading depression,

hyponatremia, and epilepsy. Cellular edema is strongly linked to brain excitability, which has historically been studied in the context of seizure (Schwartzkroin et al., 1998). In epilepsy, cell swelling precedes the initiation of seizure-like discharges *in vitro* and *in vivo* (Traynelis and Dingledine, 1989; Binder et al., 2004). Cellular edema induced by reduction of solution osmolarity can itself trigger seizure-like activity, while at lower doses it increases the amplitude and frequency of synchronous field potential bursting (Andrew et al., 1989; Dudek et al., 1990; Ballyk et al., 1991; Saly and Andrew, 1993; Kilb et al., 2006). Inhibition of cell swelling by increasing solution osmolarity prevents initiation of ictal discharges and stops spontaneously recurring seizures in progress (Andrew et al., 1989; Traynelis and Dingledine, 1989; Haglund and Hochman, 2005).

The relationship between hypoosmolarity and seizures prompted studies to understand the mechanisms underlying the effects of lowered osmolarity on neuronal excitability in brain slices. A more recently described form of excitability observed in pyramidal neurons in several brain areas are slow inward currents, or SICs (Fellin et al., 2004; Kozlov et al., 2006; Fiacco et al., 2007). SICs fit well with both non-synaptic and neurochemical properties of seizure-like discharges. SICs have been reported to be synchronized among small groups of pyramidal neurons (Angulo et al., 2004), suggesting that they may be a type of local epileptiform activity (Wetherington et al., 2008). Although SICs were first reported to be driven by Ca^{2+}-dependent glutamate release from astrocytes, subsequent

studies have pointed to a crucial role of solution osmolarity and cellular swelling to the generation of SICs (Kozlov et al., 2006; Fiacco et al., 2007).

Overall the study of SICs has been very limited. Experiments in hippocampal slices from mouse pups may provide useful information about cerebral edema and epilepsies in juveniles, but the results may not be applicable to adults. Numerous differences exist between adult (AD) and juvenile (JV) brain tissue, including degree of synaptic development, function of receptors, and regulation of neurotransmitter concentrations and reuptake (Diamond, 2005). Furthermore, interstitial space is smaller in adult tissue compared to juvenile tissue (Lehmenkühler et al., 1993; Kilb et al., 2006), suggesting that effects of cell swelling may be quite different between different age groups. To test this possibility, I conducted experiments using hippocampal slices obtained from 2- to 5-month-old adult mice. It is important to understand the relationship between hypoosmolarity, SICs, and changes in neuronal excitability in juvenile and adult mice as well as in the development of epilepsy.

Results

Obtaining healthy adult slices.

The preparation of acute brain slices allows for electrophysiological and imaging techniques to be used *in situ* in tissue that has developed normally in vivo. While this technique has been used since the 1950s and is ideal for

studying synaptic plasticity, whole cell function, and neuronal ion channels, it is not without complications (Collingridge, 1995). In terms of overall slice health, these earlier slices were of questionable quality compared to today's standards. Over the years, slices have improved drastically for electrophysiological and visualization techniques. However, while our laboratory had a protocol in place to obtain healthy juvenile slices, when this protocol was applied to adult slices it was found that the resulting slice health was less than optimal. Thus began the following series of experiments to construct a suitable adult slicing buffer and protocol for obtaining healthy adult slices.

The initial protocol for obtaining acutely isolated adult brain slices from mice was identical to that of juvenile slices (chapter 2). However the adult slicing buffer had been modified drastically over 4 to 6 months of experimentation by another graduate student in the lab attempting to obtain healthy adult slices to contain the following (in mM): 87 NaCl, 75 sucrose 2.5 KCl, 0.5 $CaCl_2$, 7 $MgCl_2$, 1.25 NaH_2PO_4, 25 $NaHCO_3$, 10 glucose, 1.3 ascorbic, acid, bubbled with 5% CO_2 + 95% O_2. Unfortunately, this protocol and adult slicing buffer were yielding poor and rather inconsistent results. After a literature search, the adult slicing protocol was modified to the use of a buffer that was partially frozen to produce a slushy like solution (Stockand and Shapiro, 2006). This is referred to as “adult slicing buffer”. First, the adult slicing buffer was oxygenated for 30 minutes. Next the slicing buffer was placed in the -80 °C for 20 to 30 minutes until partially frozen. The partially frozen adult slicing buffer was then removed, the ice broken apart

and blended so that it had a slush like consistency. Drastically improved slice health was observed in adults via this method. However, adult slice health was still not optimal. Due to the wider range of temperature deviations in the adult slicing protocol, 3.5 mM MOPS, a pH buffering compound was added in an effort to avert drastic changes in pH, and resulted in an improvement in slice health.

Although the changes to the protocol and the adult slicing buffer had improved adult slice health, it was still not on par with juvenile slices. After reviewing the literature a second time and consulting with Dr. Peter Hickmott an expert in electrophysiology, a small set of adult slicing health experiments was executed. The first small set of adult experiments evaluated two different adult slicing buffers: Our latest version of the adult slicing buffer(slicing buffer A) and a slicing buffer by Dr. Hickmott, which called for a complete NaCl replacement with sucrose, along with 100 μM DL-AP5 to block NMDA receptor activation (slicing buffer B). In addition to testing the two different adult slicing buffers I also examined the effects of pyruvate, which supplies energy to the living cells through the citric acid cycle (Krebs cycle), and has been demonstrated to help protect neurons from oxidation due to hydrogen peroxide generation (Desagher et al., 1997). One additional alteration to the protocol was also tested as outlined in Dr. Hickmott's protocol. Adult brain slices were not only sliced in adult slicing buffer, but also incubated in it as well during the recovery period after slicing for 45 minutes before being transferred to normal ACSF. In all, six separate experimental conditions were tested: 1) Slicing in slicing buffer A plus 2 mM

pyruvate; incubation in slicing buffer A plus 2 mM pyruvate; 2) Slicing in slicing buffer A plus 2 mM pyruvate; incubation in normal ACSF plus 2 mM pyruvate 3) Slicing in slicing buffer B; incubation in slicing buffer B; 4) Slicing in slicing buffer B; incubation in normal ACSF; 5) Slicing in slicing buffer B plus 5 mM pyruvate; incubation in slicing buffer B plus 5 mM pyruvate; 6) Slicing in slicing buffer B plus 5 mM pyruvate; incubation in normal ACSF plus 5 mM pyruvate. Three male adult C57BL/6J mice, all 68-days-old, were used to make a total of 33 slices split between 6 experiments. Adult brain slices were then visualized using Differential Interference Contrast (DIC) optics to determine the degree of slice health based on the number of cells that appeared alive and healthy: 1) great > 90%, 2) 90% > good > 75%, 3) 75% > fair > 50%, 4) 50% > poor > 25% 5) 25% > dead (Figure 5.1A-C). Table 5.1 summarizes the results from the small set of adult slice health experiments.

Comparison of the six experimental groups revealed that the healthiest adult slices came from experimental group 1 in which brain slices were sliced and incubated in our adult slicing buffer plus 2 mM Pyruvate. While Dr. Hickmott's slicing buffer, which did a full replacement of NaCl with sucrose, did not appear to enhance slice health above our adult slicing buffer (experimental group 1) it did yield the second best set of healthy adult slices (experiment or group 3). The inclusion of pyruvate, at least the 2 mM concentration, appeared to improve adult slice health compared to previous adult slice preparations. Addition of AP5 to the slicing buffer also appeared to increase slice health. However,

additional experiments would be needed to further examine the effects of AP5 and pyruvate on adult slice health. The most valuable discovery uncovered during this set of experiments was the vast improvement in adult brain slice health due to alteration to the protocol, as described in Dr. Peter Hickmott's slicing protocol, to slice and incubate for 45 minutes in the adult slicing buffer itself, instead of slicing in the adult slicing buffer and incubating in normal ACSF for 45 minutes.

Although immense progress was made to the adult slicing buffer and protocol, there were still a few parameters left to test in order to increase adult brain slice health which led to our second small set of experiments optimizing adult brain slices. In the second round of adult slice health experiments, the contributions of three parameters were examined: AP5 (100 μM), pyruvate (2 mM or 5 mM), and kynurenic acid (100 μM) for their effect on the health of adult brain slices (Djukic et al., 2007; Walz, 2007; Gill et al., 2010). Kynurenic acid acts as an anticonvulsant and antiexcitotoxic most likely through its antagonism of ionotropic receptors such as AMPA/kainate and NMDA receptors (Elmslie and Yoshikami, 1985). Eight experimental conditions were tested (A through H), in which adult slices were dissected in adult slicing buffer (ASB) with: A) 2 mM pyruvate, with incubation in ASB plus 2 mM pyruvate; (B) 5 mM pyruvate; C) sliced in 2 mM pyruvate and 100 μM AP5, and incubated in ASB plus 2 mM pyruvate and 100 μM AP5; (D) 5 mM pyruvate and 100 μM AP5; E) 2 mM pyruvate and 100 μM kynurenic acid, and incubated in ASB plus 2 mM pyruvate

and 100 μM kynurenic acid; (F) 5 mM pyruvate and 100 μM kynurenic acid; G) sliced in 2 mM pyruvate, 100 μM AP5, and 100 μM kynurenic acid, and incubated in ASB plus 2 mM pyruvate, 100 μM AP5, and 100 μM kynurenic acid; or H) 5 mM pyruvate, 100 μM AP5, and 100 μM kynurenic acid. After incubation at 35 °C for 45 minutes, the slices recovered at room temperature for 15 minutes and were then transferred to normal ACSF and allowed to recover for 30 to 45 minutes before imaging the slices to assess slice health (Figure 5.2A-C). Four adult male mice 97-days-old were used for this set of experiments, yielding 42 brain slices. The same criteria were used to assess the degree of slice health for this set of experiments as in the last set of experiments. Table 5.2 summarizes the results from these experiments.

Briefly, the healthiest adult slices were obtained from the experimental group E, when the adult slicing buffer with 2 mM pyruvate and 100 μM kynurenic acid was utilized for both the dissection and incubation of adult brain slices. Inclusion of AP5 did appear to improve slice health, but not to the same degree as kynurenic acid, while the combination of the two yielded similar results; observationally it is estimated that the inclusion of either one or even both would be a welcomed addition to any adult slicing buffer. In addition to experimental group E, experimental groups A, C, and G also yielded fairly healthy adult slices. All of these solutions contained 2 mM pyruvate while experimental groups B, D, F, and H, which contained 5 mM pyruvate, ended up with poorer slice health quality.

Overall experimentation into obtaining healthy adult slices drastically improved adult slice health and viability to the point of often being healthier than juvenile slices (P15-P21) . These truly striking and magnificent adult slices were produced as a result of several changes to the protocol, as well as, modifications to the adult slicing buffer. The first change in the protocol was a modification changing the ice cold slicing buffer into which the brain was initially placed after removal from the mouse into a colder adult slushy slicing buffer solution. In addition, typically after the removal of juvenile brains they are placed in an ice cold slicing buffer and immediately bisected. However, the adult brains were allowed to sit in the oxygenated adult slushy slicing buffer for at least four minutes before being bisected. Another major change to the protocol in obtaining these sublime slices, thanks to Dr. Peter Hickmott, was the technique of not only slicing the brains in the adult slicing buffer, but incubating slices in the same solution for 45 minutes after dissection, before transfer to normal ACSF. Finally, several modifications were made to the adult slicing buffer itself, including the inclusion of 3.5 mM MOPS to balance the pH, 2 mM pyruvate to protect neurons against oxidation from hydrogen peroxide generation, and 100 μM kynurenic acid to reduce overall excitation of excitatory amino acid receptors during dissection and isolation.

Slow inward currents evoked by hACSF are more pronounced in adults than juvenile mice.

To examine age related differences in neuronal excitability during osmotic stress, I conducted experiments using hippocampal slices obtained from 2- to 5-month-old adult mice and P15 to P21 juvenile mice. SICs were recorded in CA1 pyramidal neurons in adult hippocampal slices under the same conditions as those previously described in recordings from juvenile tissue (Chapter 3). SICs were readily evoked in both 17% and 40% hACSF in adult hippocampal slices (Figure 5.3 A & B). During the first application of 17% hACSF, there was a significant 2 fold increase in the frequency of SICs/min in adult animals compared to juveniles, and a 3 fold increase in the 40% hACSF (Figure 5.3 C & D and Table 5.3). For the 2nd and 3rd applications of hACSF, SICs were evoked at the same frequency as observed in juveniles (Figure 5.3 C & D). Amplitudes of SICs recorded in adults were also similar to those in juveniles, except during the 3rd application where amplitudes were larger in adults (Figure 5.3 E & F). These results suggest that on the whole, adult tissue is more susceptible to increased neuronal excitability in conditions of cellular edema compared to juvenile tissue.

Neuronal excitability following osmotic edema was also analyzed and compared between juveniles and adults to baseline activity, as well as, mild and moderate hypoosmolar insults. Adult neurons exhibited a marked increase in SIC frequency of at both the 17% (Figure 5.4 A, top) and 40% (bottom) hACSF over the baseline period prior to hACSF application, similar to juveniles (Table 5.4 and

Figure 5.4 B & C). Baseline SICs were rare or nonexistent in most cells; baseline participation: 17% AD n = 3/8 cells, 40% AD n = 0/9 cells, 17% JV n = 4/8 cells, 40% JV n = 2/9 cells). As previously stated, during the repeated applications of hACSF (above) SIC activity in both the mild and moderate osmotic insults significantly increased in adults compared to juveniles. During the mild osmotic insult adults had more than double the number of SICs/min, while in the moderate osmotic insult they had more than three times that of juveniles (Figure 5.4B &C and Table 5.4). Surprisingly, SIC activity in the wash period was increased in adults compared to juveniles for the 17% hACSF application. Curiously, the frequency of SICs in adults in the wash period after 40% hACSF was not significantly different from juveniles, despite the pronounced elevation in the wash period following 17% hACSF. Yet, SIC activity in the wash period was elevated in juveniles, and adults following the moderate osmotic insult compared to the baseline, while only the adult wash period was elevated in the mild osmotic insult compared to the baseline condition. Rise time significantly increased during the wash period compared to both the mild and moderate osmotic insults for both the juvenile and adult SICs (Table 5.4 and Figure 5.4 D &E). However, rise time also differed between juveniles and adults only during of the wash period following the 17% hACSF application (Figure 5.4 D). Interestingly, adult SICs also decayed significantly faster than juveniles during 17% hACSF application (Figure 5.4 D and Table 5.4). Neither rise time nor decay tau differed between juveniles and adults in 40% hACSF (Figure 5.4 E & G and Table 5.4), suggesting

that intrinsic properties of SICs do not change between the age groups. Rather, the kinetic differences in 17% hACSF treatment groups are likely driven by age-dependent differences in the extracellular space and tissue swelling characteristics.

Changes in neuronal action potentials and synaptic potentials in adults and juveniles during moderate osmotic stress.

In chapters 3 and 4 it was established that mild to moderate osmotic stress was capable of producing SICs as well as action potentials and burst firing in juvenile slices. Along those lines, the previous experiments in this chapter established that slow inward currents can be induced in adults by osmotic stress as well, but showed significant differences from juveniles. Next, it was decided to examine APs and EPSPs in adult animals due to osmotic insult and compare those to the juvenile animals, and some rather interesting results were observed. (Figure 5.5 A). Baseline activity was fairly quiet in both the juveniles and adults, showing no busting activity in either group and only a few single action potentials in a few juvenile slices (Figure 5.5 B). The first application of 40% hACSF produced bursting in 100% of the cells in the juveniles and adults, while single APs were observed in 70% of the juvenile slices and 100% of the adult slices. The number of cells firing single action potentials and bursting activity decreased for both the juveniles and adults in the 2nd application of 40% hACSF +NBQX (Table 5.5 and Figure 5.5 B). During osmotic stress, the frequency of APs/minute

increased during the 1st and 2nd 40% hACSF applications in the juveniles and adults compared to the baseline (Table 5.5). However, the total frequency of APs/min in the adults decreased during the 2nd application compared to the 1st. Furthermore, during the 2nd application of 40% hACSF, the adult neurons had significantly fewer APs/minute than the juvenile animals (Figure 5.5 C). These results seemed somewhat surprising at first, as I expected that the adults might have a significantly higher frequency of APs/minute during the 1st application because I observed significantly more SICs/minute in adults during the first application compared to the juveniles in the previous experiments. However, after analyzing the frequency of the bursts/minute I realized why this might be the case. In the adult animals the frequency of bursts/minute was significantly higher than the juvenile animals during the 1st 40% hACSF application (Figure 5.5 D and Table 5.5). This result was particularly interesting because it suggests that the SICs observed during osmotic insult are increasing bursting activity, and potentially synchronization of neurons within focal areas, and that this activity is more pronounced during the initial osmotic insult in adults compared to juveniles. Bursting activity in juveniles and adults was significantly increased during both osmotic insults compared to baseline, but bursting activity also decreased for both juveniles and adults from the 1st 40% hACSF application to the 2nd application (Table 5.5, and Figure 5.5 D). Another interesting result regarding bursting activity was that the number of APs/burst decreased in the 2nd application compared to the 1st but only for the adults (Table 5.5 and Figure 5.5

E). In fact, during the second application, the adult neurons had significantly fewer, APs/burst than the juveniles (Figure 5.5 E). The frequency of EPSPs/minute showed a similar trend during the 2nd osmotic insult as well, the adult animals had significantly fewer EPSPs/minute than the juveniles (Table 5.5). While the juvenile EPSPs/minute almost appear to be increasing during repeated osmotic insult, and were significant from baseline in both the 1st and 2nd 40% hACSF applications the adult EPSPs/minute were only significantly increased above baseline frequency in the 1st application (Figure 5.5 F). Overall, these results suggest that initially adult tissue is more excitable than juvenile tissue, and that neuronal action potentials for both juveniles and adults seems to decrease or be modulated in some way during repeated osmotic stress. In addition, these results along with the experiments measuring SICs, demonstrate that there are clear differences in the way that juvenile tissue and adult tissue respond to osmotic stress.

Epileptiform-like activity during mild osmotic stress in the CA1 region of adult control and IH KA acute hippocampal slices.

SICs are characteristic of epileptiform activity in their ability to depolarize the neuron above their firing threshold, and to be synchronized among small groups of pyramidal neurons (Angulo et al., 2004; Fellin et al., 2004). In fact SICs are thought to play a role in ictal discharges and possibly modulation of interictal discharges (Angulo et al., 2004; Fellin et al., 2004, 2006; Tian et al., 2005;

Gómez-Gonzalo et al., 2010). In the following set of experiments, the degree of neuronal excitability due to osmotic stress was examined in a model of epilepsy. Neuronal SICs were recorded from adult mice obtained from our collaborators, Dr. Devin Binder's laboratory at the University of California, Riverside, that had experienced intrahippocampal kainic acid (IH KA) induced status epilepticus (SE). The IH KA mouse model was chosen for these experiments because temporal lobe epilepsy with hippocampal sclerosis (TLE-HS) exhibits “reactive gliosis” in addition to axonal sprouting and a specific pattern of neuronal loss (Tauck and Nadler, 1985; Gray and Sundstrom, 1998). The changes that occur in the hypertrophic glial cells, from reactive gliosis, consist of changes in a number of different channels, receptors and proteins as well as a pronounced upregulation of glial fibrillary acidic protein (GFAP) (Aronica et al., 2000). Thus IH KA is an established TLE animal model which closely mimics the pathogenesis observed in humans with TLE (Arabadzisz et al., 2005). Control mice for these experiments were intrahippocampal saline injected littermate control male mice (Figure 5.6A, left traces) injected on the same day as IH KA mice (Figure 5.6A, right traces) and recorded from 7-day post-injection on the same day as well.

The frequency of SICs/minute increased significantly in both the control and IH KA mice during mild osmotic stress, and decreased for both groups during the wash period (Table 5.6 and Figure 5.6 B). However, no significant difference was found between the two groups. Amplitude of SICs decreased during the wash period for both the control and IH KA neurons compared to the

17% hACSF plus TTX and NBQX application (Figure 5.6 C). SIC Rise time for the IH KA mice was significantly slower than the control mice during the mild osmotic insult (Table 5.6 and Figure 5.6 D). In addition, during the wash condition for the control mice, rise time of SICs was significantly faster than during the 17% hACSF application. No significant difference was observed between IH KA mice and control mice for the decay tau of SICs, but decay tau was significantly longer during the mild osmotic insult compared to the wash period for the control and the IHKA mice (Figure 5.6 E). These results suggest that the only significant change 7-day post injection SE was an increase in rise time during the mild osmotic insult, which could suggest a number of different neuronal and/or astrocytic changes due to SE to account for the longer rise times.

Discussion

Slice preparations are well-suited for electrophysiological and imaging techniques to study neuronal excitability, intracellular calcium elevations, neuronal ion channels, and whole cell function, to name a few. Electrophysiological whole-cell patch clamp experiments in acute hippocampal slices requires that the cells be healthy, and the cell membranes directly assessable. Obtaining healthy slices can be problematic for any scientist starting out and especially when working with adult tissue even with the proper protocols and solutions in place (Aghajanian and Rasmussen, 1989). Several parameters were examined in order to improve adult slice health in this chapter. To begin

with, two different slicing buffers were examined for slice viability, original adult slicing buffer and the second one which called for a complete replacement of NaCl with sucrose. The complete replacement of sodium by sucrose is a common technique implemented in adult slicing protocol's called the 'protective cutting' method (Ting et al., 2014). The premise of this method, coincidentally, involves cell swelling by the influx of sodium and water, which constitutes the major insult during the slicing step leading to cell death and poor slice health. While I observed healthier slices using the adult slushy buffer than the adult slicing solution with complete NaCl replacement with sucrose. It should be noted that our adult slushy slicing buffer also takes advantage of this method by a partial sucrose replacement of NaCl. Decrease in the temperature of the adult slushy slicing buffer also improved adult slices, most likely by reducing cellular metabolic demands (Ozturk and Hu, 2005). Temperature plays a large role in neuronal excitability, Traynelis and Dingledine found that decreasing temperature could even abolish potassium-induced electrographic seizures in rat hippocampal slices (Traynelis and Dingledine, 1988). Finally, I found several other modifications which optimized adult brain slice health, including incubating in adult slicing buffer; inclusion of 3.5 mM MOPS to balance the pH; addition of 2 mM pyruvate to protect neurons against oxidation from hydrogen peroxide generation; and 100 μM kynurenic acid to reduce overall excitation of excitatory amino acid receptors during dissection and isolation. In healthy brain tissue astrocytes are quite effective in maintaining homeostasis but in the

pathophysiology of diseases such as epilepsy the ability of astrocytes to adequately siphon water and other ions becomes progressively impaired. Astrocytes swell as their ability to effectively maintain the extracellular homeostasis diminishes and in an effort to balance their own volume and/or osmolarity open VRACs through which water and anions such as glutamate are released.

Osmotic insult increased, EPSPs, action potentials and bursting activity for both juveniles and adults. Slow inward currents were elevated and more pronounced during mild and moderate osmotic insult in hippocampal slices from adult mice compared to juvenile mice. Lastly, I found that SICs and bursting activity were more pronounced in adult vs. juvenile tissue which suggests that activation of NMDA receptors during osmotic insult increases bursting activity, and potentially synchronization of neurons. The only significant change in IH KA mice was an increase in rise time during the mild osmotic insult, which may suggest a number of different neuronal and/or astrocytic changes due to SE to account for the longer rise times. However, seizures were not monitored over the seven-day period, and thus could not be correlated with the degree of activity for each mouse. It is possible that some mice could have had many more seizures than others.

This work provides proof-of-principle that rapid cell swelling can increase and synchronize neuronal excitability in juvenile and adult hippocampus through the generation of SICs. The greater effect observed in adult hippocampal slices

may be due to the smaller ECS in adults, which is estimated to be about half the size of juveniles (Kilb et al., 2006).

Figure 5.1

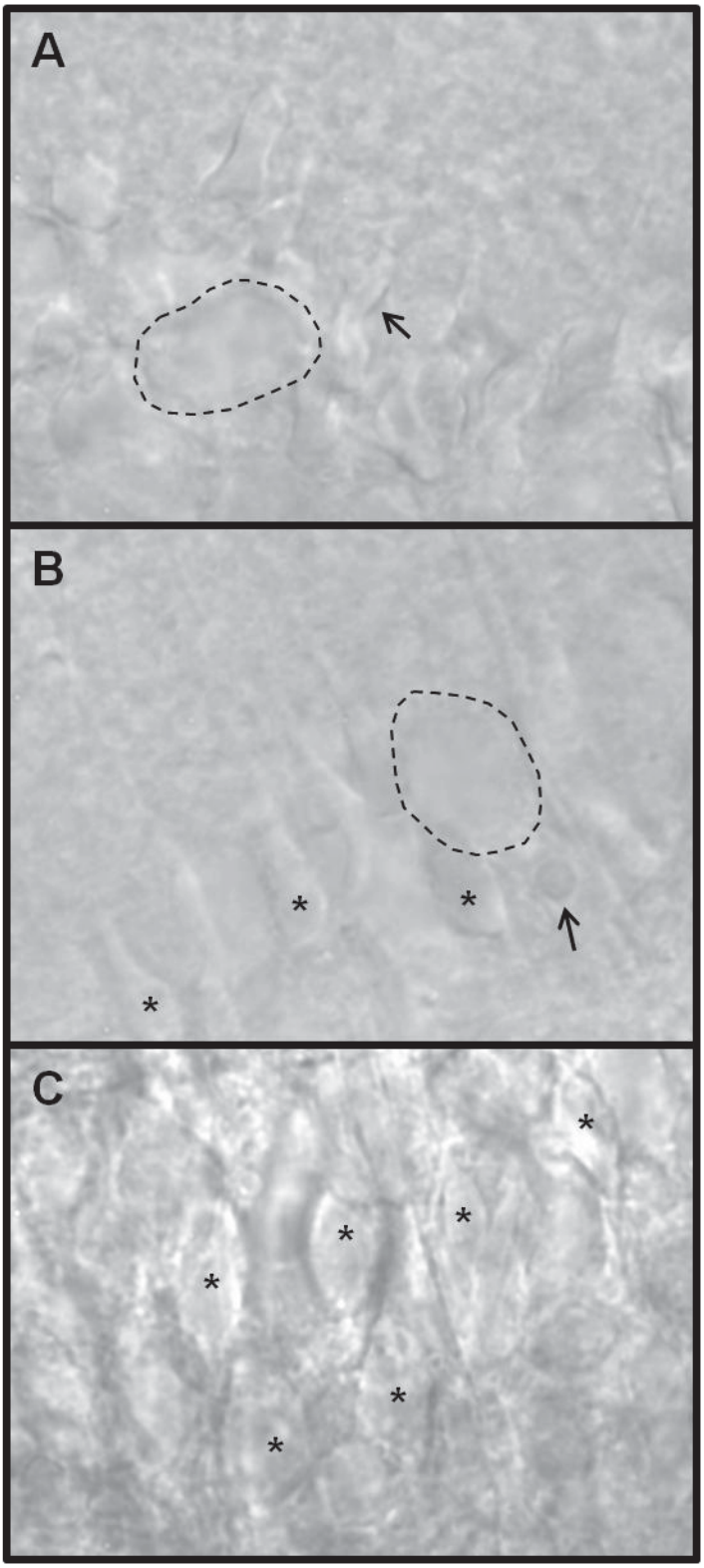

Figure 5.1: Adult slice health experiments comparing adult slicing buffer solutions and protocols. (A) Image of an adult male C57BL/6J mouse brain slice which was sliced in slicing buffer B, and incubated in normal ACSF. The dashed line surrounds the outline of a dead swollen neuron while the arrow is pointing to a shriveled dying neuron. This slice was classified as "Dead" based off our degree of slice health criterion. (B) Brain slice image of the CA1 area of the hippocampus from an adult brain slice dissected and incubated in slicing buffer B, and in classified as "Fair". The arrow points to the swollen nucleolus of a dead neuron, while the dashed line indicates the outline of a neuronal cell membrane from a dead swollen cell, and the asterisks are placed over the cell bodies of healthy CA1 neurons. (C) Image of an adult brain slice classified as "Great" which was sliced and incubated in slicing buffer A; asterisks are placed over the somas of some of the health CA1 pyramidal neurons.

Table 5.1

Small set of adult slice health experiments				
Degree of slice health (Number of cells that appear alive and healthy)				
Great > 90%	90% > Good > 75%	75% > Fair > 50%	50% > Poor > 25%	25% > Dead
1	1	1	3	2
1	2	3	3	2
1	3	3		2
2	6			2
3				4
				4
				4
				4
				4
				5
				5
				5
				5
				5
				6
				6
				6
				6
Numbers in the degree of slice health columns indicate slice health for 1 slice from the six experimental conditions.				

Table 5.1: Adult slice heath experiments evaluating the adult slicing buffers and protocols. A total of 32 brain slices from three adult male mice under six experimental conditions were evaluated for slice health based on the number of cells alive.

Figure 5.2

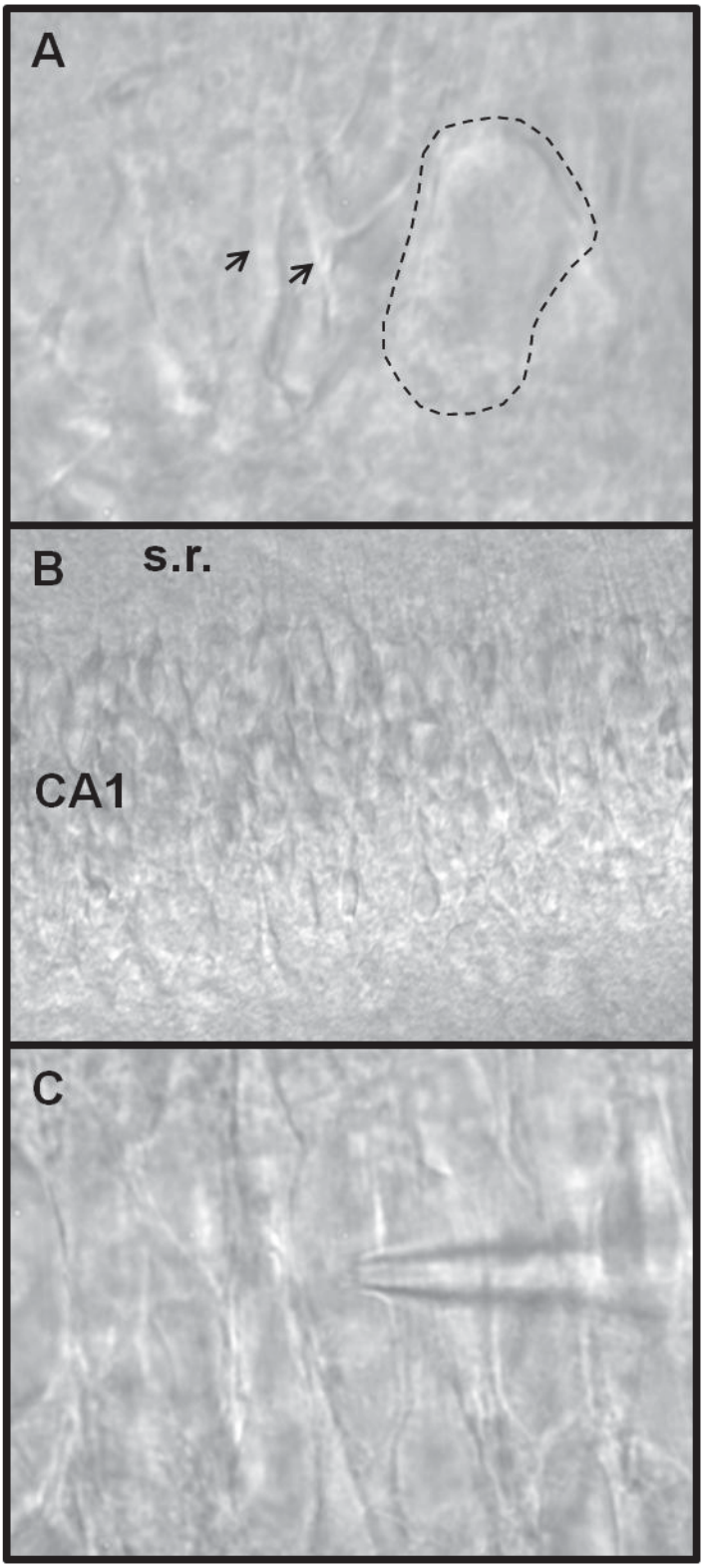

Figure 5.2: Adult slice health experiments examining effects of AP5, pyruvate and kynurenic acid. (A) Picture of the CA1 area of the hippocampus (63x) in an acutely isolated adult brain slice from experimental group D, sliced in adult slushy buffer plus 2 mM pyruvate and 100 µM AP5, then incubated in ASB plus 5 mM pyruvate and 100 µM AP5. This slice was classified as "Dead" due to the numerous dead and dying neurons, note that the dashed line surrounds a dead swollen neuron, while the arrows indicate wrinkled unhealthy neurons. (B) Zoomed out image (20x) of the CA1 and stratum radiatum (s.r.) areas within the hippocampus of a magnificent healthy adult slice, classified as "Great" from experimental condition E in which slices were dissected and incubated in adult slushy slicing buffer containing 2 mM pyruvate and 100 µM kynurenic acid. (C) . Another slice from experimental condition E, zoomed into the (63x) objective for a closer examination of adult slice condition. Notice the smooth, convex and characteristic shape of the stunning CA1 pyramidal neurons.

Table 5.2

Second small set of adult slice health experiments				
Degree of slice health (Number of cells that appear alive and healthy)				
Great > 90%	90% > Good > 75%	75% > Fair > 50%	50% > Poor > 25%	25% > Dead
A	A	A	B	A
A	C	B	F	B
C	D	C	D	B
C	E	G	F	B
E	E	F	F	B
E	G	H	H	C
E	G			D
	G			D
				D
				D
				F
				F
				G
				H
				H
				H
Letters in the degree of slice health columns indicate slice health for 1 slice from the eight experimental conditions.				

Table 5.2: The effects of AP5, pyruvate, and kynurenic acid on adult slice health. Adult slice health was evaluated based on the number of cells alive in eight experimental conditions from four adult male mice in 42 slices.

Figure 5.3

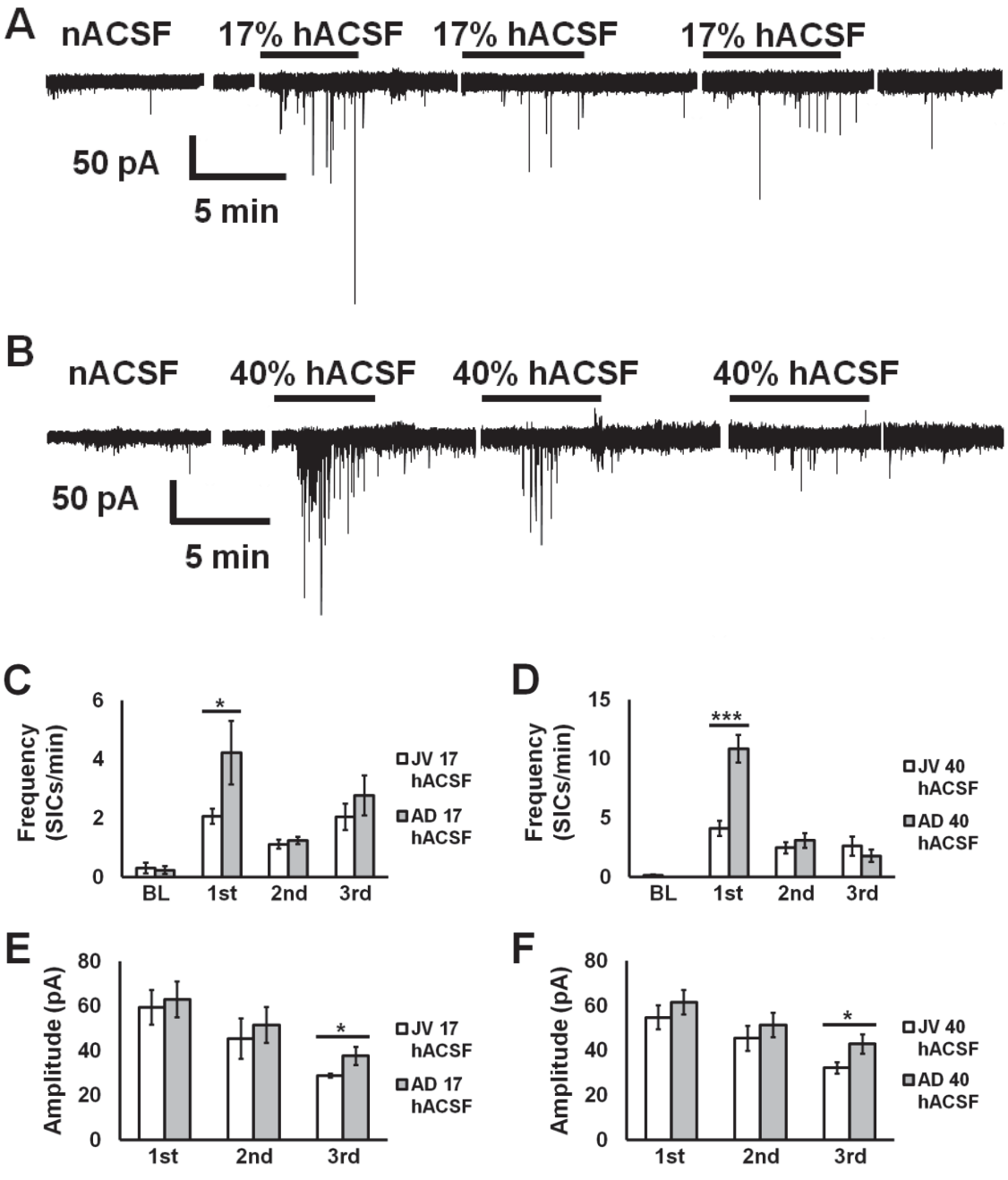
A
nACSF
17% hACSF
17% hACSF
17% hACSF
50 pA
5 min
B
nACSF
40% hACSF
40% hACSF
40% hACSF
50 pA
5 min
C
Frequency (SICs/min)
6
4
2
0
*
BL
1st
2nd
3rd
JV 17 hACSF
AD 17 hACSF
D
Frequency (SICs/min)
15
10
5
0
***
BL
1st
2nd
3rd
JV 40 hACSF
AD 40 hACSF
E
Amplitude (pA)
80
60
40
20
0
*
1st
2nd
3rd
JV 17 hACSF
AD 17 hACSF
F
Amplitude (pA)
80
60
40
20
0
*
1st
2nd
3rd
JV 40 hACSF
AD 40 hACSF

Figure 5.3 Neuronal excitability is elevated to a greater extent in adults compared to juvenile mice within the hippocampus. Representative recordings of CA1 pyramidal neurons in hippocampal slices obtained from 2- to 5-month-old adult mice during repeated applications of 17% hACSF (A) or 40% hACSF (B). Frequency of SICs in adult mice was significantly greater compared to juvenile mice for the first application of both 17 % ($p < .05$) and 40% ($p < .001$) hACSF (C and D). Amplitudes of SICs in adult tissue were larger compared to juveniles during the 3rd application of hACSF for both 17% ($p < .05$) and 40% ($p < .05$). n = 8 for 17% hACSF n = 9 for 40% hACSF.

Table 5.3

Frequency (SICs/min)				
Group	**Baseline**	**1st Application**	**2nd Application**	**3rd Application**
JV 17% hACSF	0.31 ± 0.18	2.07 ± 0.26	1.12 ± 0.15	2.04 ± 0.44
AD 17% hACSF	0.24 ± 0.13	4.22 ± 1.08	1.25 ± 0.12	2.77 ± 0.67
JV 40% hACSF	0.16 ± 0.08	3.55 ± 0.35	2.27 ± 0.48	2.81 ± 0.89
AD 40% hACSF	0 ± 0	10.85 ± 1.16	3.10 ± 0.63	1.80 ± 0.53
Amplitude (pA)				
Group	**Baseline**	**1st Application**	**2nd Application**	**3rd Application**
JV 17% hACSF		59.37 ± 7.77	45.30 ± 9.02	28.88 ± 0.93
AD 17% hACSF		62.83 ± 8.00	51.52 ± 8.05	37.67 ± 4.06
JV 40% hACSF		51.05 ± 4.19	40.90 ± 3.70	30.26 ± 1.95
AD 40% hACSF		61.54 ± 5.56	51.35 ± 5.56	42.86 ± 4.31

Table 5.3: Frequency and amplitude of SICs in juvenile and adult mice during mild and moderate osmotic insult. Mean and SE values for 17% and 40% hACSF juvenile (JV) and adult (AD) experiments plus TTX and NBQX, for frequency of SICs/minute and amplitude of SICs.

Figure5.4

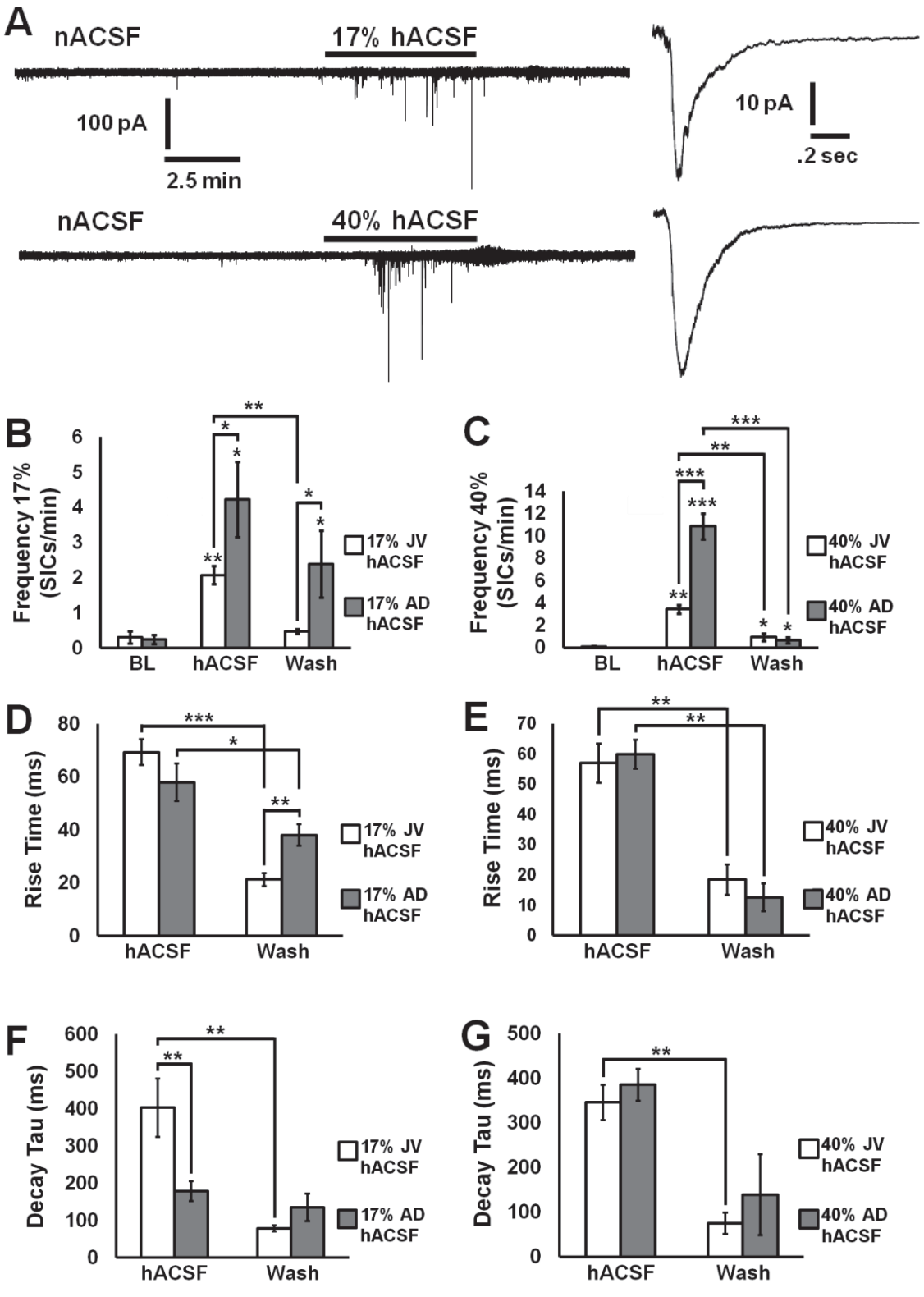
A
nACSF
17% hACSF
100 pA
2.5 min
10 pA
.2 sec
nACSF
40% hACSF
B
Frequency 17% (SICs/min)
BL
hACSF
Wash
17% JV hACSF
17% AD hACSF
C
Frequency 40% (SICs/min)
40% JV hACSF
40% AD hACSF
D
Rise Time (ms)
E
F
Decay Tau (ms)
G

Figure 5.4: Changes in neuronal excitability following osmotic edema in the adult and juvenile CA1 region of the hippocampus. (A) Representative recordings of neuronal SICs in hippocampal slices from 2- to 5-month-old adult mice before and during application of 17% hACSF (upper trace) or 40% hACSF (lower trace). To the right of each recording, the averaged SIC is shown for the hACSF period. (B, C) Frequency of SICs evoked by 17% and 40% hACSF was significantly higher in adult mice compared to juveniles. SICs remained elevated longer during the wash period in 17% hACSF in adults vs. juvenile mice (B). Rise times of SICs occurring during osmotic challenge were significantly slower in 17% (D) and 40% hACSF (E) for both juvenile and adult mice compared to SICs occurring after return to nACSF ('wash'). Not enough SICs occurred during the baseline period for comparison. (F) Decay taus of SICs evoked by 17% hACSF were significantly shorter in adult tissue compared to juvenile, and not significantly different compared to the wash period. (G) Decay taus of SICs evoked by 40% hACSF were similar to those evoked in juvenile slices. (*$p < 0.05$; **$p < 0.01$; and ***$p < 0.001$); n = 8 for 17% hACSF; n = 9 for 40% hACSF.

Table 5.4

Frequency (SICs/min)			
Group	**Baseline**	**hACSF**	**Wash**
JV 17% hACSF	0.31 ± 0.18	2.07 ± 0.26	0.47 ± 0.07
AD 17% hACSF	0.24 ± 0.13	4.22 ± 1.08	2.38 ± 0.95
JV 40% hACSF	0.10 ± 0.07	3.44 ± 0.39	0.93 ± 0.33
AD 40% hACSF	0.00 ± 0.00	10.85 ± 1.16	0.65 ± 0.26
Rise Time (ms)			
Group	**Baseline**	**hACSF**	**Wash**
JV 17% hACSF		69.31 ± 4.84	21.18 ± 2.37
AD 17% hACSF		57.87 ± 7.12	38.03 ± 4.09
JV 40% hACSF		56.94 ± 6.48	18.47 ± 5.07
AD 40% hACSF		59.80 ± 4.73	12.60 ± 4.57
Decay Tau (ms)			
Group	**Baseline**	**hACSF**	**Wash**
JV 17% hACSF		402.75 ± 78.26	78.15 ± 8.19
AD 17% hACSF		177.82 ± 27.08	134.41 ± 36.63
JV 40% hACSF		345.56 ± 39.93	74.51 ± 24.01
AD 40% hACSF		385.33 ± 35.66	139.15 ± 90.51

Table 5.4: Frequency, rise time and decay tau of SICs in juvenile and adult mice before, during and following mild and moderate osmotic insult. Mean and SE values for 17% and 40% hACSF juvenile (JV) and adult (AD) experiments plus TTX and NBQX, for frequency of SICs/minute, rise time, and decay tau of SICs.

Figure 5.5

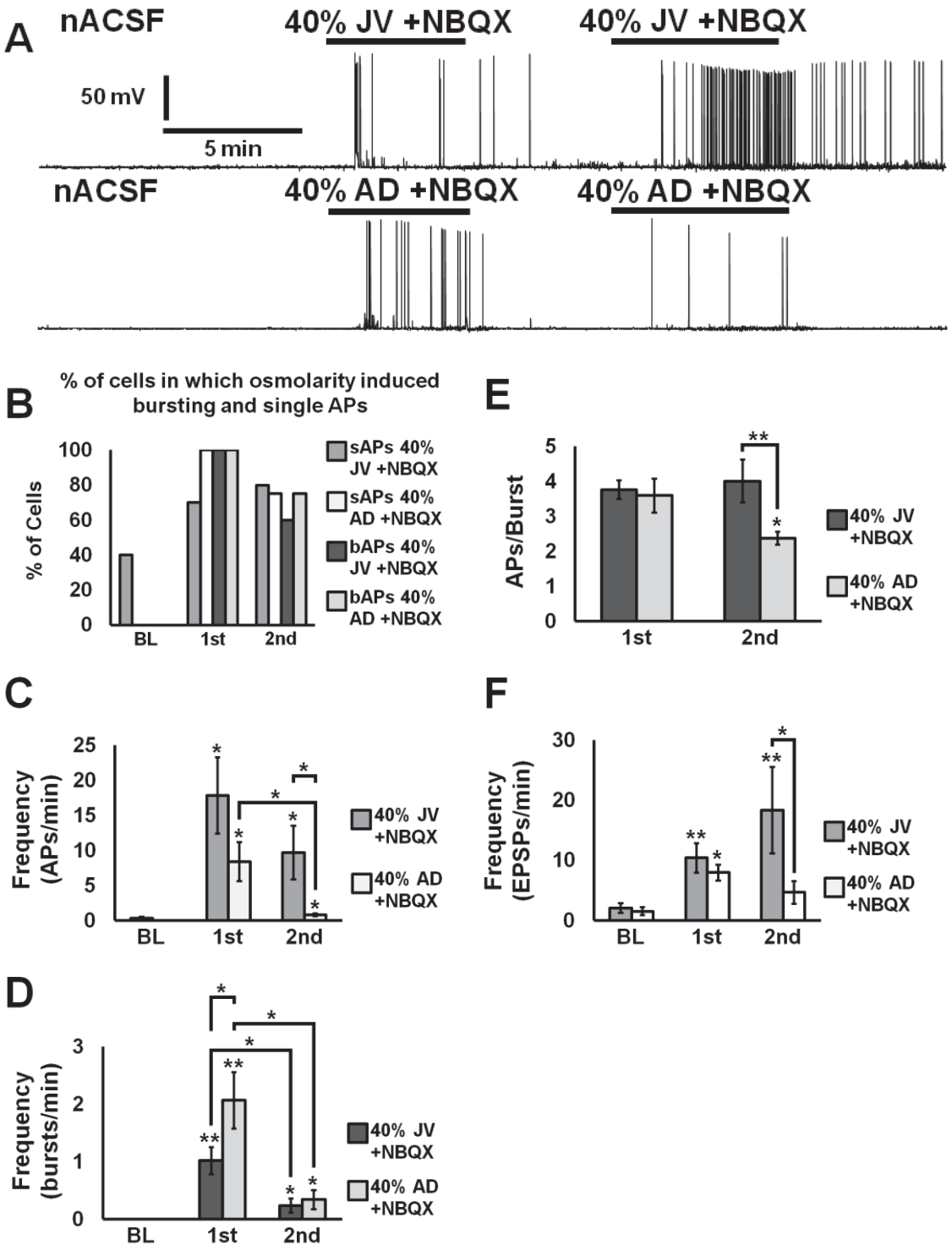
A
nACSF
40% JV +NBQX
40% JV +NBQX
50 mV
5 min
nACSF
40% AD +NBQX
40% AD +NBQX
B
% of cells in which osmolarity induced bursting and single APs
% of Cells
100
80
60
40
20
0
BL
1st
2nd
sAPs 40% JV +NBQX
sAPs 40% AD +NBQX
bAPs 40% JV +NBQX
bAPs 40% AD +NBQX
E
APs/Burst
5
4
3
2
1
0
1st
2nd
40% JV +NBQX
40% AD +NBQX
C
Frequency (APs/min)
25
20
15
10
5
0
BL
1st
2nd
40% JV +NBQX
40% AD +NBQX
F
Frequency (EPSPs/min)
30
20
10
0
BL
1st
2nd
40% JV +NBQX
40% AD +NBQX
D
Frequency (bursts/min)
3
2
1
0
BL
1st
2nd
40% JV +NBQX
40% AD +NBQX

Figure 5.5: Neuronal excitability in adults and juveniles during moderate osmotic stress. (A) Whole-cell patch-clamp recordings of action potentials and EPSPs in neurons in the CA1 area of the hippocampus of juvenile (top trace) and adult (bottom trace) mice. (B) percentage of cells urge osmolarity and is bursting and single action potentials in juvenile and adult mice due to application of 40% hACSF +NBQX. (C) The frequency of action potentials per minute increased in both adults and juveniles during the 1st and 2nd application compared to the baseline activity. In addition, there was a significant decrease the total frequency of APs/minute in adult animals during the 2nd application compared to the 1st. During the 2nd application of the 40% hACSF the frequency of APs/minute was significantly higher in the juveniles compared to the adults. (D) Interestingly, the frequency of bursts/minute was significantly higher in the 1st application of the adults compared to the juvenile animals during the moderate osmotic stress. Although the frequency of bursts/minute for both groups in the 1st and 2nd application of 40% hACSF was significantly higher compared to the baseline activity. They also followed a similar pattern over the two 40% hACSF applications, with the second application, inducing significantly fewer bursts/minute than the first application. (E) The number of action potentials per burst decreased in adults during the 2nd application compared to the 1st application. In addition, during the 2nd application of the moderate osmotic stress the juveniles had significantly more APs/burst than the adults. (F) During the 2nd application of the 40% hACSF the frequency of EPSPs per minute was significantly lower in the adult neurons than in the juvenile neurons. Furthermore, in the juvenile slices the frequency of EPSPs/ minute increased in both the 1st and 2nd application of 40% hACSF compared to baseline activity, while in the adults it was only significant increased above baseline in the 1st hACSF application but not the 2nd application. (*$p < 0.05$; **$p < 0.01$; and ***$p < 0.001$); n = 4 to 8 cells.

Table 5.5

Frequency (APs/min)			
Group	Baseline	1st App	2nd App
40% JV +NBQX	0.28 ± 0.21	17.84 ± 5.45	9.69 ± 3.85
40% AD +NBQX	0 ± 0	8.41 ± 2.77	0.78 ± 0.22
% of Cells in Which Osmolarity Induced sAPs			
Group	Baseline	1st App	2nd App
40% JV +NBQX	40	70	80
40% AD +NBQX	0	100	75
% of Cells in Which Osmolarity Induced bAPs			
Group	Baseline	1st App	2nd App
40% JV +NBQX	0	100	60
40% AD +NBQX	0	100	75
Frequency (bAPs/min)			
Group	Baseline	1st App	2nd App
40% JV +NBQX	0 ± 0	1.02 ± 0.24	0.24 ± 0.12
40% AD +NBQX	0 ± 0	2.07 ± 0.49	0.34 ± 0.16
# of APs/burst			
Group	Baseline	1st App	2nd App
40% JV +NBQX		3.75 ± 0.26	4 ± 0.61
40% AD +NBQX		3.59 ± 0.48	2.37 ± 0.19
Frequency (EPSPs/min)			
Group	Baseline	1st App	2nd App
40% JV +NBQX	2.02 ± 0.8	10.38 ± 2.41	18.32 ± 7.17
40% AD +NBQX	1.51 ± 0.68	7.93 ± 1.29	4.64 ± 1.85

Table 5.5: Action potentials and EPSPs for adult and juvenile mice during moderate osmotic stress. Mean and SE for the frequency of APs/min, frequency of bAPs/min, number of APs/burst, and frequency of EPSPs/min. Percentage of cells that responded to the 40% hACSF before, during, and after the moderate osmotic stress for adult and juvenile mice.

Figure 5.6

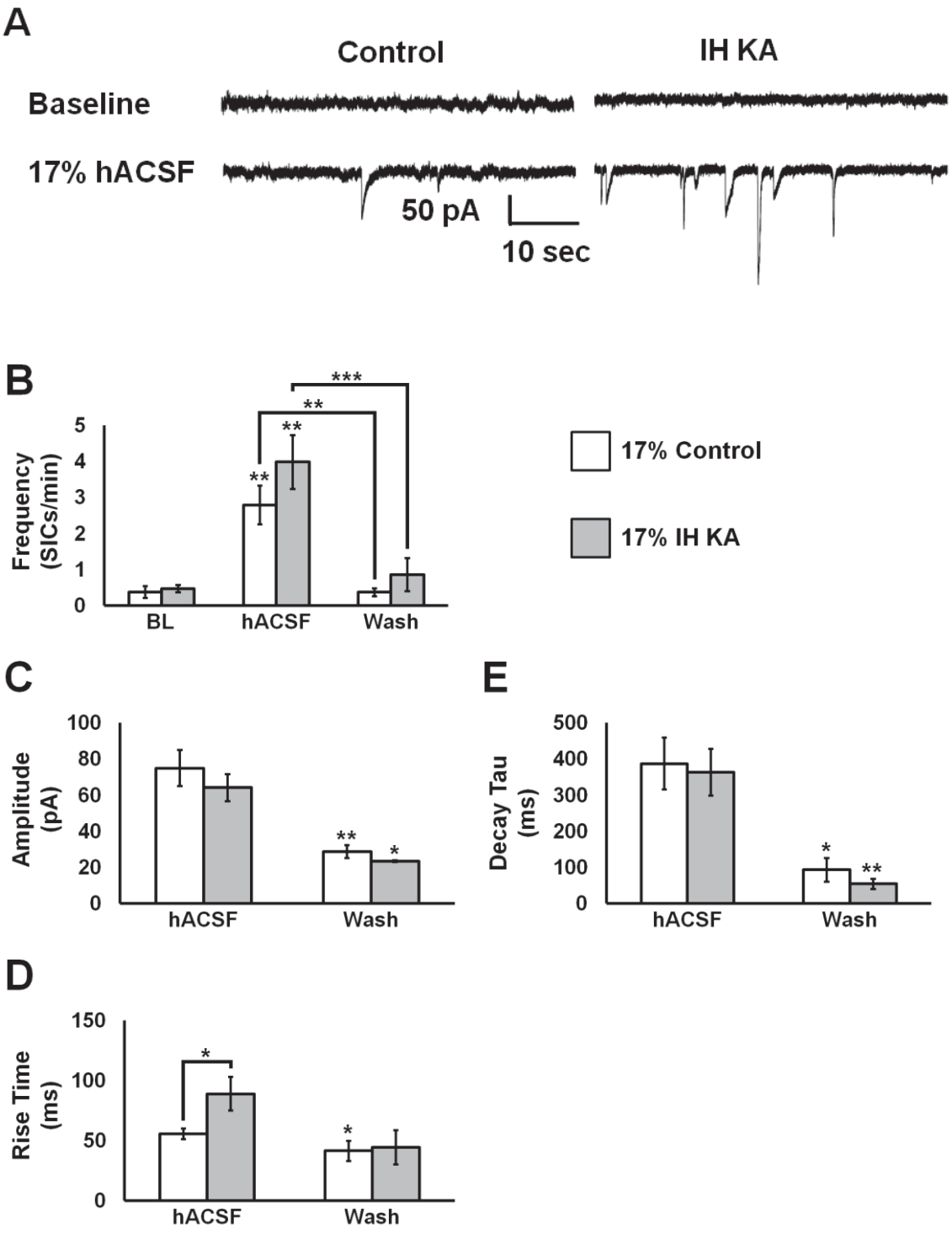
A
Control
IH KA
Baseline
17% hACSF
50 pA
10 sec
B
Frequency (SICs/min)
BL
hACSF
Wash
17% Control
17% IH KA
C
Amplitude (pA)
hACSF
Wash
D
Rise Time (ms)
hACSF
Wash
E
Decay Tau (ms)
hACSF
Wash

Figure 5.6: Epileptiform-like activity during mild osmotic stress in the CA1 region of adult control and IH KA acute hippocampal slices. (A) Whole cell voltage clamp recordings during the baseline and application of a 17% hACSF solution from adult male mice seven days after intrahippocampal injection of saline "control" (left traces) , or kainic acid (right traces) into the dorsal hippocampus. (B) The frequency of SICs increased significantly during mild osmotic stress compared to basal conditions in both the control and IH KA brain slices. Furthermore, SIC activity decreased significantly during the wash back to normal conditions following the 17% hACSF application. (C) . Amplitude of SICs was reduced in the wash condition following mild osmotic insult. (D) . Interestingly, SIC rise time in brain slices from IH KA mice were significantly longer than the saline injected controls during mild osmotic edema, but shortened to juvenile levels in the wash. In addition, rise time became significantly faster following the mild osmotic edema, but only for the saline injected controls. (D) . The decay tau of SICs for both the control and IH KA mice shortened during the wash only mild osmotic stress. (*$p < 0.05$; **$p < 0.01$; and ***$p < 0.001$); n = 5-10 cells per group.

Table 5.6

Frequency (SICs/min)			
Group	Baseline	hACSF	Wash
17% Control	0.38 ± 0.17	2.80 ± 0.54	0.37 ± 0.11
17% IH KA	0.47 ± 0.11	3.99 ± 0.75	0.86 ± 0.46
Amplitude (pA)			
Group	Baseline	hACSF	Wash
17% Control		75.01 ± 9.90	28.73 ± 3.59
17% IH KA		64.18 ± 7.44	23.43 ± 0.52
Rise Time (ms)			
Group	Baseline	hACSF	Wash
17% Control		55.71 ± 4.30	41.54 ± 8.53
17% IH KA		89.09 ± 14.02	44.43 ± 14.21
Decay Tau (ms)			
Group	Baseline	hACSF	Wash
17% Control		387.12 ± 71.61	93.46 ± 32.53
17% IH KA		363.21 ± 64.86	54.06 ± 14.61

Table 5.6: SIC frequency and kinetics in 7-day post-injection saline control and IH KA mouse contralateral hippocampal slices before, during and after a 17% hACSF application. The table displays mean and SE values for SICs before, during, and following a mild osmotic insult in adult male mice 7 days after intrahippocampal injection of either saline (control) or kainic acid.

References

Aghajanian GK, Rasmussen K (1989) Intracellular Studies in the Facial Nucleus Illustrating a Simple New Method for Obtaining Viable Motoneurons in Adult Rat Brain Slices. Synapse 338:331–338.

Andrew RD, Fagan M, Ballyk B a, Rosen a S (1989) Seizure susceptibility and the osmotic state. Brain Res 498:175–180.

Angulo MC, Kozlov AS, Charpak S, Audinat E (2004) Glutamate released from glial cells synchronizes neuronal activity in the hippocampus. J Neurosci 24:6920–6927.

Arabadzisz D, Antal K, Parpan F, Emri Z, Fritschy J-M (2005) Epileptogenesis and chronic seizures in a mouse model of temporal lobe epilepsy are associated with distinct EEG patterns and selective neurochemical alterations in the contralateral hippocampus. Exp Neurol 194:76–90.

Aronica E, Vliet EA Van, Mayboroda OA, Troost D, Lopes FH, Gorter JA (2000) Upregulation of metabotropic glutamate receptor subtype mGluR3 and mGluR5 in reactive astrocytes in a rat model of mesial temporal lobe epilepsy. 12:2333–2344.

Ballyk BA, Quackenbush SJ, Andrew RD (1991) Osmotic Effects on the CA1 Neuronal Population in Hippocampal Slices with Special Reference to Glucose. J Neurophysiol 65.

Binder DK, Papadopoulos MC, Haggie PM, Verkman a S (2004) In vivo measurement of brain extracellular space diffusion by cortical surface photobleaching. J Neurosci 24:8049–8056.

Collingridge GL (1995) The brain slice preparation : a tribute to the pioneer Henry Mcllfwain. 59:5–9.

Desagher S, Glowinski J, Premont J (1997) Pyruvate Protects Neurons against Hydrogen Peroxide-Induced Toxicity. J Neurosci 17:9060–9067.

Diamond JS (2005) Deriving the Glutamate Clearance Time Course from Transporter Currents in CA1 Hippocampal Astrocytes : Transmitter Uptake Gets Faster during Development. 25:2906–2916.

Djukic B, Casper KB, Philpot BD, Chin L-S, McCarthy KD (2007) Conditional knock-out of Kir4.1 leads to glial membrane depolarization, inhibition of potassium and glutamate uptake, and enhanced short-term synaptic potentiation. J Neurosci 27:11354–11365.

Dudek FE, Obenaus a, Tasker JG (1990) Osmolality-induced changes in extracellular volume alter epileptiform bursts independent of chemical synapses in the rat: importance of non-synaptic mechanisms in hippocampal epileptogenesis. Neurosci Lett 120:267–270.

Elmslie KS, Yoshikami D (1985) Effects of Kynurenate on Root Potentials Evoked by Synaptic Activity and Amino Acids in the Frog Spinal Cord. Brain Res 330:265–272.

Fellin T, Gomez-Gonzalo M, Gobbo S, Carmignoto G, Haydon PG (2006) Astrocytic glutamate is not necessary for the generation of epileptiform neuronal activity in hippocampal slices. J Neurosci 26:9312–9322.

Fellin T, Pascual O, Gobbo S, Pozzan T, Haydon PG, Carmignoto G (2004) Neuronal synchrony mediated by astrocytic glutamate through activation of extrasynaptic NMDA receptors. Neuron 43:729–743.

Fiacco TA, Agulhon C, Taves SR, Petravicz J, Casper KB, Dong X, Chen J, McCarthy KD (2007) Selective Stimulation of Astrocyte Calcium In Situ Does Not Affect Neuronal Excitatory Synaptic Activity. Neuron 54:611–626.

Gill MB, Frausto S, Ikoma M, Sasaki M, Oikawa M, Sakai R, Swanson GT (2010) A series of structurally novel heterotricyclic alpha-amino-3-hydroxyl-5-methyl-4-isoxazole-propionate receptor-selective antagonists. Br J Pharmacol 160:1417–1429.

Gómez-Gonzalo M, Losi G, Chiavegato A, Zonta M, Cammarota M, Brondi M, Vetri F, Uva L, Pozzan T, de Curtis M, Ratto GM, Carmignoto G (2010) An excitatory loop with astrocytes contributes to drive neurons to seizure threshold. PLoS Biol 8:e1000352.

Gray WP, Sundstrom LR (1998) Kainic acid increases the proliferation of granule cell progenitors in the dentate gyrus of the adult rat. Brain Res:52–59.

Haglund MM, Hochman DW (2005) Furosemide and mannitol suppression of epileptic activity in the human brain. J Neurophysiol 94:907–918.

Hirtz D, Thurman DJ, Mohamed M (2007) How common are the “ common ” neurologic disorders ?

Kilb W, Dierkes PW, Syková E, Vargová L, Luhmann HJ (2006) Hypoosmolar conditions reduce extracellular volume fraction and enhance epileptiform activity in the CA3 region of the immature rat hippocampus. J Neurosci Res 84:119–129.

Kozlov a S, Angulo MC, Audinat E, Charpak S (2006) Target cell-specific modulation of neuronal activity by astrocytes. PNAS 103:10058–10063.

Lehmenkühler A, Syková E, Svoboda J, Zilles K, Nicholson C (1993) Extracellular space parameters in the rat neocortex and subcortical white matter during postnatal development determined by diffusion analysis. Neuroscience 55:339–351.

Ozturk SS, Hu W eds. (2005) Cell culture technology for pharmaceutical and cell-based therapies. CRC Press.

Saly V, Andrew RD (1993) CA3 neuron excitation and epileptiform discharge are sensitive to osmolality. J Neurophysiol 69:2200–2208.

Schwartzkroin P a., Baraban SC, Hochman DW (1998) Osmolarity, ionic flux, and changes in brain excitability. Epilepsy Res 32:275–285.

Stockand JD, Shapiro MS eds. (2006) Ion Channels Methods and Protocols, Vol. 337. Humana Press Inc.

Tauck DL, Nadler JV (1985) Evidence of Functional Mossy Fiber Sprouting in Hippocampal Formation of Kainic Acid-Treated Rats. J Neurosci 5:1016–1022.

Tian G-F, Azmi H, Takano T, Xu Q, Peng W, Lin J, Oberheim N, Lou N, Wang X, Zielke HR, Kang J, Nedergaard M (2005) An astrocytic basis of epilepsy. Nat Med 11:973–981.

Ting JT, Daigle TL, Chen Q, Feng G (2014) Acute brain slice methods for adult and aging animals: application of targeted patch clampanalysis and optogenetics Martina M, Taverna S, eds. Methods Mol Biol 1183:1–21.

Traynelis SF, Dingledine R (1988) Potassium-induced spontaneous electrographic seizures in the rat hippocampal slice. J Neurophysiol 59:259–276.

Traynelis SF, Dingledine R (1989) Role of extracellular space in hyperosmotic suppression of potassium-induced electrographic seizures. J Neurophysiol 61:927–938.

Walz W ed. (2007) Patch-Clamp Analysis Advanced Techniques. Totowa: Humana Press Inc.

Wetherington J, Serrano G, Dingledine R (2008) Astrocytes in the epileptic brain. Neuron 58:168–178.

Chapter 6

A closer examination of NMDAR activation and specificity during osmotic stress and mechanisms of astrocytic glutamate release.

Abstract

Cerebral edema and seizures are associated with a plethora of diseases, disorders, and conditions such as traumatic brain injury, stroke, cardiac arrest, autism and epilepsy (Lassmann et al., 1984; Unterberg et al., 2004; Bardutzky and Schwab, 2007; Siegel, 2015). Treatments for these conditions are often limited or ineffective, substantiating the need to further understand the cell-specific contributions and mechanisms involved. It has been known for some time that cell swelling and reduction of the extracellular space can lead to increases in neuronal excitability and even to seizures *in vitro* and *in vivo* (Traynelis and Dingledine, 1988; Binder et al., 2004). The elevated neuronal excitability in these conditions has been attributed to increased ephaptic interactions between neurons. However, astrocytes may contribute actively to this process due to their selective expression of the glial water channel aquaporin 4 (AQP4), together with evidence that astrocyte swelling *in vitro* leads to significant amounts of glutamate release through astrocytic volume-regulated anion channels (VRAC) (Fellin et al., 2004; Kimelberg, 2004; Papadopoulos and Verkman, 2007). To examine the mechanisms and specificity of activation leading to neuronal excitability a number of experiments were conducted in this

chapter examining NMDARs. Using whole-cell patch clamp electrophysiological techniques, SICs were recorded in CA1 pyramidal neurons during osmotic insult in acutely isolated slices from mice. Inclusion of D-serine, a required co-agonist of NMDA receptors, significantly increased neuronal excitability during mild osmotic stress. Blocking the NR2B subunit containing NMDA receptors with Ro 25-6981 decreased neuronal SICs during both the 17% and 40% hACSF applications. Pilot experiments in which astrocytes were loaded with glutamate via patch pipette increased the amplitude and number of SICs when hACSF was applied. Future experiments will assay the effect of astrocytic AQP4 KO, glutamate loading of astrocytes, and astrocytic VRACs and pannexins/hemichannels, further defining the mechanisms underlying osmotic edema-induced increases in neuronal excitability. These studies could uncover several novel astrocytic targets and therapies to treat a vast range of CNS syndromes, diseases and disorders.

Introduction

In recent years, several researchers have proposed that astrocytes are involved in the pathophysiology of epilepsy, and that further research in extrapolating astrocytic contributions to seizures is imperative (Binder et al., 2006; Wetherington et al., 2008). Several studies indicate that ability of astrocytes to maintain the osmotic balance may be impaired in epilepsy due to

loss and redistribution of key channels and receptors like the water channel Aquaporin-4 and the Kir4.1 inwardly rectifying K^+ channel (Binder et al., 2006). Oxygen glucose deprivation, potassium and water uptake can all lead to astrocytic swelling (Andrew et al., 2007; Risher et al., 2009). Astrocytic swelling may be of particular importance to epilepsy because several studies have demonstrated that tissue swells prior to the initiation of a seizure (Traynelis and Dingledine, 1988; Binder et al., 2004). As astrocytes *in vitro* swell, they may release glutamate to regulate their volume or osmolarity, potentially through VRAC channels, which can be activated by several mechanisms, or hemichannels and/or pannexons (Pasantes-Morales et al., 2000; Mongin and Orlov, 2001; Abdullaev et al., 2006; Montero and Orellana, 2015). The glutamate released during astrocytic swelling could affect neuronal excitability through the activation of neuronal NMDA receptors, which include a population located extrasynaptically near astrocytic membranes. Activation of NMDA receptors by astrocytic glutamate is thought to produce SICs, which are NMDA dependent, and synchronous among small groups neurons (Fellin et al., 2004). The near-complete block of SICs by DL-AP5 (Chapter 3) indicated that they were NMDA receptor-dependent. I decided to pursue the role of NMDA receptors further by recording SICs during mild osmotic stress in the presence of 10 μM D-serine, a required NMDA receptor co-agonist which binds to the glycine site on the NR1 subunit. D-serine concentrations are tightly regulated *in vivo* (Danysz and Parsons, 1998), but may be partially depleted by slice preparation and the

continuous perfusion of slices by ACSF. The depletion of D-serine in slice experiments could mean that the activity I observe during osmotic stress is an underrepresentation of the actual neuronal activity. Therefore, elevating concentrations of D-serine to saturating levels in the slice is expected to potentiate NMDAR-dependent activity.

Exogenous D-serine has been suggested to specifically enhance activity of NR2B-containing NMDA receptors (Duffy et al., 2008). SICs are identified in part by their slow rise and decay times, which may partially result from the kinetics of the particular NMDA subtypes activated. Previous work has suggested that SICs (resulting from different manipulations) are mediated by NMDA receptors containing the NR2B subunit (Fellin et al., 2004). These studies revealed possible anticonvulsant effects (Wang and Bausch, 2004; Mares and Mikulecká, 2009), as well as neuroprotective effects following status epilepticus in models of epilepsy due to the NR2B antagonist ifenprodil (Ding et al., 2007; Frasca et al., 2011). Unfortunately, ifenprodil is not as selective for NMDA receptors as it was once thought to be, it also binds to α1 adrenergic receptors (Mosley et al., 2009), blocks presynaptic P/Q type calcium channels (Delaney et al., 2012), and possibly modulates other receptors (McCool and Lovinger, 1995). The highly selective NR2B antagonist Ro 25-6981 (1 μM), a derivative of ifenprodil, was selected for the experiments in this chapter to investigate whether SICs induced by osmotic stress were dependent on the NR2B subunit of the NMDA receptor.

Among local networks of neurons, SICs have been found to be synchronous and depolarize neurons above firing threshold in hippocampal pyramidal neurons, which has brought about the idea that they may have a role in epilepsy (Wetherington et al., 2008). Before the initiation of a seizure there is a decrease in the extracellular space (ECS) due to tissue swelling. Astrocytes swell and may release glutamate through VRACs, or hemichannels in certain conditions, but the significance of this observation in regard to seizure induction is not known (Zhang et al., 2011). In an effort to understand this process and determine if the SICs observed during osmotic stress are due to astrocytic release of glutamate, a set of experiments was designed to load astrocytes with glutamate and record slow inward currents. The overall purpose of the experiments in this chapter was to further investigate and understand the cellular mechanisms of neuronal excitability during cellular swelling.

Results

SICs induced by hACSF are enhanced by D-serine

Since neuronal activity may be reduced in slice preparations, due to depletion of D-serine, 10 μM D-serine was added to all of the solutions. Neuronal activity was then observed during hypoosmolar stress. Consistent with this, I observed a substantial increase in SIC frequency in slices bathed in 17% hACSF + D-serine compared to controls without D-serine (Table 6.1 and Figure 6.1 A & B). A second application of 17% hACSF without D-serine evoked SICs at a lower

frequency than the first application, whereas SIC frequency remained potentiated during the second application if D-serine was included and showed little or no attenuation. Interestingly, while SICs occurred along a similar time course with and without D-serine during the first hACSF application, D-serine appeared to shift peak SIC production ~30-60 seconds later during the second hACSF application (Figure 6.1 C).

SICs evoked by hACSF are blocked by antagonists of NR2B-containing NMDA receptors.

Using the highly selective NR2B antagonist Ro 25-6981, I investigated the role of NR2B subunit containing NMDA receptors on neuronal excitability during osmotic stress. As in the previous experiment, SICs were evoked successively using repeated applications of 17% (top traces) or 40% hACSF (bottom traces). The NMDAR antagonist Ro 25-6981 was only included 5 minutes prior to, and during the 2nd hACSF application. The SICs were almost completely abolished by the addition of Ro 25-6981 in the 17% hACSF and 40% hACSF (Table 6.2 and Figure 6.2 B & C). These data indicate that NR2B subunit containing NMDA receptors play a critical role in the increased neuronal excitability produced by acute cellular edema.

Pilot experiments suggest that neuronal SICs are enhanced during moderate osmotic stress when astrocytes are loaded with glutamate.

To investigate the contribution of astrocytic swelling-evoked glutamate release as a potential cellular mechanism in the initiation of SICs during osmotic edema, neurons in the CA1 area of the hippocampus were patch clamped and a baseline recording of NMDA receptor currents was obtained. An adjacent astrocyte in the stratum radiatum (s.r.) region of the hippocampus was also patch clamped with a pipette containing either 20 mM glutamate, or 20 mM sucrose (Control) (Figure 6.3 C). The glutamate or sucrose was allowed to dialyze into the astrocyte for 15 minutes to ensure enough time to diffuse into the smaller astrocytic compartments. After the astrocyte was patch clamped for 5 minutes, the nACSF + 1μM TTX and 10 μM NBQX was bath applied for 10 minutes to remove the Mg^{2+} block from the NMDA receptors. The patch pipette was then carefully removed from the astrocyte in order to prevent the pipette from acting as a source of intracellular ions for the astrocyte to draw from, which might prevent astrocytic swelling during hACSF application. After a 5-minute baseline recording from the neurons in nACSF, 17% hACSF + TTX and NBQX was applied to induce cellular swelling while recording SICs from CA1 pyramidal neurons (Figure 6.3 A & B). The loading of astrocytes with glutamate appeared to enhance SIC amplitude during application of 17% hACSF (Figure 6.3 D). These data provide an important insight into the role of astrocytic swelling-evoked glutamate release. Because the manipulation is specific to astrocytes, it suggests

that the astrocytes themselves are a source of glutamate triggering SICs rather than the glutamate increase coming as a result of ECS constriction alone.

Discussion

Previous research has indicated that SICs, regardless of proposed mechanism, are mediated by NMDA receptors. The main findings in this research demonstrate the specificity of NMDA receptors. In the present study, it was also observed that NMDA receptors are responsible for SICs. SICs were potentiated by D-serine, and blocked by DL-AP5 and the NR2B specific compound Ro25-6981. Previous work postulated that extrasynaptic NMDA receptors generate SICs because of their slow kinetics and block by NR2B subunit-specific antagonists such as ifenprodil (Fellin et al., 2004; Araque et al., 2014). Evidence suggests that synaptic and extrasynaptic NMDA receptors are triheteromeric, containing GluN1, GluN2A (NR2A) and GluN2B (NR2B) subunits (Harris and Pettit, 2007; Rauner and Köhr, 2011; Tovar et al., 2013). Therefore, subunit selective pharmacology cannot distinguish between synaptic vs. extrasynaptic pools of NMDA receptors. Although pilot data, loading astrocytes with glutamate, and inducing slow inward currents during osmotic stress appear to enhance slow inward currents, which is suggestive that astrocytes are the cells releasing glutamate during osmotic edema.

Figure 6.1:

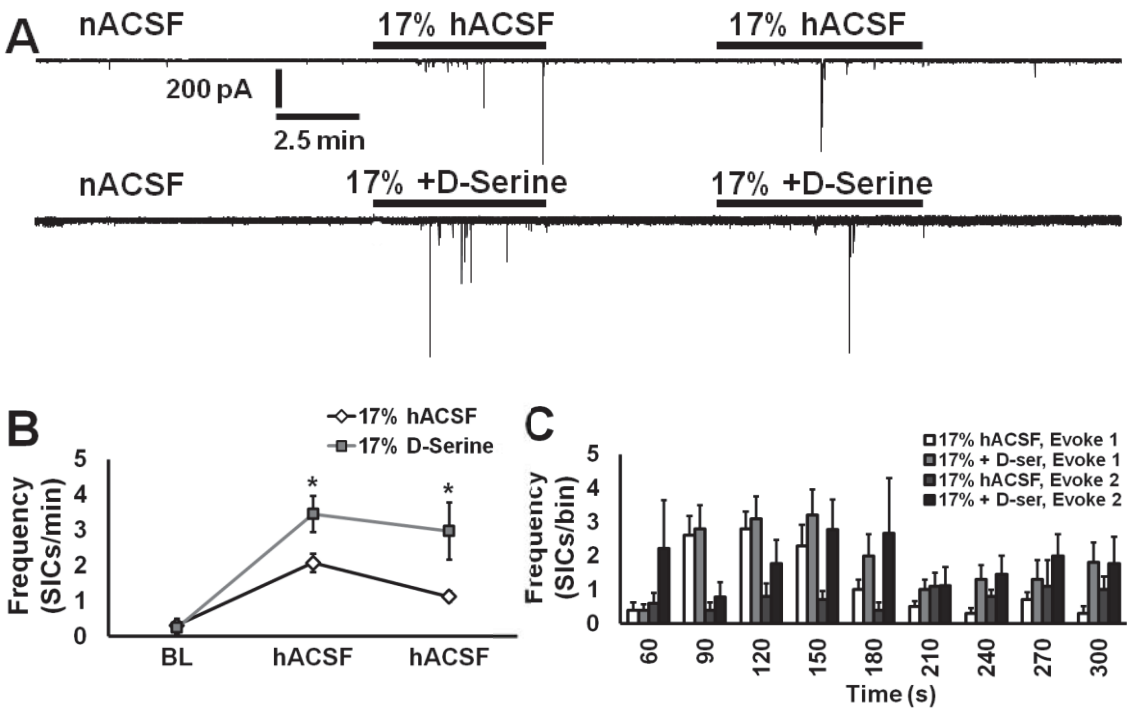

Figure 6.1: SICs are enhanced by D-Serine, a coagonist of the NMDA receptor. (A) Representative recordings of excitatory currents in CA1 pyramidal neurons before, during and after 17% hACSF (upper trace) and 17% hACSF + D-serine (lower trace). In order to isolate SICs, both of the experiments also contained 1 μM TTX and 10 μM NBQX in order to block neuron firing of action potentials and AMPA receptor activation. (B) On average, D-serine significantly enhanced the frequency of SICs during both hACSF applications compared to baseline and also compared to recordings in separate slices in which hACSF was re-applied without D-serine. (C) Frequency histogram of the hACSF period organized into 30 s bins revealed a right-ward shift in SIC frequency in the presence of D-serine (see 150 and 180s bins). (D) Representative recordings of successive hACSF applications with or without the addition of 1 μM Ro 25-6981 for 17% hACSF (upper panels) or 40% hACSF (lower panels). Antagonism of NR2B subunit-containing NMDARs nearly completely blocked SICs evoked during osmotic challenge, as summarized in (E) and (F). (*$p < 0.05$; and **$p < 0.01$); n = 8 cells per group.

Table 6.1

Frequency (SICs/min)			
Group	**Baseline**	**1st App**	**2nd App**
17% hACSF	0.31 ± 0.18	2.07 ± 0.26	1.12 ± 0.15
17% D-Serine	0.24 ± 0.18	3.46 ± 0.51	2.97 ± 0.80

Table 6.1: Frequency of SICs/minute increases during osmotic insult in the presence of D-serine. Mean and SE values for the frequency of SICs/minute before, and during repeated 17% hACSF plus TTX and NBQX (17% hACSF) applications and in the presence of 10 μM d-serine (17% D-Serine).

Figure 6.2

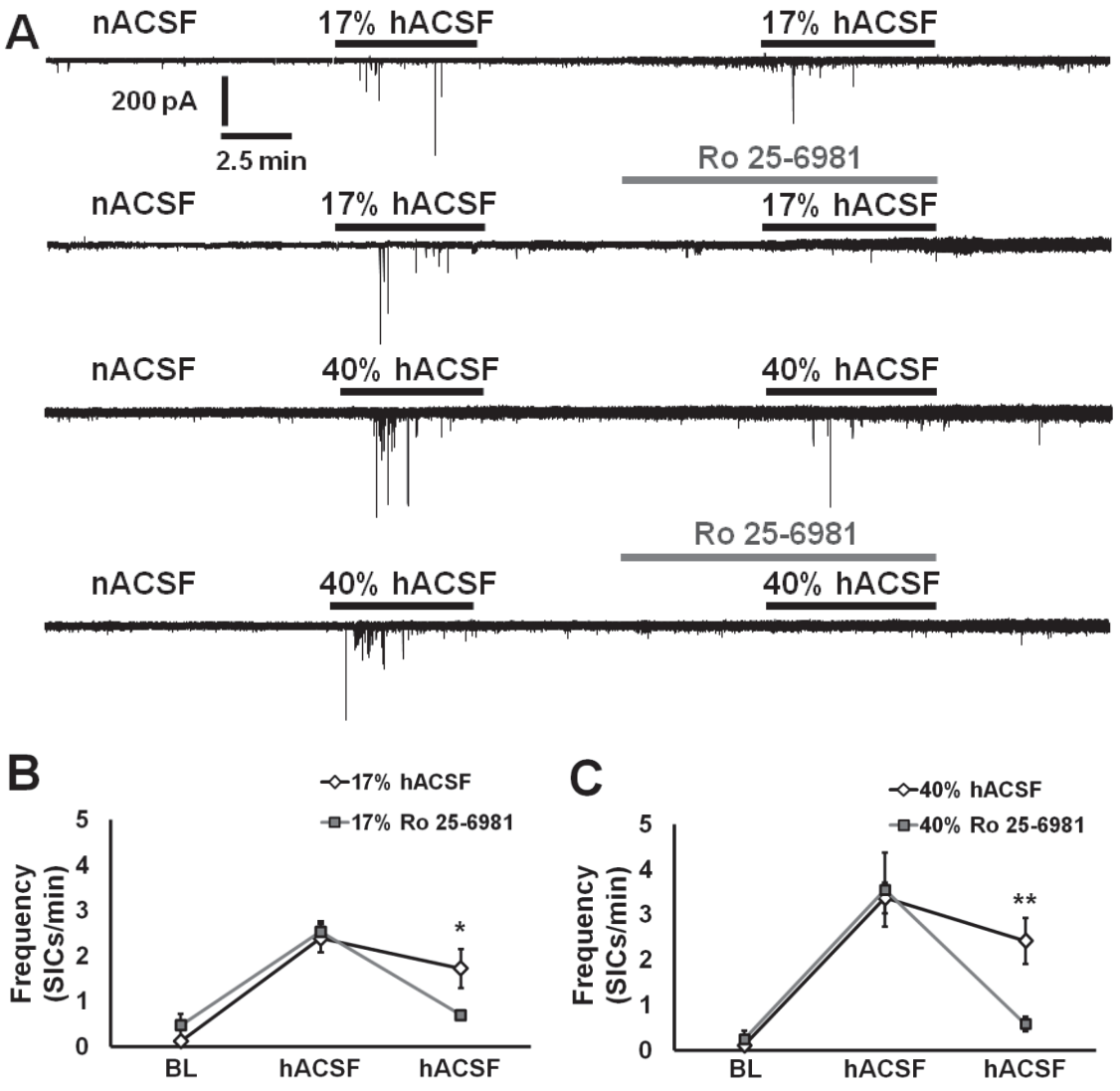

Figure 6.2: SICs are blocked by the NR2B subunit NMDA receptor antagonist Ro 25-6981. (A) Representative recordings of successive hACSF applications with or without the addition of 1 μM Ro 25-6981 for 17% hACSF (upper panels) or 40% hACSF (lower panels). To isolate SICs, all of the recordings also contained 1 μM TTX and 10 μM NBQX in order to block neuron firing of action potentials and AMPA receptor activation. Antagonism of NR2B subunit-containing NMDARs nearly completely blocked SICs evoked during both the moderate and severe osmotic challenge, as summarized in (B) and (C). (*$p < 0.05$; and **$p < 0.01$); n = 8 cells per group.

Table 6.2

Frequency (SICs/min)			
Group	**Baseline**	**1st App**	**2nd App**
17% hACSF	0.12 ± 0.07	2.39 ± 0.31	1.73 ± 0.43
17% Ro 25-6981	0.47 ± 0.25	2.53 ± 0.23	0.70 ± 0.08
40% hACSF	0.11 ± 0.08	3.37 ± 0.34	2.42 ± 0.51
40% Ro 25-6981	0.24 ± 0.18	3.55 ± 0.82	0.58 ± 0.16

Table 6.2: Frequency of SICs/minute during mild and moderate osmotic insult in the presence of the NR2B subunit containing NMDA antagonist Ro 25-6981. Mean and SE values for the frequency of SICs/minute in the presence or absence of 1 μM Ro 25-6981 (2nd App only) during mild and moderate osmotic stress.

Figure 6.3

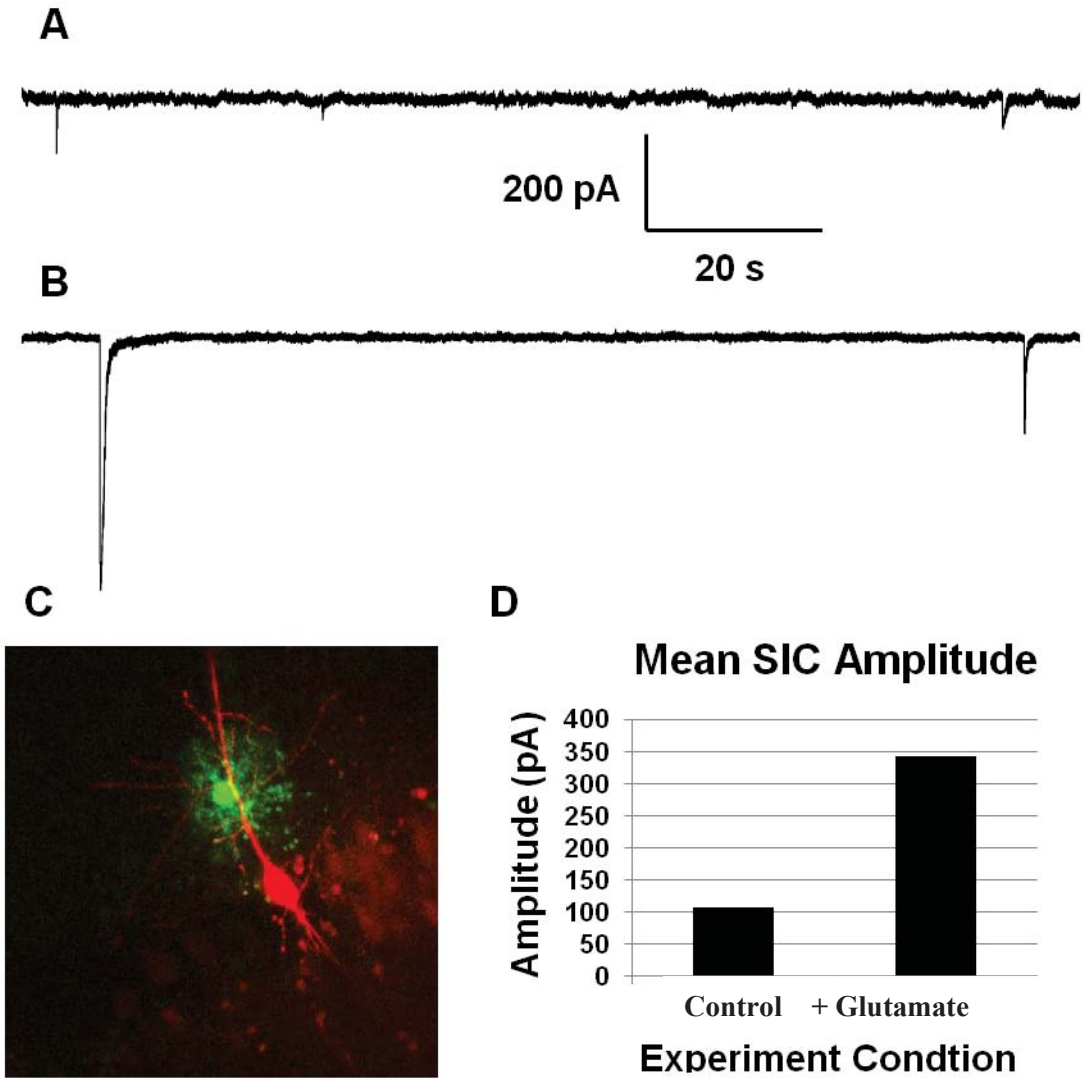

Figure 6.3: Neuronal SICs appear to be enhanced during moderate osmotic stress when astrocytes are loaded with glutamate. Representative traces of SICs during a 17% hACSF application, after a 15 min patch clamp of astrocytes to load them with either + 20 mM sucrose, control condition (A), or + 20 mM glutamate (B). Confocal image of the experimental arrangement for the patch clamped, dye filled cells within the hippocampus showing the CA1 pyramidal neuron (red) and nearby, striatum radiatum, astrocyte (green) (C). Preliminary data suggests that SICs from neurons next to astrocytes loaded with sucrose appear to have smaller absolute amplitudes (A) than neurons near astrocytes loaded with glutamate (B & D). n = 2

References

Abdullaev IF, Rudkouskaya A, Schools GP, Kimelberg HK, Mongin A a (2006) Pharmacological comparison of swelling-activated excitatory amino acid release and Cl- currents in cultured rat astrocytes. J Physiol 572:677–689.

Andrew RD, Labron MW, Boehnke SE, Carnduff L, Kirov S a (2007) Physiological evidence that pyramidal neurons lack functional water channels. Cereb Cortex 17:787–802.

Bardutzky J, Schwab S (2007) Antiedema therapy in ischemic stroke. Stroke 38:3084–3094.

Binder DK, Auser CS, Words KEY (2006) Functional Changes in Astroglial Cells in Epilepsy. 368:358–368.

Binder DK, Papadopoulos MC, Haggie PM, Verkman a S (2004) In vivo measurement of brain extracellular space diffusion by cortical surface photobleaching. J Neurosci 24:8049–8056.

Danysz W, Parsons CG (1998) Glycine and N-Methyl-D-Aspartate Receptors: Physiological Significance and Possible Therapeutic Applications. Pharmacol Rev 50.

Delaney AJ, Power JM, Sah P (2012) Ifenprodil reduces excitatory synaptic transmission by blocking presynaptic P/Q type calcium channels. J Neurophysiol 107:1571–1575.

Ding S, Fellin T, Zhu Y, Lee S-Y, Auberson YP, Meaney DF, Coulter D a, Carmignoto G, Haydon PG (2007) Enhanced astrocytic Ca2+ signals contribute to neuronal excitotoxicity after status epilepticus. J Neurosci 27:10674–10684.

Duffy S, Labrie V, Roder JC (2008) D-serine augments NMDA-NR2B receptor-dependent hippocampal long-term depression and spatial reversal learning. Neuropsychopharmacology 33:1004–1018.

Fellin T, Pascual O, Gobbo S, Pozzan T, Haydon PG, Carmignoto G (2004) Neuronal synchrony mediated by astrocytic glutamate through activation of extrasynaptic NMDA receptors. Neuron 43:729–743.

Frasca A, Aalbers M, Frigerio F, Fiordaliso F, Salio M, Gobbi M, Cagnotto A, Gardoni F, Battaglia GS, Hoogland G, Di Luca M, Vezzani A (2011) Misplaced NMDA receptors in epileptogenesis contribute to excitotoxicity. Neurobiol Dis 43:507–515.

Kimelberg HK (2004) Increased release of excitatory amino acids by the actions of ATP and peroxynitrite on volume-regulated anion channels (VRACs) in astrocytes. 45:511–519.

Lassmann H, Petsche U, Kitz K, Baran H, Sperk G, Seitelberger F, Hornykiewicz O (1984) The role of brain edema in epileptic brain damage induced by systemic kainic acid injection. Neuroscience 13:691–704.

Mares P, Mikulecká A (2009) Different effects of two N-methyl-D-aspartate receptor antagonists on seizures, spontaneous behavior, and motor performance in immature rats. Epilepsy Behav 14:32–39.

McCool BA, Lovinger DM (1995) Ifenprodil Inhibition of the 5-Hydroxytryptamine3 Receptor. Neuropharmacology 34:621–629.

Mongin AA, Orlov SN (2001) Mechanisms of cell volume regulation and possible nature of the cell volume sensor. Pathophysiology 8:77–88.

Montero TD, Orellana J a (2015) Hemichannels: new pathways for gliotransmitter release. Neuroscience 286:45–59.

Mosley C a, Myers SJ, Murray EE, Santangelo R, Tahirovic Y a, Kurtkaya N, Mullasseril P, Yuan H, Lyuboslavsky P, Le P, Wilson LJ, Yepes M, Dingledine R, Traynelis SF, Liotta DC (2009) Synthesis, structural activity-relationships, and biological evaluation of novel amide-based allosteric binding site antagonists in NR1A/NR2B N-methyl-D-aspartate receptors. Bioorg Med Chem 17:6463–6480.

Papadopoulos MC, Verkman AS (2007) Aquaporin-4 and brain edema. Pediatr Nephrol 22:778–784.

Pasantes-Morales H, Franco R, Torres-Marquez E, Hernández-Fonseca K, Ortega A (2000) Amino Acid Osmolytes in Regulatory Volume Decrease and Isovolumetric Regulation in Brain Cells: Contribution and Mechanisms. Cell Physiol Biochem:361–370.

Risher WC, Andrew RD, Kirov SA (2009) Real-Time Passive Volume Responses of Astrocytes to Acute Osmotic and Ischemic Stress in Cortical Slices and In Vivo Revealed by Two-Photon Microscopy. 221:207–221.

Siegel AJ (2015) Fatal Water Intoxication and Cardiac Arrest in Runners during Marathons: Prevention and Treatment Based on Validated Clinical Paradigms. Am J Med.

Traynelis SF, Dingledine R (1988) Potassium-induced spontaneous electrographic seizures in the rat hippocampal slice. J Neurophysiol 59:259–276.

Unterberg a W, Stover J, Kress B, Kiening KL (2004) Edema and brain trauma. Neuroscience 129:1021–1029.

Wang X-M, Bausch SB (2004) Effects of distinct classes of N-methyl-D-aspartate receptor antagonists on seizures, axonal sprouting and neuronal loss in vitro: suppression by NR2B-selective antagonists. Neuropharmacology 47:1008–1020.

Wetherington J, Serrano G, Dingledine R (2008) Astrocytes in the epileptic brain. Neuron 58:168–178.

Zhang H, Cao HJ, Kimelberg HK, Zhou M (2011) Volume regulated anion channel currents of rat hippocampal neurons and their contribution to oxygen-and-glucose deprivation induced neuronal death. PLoS One 6:e16803.

Chapter 7

Conclusion and Perspective

It seems clear that non-synaptic sources of glutamate during osmotic edema contribute to neuronal excitability, to synchronization of neuronal networks, and potentially to seizure generation in some way. However, much work needs to be done to understand this process at the physiological level as well as the pathological. Unfortunately, research has been lacking to a great extent in this area, focused on neuronal mechanisms including augmented excitatory inputs through increased synchrony and/or activation due to recurrent excitatory collaterals (Wong et al., 1986) or global decrease in inhibitory input via defective GABAergic inhibition (Lloyd et al., 1986).

The results of this study demonstrate that one of the very first effects produced in CA1 pyramidal neurons by osmotic edema are NMDA receptor-dependent slow inward currents. SICs were generated within around 60 seconds in hypoosmolar ACSF at all concentrations tested. Even a 5% reduction in osmolarity evoked SICs in neurons, although SICs were larger and more frequent as osmolarity decreased. SICs are typically evoked in Mg^{2+}-free conditions or depolarized holding potentials, during voltage-clamp of neurons, and in the presence of the NMDA receptor co-agonist D-serine, the AMPA receptor antagonist NBQX, and in TTX and/or bafilomycin to block action

potentials and quantal vesicular release (Angulo et al., 2004; Fellin et al., 2004; Fiacco et al., 2007; Shigetomi et al., 2008). These conditions make it difficult to ascertain what effect SICs might have on neuronal excitability under more physiological conditions. Therefore, the effect of hypoosmolarity was measured while systematically removing pharmacological and electrophysiological manipulations. In all cases tested, including in the absence of any added reagents or voltage clamps reducing osmolarity of the ACSF significantly increased neuronal excitability. Action potentials were evoked over the same timecourse as SICs, and were also blocked by AP5, suggesting that activation of NMDA receptors during cell swelling significantly depolarizes neurons above action potential threshold. Action potentials also displayed more bursting characteristics during osmotic challenge compared to the few APs occurring spontaneously in the baseline period prior to hACSF application. Lastly, I found that SICs and bursting activity were more pronounced in adult vs. juvenile tissue which suggests that activation of NMDA receptors during osmotic insult are increasing bursting activity, and potentially synchronization of neurons. Our results suggest that significant increases in neuronal excitability are produced at the very onset of cell swelling, likely before cellular volume increases have stabilized.

Previous work has recorded the effects of reduced osmolarity on evoked neuronal activity in the hippocampus. Andrew et al. (1989) and Ballyk et al. (1991) observed effects of hypoosmolality on evoked CA1 pyramidal cell field

potentials and on the population spike (PS) amplitude, with no evidence for changes in chemical synaptic transmission. Because the increase in PS amplitude was similar when antidromically stimulating CA1 axons or orthodromic stimulation of Schaffer collaterals, the changes observed were entirely explained by the increased extracellular resistance directing more voltage across the neuronal membrane, as described by Ohm's law (voltage = current * resistance) (Andrew et al., 1989). These ephaptic, or field effects help to synchronize neuronal excitability across the population of neurons and therefore contribute to seizure-like discharges (Andrew et al., 1989; Ballyk et al., 1991). Similar results were obtained from recordings in CA3 by the same group (Saly and Andrew, 1993). Later, Somjen and others challenged these findings by providing evidence from recording evoked potentials and whole-cell synaptic currents that synaptic transmission is also enhanced by lowered osmolarity ACSF (Chebabo et al., 1995a; Huang et al., 1997). These authors hypothesized that buildup of transmitter concentration in the reduced extracellular space at the receptive surface may be the mechanism underlying the increased EPSCs. Together, these seminal studies provided strong evidence that osmotically-induced edema enhances evoked synaptic transmission, electrical field effects, and population discharges. However, none of these earlier studies mentioned SICs, nor found changes in electrophysiological properties of individual neurons. It now seems likely that this activity was missed in the previous work due to the methods used to record neuronal activity. Episodic rather than continuous recordings were

performed, usually after several minutes (10 - 20 min) in hACSF when cell swelling and reduction of the ECS had largely stabilized. In contrast, the experiments in this body of work were continuous recordings of spontaneous neuronal activity throughout the process of solution exchange from normosmolar to hypoosmolar ACSF. These findings, therefore, add to and expand upon earlier studies by identifying NMDA receptor activation and SICs as one of the first events that significantly increase neuronal excitability at the onset of osmotic edema.

Slow inward currents have been predominantly discussed in the context of astrocytes. The first reports of SICs suggested that astrocyte Ca^{2+}-dependent glutamate release activated extrasynaptic NMDA receptors on adjacent neuronal compartments to generate SICs (Angulo et al., 2004; Fellin et al., 2004). However, these findings were later questioned by data suggesting that reduced osmolarity and cellular swelling were important for SICs. First, Kozlov et al. (2006) found that SICs in olfactory bulb granule cells were evoked by various types of mechanical stimulation including cyclic stretch to blood vessels, and that reducing extracellular osmolarity significantly increased SIC frequency. These data suggested a role for volume-regulated anion channels (VRAC) in the generation of SICs (Kozlov et al., 2006). Subsequently, Fiacco et al. (2007) demonstrated that SICs could be evoked in CA1 pyramidal neurons by application of -25 mM NaCl ACSF in slices from $IP_3R2^{-/-}$ mice, in which Gq GPCR-driven astrocyte Ca^{2+} activity is significantly reduced (Petravicz et al.,

2008; Srinivasan et al., 2015). These findings suggested that SICs are predominantly driven by reduced osmolarity, although there is ample evidence to suggest that astrocyte Ca^{2+} activity amplifies or modulates volume-regulated release pathways that may be involved in the generation of SICs (Mongin and Kimelberg, 2005; Takano et al., 2005; Ramos-mandujano et al., 2007).

Are astrocytes responsible for SICs? This remains an open question that requires further study. A hypothesis for how SICs are generated during the onset of cellular edema can be made after taking into consideration the cells that swell, the receptors involved, and where the glutamate is coming from (Figure 7.1). Evidence to date suggests that neurons are very resistant to osmotic changes. This has been demonstrated in acutely dissociated neurons (Somjen et al., 1993) and in recordings of real-time volume responses during acute osmotic stress *in situ* (Andrew et al., 2007) and *in vivo* (Risher et al., 2009). However, recently our laboratory has obtained data using confocal imaging to visualize neurons during mild and moderate osmotic stress which may refute their findings. Astrocytes readily swell in osmotic stress, and has been attributed to their selective expression of the functional water channel aquaporin 4 (Andrew et al., 2007; Hirrlinger et al., 2008; Risher et al., 2009). Therefore, astrocytes appear to be one of the cells in the brain that swell during cellular edema brought on by acute reductions in extracellular osmolarity, and may therefore be a driving force behind reduction of the ECS.

All studies of SICs, regardless of proposed mechanism, have found that SICs are mediated by NMDA receptors. In the present study, it is also observed that NMDA receptors are responsible for SICs. SICs were potentiated by D-serine, and blocked by both DL-AP5 and the NR2B specific compound Ro25-6981. Previous work postulated that extrasynaptic NMDA receptors generate SICs because of their slow kinetics and block by NR2B subunit-specific antagonists such as ifenprodil (Fellin et al., 2004; Araque et al., 2014). However, accumulating evidence suggests that synaptic and extrasynaptic NMDA receptors are triheteromeric, containing GluN1, GluN2A (NR2A) and GluN2B (NR2B) subunits (Harris and Pettit, 2007; Rauner and Köhr, 2011; Tovar et al., 2013). Therefore, subunit selective pharmacology cannot be used to distinguish between synaptic vs. extrasynaptic pools of NMDA receptors. If receptor composition is similar within and outside the synapse, kinetic properties of the channels themselves are not likely to play much of a role in the slow kinetics of SICs. Whether synaptic or extrasynaptic, a more likely scenario for the slow rise and decay times of SICs is the increased tortuosity of the ECS brought about by cell swelling. The ECS is not simply a fluid-filled space, but rather contains a rich meshwork of extracellular matrix molecules (Vargova and Sykova, 2014). The ECS can be likened to a wet sponge, which gets compressed when cells swell. Within this collapsed meshwork, diffusion of glutamate will be significantly impeded, leading to currents with slow kinetics. While a role for extrasynaptic NMDA receptors in the generation of SICs still seems likely based on their

location and high binding affinity for glutamate, additional work is required to substantiate this possibility. Incorporation of stimulation protocols with the use-dependent channel blocker MK-801 seems like a logical approach to isolate the extrasynaptic fraction of NMDA receptors (Harris and Pettit, 2007).

Because SICs can be evoked in the absence of neuronal action potentials or miniature spontaneous vesicular release, the glutamate binding NMDA receptors must be predominantly non-synaptic in origin. This leaves two possible sources of glutamate leading to SICs: Release from non-neuronal cells, or ambient glutamate already present in the ECS which increases in concentration and proximity to receptors as the ECS shrinks. Astrocytes represent a potentially significant source of glutamate when they swell. It is well-established that astrocytes *in vitro* release large quantities of glutamate from VRAC in hypoosmolar conditions (Abdullaev et al., 2006; Kimelberg et al., 2006; Liu et al., 2006). However, there is some uncertainty in the literature with regard to when and how VRAC open in the process of osmotic edema. Purified astrocytes in culture initially swell in response to hypoosmolar treatment, and then undergo a regulatory volume decrease (RVD) due to opening of VRAC (Kimelberg et al., 2006; Andrew et al., 2007). VRAC opening causes compensatory loss of K^+, Cl^-, and excitatory amino acids including glutamate, accompanied by water, leading to recovery of cell volume. However, a number of studies have provided evidence that RVD does not occur in intact tissue preparations, as demonstrated by recording intrinsic optical signals (Andrew et al., 1997, 2007) and real-time

volume measurements of fluorescently-labeled astrocytes *in situ* (Neusch et al., 2006; Andrew et al., 2007) and *in vivo* (Risher et al., 2009). In few instances when RVD has been observed, it occurs gradually, proceeding over tens of minutes, and does not appear to initiate for ~10-20 min. in hypoosmolar solution (Chebabo et al., 1995a, 1995b; Andrew et al., 1997). In the present study, hACSF was only applied for 5 to 7 minutes at a time. Our real-time volume measurements of astrocytes indicate that astrocyte volume increases are just starting to peak after 5 minutes in hACSF. This means that SICs and APs occurred over a period of time in which the ECS was still shrinking, and normosmolar ACSF was re-applied before RVD had a chance to begin. Previous studies that recorded changes in light transmittance and extracellular resistance measurements also suggest that cell swelling and reduction of the ECS is still occurring during this time (Andrew and MacVicar, 1994; Chebabo et al., 1995b; Kilb et al., 2006; Andrew et al., 2007). Initiation of SICs within one minute suggests - at least in the context of RVD measurements - that sufficient glutamate is available to activate NMDARs before VRAC ever have a chance to open. If, however, VRAC are triggered to open by the initial stretch of the membrane as the cell volume is increasing, they may play a role. Based on measurements of glutamate accumulation in the ECS by enzymatic assay and D-[^{3}H]aspartate release *in vitro*, and microdialysis measurements *in vivo*, significant release of glutamate from VRAC takes place within 3-5 minutes, likely while cells are still swelling (Abdullaev et al., 2006; Liu et al., 2006; Haskew-Layton et al.,

2008). Alternatively, other mechanically-sensitive channels may be involved in generation of SICs. The NMDA receptors themselves have been reported to be osmosensitive (Paoletti and Ascher, 1994), and connexin/pannexin hemichannels are sensitive to both stretch and reduced divalent cation solution (Ye et al., 2003; Montero and Orellana, 2015; Voigt et al., 2015) - precisely the conditions presented by hypoosmolar challenge. Further complicating matters is that the traditional pharmacological agents used to block VRAC are nonspecific, including the most promising of those - DCPIB - which has been shown recently to also block hemichannels (Bowens et al., 2013). At this time, it is not possible to determine if SICs are generated by an active release mechanism or by glutamate already present in the ECS. A careful series of experiments will need to be performed to determine the role of VRAC or other channels in the generation of SICs and increased neuronal excitability during acute osmotic edema. An intriguing possibility is that hemichannels release glutamate in the early phase while cell volume is increasing, while VRAC are involved in sustained release of glutamate during prolonged RVD.

These findings have important implications for understanding the underpinnings of epilepsy. Non-synaptic mechanisms are critical for the initiation and maintenance of recurring seizure-like activity in the hippocampus. Ictal discharges have actually been shown to occur in the complete absence of chemical synaptic transmission (Jensen and Yaari, 1988; Dudek et al., 1990; Roper et al., 1992). Undoubtedly, increased electrical field effects due to

reduction of the ECS play a major role in synchronization of neuronal bursts underlying seizure (Taylor and Dudek, 1984; Andrew et al., 1989; Jensen and Yaari, 1997; Dudek et al., 1999). Chemical synaptic transmission has also been shown to play a role (Huang et al., 1997), likely amplifying seizure activity through activation of excitatory AMPA and NMDA receptors to increase neuronal depolarization. While blocking AMPA receptors with NBQX I observed a significant decrease in the frequency of currents, during a mild osmotic insult, in the baseline and all three hypoosmolar applications. These findings suggest that AMPA receptors are also activated during osmotic edema and increase neuronal excitability. Dingledine et al. (1986) found that a significant component of the slow depolarization underlying burst firing is synaptic in origin and mediated by NMDA receptors. Later, Traynelis and Dingledine (1988) demonstrated that recurring potassium-induced hippocampal seizures (ictal discharges) are blocked by the NMDA receptor antagonist D-AP5. Slow inward currents are intriguing in the context of epilepsy, as they are non-synaptic in origin, chemically-mediated, and NMDA receptor-dependent. SICs enhance synchrony of neuronal activity, as demonstrated in this body of work, by increased bursting of neuronal action potentials evoked by hACSF application, an effect that was dependent on NMDA receptors. This work provides proof-of-principle that rapid cell swelling can increase and synchronize neuronal excitability in juvenile and adult hippocampus through the generation of SICs. The greater effect observed in adult hippocampal slices may be due to the smaller ECS in adults, which is estimated to be about

half the size of juveniles (Kilb et al., 2006). Overall, the consistent effect of osmotic edema on neuronal excitability across a variety of conditions suggests that cell swelling may be a universal mechanism contributing to seizures across multiple forms of epilepsy and seizure disorders. The rapid timecourse of evoking SICs by hACSF in our study fits well with the timing of glial depolarization, increased CA1 burst intensity, and ECS reduction, which occur 1-2 minutes prior to ictal discharge in the elevated potassium model of epilepsy (Traynelis and Dingledine, 1988, 1989). Similar observations have been made in studies of seizure *in vivo* (Binder et al., 2006). It may be that elevated potassium, which has also been shown to cause cell swelling (Andrew et al., 2007; Risher et al., 2009) leads to opening of VRAC, RVD, and release of glutamate to trigger the NMDA receptor-dependent ictal discharge.

Figure 7.1

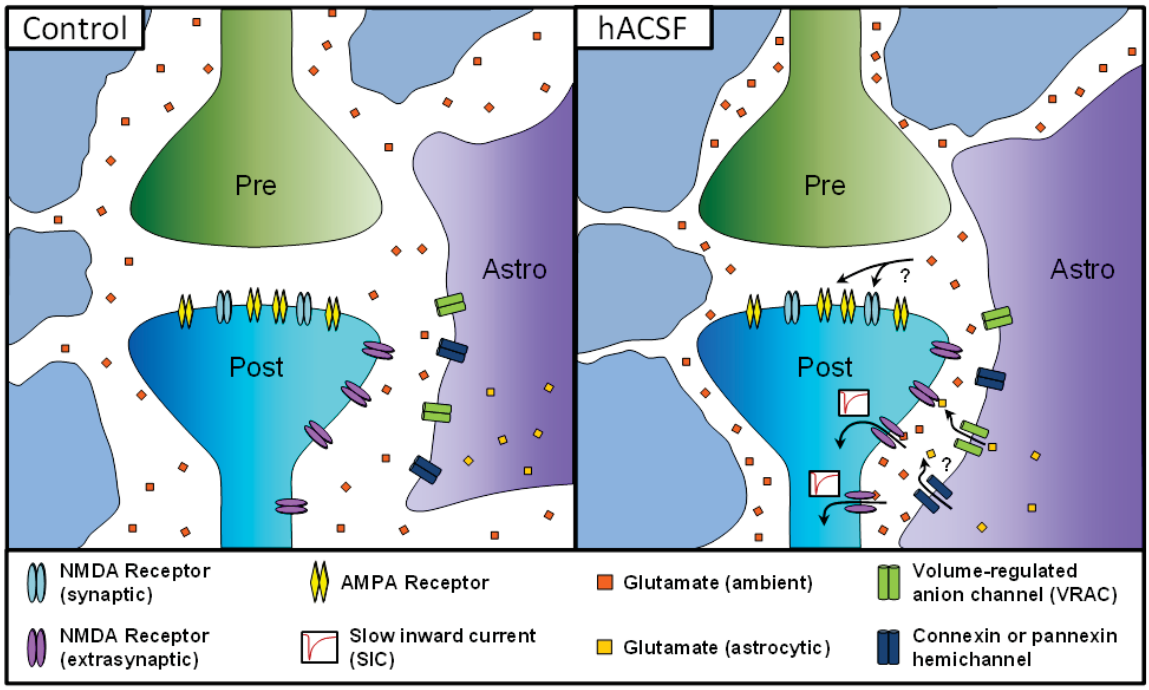

Figure 7.1: Hypothesized model for neuronal excitability increases in hACSF. In control conditions (left panel), ambient glutamate diffuses through the extracellular space around the synapse at low concentration. Neuronal excitability is mostly synaptic. Upon addition of hACSF (right panel), tissue (including astrocyte) swelling leads to constriction of the ECS. This increases local glutamate concentrations near extrasynaptic (and possibly synaptic) NMDA receptors, increasing neuronal excitability through NMDA receptor activation. Resultant currents (SICs) are large and slow due in part to the restricted diffusion of glutamate within the compressed ECS. Ambient glutamate concentration may be augmented by astrocytic glutamate released through volume-regulated anion channels (VRAC) and/or connexin/pannexin hemichannels.

References

Abdullaev IF, Rudkouskaya A, Schools GP, Kimelberg HK, Mongin A a (2006) Pharmacological comparison of swelling-activated excitatory amino acid release and Cl- currents in cultured rat astrocytes. J Physiol 572:677–689.

Andrew RD, Fagan M, Ballyk B a, Rosen a S (1989) Seizure susceptibility and the osmotic state. Brain Res 498:175–180.

Andrew RD, Labron MW, Boehnke SE, Carnduff L, Kirov SA (2007) Physiological Evidence That Pyramidal Neurons Lack Functional Water Channels. Cereb Cortex 17:787–802.

Andrew RD, Lobinowich ME, Osehobo EP (1997) Evidence against volume regulation by cortical brain cells during acute osmotic stress. Exp Neurol 143:300–312.

Andrew RD, MacVicar B a (1994) Imaging cell volume changes and neuronal excitation in the hippocampal slice. Neuroscience 62:371–383.

Angulo MC, Kozlov AS, Charpak S, Audinat E (2004) Glutamate released from glial cells synchronizes neuronal activity in the hippocampus. J Neurosci 24:6920–6927.

Araque A, Carmignoto G, Haydon PG, Oliet SHR, Robitaille R, Volterra A (2014) Gliotransmitters travel in time and space. Neuron 81:728–739.

Ballyk BA, Quackenbush SJ, Andrew RD (1991) Osmotic Effects on the CA1 Neuronal Population in Hippocampal Slices with Special Reference to Glucose. J Neurophysiol 65.

Binder DK, Yao X, Zador Z, Sick TJ, Verkman AS (2006) Increased Seizure Duration and Slowed Potassium Kinetics in Mice Lacking Aquaporin-4 Water Channels. 636:631–636.

Bowens NH, Dohare P, Kuo Y, Mongin AA (2013) DCPIB , the Proposed Selective Blocker of Volume-Regulated Anion Channels , Inhibits Several Glutamate Transport Pathways in Glial Cells s. :22–32.

Chebabo SR, Hester M a, Aitken PG, Somjen GG (1995a) Hypotonic exposure enhances synaptic transmission and triggers spreading depression in rat hippocampal tissue slices. Brain Res 695:203–216.

Chebabo SR, Hester MA, Jing J, Aitken PG, Somjen GG (1995b) Interstitial space , electrical resistance and ion concentrations during hypotonia of rat hippocampal slices. J Physiol:685–697.

Dudek FE, Obenaus a, Tasker JG (1990) Osmolality-induced changes in extracellular volume alter epileptiform bursts independent of chemical synapses in the rat: importance of non-synaptic mechanisms in hippocampal epileptogenesis. Neurosci Lett 120:267–270.

Dudek FE, Patrylo PR, J.P. W (1999) Mechanisms of neuronal synchronization during epileptiform activity. Adv Neurol 79:699–708.

Fellin T, Pascual O, Gobbo S, Pozzan T, Haydon PG, Carmignoto G (2004) Neuronal synchrony mediated by astrocytic glutamate through activation of extrasynaptic NMDA receptors. Neuron 43:729–743.

Fiacco TA, Agulhon C, Taves SR, Petravicz J, Casper KB, Dong X, Chen J, McCarthy KD (2007) Selective stimulation of astrocyte calcium in situ does not affect neuronal excitatory synaptic activity. Neuron 54:611–626.

Harris AZ, Pettit DL (2007) Extrasynaptic and synaptic NMDA receptors form stable and uniform pools in rat hippocampal slices. J Physiol 584:509–519.

Haskew-Layton RE, Rudkouskaya A, Jin Y, Feustel PJ, Kimelberg HK, Mongin A a (2008) Two distinct modes of hypoosmotic medium-induced release of excitatory amino acids and taurine in the rat brain in vivo. PLoS One 3:e3543.

Hirrlinger PG, Wurm A, Hirrlinger J, Bringmann A, Reichenbach A (2008) Osmotic swelling characteristics of glial cells in the murine hippocampus, cerebellum, and retina in situ. J Neurochem 105:1405–1417.

Huang R, Bossut DF, Somjen GG (1997) Enhancement of Whole Cell Synaptic Currents by Low Osmolarity and by Low [NaCl] in Rat Hippocampal Slices. :2349–2359.

Jensen MS, Yaari Y (1988) The Relationshp Between Interictal and Ictal Paroxysms in an In Vitro Model o f rocal Hippocampal kpuepsy. :591–598.

Jensen MS, Yaari Y (1997) Role of Intrinsic Burst Firing , Potassium Accumulation , and Electrical Coupling in the Elevated Potassium Model of Hippocampal Epilepsy.

Kilb W, Dierkes PW, Syková E, Vargová L, Luhmann HJ (2006) Hypoosmolar conditions reduce extracellular volume fraction and enhance epileptiform activity in the CA3 region of the immature rat hippocampus. J Neurosci Res 84:119–129.

Kimelberg HK, Macvicar BA, Sontheimer H (2006) Anion Channels in Astrocytes : Biophysics , Pharmacology , and Function. 757:747–757.

Kozlov a S, Angulo MC, Audinat E, Charpak S (2006) Target cell-specific modulation of neuronal activity by astrocytes. PNAS 103:10058–10063.

Liu H, Tashmukhamedov BA, Inoue H, Okada Y (2006) Roles of Two Types of Anion Channels in Glutamate Release from Mouse Astrocytes Under Ischemic or Osmotic Stress. 357:343–357.

Lloyd KG, Bossi L, Morselli C, Rougier M, Loiseau H (1986) Alterations in human epilepsy. Adv Neurol 44:1033–1044.

Mongin AA, Kimelberg HK (2005) ATP regulates anion channel-mediated organic osmolyte release from cultured rat astrocytes via multiple Ca2+-sensitive mechanisms. Am J Physiol Cell Physiol:204–213.

Montero TD, Orellana J a (2015) Hemichannels: new pathways for gliotransmitter release. Neuroscience 286:45–59.

Neusch C, Papadopoulos N, Müller M, Maletzki I, Winter SM, Hirrlinger J, Handschuh M, Bähr M, Richter DW, Kirchhoff F, Hülsmann S (2006) Lack of the Kir4.1 channel subunit abolishes K+ buffering properties of astrocytes in the ventral respiratory group: impact on extracellular K+ regulation. J Neurophysiol 95:1843–1852.

Paoletti P, Ascher P (1994) Mechanosensitivity of NMDA Receptors in Cultured Mouse Central Neurons. Neuron 13:645–655.

Petravicz J, Fiacco T a, McCarthy KD (2008) Loss of IP3 receptor-dependent Ca2+ increases in hippocampal astrocytes does not affect baseline CA1 pyramidal neuron synaptic activity. J Neurosci 28:4967–4973.

Ramos-mandujano G, Vazquez-Juarez E, Hernandez-Benitez R, Pasantes-Moreales H (2007) Thrombin Potently Enhances Swelling-Sensitive Glutamate Efflux from Cultured Astrocytes. Glia:917–925.

Rauner C, Köhr G (2011) Triheteromeric NR1/NR2A/NR2B receptors constitute the major N-methyl-D-aspartate receptor population in adult hippocampal synapses. J Biol Chem 286:7558–7566.

Risher WC, Andrew RD, Kirov SA (2009) Real-Time Passive Volume Responses of Astrocytes to Acute Osmotic and Ischemic Stress in Cortical Slices and In Vivo Revealed by Two-Photon Microscopy. 221:207–221.

Roper SN, Obenaus a, Dudek FE (1992) Osmolality and nonsynaptic epileptiform bursts in rat CA1 and dentate gyrus. Ann Neurol 31:81–85.

Saly V, Andrew RD (1993) CA3 neuron excitation and epileptiform discharge are sensitive to osmolality. J Neurophysiol 69:2200–2208.

Shigetomi E, Bowser DN, Sofroniew M V, Khakh BS (2008) Two Forms of Astrocyte Calcium Excitability Have Distinct Effects on NMDA Receptor-Mediated Slow Inward Currents in Pyramidal Neurons. 28:6659–6663.

Somjen GG, Faas GC, Vreugdenhil M, Wadman WJ (1993) Channel shutdown: a response of hippocampal neurons to adverse environments. Brain Res 632:180–194.

Srinivasan R, Huang BS, Venugopal S, Johnston AD, Chai H, Zeng H, Golshani P, Khakh BS (2015) Ca2+ signaling in astrocytes from Ip3r2−/− mice in brain slices and during startle responses in vivo. Nat Neurosci 18.

Takano T, Kang J, Jaiswal JK, Simon SM, Lin JH-C, Yu Y, Li Y, Yang J, Dienel G, Zielke HR, Nedergaard M (2005) Receptor-mediated glutamate release from volume sensitive channels in astrocytes. PNAS 102:16466–16471.

Taylor CP, Dudek FE (1984) Excitation of Hippocampal Pyramidal Cells by an Electrical Field Effect. J Neurophysiol 52.

Tovar KR, McGinley MJ, Westbrook GL (2013) Triheteromeric NMDA receptors at hippocampal synapses. J Neurosci 33:9150–9160.

Traynelis SF, Dingledine R (1988) Potassium-induced spontaneous electrographic seizures in the rat hippocampal slice. J Neurophysiol 59:259–276.

Traynelis SF, Dingledine R (1989) Role of extracellular space in hyperosmotic suppression of potassium-induced electrographic seizures. J Neurophysiol 61:927–938.

Vargova L, Sykova E (2014) Astrocytes and extracellular matrix in extrasynaptic volume transmission. Phil Trans R Soc B.

Voigt J, Grosche A, Vogler S, Pannicke T, Hollborn M, Kohen L, Wiedemann P, Reichenbach A, Bringmann A (2015) Nonvesicular release of ATP from rat retinal glial (Müller) cells is differentially mediated in response to osmotic stress and glutamate. Neurochem Res 40:651–660.

Wong RK, Traub RD, Miles R (1986) Cellular basis of neuronal synchrony in epilepsy. Adv Neurol 44:583–592.

Ye Z-C, Wyeth MS, Baltan-Tekkok S, Ransom BR (2003) Functional hemichannels in astrocytes: a novel mechanism of glutamate release. J Neurosci 23:3588–3596.